Greased lighting : implications of circadian lipid metabolism for cardiometabolic health

Berg, R. van den; Berg R. van den

GREASED LIGHTING

IMPLICATIONS OF CIRCADIAN LIPID METABOLISM FOR CARDIOMETABOLIC HEALTH

Rosa van den Berg

GREASED LIGHTING

IMPLICATIONS OF CIRCADIAN LIPID METABOLISM
FOR CARDIOMETABOLIC HEALTH

Rosa van den Berg

Greased lighting:
implications of circadian lipid metabolism for cardiometabolic health

Layout & printing by Sidestone Press
ISBN: 978-90-8890-542-1

GREASED LIGHTING

IMPLICATIONS OF CIRCADIAN LIPID METABOLISM FOR CARDIOMETABOLIC HEALTH

PROEFSCHRIFT

Ter verkrijging van
de graad van Doctor aan de Universiteit Leiden,
op gezag van Rector Magnificus prof. Mr. C.J.J.M. Stolker,
volgens besluit van het College voor Promoties
te verdedigen op donderdag 12 oktober 2017
klokke 16.15 uur

door

Rosa van den Berg
Geboren te Voorburg
In 1985

Promotor Prof. dr. P.C.N. Rensen

Copromotor Dr. N.R. Biermasz

Leden promotiecommissie

Prof. dr. A.M. Pereira Arias
Prof. dr. J.H. Meijer
Prof. dr. J.A. Romijn (Amsterdam Medisch Centrum)
Prof. dr. S. Kersten (Wageningen University & Research)

The work described in this thesis was performed at the department of Medicine, division of Endocrinology, Leiden University Medical Center, Leiden, The Netherlands, and at Einthoven Laboratory for Experimental Vascular Medicine, Leiden, The Netherlands.

Financial support by the Dutch Heart Foundation for the publication of this thesis is gratefully acknowledged.

TABLE OF CONTENTS

Chapter 1

General Introduction and outline

GENERAL INTRODUCTION AND OUTLINE

Cardiovascular disease (CVD) is the leading cause of mortality worldwide [1]. The main contributor to CVD is the formation of atherosclerotic plaques in the vessel wall, a process largely driven by hypercholesterolemia [2]. Indeed, cholesterol-lowering drugs such as statins have substantially lowered CVD related mortality [3]. In spite of this success, the incidence of CVD has continued to rise, prompting the search for additional modifiable risk factors. Perturbation of our biological clock has recently been recognized as a potential modifiable risk factor for metabolic diseases [4]. Epidemiological studies demonstrated an association between disturbed day-night rhythms, such as due to shift work [5], short sleep [6] and light at night [7-9], and several metabolic disturbances, such as obesity, dyslipidemia, insulin resistance and coronary heart disease. The overall aim of the projects described in this thesis is to investigate the mechanisms by which the biological clock contributes to lipid metabolism and how derangement of the biological clock may contribute to metabolic disorders. I will therefore provide an overview of the basic aspects of lipid metabolism and mammalian chronobiology, and the interplay between these two fields.

Within the topic of lipid metabolism, I will focus on lipoprotein metabolism and the role of brown adipose tissue (BAT) in lipoprotein metabolism. I will discuss the pathophysiology of atherosclerosis with a focus on dyslipidemia and obesity as risk factors. Within the topic of chronobiology, I will briefly address the basic organization of the mammalian biological clock, as this thesis describes studies performed in mice and humans. In this thesis, I will also explore the role of the hypothalamus-pituitary-adrenal (HPA)-axis in circadian rhythms. Therefore, the HPA-axis will be addressed in more detail. Next, since in humans short sleep duration is a common behavioral disruption of physiological day-night rhythms, I will briefly introduce human sleep physiology with a focus on short sleep duration and energy metabolism. Finally, I will combine these two fields and discuss circadian rhythmicity in lipid metabolism and give an overview of the evidence for a causal role of disturbed rhythms in metabolic disease.

Metabolism

Lipoprotein physiology

Lipids are hydrophobic molecules which encompass different molecular substances. For this thesis, I will focus on triglycerides (TG) and cholesterol, since these lipids are most involved in metabolic health and development of CVD. TGs are the most abundant lipids in human diet and their function for metabolism is to deliver energy in the form of fatty acids (FAs). TG consists of three FA chains esterified to a glycerol backbone. Cholesterol is an abundant dietary lipid in a typical Western type diet, with an entirely different structure and function. Cholesterol serves to build membranes, and serves as a precursor molecule for synthesis of bile acids and steroid hormones. Due to their hydrophobic nature, both TGs and cholesteryl esters, the storage form of cholesterol, have to be properly packaged into lipoprotein particles to be transported in the circulation. Lipoproteins are large spherical

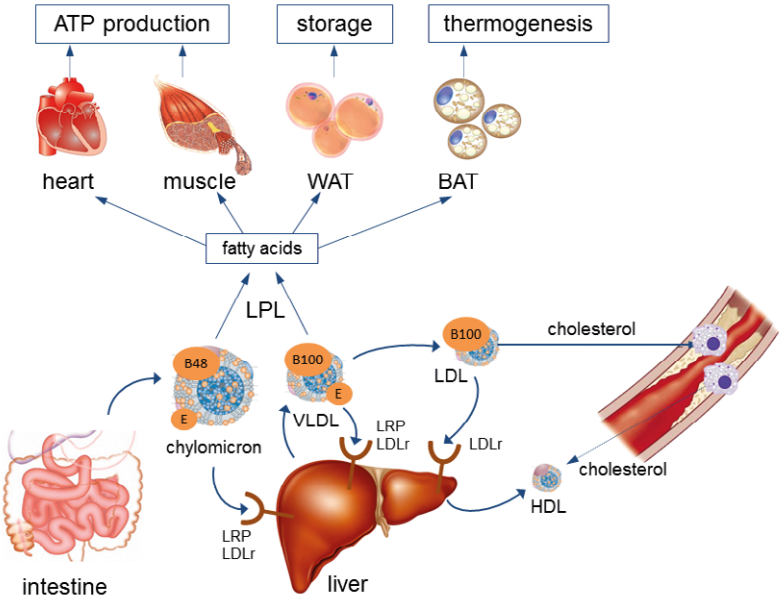

Figure 1. Overview of lipoprotein metabolism. *ATP = adenosine triphosphate, BAT = brown adipose tissue, LDLr = LDL receptor, LPL = lipoprotein lipase, LRP = LDL-receptor related protein, TG = triglyceride, WAT = white adipose tissue. See text for explanation.*

macromolecular complexes, with a lipid rich core consisting of TGs and cholesteryl esters and an outer layer composed of proteins, free cholesterol and phospholipids. They are classified based on their diameter and density: very low density lipoproteins (VLDL), low density lipoproteins (LDL), intermediate density lipoproteins (IDL), high density lipoproteins (HDL), and chylomicrons (CM) (chyle refers to lymph).

Since TGs either derive either from the diet or from de novo synthesis in the liver, the latter predominating during fasting, there are two lipoprotein synthesis routes: the endogenous and exogenous pathway [10]. After feeding, dietary TGs within the intestinal lumen are hydrolyzed into FAs and 2-monoacylglycerol, both of which are taken up by enterocytes and re-esterified into TGs. Likewise, cholesteryl esters are hydrolyzed an cholesterol is taken up by enterocytes and re-esterified. In the enterocytes, apolipoprotein B (apoB48 in humans, apoB100 in rodents) is added onto droplets consisting of TGs and cholesteryl esters by the enzyme microsomal triglyceride transfer protein (MTP), eventually producing chylomicrons during exit of enterocytes by coating with a shell composed of phospholipids, cholesterol and additional apolipoproteins. These particles are secreted into the lymphatic fluid, and eventually reaches metabolically active cells via the circulation. In case of fasting, this role is taken over by the liver, which continuously produces VLDL particles according to intracellular mechanisms similar to chylomicrons, although they are built from apoB100 in both humans and rodents [11-13]. In the circulation, these large TG-rich VLDLs or CM are trapped onto the endothelium by proteoglycans in metabolically

active tissues where TGs are hydrolyzed by lipoprotein lipase (LPL) [14]. The liberated FA can then be taken up by parenchymal cells via FA transporters such as CD36 and FA acid transport protein (FATP). Over time, VLDL and CM are delipidated; they decrease in size and increase in relative density, turning into remnant particles, namely VLDL remnants, or IDL, and CM remnants. In the blood stream, they acquire additional apolipoproteins, importantly ApoE. ApoE can bind to both the LDL-receptor (LDLr) and LDLr-related protein (LRP) on hepatocytes, mediating their uptake [15]. Further delipidation of IDL results in LDL, which have lost all apolipoproteins except for ApoB100 that induces uptake by the LDLr only. HDL is a separately synthesized particle within the liver and intestine uniquely containing ApoA1 and/or ApoA2. HDL is secreted as a cholesterol-poor discoid particle, which has the capacity to take up cholesterol from various peripheral tissues, including macrophages. Also, in humans, HDL can take up cholesteryl esters from LDL particles, in exchange for TG via cholesteryl ester transfer protein (CETP). While ApoB-containing lipoproteins are associated with increased risk for CVD, ApoA-containing HDL is associated with a decreased risk for CVD [10] (Figure 1).

Dyslipidemia and the development of atherosclerosis

The major part of CVD is attributable to atherosclerotic disease [16]. Atherosclerosis is a chronic and active pathological process within the vessel wall, consisting of an inflammatory and a lipid-driven component. The lipid-component is driven by elevated circulating concentrations of LDL particles. LDL particles can enter the vessel wall, where they are prone to modification by *e.g.* oxidation and aggregation. Macrophages take up these modified LDL particles via SRA and CD36, resulting in 'foam cells': large cholesterol-rich macrophages. Eventually, foam cells die and attract more immune cells, precipitating a pro-inflammatory cascade. On the other hand, HDL is described as anti-atherogenic, not only because of its anti-oxidative and anti-inflammatory properties, but mainly by its ability to extract cholesterol from macrophages via ABCA1 and ABCG1 for transport to the liver for excretion into the feces, a process that is termed reverse cholesterol transport [17]. Atherosclerotic plaques occlude the vascular lumen, diminishing laminar blood flow, without prominent clinical symptoms. However, upon plaque rupture, rapid platelet aggregation results in formation of thrombi that can completely occlude the lumen of a blood vessel, resulting in hypoxia and death of tissues downstream of the occlusion. Occlusion of the carotid artery results in a stroke, while in the coronary artery this results in a myocardial infarction.

White adipose tissue and its role in obesity

The prevalence of overweight and obesity has reached epidemic numbers worldwide. According to the World Health Organization, in 2014 1.9 billion people were overweight and 600 million were obese [18]. Obesity is a major risk factor for dyslipidemia and cardiovascular disease, but also for development of a myriad of other diseases, such as type 2 diabetes (T2D) and cancer [19, 20]. Although obesity is classified most commonly according to the body mass index (BMI, in kg/m^2), this poorly reflects the underlying

pathophysiology, since it ignores body composition. The body composition plays an important role in the predisposition to metabolic disease, where the accumulation of white adipose tissue (WAT) is pivotal. Upon a positive energy balance, i.e. a surplus of energy intake over energy expenditure, excess energy is stored in WAT in the form of TGs. When a critical level of TGs in WAT is reached, the white adipocytes produce pro-inflammatory mediators, initiating a pro-inflammatory state within the WAT which perpetuates itself. This low-grade inflammatory status induces insulin resistance and leads to steatosis of other organs including skeletal muscles and the liver by 'lipid overflow', causing insulin resistance in those tissues. Prolonged insulin resistance may result in the development of T2D where insulin sensitizers and eventually insulin is administered to control pathological consequences to high blood glucose levels. Insulin resistance of the liver results in a higher VLDL particle output, which increases circulating TG levels, thus aggravating dyslipidemia [21]. Therefore, promoting weight loss and preventing obesity are key strategies to prevent CVD.

Brown adipose tissue: a target to promote metabolic health

Besides the white fat depots which have an important role in obesity, both humans and rodents also possess brown fat depots. In contrast to WAT, BAT burns energy to produce heat. Cold is the most important physiological stimulus to activate BAT. Cold signals from the skin are processed by the anterior hypothalamus, which increases the sympathetic outflow towards the densely innervated BAT. Upon release of noradrenalin, the β3-adrenergic receptor on brown adipocytes is activated, leading to a downstream signaling cascade, ultimately resulting in increased hydrolysis of intracellular TG stores and increased FA oxidation by mitochondria. The mitochondria-dense brown adipocytes uniquely express uncoupling protein 1 (UCP1), which allows dissipation of the proton gradient generated by the electron transport chain into heat instead of ATP production. To replenish intracellular lipid stores, brown adipocytes increase the uptake of TG-derived FA as well as glucose from the circulation (Figure 2) [22].

In rodents, increasing BAT activity, either by physiological or pharmacological stimuli, has been proven to prevent and diminish diet-induced obesity and to lower dyslipidemia and atherosclerosis development [24-26]. In recent years, efforts have been made to translate these results to humans. In healthy young volunteers, a 3 week mild cold exposure intervention increased BAT volume (as detected by [^{18}F]fluorodeoxyglucose uptake by PET-CT) and decreased fat mass by approx. 800 g [27]. Additionally, BAT activation by cold acclimation improved insulin sensitivity in individuals with T2D [28]. South Asians, an ethnic group with a predisposition for dyslipidemia, obesity and CVD, have lower BAT detectability accompanied by lower resting energy expenditure [29]. Therefore, the activation of BAT in humans is a viable therapeutic strategy to combat cardiometabolic diseases including adiposity, dyslipidemia and CVD. Current treatment strategies aim to recruit more BAT volume and/or to stimulate BAT activity to increase energy expenditure [30].

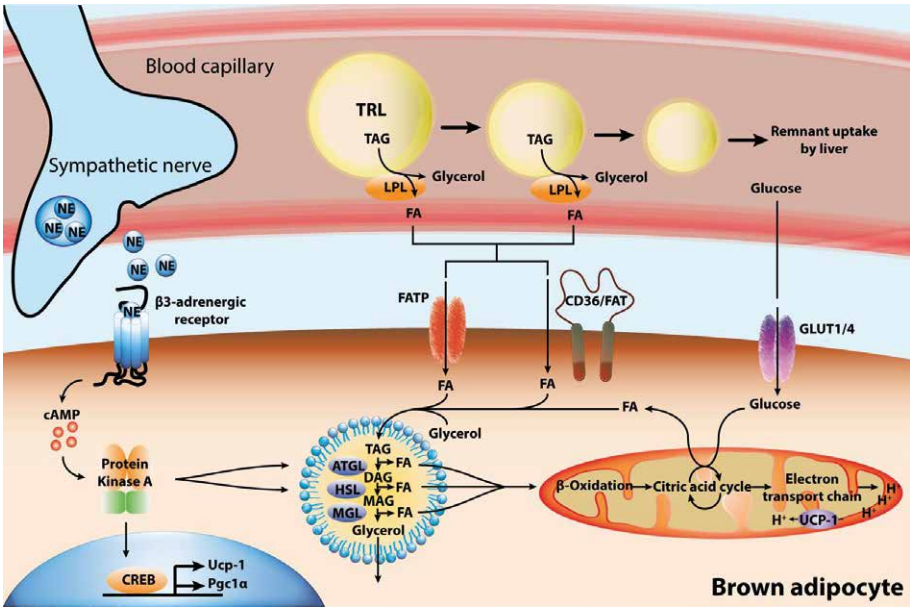

Figure 2. Brown adipocyte physiology. *DG = diglyceride, FA = fatty acid, FATP = fatty acid transport protein, LPL = lipoprotein lipase, MG = monoglyceride, TG= triglyceride, TRL = triglyceride-rich lipoprotein, UCP-1 = uncoupling protein-1 . See text for explanation. From Hoeke et al. [23]*

Chronobiology

Organization of the mammalian biological clock

The earth turns around its axis, resulting in the daily rhythm of light and dark, while the rotation of the earth around the sun results in a yearly rhythm of different day length. These 'circadian' (from Latin *circa*= about; *dies*=day) and seasonal rhythms have resulted in the evolution of biological clock systems throughout living organisms on earth (see box for more circadian terminology). Biological clocks are ubiquitous; they are present in bacteria, fungi, plants and animals. Presumably, the DNA damaging effects of ultraviolet radiation during the day has been one of the first triggers for a compartmentalization of cellular processes. DNA has to be unfolded for replication which renders it more susceptible to breaks. Darkness is therefore a more favorable period for DNA replication and repair. Furthermore, during the light period, energy from sunlight is available for photosynthesis, giving rise to a natural circadian rhythm in energy availability. Seasonal rhythms are represented by changing light exposure duration and are highly associated with changes in temperature. Rather than reacting to these changing environmental circumstances, the biological clock system evolved to anticipate to these recurrent events [31].

The light-dark cycle is the most important cue for the mammalian biological clock. The biological clock system is hierarchy organized, with a central clock, located in the suprachiasmatic nuclei (SCN) of the hypothalamus, which governs peripheral clocks throughout the body. Light is perceived by the eye and information about the intensity and wavelength of light is transferred directly to the SCN via the retino-hypothalamic tract [32]. The SCN, consisting of approx. 20,000 individual neurons, has the unique capacity to produce a rhythmic electrical firing rate, which is sustained *ex vivo*. The individual neurons synchronize each other through neuropeptide coupling, synaptic signaling and gap junctions [33]. The output of the SCN consists of this rhythmic electrical signal as well as an endocrine output, most importantly vasoactive intestinal polypeptide and arginine vasopressin [34, 35]. The SCN is the only part of the biological clock which allows entrainment of our biological clocks to light. However, light is not the only environmental cue conferring information on 24h rhythms and indeed the SCN can be synchronized by other "Zeitgebers" (German for 'time givers'). These Zeitgebers include food intake and physical activity [36] (Figure 3).

BOX: RELEVANT CIRCADIAN TERMINOLOGY

Amplitude: the distance between the peak or trough and the mean value of an oscillatory function
Chronobiology: the scientific field that studies biological rhythms

Chronotherapy: treatment based on knowledge of chronobiology. May be used for different aspects, such as timing of drug administration, using of light as treatment or treatments aimed to improve sleep-wake rhythms.

Circadian: taking place or functioning in cycles of approximately 24 hours. Conventionally, circadian rhythms are required to be endogenously generated and therefore must be determined under constant conditions (such as in mice under constant darkness).

Daily: taking placing every 24 hours

Diurnal: for this thesis same as daily. Can also refer to species which have their habitual activity period during the light phase (contrary to *nocturnal*)

Free-running period: the period of an oscillation (rhythm) in the freerun state

Jet lag: adverse health effects associated with the disruption of circadian rhythms, typically caused by time zone travel

Peak: highest value within a cycle

Period: the amount of time between the completion of one cycle

Trough: lowest value within a cycle

Zeitgebers: synchronizing environmental signals

Zeitgeber time: convention to display time where onset of light is defined as ZT0. Measured in hours

The SCN orchestrates 24h rhythms in physiological processes and behavior to align them to the environment. The SCN synchronizes peripheral tissues both directly via hormonal and neuronal output originating from the SCN and indirectly, via regulating brain areas and dictating rhythmicity in hormonal output that is generated outside the SCN. The SCN has many direct neuronal connections to other brain regions, *e.g.* nuclei that control food intake behavior (e.g. the arcuate nucleus), body temperature (the pre-optic area) and hormonal output (e.g. pineal gland and paraventricular nucleus (PVN)) [37]. In addition, direct neuronal connections exist with peripheral tissues, including metabolic organs such as liver, adipose tissue and muscle. Likely, this holds true for additional metabolic organs which have not been investigated up to now [38-40].

Peripheral tissues exhibit rhythmicity in their tissue-specific function. While not every cell of the mammalian body has been studied, for now it seems safe to state that all tissues display a degree of rhythmicity. Estimates of the extent of rhythmicity in peripheral tissues are often derived from microarray studies, which report that 5-10% of the transcriptome displays a circadian rhythm [41, 42]. Data derived from transcriptome analysis are probably an underestimation of the cellular circadian processes, since besides transcription, also histone modification, translation, post-translational modification and protein degradation display a circadian rhythm, [43, 44]. All mammalian cells that have been studied so far contain a molecular clock, driven by a transcriptional-translational feedback loop. In the past decade, the most important proteins of the molecular clock have been elucidated. Upon dimerization of core clock proteins BMAL1 and CLOCK (or within the same tissues their analogues BMAL2 and NPAS2), they form an active transcription factor. They bind to the promotor element E-Box, which promotes the transcription of downstream genes. Among these genes are both clock gene repressors and the 'clock controlled genes' (ccgs), which exert their tissue-specific functions. The clock gene repressor genes encode for proteins, namely PERIOD (PER1, PER2), CRYPTOCHROME (CRY1, CRY2) and NR1D1 (better known as REV-ERBα), which translocate back to the nucleus and inhibit the BMAL1-CLOCK dimer, thereby forming the negative arm of the transcription-translation feedback loop. This molecular clock system is equal amongst different cell types, also within the SCN (Figure 4) [45, 46].

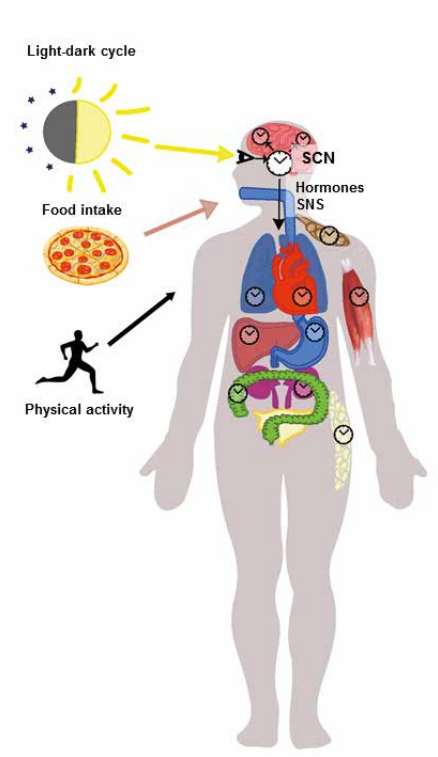

Figure 3. Organization of mammalian circadian clock system. *SCN = suprachiasmatic nuclei; SNS = sympathetic nervous system. See text for explanation.*

HPA-axis physiology and its role in chronobiology

The SCN function and the molecular clock in peripheral tissues are well-described. Nevertheless, the exact signals that transfer the timing signal of the SCN to peripheral tissues are still largely unknown. There is some evidence for glucocorticoids to confer timing signal to peripheral tissues [47, 48]. Glucocorticoids are able to synchronize the circadian rhythm in clock gene expression *in vitro* [49, 50]. Also, complete absence of endogenous

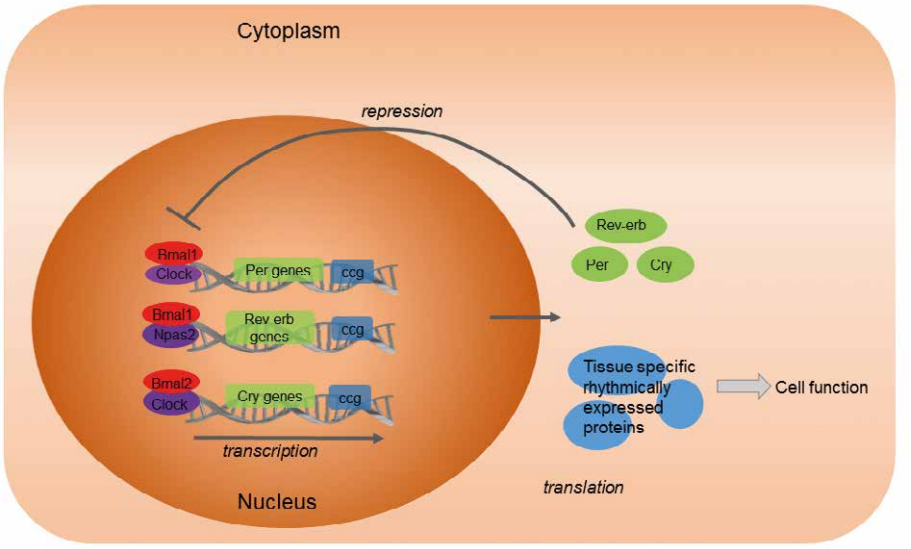

Figure 4. Cell autonomous clock. *Every mammalian cell contains a core clock machinery which controls circadian gene expression via transcriptional translational feedback loop. Ccg = clock controlled gene. See text for explanation.*

glucocorticoids by adrenalectomy shifts the circadian rhythm in clock genes in peripheral tissues [51]. In humans subjected to a constant food, sleep and activity protocol, an oral dose of glucocorticoids also shifted clock gene expression pattern in peripheral blood mononuclear cells [52].

Glucocorticoid secretion is regulated via the HPA-axis, which is the endocrine system that is best known for its response to stress. Upon a physiological or psychological stressor, the PVN secretes corticotrophin-releasing hormone (CRH). CRH stimulates the pituitary to secrete adrenocorticotropic hormone (ACTH) into the circulation, which stimulates the adrenals to secrete glucocorticoid hormones (cortisol in humans, corticosterone in rodents). ACTH and glucocorticoids exert a negative feedback on the hypothalamus and on the pituitary which dampen the response. Interestingly, in absence of stress, plasma glucocorticoid concentrations are highly rhythmic. In both humans and rodents, glucocorticoids reach a peak concentration before waking up ('arousal') and decrease throughout the wakeful period reaching the trough before sleep [53].

Glucocorticoids are steroid hormones which travel to the cell nucleus where they bind to their receptors: the mineralocorticoid receptor (MR) and the glucocorticoid receptor (GR). Since the MR has a higher binding affinity than the GR, the MR is bound throughout the 24h period, while the GR is only bound during the peak concentrations, such as during stress or the circadian peak [54]. MR and GR are present throughout the body, including the brain and metabolic organs such as liver, adipose tissue and muscle. In metabolism, glucocorticoids act as catabolic hormones, i.e. to increase available energy. GR agonism

increases glucose release, gluconeogenesis, and lipolysis while inhibiting glucose uptake by muscle and adipose tissue. The circadian peak of glucocorticoids thereby increases energy availability before waking up.

Human sleep physiology and sleep insufficiency

Humans have a well-defined circadian sleep-wake rhythm. Sleep takes place during the night, while during the day we are awake and active. It is important to note that sleep physiology is not solely an output of the biological clock, but two processes: sleep timing and sleep pressure. Therefore, sleep insufficiency is not synonymous to a disturbance of the biological clock, but also affects the sleep pressure physiology. Sleep timing is the process determined by the biological clock. The SCN determines a circadian rhythm in wakefulness which is aligned with the light-dark cycle. Furthermore, sleep timing ensures that sleep-wake cycles are synchronized to circadian rhythms in other bodily functions [55]. This is relevant to energy metabolism, as sleep coincides with fasting and a nearly absent physical activity levels. Sleep pressure is a direct function of wakefulness. Upon wakening, sleep pressure builds up and upon sleep, sleep pressure decreases. The regulation of onset of sleep and maintaining sleep is a delicate interplay of brain areas promoting wakefulness, suppressing wakefulness and promoting sleep. For the regulation of sleep timing, it is clear that melatonin plays an important role. How sleep pressure is regulated is not completely understood [56].

Sleep insufficiency is highly prevalent, with 70.1 million adults reporting less than 6 hours sleep per night [57]. Epidemiological studies strongly associate habitual short sleep duration (<5 hours per night) with many metabolic disorders [6, 58-60]. Interestingly, while most studies report a linear relationship between sleep duration and metabolic outcome parameters, others also report an association between long sleep duration (usually >9-10 hours per night) and metabolic disorders, resulting in a U-shaped association [61, 62]. A recent study demonstrated that short sleep duration was a risk factor for BMI, but not perceived sleep loss [63]. The notion that optimal sleep duration exists, is supported by studies on sleep duration in absence of modern lifestyle demands such as artificial light and setting an alarm clock. Individuals living in pre-industrialized communities have a reported sleep duration of approximately 7 hours per night [64]. Likewise, young adults camping one week outdoors, banned from electrical lights, alarm clocks and watches, display similar sleep-wake cycles [65]. In both cases, sleep duration was not equal to the total hours of darkness, but rather was kept constant by staying awake by making campfires. Together these data suggest that the optimal sleep duration is about 7 hours sleep per night.

Interplay between lipid metabolism and the biological clock

Rhythms in lipid metabolism

It has long been investigated whether human plasma lipids display circadian variation. Under standardized meal circumstances, it is clear that TG levels are highly rhythmic with a reported variation of 30-60%. TG levels also display a clear postprandial excursion [66-68].

The postprandial TG excursion shows variable peak levels throughout the day, with a higher excursion in the morning than in the afternoon [66, 69]. Circadian rhythm in TG uptake by the intestine may be a contributor, since enterocytes express clock genes [70]. Mice with a mutation of the *Clock* gene have increased lipid absorption and doubled plasma TG and cholesterol levels [71]. Cholesterol levels seem more stable throughout the day; some studies show some degree of rhythmicity [67, 72] while others do not [66, 73]. Furthermore, extensive lipidome analysis demonstrated that circulating plasma lipids are rhythmic independent of food intake in humans [74, 75] and rodents [76]. Therefore, the production and/or uptake of lipids by metabolic organs must be rhythmic. In rodents, genes involved in both TG and cholesterol production and uptake in the liver were shown to be rhythmic [76, 77]. In humans, cholesterol synthesis was estimated by determination of cholesterol precursors in plasma, and appeared to display a diurnal variation [73]. It is currently not yet known, whether the lipid uptake by metabolically active tissues displays a circadian rhythm.

Circadian disruption as a causal risk factor for metabolic disorders

In the past decade, animal studies have provided ample evidence for a causative link between disturbance of the biological clock and cardiometabolic disorders. Specific electrical ablation of the SCN induces obesity and insulin resistance in rodents [78]. Also, several genetic knock-out models of clock genes have been generated, which resulted in adverse metabolic phenotypes, including dyslipidemia and obesity [79-82]. The adverse metabolic phenotype observed in whole-body knock-out of clock genes may have a similar etiology as the SCN ablation, since the genetic deficiencies also affect the SCN [83]. Interestingly, tissue-specific disturbances of rhythm also induce metabolic disturbances. Mice with an adipocyte-specific knock-out of *Bmal1* have higher body weight than control animals due to increased food intake. Interestingly, this was attributed to an increased FA release by WAT during daytime, which increases orexigenic signals in the hypothalamus [84]. Furthermore, tissue-specific disruption of clock genes can enhance atherosclerosis formation. *Ldlr-/-* mice that received bone marrow from *Rev-erbα-/-* mice exhibit a pro-inflammatory phenotype due to M1 polarization of macrophages [85]. *Apoe-/-* mice that received bone marrow from *Clock* mutant mice have impaired cholesterol efflux from macrophages [71].

Unfortunately, these genetic models for disturbed circadian rhythms are not readily translatable to humans. Alternatively, light exposure changes can modulate the biological clock output without inducing genetic defects. In mice, constant light exposure induces a fast increase in weight gain, independent of physical activity and food intake. Instead, constant light exposure lowers total energy expenditure [86-88]. Mechanistically, constant light dampens the circadian electrical output of the SCN [86] and it was previously shown that constant light dampens circadian glucocorticoid levels [89, 90]. In humans, an experimental study showed that 2 hours of blue light exposure in the evening changes energy expenditure the following morning. This indicates that light exposure, presumably via the SCN, can causally influence metabolism in humans [91].

OUTLINE OF THIS THESIS

The overall aim of this thesis is to investigate the role of circadian rhythm in metabolism, specifically involving lipid metabolism and its implications for metabolic disease.

Part I describes animal models of circadian rhythms with particular focus on the role of BAT. Since light exposure has been associated to increased body weight and BMI in humans, we set out to investigate how light exposure affects metabolism. In **chapter 2** we investigated the effect of prolonged light exposure on body composition and evaluated underlying mechanisms to show that prolonged light dampens BAT activity. In **chapter 3**, we included both shortened and prolonged light exposure as modulators of the biological clock, and investigated diurnal rhythms in BAT activity and their consequences for plasma lipid metabolism. Next, we set out to further elucidate the mechanism by which the biological clock regulates BAT rhythmicity. We focused on the role of the HPA-axis by evaluating the effect of a dampened glucocorticoid rhythm on BAT rhythmicity in **chapter 4**. Since light exposure can alter metabolism, at least via BAT activity, we hypothesized that rotating light schedules may also underlie the association between shift work and atherosclerotic disease. In **chapter 5** we, therefore, investigated the effect of light schedules on atherosclerosis development.

Part 2 focuses on human models for circadian rhythms. A common human disturbance of physiological day-night rhythms is shortened sleep duration. Previously, it was found that one night of short sleep increases insulin resistance. In **chapter 6**, we aimed to better understand the underlying mechanism for this finding by performing metabolomic analysis on plasma. Another human condition associated with deterioration of circadian rhythms is aging. We made use of this fact to better understand whether circadian rhythms in cholesterol levels are affected by the biological clock and may relate to human health. In **chapter 7** we, therefore, determined diurnal plasma cholesterol concentrations in a cohort of individuals with a familial predisposition for longevity and their spouses.

The results and implications of these studies are discussed in **chapter 8**.

REFERENCES

1. Alwan, A., *Global status report on noncommunicable diseases 2010*. 2011: World Health Organization.
2. raham, I., *et al.*, *Dyslipidemias in the prevention of cardiovascular disease: risks and causality.* Curr. Cardiol. Rep, 2012. **14**(6): p. 709-720.
3. aylor, F., *et al.*, *Statins for the primary prevention of cardiovascular disease.* Cochrane. Database. Syst. Rev, 2013. **1**: p. CD004816.
4. oung, M.E. and M.S. Bray, *Potential role for peripheral circadian clock dyssynchrony in the pathogenesis of cardiovascular dysfunction.* Sleep Med, 2007. **8**(6): p. 656-667.
5. squirol, Y., *et al.*, *Shift work and cardiovascular risk factors: new knowledge from the past decade.* Arch Cardiovasc Dis, 2011. **104**(12): p. 636-68.
6. appuccio, F.P., *et al.*, *Sleep duration and all-cause mortality: a systematic review and meta-analysis of prospective studies.* Sleep, 2010. **33**(5): p. 585-592.
7. cFadden, E., *et al.*, *The Relationship Between Obesity and Exposure to Light at Night: Cross-Sectional Analyses of Over 100,000 Women in the Breakthrough Generations Study.* Am. J Epidemiol, 2014.
8. ybnikova, N.A., A. Haim, and B.A. Portnov, *Does artificial light-at-night exposure contribute to the worldwide obesity pandemic?* Int J Obes. (Lond), 2016.
9. attinson, C.L., *et al.*, *Environmental Light Exposure Is Associated with Increased Body Mass in Children.* PLoS One, 2016. **11**(1): p. e0143578.
10. insberg, H.N., *Lipoprotein physiology.* Endocrinol Metab Clin North Am, 1998. **27**(3): p. 503-19.
11. Kindel, T., D.M. Lee, and P. Tso, *The mechanism of the formation and secretion of chylomicrons.* Atheroscler Suppl, 2010. **11**(1): p. 11-6.
12. Mansbach, C.M., 2nd and F. Gorelick, *Development and physiological regulation of intestinal lipid absorption. II. Dietary lipid absorption, complex lipid synthesis, and the intracellular packaging and secretion of chylomicrons.* Am J Physiol Gastrointest Liver Physiol, 2007. **293**(4): p. G645-50.
13. Black, D.D., *Development and physiological regulation of intestinal lipid absorption. I. Development of intestinal lipid absorption: cellular events in chylomicron assembly and secretion.* Am J Physiol Gastrointest Liver Physiol, 2007. **293**(3): p. G519-24.
14. Merkel, M., R.H. Eckel, and I.J. Goldberg, *Lipoprotein lipase: genetics, lipid uptake, and regulation.* J Lipid Res, 2002. **43**(12): p. 1997-2006.
15. Mahley, R.W., *et al.*, *Chylomicron remnant metabolism. Role of hepatic lipoprotein receptors in mediating uptake.* Arteriosclerosis, 1989. **9**(1 Suppl): p. I14-8.
16. Lusis, A.J., *Atherosclerosis.* Nature, 2000. **407**(6801): p. 233-241.
17. Favari, E., *et al.*, *Cholesterol efflux and reverse cholesterol transport.* Handb Exp Pharmacol, 2015. **224**: p. 181-206.
18. Organization, W.H. *Factsheet obesity and overweight*. June 2016; Available from: http://www.who.int/mediacentre/factsheets/fs311/en.
19. Eckel, R.H., S.M. Grundy, and P.Z. Zimmet, *The metabolic syndrome.* Lancet, 2005. **365**(9468): p. 1415-1428.
20. Reilly, J.J., *et al.*, *Health consequences of obesity.* Archives of Disease in Childhood, 2003. **88**(9): p. 748-752.
21. DeFronzo, R.A. and E. Ferrannini, *Insulin resistance. A multifaceted syndrome responsible for NIDDM, obesity, hypertension, dyslipidemia, and atherosclerotic cardiovascular disease.* Diabetes Care, 1991. **14**(3): p. 173-94.
22. Cannon, B. and J. Nedergaard, *Brown adipose tissue: function and physiological significance.* Physiol Rev, 2004. **84**(1): p. 277-359.
23. Hoeke, G., *et al.*, *Role of Brown Fat in Lipoprotein Metabolism and Atherosclerosis.* Circ. Res, 2016.

118(1): p. 173-182.

24. Berbee, J.F., *et al.*, *Brown fat activation reduces hypercholesterolaemia and protects from atherosclerosis development.* Nat Commun, 2015. **6**: p. 6356.
25. Bartelt, A., *et al.*, *Brown adipose tissue activity controls triglyceride clearance.* Nat. Med, 2011. **17**(2): p. 200-205.
26. van Dam, A.D., *et al.*, *Salsalate activates brown adipose tissue in mice.* Diabetes, 2015. **64**(5): p. 1544-1554.
27. Yoneshiro, T., *et al.*, *Recruited brown adipose tissue as an antiobesity agent in humans.* J Clin Invest, 2013. **123**(8): p. 3404-3408.
28. Hanssen, M.J., *et al.*, *Short-term cold acclimation improves insulin sensitivity in patients with type 2 diabetes mellitus.* Nat Med, 2015. **21**(8): p. 863-5.
29. Bakker, L.E., *et al.*, *Brown adipose tissue volume in healthy lean south Asian adults compared with white Caucasians: a prospective, case-controlled observational study.* Lancet Diabetes Endocrinol, 2014. **2**(3): p. 210-217.
30. Lidell, M.E., M.J. Betz, and S. Enerback, *Brown adipose tissue and its therapeutic potential.* J Intern Med, 2014. **276**(4): p. 364-77.
31. Paranjpe, D.A. and V.K. Sharma, *Evolution of temporal order in living organisms.* J Circadian Rhythms, 2005. **3**(1): p. 7.
32. Reppert, S.M. and D.R. Weaver, *Coordination of circadian timing in mammals.* Nature, 2002. **418**(6901): p. 935-941.
33. Welsh, D.K., *et al.*, *Individual neurons dissociated from rat suprachiasmatic nucleus express independently phase circadian firing rhythms.* Neuron, 1995. **14**: p. 697-706.
34. Welsh, D.K., J.S. Takahashi, and S.A. Kay, *Suprachiasmatic nucleus: cell autonomy and network properties.* Annu Rev Physiol, 2010. **72**: p. 551-77.
35. Reghunandanan, V. and R. Reghunandanan, *Neurotransmitters of the suprachiasmatic nuclei.* J Circadian Rhythms, 2006. **4**: p. 2.
36. Mrosovsky, N., *Locomotor activity and non-photic influences on circadian clocks.* Biol Rev Camb Philos Soc, 1996. **71**(3): p. 343-72.
37. Morin, L.P., *Neuroanatomy of the extended circadian rhythm system.* Exp. Neurol, 2013. **243**: p. 4-20.
38. Buijs, R.M., *et al.*, *Parasympathetic and sympathetic control of the pancreas: a role for the suprachiasmatic nucleus and other hypothalamic centers that are involved in the regulation of food intake.* J Comp Neurol, 2001. **431**(4): p. 405-23.
39. Kreier, F., *et al.*, *Tracing from fat tissue, liver, and pancreas: a neuroanatomical framework for the role of the brain in type 2 diabetes.* Endocrinology, 2006. **147**(3): p. 1140-7.
40. Bartness, T.J., C.K. Song, and G.E. Demas, *SCN efferents to peripheral tissues: implications for biological rhythms.* J. Biol. Rhythms, 2001. **16**: p. 196-204.
41. Akhtar, R.A., *et al.*, *Circadian cycling of the mouse liver transcriptome, as revealed by cDNA microarray, is driven by the suprachiasmatic nucleus.* Curr. Biol, 2002. **12**(7): p. 540-550.
42. McCarthy, J.J., *et al.*, *Identification of the circadian transcriptome in adult mouse skeletal muscle.* Physiol Genomics, 2007. **31**(1): p. 86-95.
43. Koike, N., *et al.*, *Transcriptional architecture and chromatin landscape of the core circadian clock in mammals.* Science, 2012. **338**(6105): p. 349-354.
44. Reddy, A.B., *et al.*, *Circadian orchestration of the hepatic proteome.* Curr Biol, 2006. **16**(11): p. 1107-15.
45. Mohawk, J.A., C.B. Green, and J.S. Takahashi, *Central and peripheral circadian clocks in mammals.* Annu. Rev. Neurosci, 2012. **35**: p. 445-462.
46. Zhang, J., *et al.*, *Molecular signals of Mammalian circadian clock.* Kobe J Med Sci, 2004. **50**(3-4): p. 101-9.

47. Kalsbeek, A., *et al., SCN outputs and the hypothalamic balance of life.* J. Biol. Rhythms, 2006. **21**(6): p. 458-469.
48. Patton, D.F. and R.E. Mistlberger, *Circadian adaptations to meal timing: neuroendocrine mechanisms.* Frontiers in Neuroscience, 2013. **7**: p. 185.
49. Balsalobre, A., *Resetting of circadian time in peripheral tissues by glucocorticoid signaling.* Science, 2000. **289**: p. 2344-2347.
50. Reddy, A.B., *et al., Glucocorticoid signaling synchronizes the liver circadian transcriptome.* Hepatology, 2007. **45**(6): p. 1478-88.
51. Pezuk, P., *et al., Glucocorticoids as entraining signals for peripheral circadian oscillators.* Endocrinology, 2012. **153**(10): p. 4775-83.
52. Cuesta, M., N. Cermakian, and D.B. Boivin, *Glucocorticoids entrain molecular clock components in human peripheral cells.* Faseb j, 2015. **29**(4): p. 1360-70.
53. Koch, C.E., *et al., Interaction between circadian rhythms and stress.* Neurobiol Stress, 2017. **6**: p. 57-67.
54. Herman, J.P., *et al., Regulation of the Hypothalamic-Pituitary-Adrenocortical Stress Response.* Compr Physiol, 2016. **6**(2): p. 603-21.
55. Porkka-Heiskanen, T., *Sleep homeostasis.* Curr Opin Neurobiol, 2013. **23**(5): p. 799-805.
56. Schwartz, J.R.L. and T. Roth, *Neurophysiology of Sleep and Wakefulness: Basic Science and Clinical Implications.* Current Neuropharmacology, 2008. **6**(4): p. 367-378.
57. Ford, E.S., T.J. Cunningham, and J.B. Croft, *Trends in Self-Reported Sleep Duration among US Adults from 1985 to 2012.* Sleep, 2015. **38**(5): p. 829-32.
58. Cappuccio, F.P., *et al., Quantity and quality of sleep and incidence of type 2 diabetes: a systematic review and meta-analysis.* Diabetes Care, 2010. **33**(2): p. 414-420.
59. Gallicchio, L. and B. Kalesan, *Sleep duration and mortality: a systematic review and meta-analysis.* J. Sleep Res, 2009. **18**(2): p. 148-158.
60. Killick, R., S. Banks, and P.Y. Liu, *Implications of sleep restriction and recovery on metabolic outcomes.* J. Clin. Endocrinol. Metab, 2012. **97**(11): p. 3876-3890.
61. Liu, Y., *et al., Sleep duration and chronic diseases among U.S. adults age 45 years and older: evidence from the 2010 Behavioral Risk Factor Surveillance System.* Sleep, 2013. **36**(10): p. 1421-7.
62. Ohkuma, T., *et al., Impact of sleep duration on obesity and the glycemic level in patients with type 2 diabetes: the Fukuoka Diabetes Registry.* Diabetes Care, 2013. **36**(3): p. 611-7.
63. Altman, N.G., *et al., Sleep duration versus sleep insufficiency as predictors of cardiometabolic health outcomes.* Sleep Med, 2012. **13**(10): p. 1261-70.
64. Yetish, G., *et al., Natural Sleep and Its Seasonal Variations in Three Pre-industrial Societies.* Current Biology. **25**(21): p. 2862-2868.
65. Wright, K.P., Jr., *et al., Entrainment of the human circadian clock to the natural light-dark cycle.* Curr Biol, 2013. **23**(16): p. 1554-8.
66. Mirani-Oostdijk, C.P., *et al., Diurnal changes in serum triglycerides as related to changes in lipolytic enzymes, (apo) lipoproteins and hormones in normal subjects on a carbohydrate-rich diet.* Eur J Clin Invest, 1983. **13**(4): p. 301-9.
67. Rivera-Coll, A., X. Fuentes-Arderiu, and A. Diez-Noguera, *Circadian rhythmic variations in serum concentrations of clinically important lipids.* Clin. Chem, 1994. **40**(8): p. 1549-1553.
68. van Wijk, J.P., A.J. van Oostrom, and C.M. Castro, *Normal ranges of non-fasting triglycerides in healthy Dutch males and females.* Clin Chim. Acta, 2003. **337**(1-2): p. 49-57.
69. Klop, B., *et al., Daytime triglyceride variability in men and women with different levels of triglyceridemia.* Clin Chim. Acta, 2011. **412**(23-24): p. 2183-2189.
70. Hoogerwerf, W.A., *et al., Clock gene expression in the murine gastrointestinal tract: endogenous rhythmicity and effects of a feeding regimen.*

Gastroenterology, 2007. **133**(4): p. 1250-1260.

71. Pan, X., X.C. Jiang, and M.M. Hussain, *Impaired Cholesterol Metabolism and Enhanced Atherosclerosis in Clock Mutant Mice.* Circulation, 2013.
72. Singh, R., *et al.*, *Circadian Time Structure of Circulating Plasma Lipid Components in Healthy Indians of Different Age Groups.* Indian Journal of Clinical Biochemistry, 2016. **31**(2): p. 215-223.
73. Miettinen, T.A., *Diurnal variation of cholesterol precursors squalene and methyl sterols in human plasma lipoproteins.* J Lipid Res, 1982. **23**(3): p. 466-73.
74. Chua, E.C., *et al.*, *Extensive diversity in circadian regulation of plasma lipids and evidence for different circadian metabolic phenotypes in humans.* Proc. Natl Acad. Sci. U. S. A, 2013. **110**(35): p. 14468-14473.
75. Dallmann, R., *et al.*, *The human circadian metabolome.* Proceedings of the National Academy of Sciences, 2012. **109**(7): p. 2625-2629.
76. Adamovich, Y., *et al.*, *Circadian clocks and feeding time regulate the oscillations and levels of hepatic triglycerides.* Cell Metab, 2014. **19**(2): p. 319-30.
77. Davidson, A.J., O. Castanon-Cervantes, and F.K. Stephan, *Daily oscillations in liver function: diurnal vs circadian rhythmicity.* Liver Int, 2004. **24**(3): p. 179-86.
78. Coomans, C.P., *et al.*, *The suprachiasmatic nucleus controls circadian energy metabolism and hepatic insulin sensitivity.* Diabetes, 2013. **62**(4): p. 1102-1108.
79. Turek, F.W., *et al.*, *Obesity and metabolic syndrome in circadian Clock mutant mice.* Science, 2005. **308**(5724): p. 1043-1045.
80. Shimba, S., *et al.*, *Deficient of a clock gene, brain and muscle Arnt-like protein-1 (BMAL1), induces dyslipidemia and ectopic fat formation.* PLoS. One, 2011. **6**(9): p. e25231.
81. Shi, S.Q., *et al.*, *Circadian disruption leads to insulin resistance and obesity.* Curr. Biol, 2013. **23**(5): p. 372-381.
82. Rudic, R.D., *et al.*, *BMAL1 and CLOCK, two essential components of the circadian clock, are involved in glucose homeostasis.* PLoS Biol, 2004. **2**(11): p. 377.
83. Maury, E., H.K. Hong, and J. Bass, *Circadian disruption in the pathogenesis of metabolic syndrome.* Diabetes Metab, 2014. **40**(5): p. 338-46.
84. Paschos, G.K., *et al.*, *Obesity in mice with adipocyte-specific deletion of clock component Arntl.* Nat. Med, 2012. **18**(12): p. 1768-1777.
85. Ma, H., *et al.*, *Increased Atherosclerotic Lesions in LDL Receptor Deficient Mice With Hematopoietic Nuclear Receptor Rev-erbalpha Knock- Down.* J. Am. Heart Assoc, 2013. **2**(4): p. e000235.
86. Coomans, C.P., *et al.*, *Detrimental effects of constant light exposure and high-fat diet on circadian energy metabolism and insulin sensitivity.* FASEB J, 2013. **27**(4): p. 1721-1732.
87. Fonken, L.K., *et al.*, *Dim light at night disrupts molecular circadian rhythms and increases body weight.* J. Biol. Rhythms, 2013. **28**(4): p. 262-271.
88. Fonken, L.K., *et al.*, *Light at night increases body mass by shifting the time of food intake.* Proc. Natl. Acad. Sci. U. S. A, 2010. **107**(43): p. 18664-18669.
89. Park, S.Y., *et al.*, *Constant light disrupts the circadian rhythm of steroidogenic proteins in the rat adrenal gland.* Mol Cell Endocrinol, 2013. **371**(1-2): p. 114-23.
90. Waite, E.J., *et al.*, *Ultradian corticosterone secretion is maintained in the absence of circadian cues.* Eur J Neurosci, 2012. **36**(8): p. 3142-50.
91. Kayaba, M., *et al.*, *The effect of nocturnal blue light exposure from light-emitting diodes on wakefulness and energy metabolism the following morning.* Environ Health Prev Med, 2014. **19**(5): p. 354-61.

PART I

Circadian rhythms in animal models: regulation of brown fat activity and consequences for metabolic disease

Chapter 2

Prolonged daily light exposure increases body fat mass through attenuation of brown adipose tissue activity

Rosa van den Berg, Sander Kooijman*, Ashna Ramkisoensing, Mariëtte R. Boon, Eline N. Kuipers, Marieke Loef, Tom C.M. Zonneveld, Eliane A. Lucassen, Hetty C.M. Sips, Iliana A. Chatzispyrou, Riekelt H. Houtkooper, Johanna H. Meijer, Claudia P. Coomans, Nienke R. Biermasz*, Patrick C.N. Rensen**

Proc Natl Acad Sci USA 2015; 112: 6748-53

**Authors contributed equally*

ABSTRACT

Disruption of circadian rhythmicity is associated with obesity and related disorders including type 2 diabetes and cardiovascular disease. Specifically, prolonged artificial light exposure associates with obesity in humans, although the underlying mechanism is unclear. Here, we report that increasing the daily hours of light exposure increases body adiposity through attenuation of brown adipose tissue (BAT) activity, a major contributor of energy expenditure. Mice exposed to a prolonged day length of 16 h and 24 h light, compared to regular 12 h light, showed increased adiposity without affecting food intake or locomotor activity. Mechanistically, we demonstrated that prolonged day length decreases sympathetic input into BAT and reduces β3-adrenergic intracellular signaling. Concomitantly, prolonging day length decreased the uptake of fatty acids from triglyceride-rich lipoproteins as well as of glucose from plasma selectively by BAT. We conclude that impaired BAT activity is an important mediator in the association between disturbed circadian rhythm and adiposity and anticipate that activation of BAT may overcome the adverse metabolic consequences of disturbed circadian rhythmicity.

INTRODUCTION

Modern world society is subjected to disturbances of circadian rhythms by shift work, sleep deprivation and environmental light pollution. Importantly, increasing prevalence of obesity is associated with disrupted sleep-wake pattern in humans [1] and coincides with the availability of artificial light [2, 3]. Additionally, a recent study revealed a relationship between exposure to light at night and obesity in a cross-sectional analysis of over 100,000 women [4]. Light input is the most important cue for generation of circadian (~24 h) rhythms by the master clock. Both in rodents and humans the master clock is situated in the suprachiasmatic nucleus (SCN) of the hypothalamus. The SCN is responsible for synchronization of peripheral clocks throughout the body, which is mediated by endocrine and neuronal signals [5]. A causal role for a disturbed circadian rhythm in the development of obesity has been demonstrated by animal studies. Mice with genetically dysfunctional clock genes develop obesity and insulin resistance [6-9]. Moreover, specific ablation of the SCN induces acute weight gain [10]. These results indicate a crucial role for the SCN in the regulation of adiposity.

Interestingly, we previously showed that prolonged light exposure only is sufficient to enhance weight gain in mice. Constant light disrupts the central circadian clock, evidenced by an immediate reduction in the circadian amplitude of SCN electrical activity. Moreover, constant light induces body weight gain and insulin resistance, even faster than high-fat diet, which was not due to increased food intake or reduced locomotor activity [11]. Therefore, disruption of the central biological clock likely induces weight gain by decreasing energy expenditure.

Recently, it has been recognized that brown adipose tissue (BAT) importantly contributes to energy expenditure. BAT combusts high amounts of triglycerides (TG) into heat, a process called thermogenesis that is mediated by uncoupling protein 1 (UCP1). Interestingly, SCN neurons project onto BAT and injection of glutamate into the SCN increases BAT thermogenesis in rats [12, 13]. This indicates that BAT may mediate the association between circadian rhythmicity and energy expenditure. Therefore, the aim of this study was to shed light on the association between prolonged light exposure and obesity in humans by investigating the effect of day length on BAT activity in mice in relation to body fat gain, independent of ambient temperature. We demonstrate that daily light exposure negatively associates with the uptake of TG-derived fatty acids and glucose from plasma by BAT, pointing to decreased activity of the tissue. Furthermore, we show that increasing daily light exposure decreases BAT activity through reduced sympathetic stimulation.

MATERIALS AND METHODS

Animal study

All animal experiments were approved by the institutional ethics committee on animal care and experimentation at Leiden University Medical Center (LUMC), Leiden, The Netherlands. 9-12 week old male C57Bl/6J mice (Charles River) were single housed in clear plastic cages within light-tight cabinets at constant room temperature of 22°C. Stable temperature inside the light-tight cabinets was verified in 12 h vs. 24 h light conditions. The cages were illuminated with white fluorescent light with an intensity of approximately 85 µW/cm^2. Before start of the experiment, mice were kept on a regular 12:12 light-dark cycle. Mice had ad libitum access to standard laboratory chow (Special Diets Services, UK) and water throughout experiments. Mice were matched on body weight and light intervention consisted of subjecting mice to either 12, 16 or 24 h light exposure per day (i.e. 24 h) for the duration of five weeks (n= 9).

In a second study, mice were randomized to either bilateral selective sympathetic denervation (n=17) of iBAT or sham surgery (n=6). Mice were anesthetized (isofluorane inhalation) and a midline incision of the skin was made, exposing both iBAT pads. Sympathetic branches were visualized and cut on both sides. Wounds were closed and mice received post-operative analgesia (0.03 mg/kg buprenorphine, Temgesic, Merck). Successful denervation was confirmed retrospectively by absence of TH in iBAT sections (see below). After four days of recovery, mice that underwent denervation were randomized based on body weight and exposed to 12, 16, or 24 h light per day for five weeks while sham operated mice were exposed to 12 h light per day and served as a reference group.

Body composition, food intake and locomotor activity

At the end of the experiment, body weight was measured and body composition (i.e., lean mass and fat mass) was determined in conscious mice using an EchoMRI-100 (EchoMRI, Houston, Texas). Food intake was monitored by weighing food on lids either during last two weeks of light intervention or throughout the five weeks of light exposure (denervation experiment). Behavioural activity of mice was assessed with passive infrared detectors and recorded using Actimetrics software (Wilmette, IL, USA).

TG and glucose clearance

At the end of the experiments, the clearance of TG and glucose was assessed. Glycerol tri[^{3}H] oleate ([^{3}H]TO) labeled VLDL-like emulsion particles (80 nm) were prepared as previously described [14] and [^{14}C]deoxyglucose ([^{14}C]DG) was added (ratio ^{3}H:^{14}C = 6:1). After 5 weeks of light intervention, mice were fasted for 4 h (9AM to 1PM clock time, corresponding to Zeitgeber time (ZT) 2-6 for 12 h group and ZT 4-8 for 16 h group) and intravenously injected with the radiolabeled emulsion particles (1.0 mg TG in 200 µL PBS) and glucose via the tail vein. At time points t=2, 5, 10 and 15 min after injection, blood was taken from the tail vein to determine the serum decay of both radiolabels. Immediately after the last blood withdrawal, mice were euthanized by cervical dislocation and perfused with ice-cold PBS

for 5 min. Organs were harvested, weighed, and the uptake of ^{3}H and ^{14}C radioactivity was determined.

Histology

Formalin-fixed paraffin-embedded iBAT and gWAT sections were cut (5 µm). To determine gWAT cell size, sections were stained with Mayer's haematoxylin and eosin. White adipocyte size was quantified using ImageJ software. To determine sympathetic activation of iBAT a TH staining was performed. Sections were rehydrated and incubated 15 min with 10 mM citrate buffer (pH 6.0) at 120°C for antigen retrieval. Sections were blocked with 5% BSA/PBS followed by overnight incubation with anti-TH antibody (1:2000, AB-112, Abcam) at 4°C. Next, sections were incubated with a secondary antibody (anti-rabbit antibody, DAKO enVision), stained with Nova Red and counterstained with Mayer's haematoxylin. Percentage of area positive for TH staining was quantified using Image J software.

Gene expression analysis and mitochondrial assays

A part of iBAT and sBAT was snap frozen and stored at -80°C for gene expression analysis and protein analysis (see below). Total RNA was isolated using TriPure (Roche) according to the manufacturer's instructions. 1 µg of total RNA was reverse-transcribed using M-MLV reverse transcriptase (Promega, Madison, WI, USA). Real-time PCR was carried out on a CFX96 PCR machine (Bio-Rad) using IQ SYBR-Green Supermix (Bio-Rad). Expression levels were normalized to 36B4 as housekeeping gene. Expression of mitochondrial genes was measured with quantitative PCR on a Roche Lightcycler 480 using Roche SYBR-green mastermix, using mitochondrial specific primers (Table S1). Mitochondrial DNA (mtDNA) abundance was quantified as described before [15]. In short, total DNA was extracted from sBAT tissue, using the QIAamp DSP DNA Mini Kit (Qiagen). Citrate synthase activity was measured in sBAT tissue as described before [16].

Western blot analysis

The iBAT samples stored at -80°C were homogenized in lysis buffer. Samples were diluted and denatured for 5 min at 95°C after adding Laemmli Sample Buffer (1:1, vol/vol; Serva, Heidelberg, Germany). Proteins within homogenates (15 µg) were separated on a 10% SDS-page gel and subsequently transferred onto blotting membranes. The blotting membranes were blocked with 5% milk powder and incubated overnight at 4°C with the primary antibody β-actin, pCREB, pAMPK or pHSL S565 (Cell Signaling). Secondary antibody (anti-rabbit IgG HRP conjugate; 1:5000; Promega, Madison, WI, USA) was added and SuperSignal Western Blot Enhancer (Thermo Scientific, Rockford, IL, USA) was used to visualize protein bands. Blots were analysed with Bio-Rad Quantity One and normalized to β-actin.

Statistical analysis

Data are presented as means ± SEM. Correlations between two dependent variables were made using Pearson's correlation. Associations of variables with day length were assessed by linear regression analysis. Differences between groups were determined

using T-tests for normally distributed data. Contribution of light exposure as a covariate to body weight gain was analysed by mixed model analysis using IBM SPSS Statistics version 20. To assess behavioural activity, actograms were analysed using Clock lab and rhythmicity F periodogram analysis was performed on activity bins of 10 minutes of the last 10 consecutively recorded days, based on the algorithm of Dörrscheidt and Beck [17]. Differences at P values < 0.05 were considered statistically significant.

RESULTS

Entrainment to light schedules

Male 12 week old C57Bl/6J mice, fed ad libitum a regular chow diet, were exposed to daily light exposure of either 12 h, 16 h or to 24 h during 5 weeks at a constant ambient temperature of 22°C. During the last 2 weeks of light intervention, circadian rhythm in behavioural activity was assessed in their home cages. As compared to a day length of 12 h (Supplemental Figure 1A), mice exposed to a day length of 16 h showed a retained circadian (24 h) rhythm in behavioural activity, with high activity during night-time (Supplemental Figure 1B). In contrast, circadian rhythmicity of behavioural activity was largely reduced in mice exposed to constant light (Supplemental Figure 1c).

Prolonged daily light exposure increases adiposity without increasing food intake

After 5 weeks of light intervention, body weight was determined and body composition was assessed by EchoMRI. Prolonged light exposure did not significantly increase total body weight (Figure 1a) or lean mass (Figure 1b). Interestingly, we observed a daily light exposure-dependent increase in fat mass which reached significance for 24 h versus 12 h exposure (+57%; p=0.01; Figure 1c). In fact, duration of light exposure positively correlated with the body fat mass (β=0.053; r^2=0.21; p=0.02) (Figure 1d). Mixed model analysis of weekly body weight development showed that light exposure significantly contributed to weight gain (p=0.028). After 5 weeks of light intervention, mice were sacrificed after a kinetic experiment with radioactive tracers (see below), and gonadal white adipose tissue (gWAT) was quantitatively weighed and examined histologically. A positive correlation was found between light exposure duration and gWAT weight (β=0.005; r^2=0.20; p=0.02) (Figure 1e) as well as average adipocyte size (β=0.08; r^2=0.20; p=0.04) (Figure 1f, g). The gWAT weight and adipocyte size were significantly increased in mice exposed to 24 h light compared to 12 h (+21%; p=0.02 and +21%; p=0.04, respectively). Notably, food intake was not different in mice exposed to 16 h light, and even tended to be reduced in mice continuously exposed to light (-13%; p=0.08) compared to mice exposed to 12 h light per day, (Figure 1h). Therefore, the positive correlation between day length and adiposity is not explained by hyperphagia, consistent with our previous observations that exposure of mice to constant light decreases energy expenditure rather than increasing food intake [11].

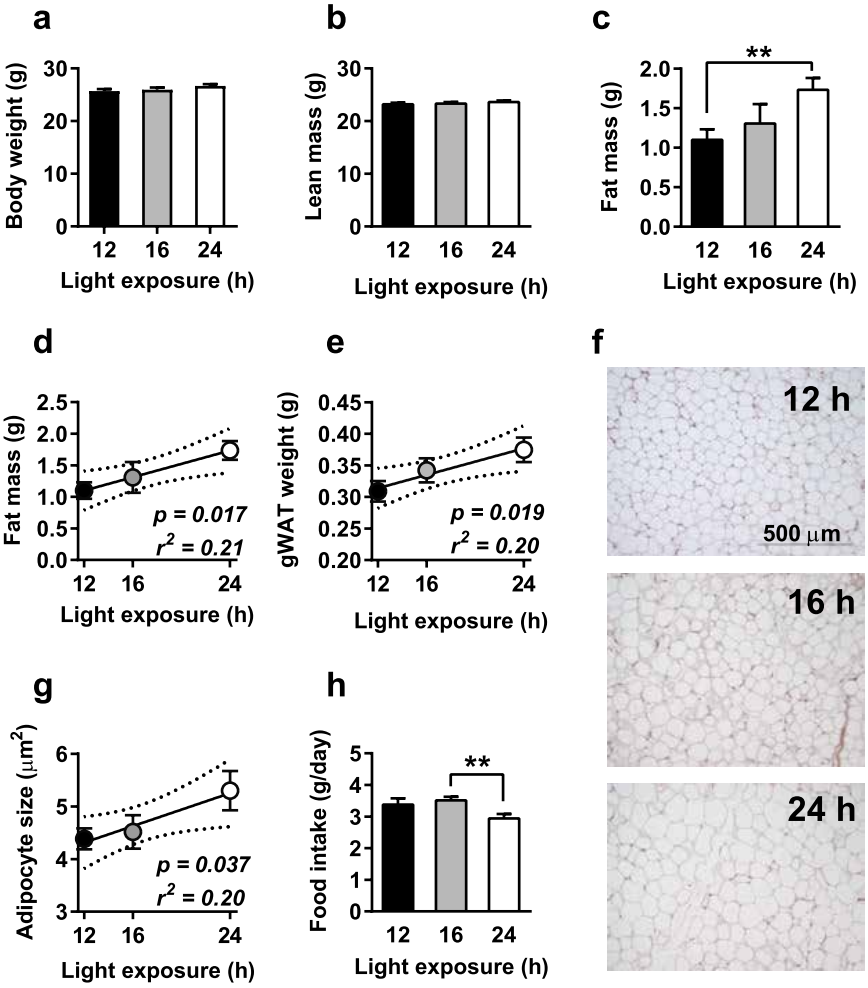

Figure 1: Mice were exposed to either 12, 16 or 24 h light (n = 9) for 5 weeks, and body weight (a), lean mass (b) and fat mass (c) were determined. *Correlations are depicted between the light exposure period and total fat mass (d), gWAT weight (e) and adipocyte size in gWAT (g). Representative images of gWAT stained with haematoxylin and eosin are shown (f). Food intake of the last two weeks of light intervention was measured (h). Data are presented as means ± SEM. Dotted lines represent 95% confidence interval of the regression line. **p<0.01.*

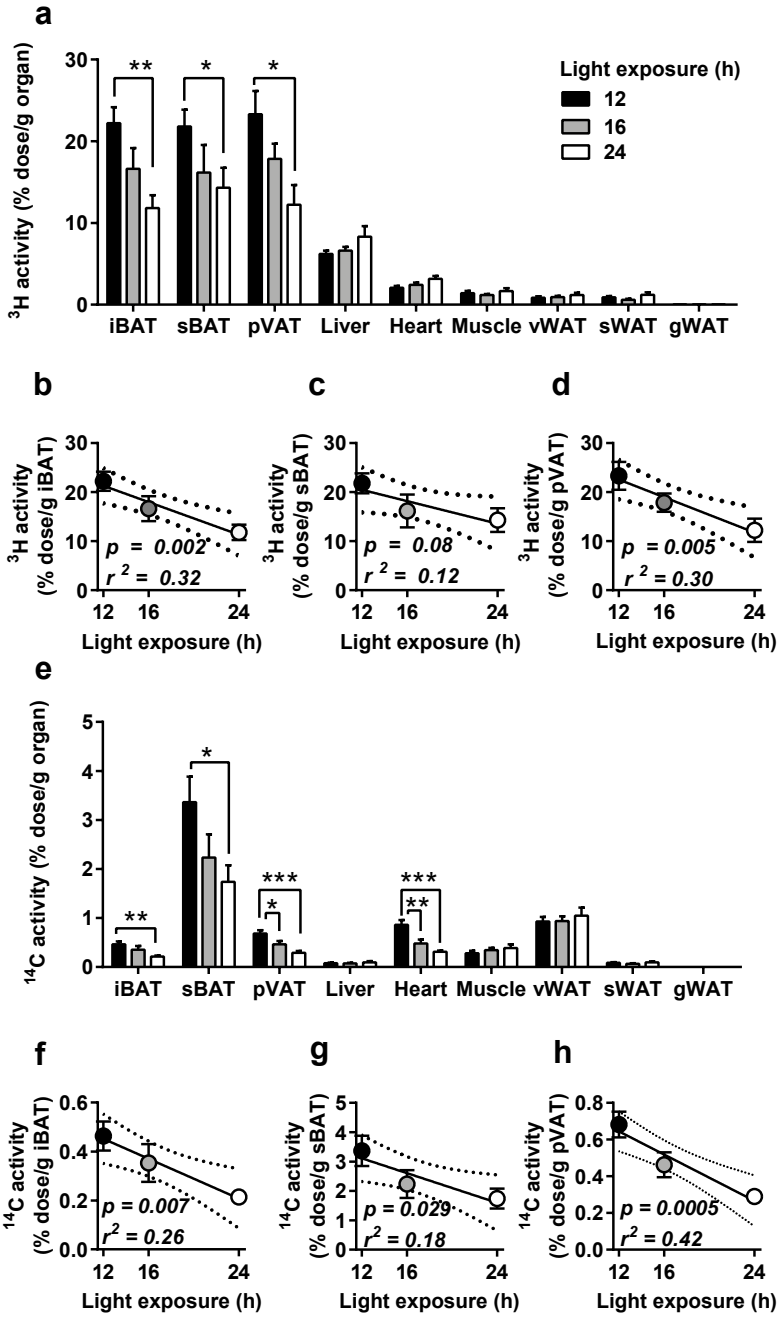
a
^{3}H activity (% dose/g organ)
Light exposure (h)
12
16
24
iBAT sBAT pVAT Liver Heart Muscle vWAT sWAT gWAT
b
^{3}H activity (% dose/g iBAT)
p = 0.002
r 2 = 0.32
c
^{3}H activity (% dose/g sBAT)
p = 0.08
r 2 = 0.12
d
^{3}H activity (% dose/g pVAT)
p = 0.005
r 2 = 0.30
Light exposure (h)
e
^{14}C activity (% dose/g organ)
iBAT sBAT pVAT Liver Heart Muscle vWAT sWAT gWAT
f
^{14}C activity (% dose/g iBAT)
p = 0.007
r2 = 0.26
g
^{14}C activity (% dose/g sBAT)
p = 0.029
r2 = 0.18
h
^{14}C activity (% dose/g pVAT)
p = 0.0005
r2 = 0.42
Light exposure (h)

Prolonged daily light exposure decreases the nutrient uptake by brown adipose tissue

To investigate whether prolonged daily light exposure reduces BAT activity, consistent with decreased energy expenditure, we determined the effect of light exposure duration on the ability of BAT to take up TG-derived free fatty acids and glucose from plasma. Hereto, we assessed the kinetics of intravenously injected glycerol tri[^{3}H]oleate ([^{3}H]TO)-labeled VLDL-like emulsion particles and [^{14}C]deoxyglucose ([^{14}C]DG) and determined the distribution of radiolabels at 15 min after injection.

Prolonged daily light exposure did not substantially alter the kinetics of plasma clearance of [^{3}H]TO and [^{14}C]DG (Supplemental Figure 2a,B). In mice exposed to a 12 h light per day, the uptake of [^{3}H]TO-derived radioactivity was much higher in the various BAT depots (interscapular BAT (iBAT), subscapular BAT (sBAT), and perivascular adipose tissue (pVAT)) as compared to liver (~3.5-fold), heart (~10-fold), muscle (~15-fold) and white adipose tissue (WAT) (~25-650-fold) (Figure 2a). Interestingly, the uptake of [^{3}H]TO-derived activity by iBAT, sBAT and pVAT decreased with prolonged light exposure reaching -47% (p=0.001), -34% (p=0.03) and -48% (p=0.01) for 24 h versus 12 h light exposure (Figure 2a). Accordingly, the day length negatively associated with the uptake of [^{3}H]TO-derived activity by iBAT (β=-0.83; r^2= 0.32; p=0.002) (Figure 2b), sBAT (β=-0.58; r2= 0.12; p=0.08) (Figure 2c) and pVAT (β=-0.90; r2=0.30; p=0.005) (Figure 2d). Prolonged light exposure did not alter the uptake of [^{3}H]TO-derived radioactivity by organs other than BAT. Consistent with reduced TG-derived free fatty acid uptake by BAT, we found that prolonged light exposure associated to increased plasma free fatty acid levels (β= 0.03; r^2=0.45; p<0.001) (Supplemental Figure 2c).

Prolonged daily light exposure also decreased the uptake of [^{14}C]DG by BAT. As compared to 12 h light exposure, 24 h light exposure decreased the uptake of [^{14}C]DG by iBAT (-54%; p=0.002), sBAT (-48%; p=0.02) and pVAT (-57%; p=0.001) (Figure 2f). Additionally, 16 h of light a day significantly decreased glucose uptake in pVAT (-32%; p=0.04) compared to 12 h (Figure 2e). Similar to the uptake of [3H]TO-derived radioactivity, day length negatively associated with the uptake of glucose by iBAT (β=-0.02; r2=0.26; p=0.007) (Figure 2f), sBAT (β= -0.13; r2=0.18; p=0.03) (Figure 2g) and pVAT (β=-0.03; r2=0.42; p=0.0005) (Figure 2h).

Figure 2: (left page) Mice were exposed to either 12, 16 or 24 h light (n = 8-9) for 5 weeks, and the VLDL-TG and glucose kinetics were assessed by injection of glycerol tri[^{3}H]oleate ([^{3}H]TO)-labeled emulsion particles and [^{14}C]deoxyglucose ([^{14}C]DG). *Uptake of [^{3}H]TO-derived activity by the various organs was determined (a), and correlations were determined between light exposure and [^{3}H]TO-derived activity in iBAT (b), sBAT (c) and pVAT (d). Concomitantly, the uptake of [^{14}C]DG by the various organs was determined (e), and correlations were determined between light exposure and the uptake of [^{14}C]DG by iBAT (f), sBAT (g) and pVAT (h). Data are presented as means ±SEM. Dotted lines represent 95% confidence interval of the regression line.*p<0.05, **p<0.01, *** p<0.001. Abbreviations of organs: iBAT, interscapular BAT; sBAT, subscapular BAT; pVAT, perivascular adipose tissue; vWAT, visceral WAT; sWAT, subcutaneous WAT; gWAT, gonadal WAT.*

These data imply that prolonged daily light exposure decreases the uptake of nutrients from plasma quite specifically by the various BAT depots, indicating that prolonged daily light exposure decreases the activity of brown adipocytes.

Prolonged daily light exposure decreases intracellular adrenergic signalling in BAT

As the SCN is directly connected to BAT via the sympathetic nervous system, we reasoned that prolonged daily light exposure decreases sympathetic activation of BAT. Indeed, immunohistochemical analysis of iBAT showed that the amount of tyrosine hydroxylase (TH), the rate-limiting enzyme in the synthesis of noradrenalin tended to decrease with increasing day length, up to -42% in 24 h compared to 12 h (p=0.10) (Figure 3a,B). Additionally, the amount of TH detected in BAT correlated with the uptake of [^{3}H]TO-derived activity by BAT (r2=0.17; p=0.056) (Figure 3c) as well as with the uptake of [^{14}C]DG by BAT (r2=0.43; p=0.001) (Figure 3d).

Since activation of the β3-adrenergic receptor by noradrenalin increases intracellular levels of cyclic AMP (cAMP) which activates protein kinase A (PKA), resulting in phosphorylation of cAMP response-binding element (CREB) and activates AMP-activated protein kinase (AMPK), we next determined the phosphorylation status of these proteins involved in thermogenesis in iBAT. Phosphorylated CREB (pCREB) was decreased in 24 h light exposure compared to 12 h (-27%; p=0.009) (Figure 3e). Phosphorylated AMPK (pAMPK) was decreased in mice on a day length of 16 h (-14%; p=0.05) and 24 h (-32%; p=0.002) (Figure 3f, h) compared to 12 h of light exposure per day, independent of total AMPK levels (Supplemental Figure 3a,b). Daily light duration negatively associated with levels of both pCREB (β= -0.03, r2=0.29, p=0.006) (Figure 3e, h) and pAMPK (β= -0.04, r2=0.47, p=0.0003) (Figure 3f,h). Both pAMPK and pCREB induce phosphorylation of the lipolytic enzyme hormone-sensitive lipase (HSL). While day length did not affect PKA-mediated phosphorylation of HSL on serine 563 position (pHSL S^{563}) (Supplemental Figure 3a,c), it reduced AMPK-mediated phosphorylation of HSL on serine 565 (pHSL S^{565}). A day length of 24 h decreased pHSL S^{565} compared to a day length of 12 h (-39%; p=0.009) and day length negatively correlated with pHSL S^{565} (β= -0.04, r^2=0.33, p=0.0031) (Figure 3g, h).

Gene targets of pCREB include peroxisome proliferator-activated receptor 1α (PPARGC1α or PGC1α) that drives transcription of genes involved in mitochondrial biogenesis, and UCP1, which is essential for BAT thermogenesis. Prolonged daily light exposure (24 h vs. 12 h) decreased gene expression of *Pgc1α* (-55%; p<0.05) (Figure 3I) and tended to decrease gene expression of *Ucp1* (-37%; p=0.08) (Figure 3J). Increasing day length negatively associated with expression of *Ucp1* (β= -0.03, r^2=0.39, p=0.0005) (Figure 3j).

Next, we examined the possibility that prolonged light exposure reduces BAT thermogenic capacity by decreasing mitochondrial function. Prolonged light exposure did not affect gene expression of genes involved in mitochondrial biogenesis (*Tfam, Cox7a1, Cyc1, Atp5g1*), fatty acid oxidation enzymes (*Acadvl, Acadl, Acadm*) or mitochondrial fusion (*Mfn2*) (Supplemental Figure 4a). Additionally, the amount of mitochondrial DNA

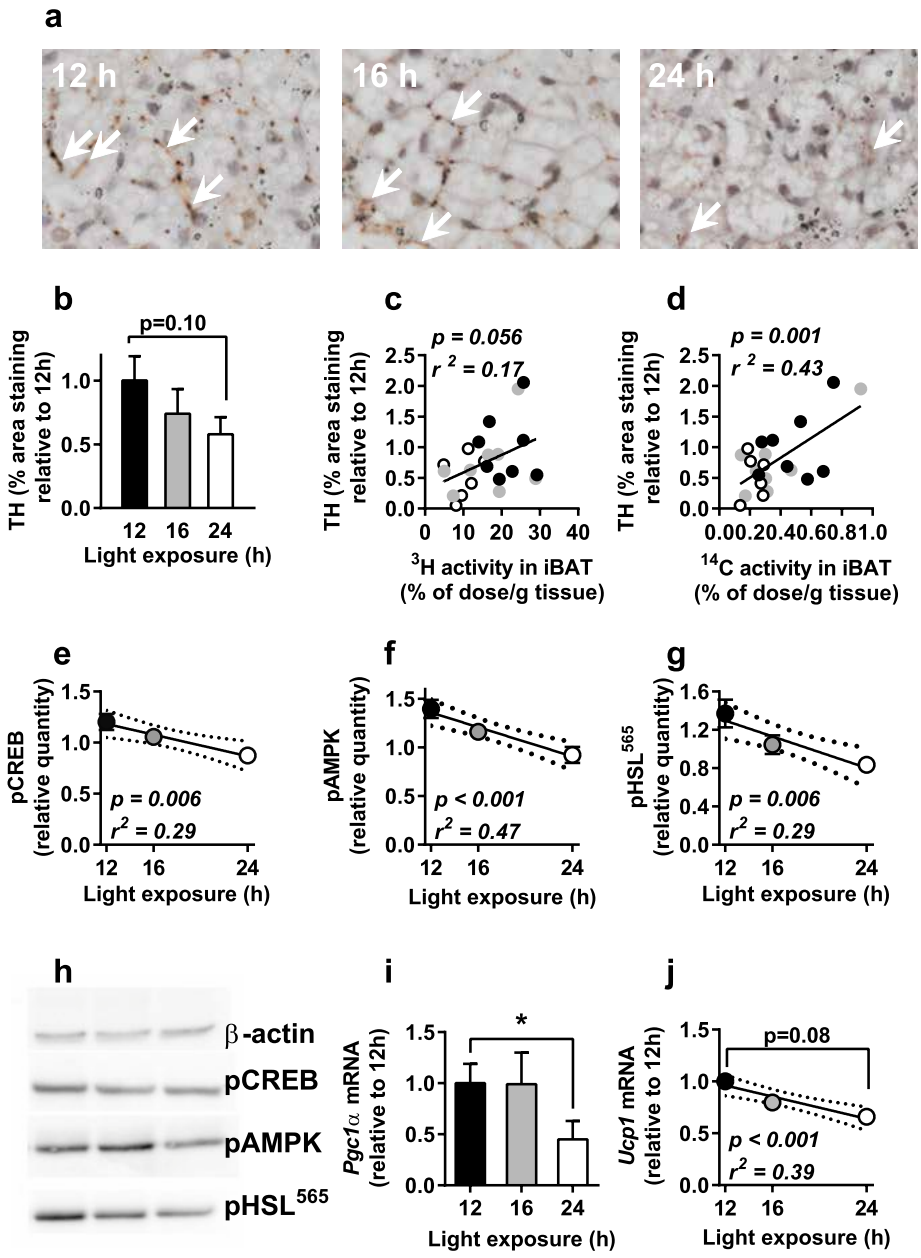

Figure 3: Mice were exposed to either 12, 16, or 24 h light (n = 9) for 5 weeks, and interscapular BAT was isolated. *Histological sections were stained for tyrosine hydroxylase (TH), representative images are shown (a; arrows indicate TH staining), and quantified (**b**). Correlation was determined between TH staining and uptake of [^{3}H]TO-derived activity (c) and [^{14}C]DG (d). Also, correlations were determined between light exposure and protein levels of pCREB (e), pAMPK (f), and pHSL S^{565} (g). Protein levels were normalized to β-actin levels. Representative blots for β-actin, pCREB, pAMPK and pHSL S^{565} are shown (h). Gene expression of Pgc1α (i) and Ucp1 (j) were determined and normalized to 36B4 expression. Data are presented as means ± SEM. Dotted lines represent 95% confidence interval of the regression line. *p<0.05.*

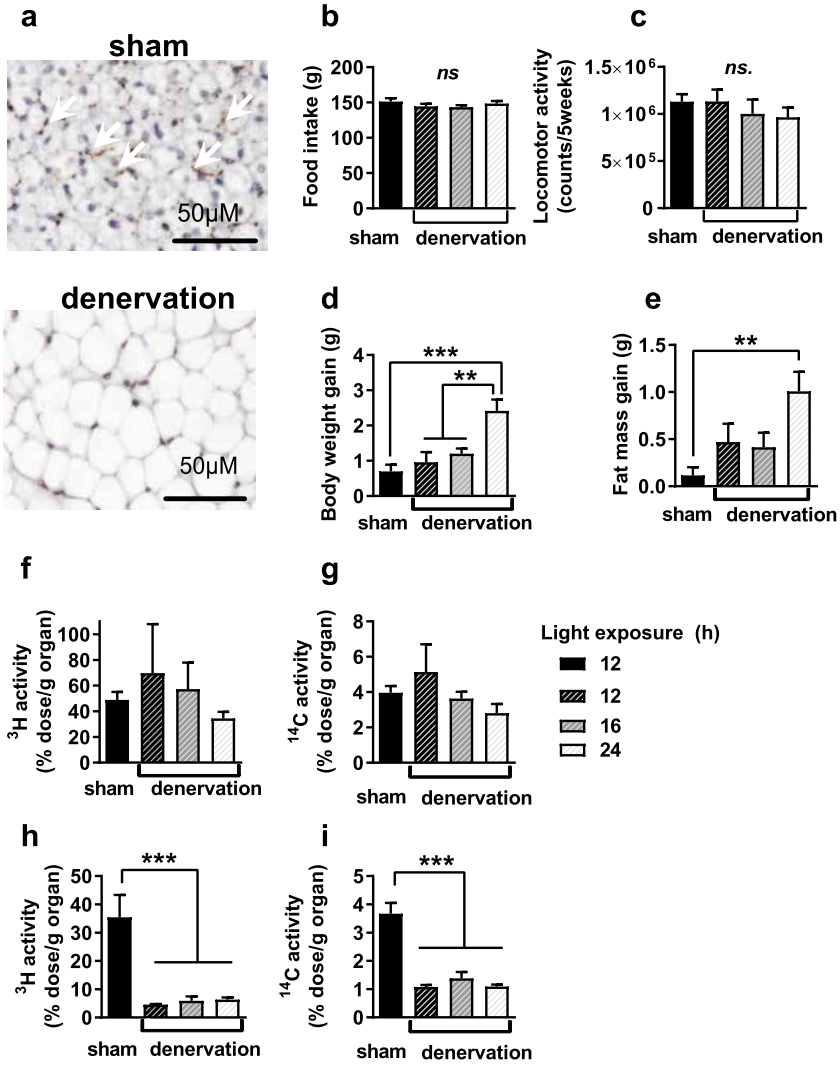

Figure 4: Mice underwent bilateral sympathetic denervation of iBAT or sham surgery. *Denervated mice were exposed to either 12, 16 or 24 h light (n = 5-6) while sham mice were exposed to 12 h light exposure (n=6). After 5 weeks, iBAT was isolated and histologically stained for tyrosine hydroxylase (TH). Representative images are shown (a). Total food intake (b), locomotor activity* ***(c)*** *, body weight gain (d) and fat mass gain (e) were determined. VLDL-TG and glucose kinetics were assessed by injection of glycerol tri[^{3}H]oleate ([^{3}H]TO)-labeled emulsion particles and [^{14}C]deoxyglucose ([^{14}C]DG). Uptake of [^{3}H]TO-derived and [^{14}C]DG activity by sBAT (f,g) and by iBAT was determined (h,i). Data are presented as means ±SEM. ns. = not significant, *p<0.05, **p<0.01, *** p<0.001.*

(supplemental figure 4b) as well as citrate synthase activity (supplemental figure 4c) was similar between the different light exposure groups. In line with this finding, total BAT amount was not different upon prolonged light exposure (supplemental figure 4d).

Together, these data indicate that prolonged daily light exposure reduces sympathetic signalling in BAT that is not accompanied by a decrease in mitochondrial capacity, but does result in reduced uptake of TG-derived fatty acids and glucose.

Sympathetic denervation of iBAT largely reduces nutrient uptake and abolishes effects of prolonged light exposure

To confirm that sympathetic outflow is crucial for the observed effects of prolonged daily light exposure, we performed selective, bilateral denervation of the iBAT prior to exposing mice to 12, 16 or 24 h light per day. A reference group of mice underwent sham surgery and were exposed to 12 h light per day. Denervation completely abolished sympathetic input into iBAT, as evidenced by absence of TH (Figure 4a). In line with the previous experiment, light exposure did not affect food intake (Figure 4b). Additionally, spontaneous locomotor activity was similar between all groups (Figure 4c). Interestingly, body weight gain only increased in mice that were subjected to 24 h light exposure (Figure 4d). This increase was likely due to increased fat mass gain in these animals (Figure 4e).

Next, iBAT and sBAT activity was investigated by determining the ability to take up TG-derived fatty acids and glucose from plasma by injection of radiolabeled particles as described above. While the uptake of [^{3}H]TO and [^{14}C]DG by non-denervated sBAT remained high (Figure 4f and Figure 4g resp.), specific iBAT denervation lowered the uptake of [^{3}H]TO-derived activity (Figure 4h) and [^{14}C]DG (Figure 4i) by iBAT with approximately 70-80% compared to sham operated animals ($p<0.001$), indicating the importance of noradrenergic input in BAT activity. Importantly, prolonged daily light exposure did not further decrease the uptake of [^{3}H]TO and [^{14}C]DG. These data indicate the reduction in adrenergic signalling may be causal in the negative correlations of hours of light exposure and BAT activity.

DISCUSSION

This study addressed the effect of daily light exposure (12, 16 and 24 h) on energy metabolism in chow-fed C57Bl/6J mice. We show that prolonging the daily light exposure increases adiposity and reduces the uptake of TG-derived fatty acids and glucose specifically by BAT, accompanied by decreased ß-adrenergic signalling in BAT and decreased phosphorylation of intracellular proteins involved in thermogenesis.

Daily light exposure duration positively associated with body fat mass and white adipocyte hypertrophy. These data are in line with observations in field voles, switching the day length from 8 h to 16 h increased body weight by 24% in 4 weeks compared to animals that remained on a day length of 8 h [18]. Accordingly, we previously showed that prolonging day length from 12 h to 24 h decreases energy expenditure in mice without increasing food intake or locomotor activity [11]. Although acute light exposure at night can reduce

locomotor activity [19] and prolonged light exposure affects wheel running activity [20, 21], our present study confirms previous reports from us [11] and others [22] that prolonged light exposure does not decrease spontaneous locomotor activity. Together, these studies support the idea that prolonged daily light exposure increases body fat mass through a decrease in energy expenditure rather than to an increase in food intake or decrease of locomotor activity.

The present study strongly suggests that prolonged daily light exposure increases adiposity due to attenuation of BAT activity as reflected by the negative association between daily light exposure and the uptake of fatty acids and glucose by several BAT depots. Of note, prolonged daily light exposure did not affect uptake of nutrients by other metabolic organs, such as WAT. These data are consistent with our recent findings that attenuating BAT activity by inhibiting the central melanocortin system also reduces the influx of nutrients into BAT [23]. In fact, activation of BAT, *e.g.* by cold exposure, increases expression of genes involved in fatty acid oxidation, glucose uptake and lipogenesis [24] and strongly increases the uptake of TG-derived fatty acids [25] and glucose [24].

Our data are consistent with the hypothesis that prolonged daily light exposure decreases BAT activity through reduction of the sympathetic outflow towards BAT. Tyrosine hydroxylase (TH), the rate limiting enzyme in noradrenalin production, correlates with nutrient uptake by BAT and we observed a decrease in sympathetic signalling pathways in BAT. Prolonged light exposure decreased phosphorylation of CREB and AMPK, two main targets of β3-adrenergic signalling in the brown adipocyte. AMPK not only modulates intracellular lipolysis by phosphorylation of HSL, but also regulates uptake of lipids and glucose by inducing translocation of CD36, LPL and GLUT4 to the plasma membrane [26, 27], which may explain the reduced nutrient uptake by BAT. Moreover, we showed that in the absence of sympathetic input, BAT activity is equal among the various light exposure groups.

We propose that the SCN directly mediates the decrease in sympathetic outflow upon prolonging daily light exposure. In previous studies we demonstrated that prolonged light exposure dampens the amplitude of electrical activity in the SCN in vitro [28] and in vivo [10]. Interestingly, the amplitude of electrical activity in the SCN is linked to sympathetic outflow towards multiple organs [29]. This mechanism also explains previous findings that exposure of mice to dim light (5 lux) during 10 h nights for 4 weeks already results in an increase in body weight, which was accompanied by an attenuated amplitude of circadian gene expression in the hypothalamus [30]. Also, sympathetic outflow towards BAT depots other than interscapular BAT would explain our observations that denervation of iBAT does not increase body weight. Only 24 h light exposure decreases sympathetic outflow to such an extent, that mice increase significantly in body weight. Of note, the effects of light exposure on BAT are independent of melatonin secretion, since C57Bl/6J mice are genetically melatonin deficient [31]. However, we cannot exclude the possibility that in humans melatonin does play a role in the association between light pollution and adiposity as administration of melatonin increases BAT growth [32] and activity [33, 34] in hamsters and rats.

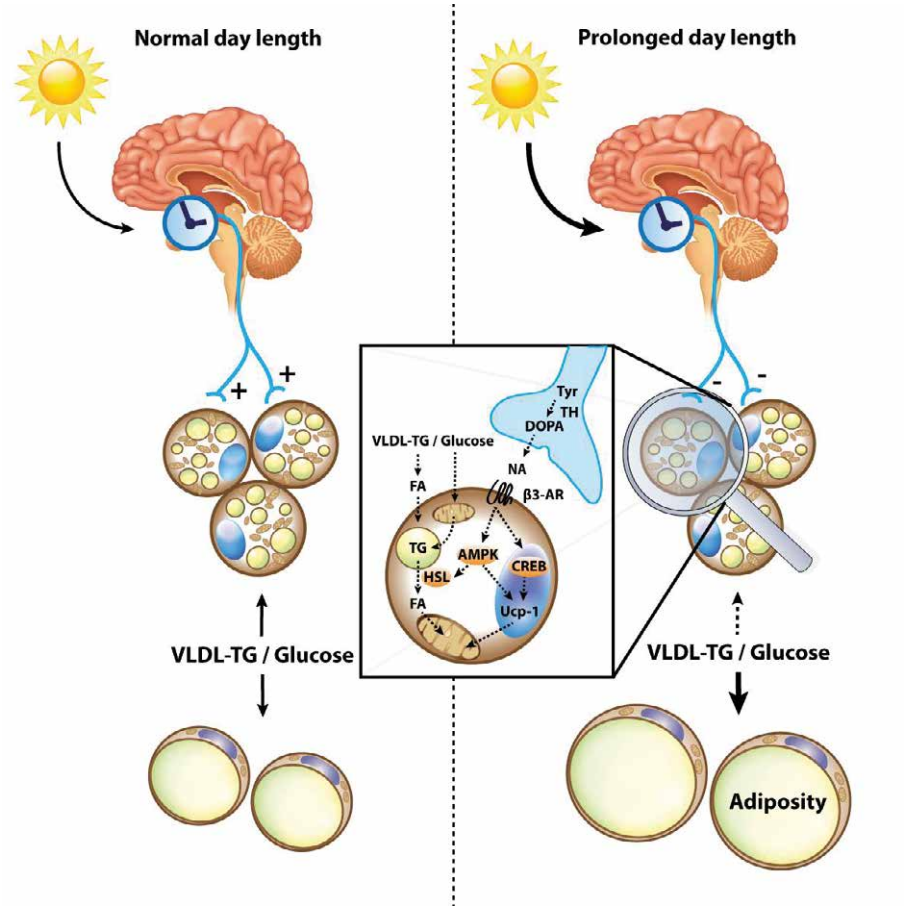

Figure 5: Proposed model on how light exposure modulates body fat mass through brown adipose tissue activity. *Daily light exposure duration is perceived by the suprachiasmatic nucleus, that signals towards BAT via the sympathetic nervous system. At normal day length uptake of nutrients by BAT and WAT is in balance, while increasing daily light exposure result in reduced BAT activation and subsequent storage of excess energy in WAT. The decrease in noradrenaline (NA) availability for stimulation of the β3-adrenergic receptor (B3-AR) leads 1) reduced phosphorylation of CREB, which decreases transcription of UCP1; 2) reduced phosphorylation of AMPK resulting in decreased phosphorylation of HSL and thus decreased lipolysis.*

Based on our collective data, we thus propose the following mechanism by which prolonging daily light exposure increases adiposity: prolonged day length dampens the SCN amplitude thereby lowering sympathetic outflow towards BAT resulting in decreased β3-adrenergic signalling and thermogenesis in brown adipocytes. As a consequence, the uptake of VLDL-TG derived fatty acids and glucose by BAT is reduced. The decreased

combustion of fatty acids by BAT at equal energy intake thus results in a positive energy balance and therefore storage of lipids in WAT (Figure 5).

Recent evidence suggests that BAT activity in humans is physiologically regulated by the biological clock. The detectability of BAT by [^{18}F]fluorodeoxyglucose (FDG)-PET-CT imaging at room temperature follows a circannual cycle, both in the northern and southern hemisphere [35-37], with low detectability of BAT in summer (i.e., short day) as compared to winter (i.e., long day). Although differences in outside temperature over the year would be a likely explanation for this phenomenon, the detectability of BAT showed a stronger correlation with day length than with outside temperature [35]. Based on our present data, the daily light exposure may thus well explain the circannual cycle of BAT detectability. Likewise, impaired BAT activity may also explain, at least partly, the relationship between obesity and disturbances in circadian rhythmicity in humans by light pollution [2, 3, 38], and possibly also by shift work [39-41] and sleep curtailment [1, 42, 43]. Additionally, our data may provide the link in the relationship between exposure to light in the bedroom and obesity [4]. The suggested causal relationship has clear implications for the prevention of obesity in humans. Although the association between light in the bedroom and BAT activity in humans remains to be investigated, future lifestyle advice could include instructing people to darken their bedroom.

In conclusion, our study provides evidence that prolonged daily light exposure increases body fat mass through reduction of BAT activity. The present findings support the hypothesis that the relationship between disturbed circadian rhythmicity and adiposity in humans is mediated by impaired BAT activity.

ACKNOWLEDGMENTS

The authors thank Simone Denis, Julia Melia Aloma and Lianne van der Wee-Pals for excellent technical support. This research was supported by the Netherlands Organisation for Scientific Research (NWO-VENI grants 016.136.125 to NR Biermasz and 91613050 to RH Houtkooper), the European Foundation for the Study of Diabetes and the Programme Partner Novo Nordisk (grant 94802 to CP Coomans, JH Meijer and PCN Rensen), the Dutch Diabetes Research Foundation (grant 2013.81.1663 to CP Coomans), the Rembrandt Institute for Cardiovascular Science (RICS) (Rembrandt Research Award to MR Boon and RH Houtkooper) and an AMC PhD fellowship (to IA Chatzispyrou). PCN Rensen is an Established Investigator of the Dutch Heart Foundation (grant 2009T038).

REFERENCES

1. Killick, R., S. Banks, and P.Y. Liu, *Implications of sleep restriction and recovery on metabolic outcomes.* J. Clin. Endocrinol. Metab, 2012. **97**(11): p. 3876-3890.
2. bayashi, K., *et al.*, *Exposure to light at night, nocturnal urinary melatonin excretion, and obesity/dyslipidemia in the elderly: a cross-sectional analysis of the HEIJO-KYO study.* J Clin Endocrinol. Metab, 2013. **98**(1): p. 337-344.
3. yse, C.A., *et al.*, *Circadian desynchrony and metabolic dysfunction; did light pollution make us fat?* Med Hypotheses, 2011. **77**(6): p. 1139-1144.
4. cFadden, E., *et al.*, *The Relationship Between Obesity and Exposure to Light at Night: Cross-Sectional Analyses of Over 100,000 Women in the Breakthrough Generations Study.* Am. J Epidemiol, 2014.
5. erreau-Lenz, S., *et al.*, *The biological clock: the bodyguard of temporal homeostasis.* Chronobiol Int, 2004. **21**(1): p. 1-25.
6. ho, H., *et al.*, *Regulation of circadian behaviour and metabolism by REV-ERB-alpha and REV-ERB-beta.* Nature, 2012. **485**(7396): p. 123-127.
7. hi, S.Q., *et al.*, *Circadian disruption leads to insulin resistance and obesity.* Curr. Biol, 2013. **23**(5): p. 372-381.
8. himba, S., *et al.*, *Brain and muscle Arnt-like protein-1 (BMAL1), a component of the molecular clock, regulates adipogenesis.* Proc. Natl Acad. Sci. U. S. A, 2005. **102**(34): p. 12071-12076.
9. urek, F.W., *et al.*, *Obesity and metabolic syndrome in circadian Clock mutant mice.* Science, 2005. **308**(5724): p. 1043-1045.
10. Coomans, C.P., *et al.*, *The suprachiasmatic nucleus controls circadian energy metabolism and hepatic insulin sensitivity.* Diabetes, 2013. **62**(4): p. 1102-1108.
11. Coomans, C.P., *et al.*, *Detrimental effects of constant light exposure and high-fat diet on circadian energy metabolism and insulin sensitivity.* FASEB J, 2013. **27**(4): p. 1721-1732.
12. Amir, S., *Retinohypothalamic tract stimulation activates thermogenesis in brown adipose tissue in the rat.* Brain Res, 1989. **503**(1): p. 163-166.
13. Bamshad, M., C.K. Song, and T.J. Bartness, *CNS origins of the sympathetic nervous system outflow to brown adipose tissue.* Am. J. Physiol, 1999. **276**(6 Pt 2): p. R1569-R1578.
14. Rensen, P.C., *et al.*, *Particle size determines the specificity of apolipoprotein E-containing triglyceride-rich emulsions for the LDL receptor versus hepatic remnant receptor in vivo.* J. Lipid Res, 1997. **38**(6): p. 1070-1084.
15. Houtkooper, R.H., *et al.*, *The metabolic footprint of aging in mice.* Sci Rep, 2011. **1**: p. 134.
16. Ventura, F.V., *et al.*, *Differential inhibitory effect of long-chain acyl-CoA esters on succinate and glutamate transport into rat liver mitochondria and its possible implications for long-chain fatty acid oxidation defects.* Mol Genet Metab, 2005. **86**(3): p. 344-52.
17. Dörrscheidt GL and B. L., *Advanced methods for evaluating characteristic parameters of circadian rhythms.* J Mathemat Biol, 1975. **2**: p. 107-121.
18. Krol, E., *et al.*, *Effect of photoperiod on body mass, food intake and body composition in the field vole, Microtus agrestis.* J Exp. Biol, 2005. **208**(Pt 3): p. 571-584.
19. Redlin, U., *Neural basis and biological function of masking by light in mammals: suppression of melatonin and locomotor activity.* Chronobiol Int, 2001. **18**(5): p. 737-58.
20. orin, L.P., P.J. Lituma, and K.M. Studholme, *Two components of nocturnal locomotor suppression by light.* J Biol Rhythms, 2010. **25**(3): p. 197-207.
21. Mrosovsky, N., R.G. Foster, and P.A. Salmon, *Thresholds for masking responses to light in three strains of retinally degenerate mice.* J Comp

Physiol A, 1999. **184**(4): p. 423-8.

22. Fonken, L.K., *et al.*, *Light at night increases body mass by shifting the time of food intake.* Proc. Natl. Acad. Sci. U. S. A, 2010. **107**(43): p. 18664-18669.
23. Kooijman, S., *et al.*, *Inhibition of the central melanocortin system decreases brown adipose tissue activity.* J. Lipid Res (Submitted), 2014.
24. Yu, X.X., *et al.*, *Cold elicits the simultaneous induction of fatty acid synthesis and beta-oxidation in murine brown adipose tissue: prediction from differential gene expression and confirmation in vivo.* FASEB J, 2002. **16**(2): p. 155-168.
25. Bartelt, A., *et al.*, *Brown adipose tissue activity controls triglyceride clearance.* Nat. Med, 2011. **17**(2): p. 200-205.
26. Samovski, D., *et al.*, *Insulin and AMPK regulate FA translocase/CD36 plasma membrane recruitment in cardiomyocytes via Rab GAP AS160 and Rab8a Rab GTPase.* J Lipid Res, 2012. **53**(4): p. 709-717.
27. Jeppesen, J., *et al.*, *Contraction-induced skeletal muscle FAT/CD36 trafficking and FA uptake is AMPK independent.* J Lipid Res, 2011. **52**(4): p. 699-711.
28. VanderLeest, H.T., *et al.*, *Seasonal encoding by the circadian pacemaker of the SCN.* Curr. Biol, 2007. **17**(5): p. 468-473.
29. Kalsbeek, A., *et al.*, *SCN outputs and the hypothalamic balance of life.* J. Biol. Rhythms, 2006. **21**(6): p. 458-469.
30. Fonken, L.K., *et al.*, *Dim light at night disrupts molecular circadian rhythms and increases body weight.* J. Biol. Rhythms, 2013. **28**(4): p. 262-271.
31. Roseboom, P.H., *et al.*, *Natural melatonin 'knockdown' in C57BL/6J mice: rare mechanism truncates serotonin N-acetyltransferase.* Brain Res Mol Brain Res, 1998. **63**(1): p. 189-197.
32. Heldmaier, G. and K. Hoffmann, *Melatonin stimulates growth of brown adipose tissue.* Nature, 1974. **247**(5438): p. 224-5.
33. Holtorf, A.P., *et al.*, *Diurnal changes in sensitivity to melatonin in intact and pinealectomized Djungarian hamsters: effects on thermogenesis, cold tolerance, and gonads.* J Pineal Res, 1985. **2**(4): p. 393-403.
34. Hagelstein, K.A. and G.E. Folk, Jr., *Effects of photoperiod, cold acclimation and melatonin on the white rat.* Comp Biochem Physiol C, 1979. **62c**(2): p. 225-9.
35. Au-Yong, I.T., *et al.*, *Brown adipose tissue and seasonal variation in humans.* Diabetes, 2009. **58**(11): p. 2583-2587.
36. Perkins, A.C., *et al.*, *Prevalence and pattern of brown adipose tissue distribution of 18F-FDG in patients undergoing PET-CT in a subtropical climatic zone.* Nucl. Med Commun, 2013. **34**(2): p. 168-174.
37. Persichetti, A., *et al.*, *Prevalence, mass, and glucose-uptake activity of (1)(8)F-FDG-detected brown adipose tissue in humans living in a temperate zone of Italy.* PLoS. One, 2013. **8**(5): p. e63391.
38. Reid, K.J., *et al.*, *Timing and intensity of light correlate with body weight in adults.* PLoS One, 2014. **9**(4): p. e92251.
39. Karlsson, B.H., *et al.*, *Metabolic disturbances in male workers with rotating three-shift work. Results of the WOLF study.* Int Arch. Occup. Environ. Health, 2003. **76**(6): p. 424-430.
40. L., D.L., *et al.*, *Effect of shift work on body mass index: results of a study performed in 319 glucose-tolerant men working in a Southern Italian industry.* Int J. Obes. Relat Metab Disord, 2003. **27**(11): p. 1353-1358.
41. Barbadoro, P., *et al.*, *Rotating shift-work as an independent risk factor for overweight italian workers: a cross-sectional study.* PLoS. One, 2013. **8**(5): p. e63289.
42. Watanabe, M., *et al.*, *Association of short sleep duration with weight gain and obesity at 1-year follow-up: a large-scale prospective study.* Sleep, 2010. **33**(2): p. 161-167.
43. Hairston, K.G., *et al.*, *Sleep duration and five-year abdominal fat accumulation in a minority cohort: The IRAS family study.* Sleep, 2010. **33**(3): p. 289-295.

SUPPLEMENTARY APPENDIX

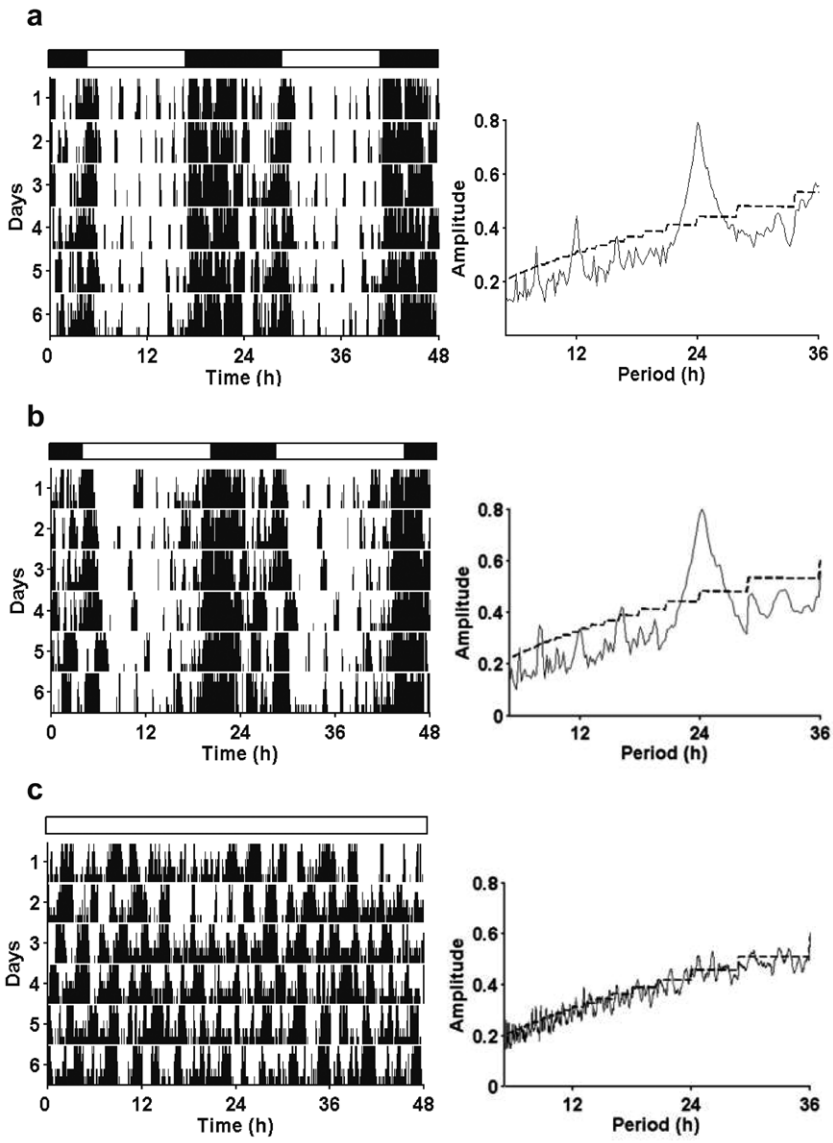

Supplemental Figure 1. Prolonged daily light exposure affects behavioural rhythms in mice. *Mice were exposed to either 12, 16 or 24 h light (n = 9) for 5 weeks, and behavioural activity was monitored by passive infrared detectors. Representative actograms (left panels) and the pertaining F periodogram (right panels) are shown of a mouse exposed to 12 (a), 16 (b) and 24 h (c) of light. The double-plotted actograms show consecutive days on successive lines and the vertical black upticks indicate behavioural activity measured by passive infrared detectors. The light regimes are plotted on top of the actograms; white areas represent light and black areas represent darkness. Periodogram analysis visualizes the strength of behavioural rhythmicity. The dotted lines in the periodograms indicate the 0.05 level of significance.*

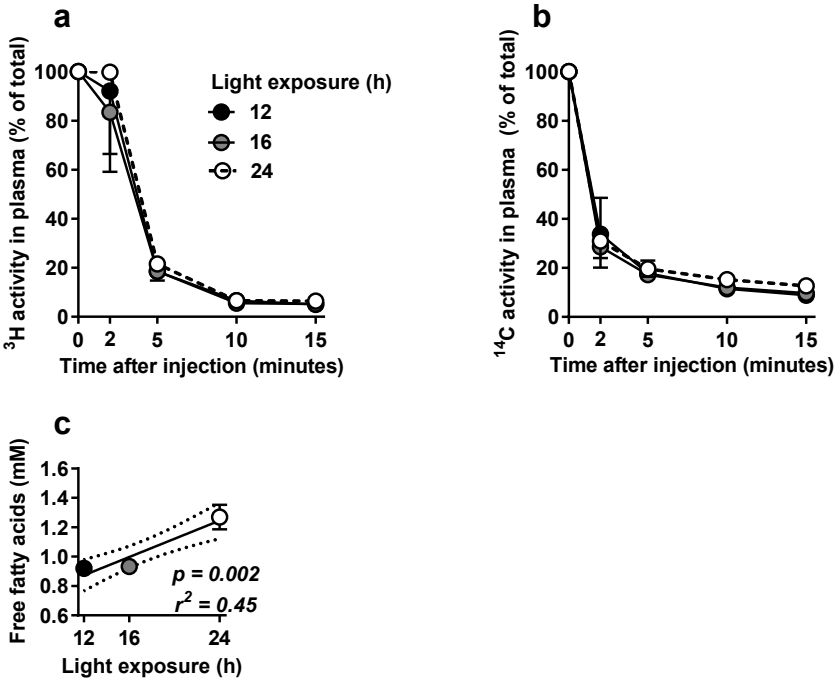

Supplemental Figure 2. Effect of light exposure on TG and glucose plasma clearance. *Prolonged daily light exposure does not affect TG and glucose plasma clearance. Mice were exposed to either 12, 16 or 24 h light for 5 weeks, and the VLDL-TG and glucose kinetics were assessed by injection of glycerol tri[^{3}H] oleate ([^{3}H]TO)-labeled emulsion particles and [^{14}C]deoxyglucose ([^{14}C]DG). Blood was drawn 2, 5, 10 and 15 min after injection. [^{3}H]TO (n=8-9) (a) and [^{14}C]DG (n=6-7) (b) derived activity was assessed in plasma samples by liquid oscillation counting. Data are represented as means ±SEM. Statistical significance was determined by unpaired two-tailed Student's t-test.*

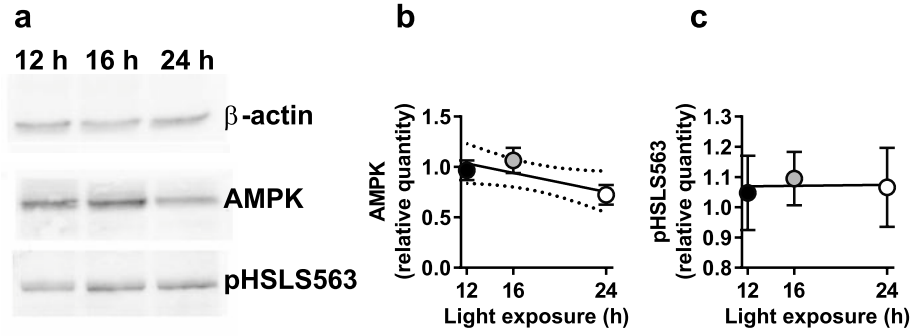

Supplemental Figure 3. Prolonged daily light exposure does not affect AMPK and pHSL S^{563} in BAT. *Prolonged daily light exposure does not affect AMPK and pHSL S^{563} in BAT. Mice exposed to either 12, 16, or 24 h light (n= 9) for 5 weeks, and interscapular BAT was isolated for protein quantification. Representative western blots are shown for β-actin, total AMPK and pHSL S^{563} (a). Correlation was determined between hours of light exposure and protein levels of AMPK (b) and pHSL S^{563} (c). Protein levels were normalized to β-actin levels. Data are represented as means ± SEM. Statistical significance between groups was determined by unpaired two-tailed Student's t-test, linear regression analysis was performed to analyse the association of gene expression with light exposure.*

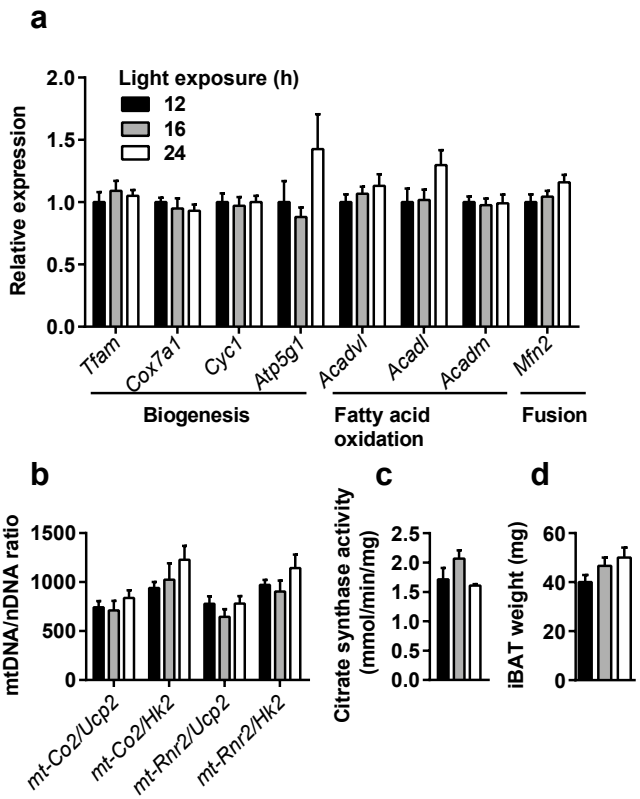

Supplemental Figure 4. Effects of prolonged light exposure on mitochondrial function. *Prolonged daily light exposure does not decrease structural mitochondrial function in BAT and quantity of BAT. Mice were exposed to either 12, 16, or 24 h light (n= 9) for 5 weeks, and interscapular and subscapular BAT was isolated for gene expression and mitochondrial function analysis. Expression of genes involved in mitochondrial biogenesis, fatty acid oxidation and fusion genes did not change upon prolonged light exposure (a). The same is true for relative mitochondrial DNA quantity (b) and mitochondrial citrate synthase activity (c). iBAT was removed quantitatively and weighed (d). Gene expression levels were normalized to 36B4 levels. Mitochondrial DNA quantity is expressed as ratio of mitochondrial gene expression relative to nuclear gene expression (genes indicated below). Data are represented as means ± SEM. Abbreviations: Tfam, transcription factor A, mitochondrial; Cox7a1, cytochrome c oxidase subunit VIIa 1; Cyc1, cytochrome C-1; Atp5g1, ATP synthase, H+ transporting, mitochondrial F0 complex, subunit C1; Acadvl, acyl-Coenzyme A dehydrogenase, very long chain; Acadl, acyl-Coenzyme A dehydrogenase, long-chain; Acadm, acyl-Coenzyme A dehydrogenase, medium chain; Mfn2, mitofusin 2; mtCo2, cytochrome c oxidase II, mitochondrial; mt-Rnr2, 16S rRNA, mitochondrial; Ucp2, uncoupling protein 2; Hk2, hexokinase 2.*

Chapter 3

Diurnal regulation of plasma lipid levels by brown adipose tissue

Rosa van den Berg, Sander Kooijman*, Raymond Noordam, Ashna Ramkisoensing, Wieneke Dijk, Lauren L. Tambyrajah, Gustavo Abreu-Vieira, Isabel M. Mol, Barbara Kramar, Rosanna Caputo, Laura Sardón Puig, Evelien M. de Ruiter, Linda W.M. van Kerkhof, Constantinos Christodoulides, Fredrik Karpe, Zachary Gerhart-Hines, Sander Kersten, Johanna H. Meijer, Claudia P. Coomans, Diana van Heemst, Nienke R. Biermasz#, Patrick C.N. Rensen#*

Submitted

**,# Authors contributed equally.*

ABSTRACT

Brown adipose tissue (BAT) activation leads to a fast removal of lipids from the circulation in order to produce heat. Recently, diurnal BAT activity was demonstrated to determine rhythms in daily body temperature and glucose handling. In this paper, we have characterized the involvement of diurnal BAT activitiy in plasma lipid metabolism. We observed a high amplitude 24h rhythm in the fatty acid uptake by BAT with highest uptake at the onset of the active period coinciding with high LPL expression and low Angptl4 expression. Diurnal rhythmicity in BAT activity dictated a daily rhythm in plasma lipid concentrations as well as lipid clearance. Strikingly, in mice as well as humans we found postprandial lipid excursions to be nearly absent at the onset of the active period and high before sleep, consistent with the diurnal BAT activity pattern. We anticipate that restriction of food intake to the early wakeful period improves metabolic health related to high BAT activity.

INTRODUCTION

Brown adipose tissue (BAT) is a key site of mammalian thermogenesis and its activity is critical for the survival of small mammals in cold environments and for arousal in hibernators. Heat arises primarily from mitochondrial uncoupling during the combustion of intracellularly stored lipids. To replenish these lipid stores, brown adipocytes take up triglyceride (TG)-derived fatty acids (FA) from the circulation in a lipoprotein lipase (LPL)-dependent matter. Activation of BAT results in increased energy expenditure (EE) and a marked lowering of plasma TG levels [1, 2]. Therefore, BAT activation is considered a target for the treatment of metabolic disorders.

Recent studies linked control of the daily rhythm in body temperature of mice and their ability to adapt to cold to diurnal BAT activity [3, 4], which is consistent with earlier reports demonstrating circadian expression of clock genes in murine BAT [5] and oscillations in glucose uptake as determined by PET-FDG imaging [6]. Notably, human brown adipocytes also exhibit a rhythm in clock gene expression and glucose uptake [7]. Interestingly, in both mice [8] and humans [9, 10] variations in daily light exposure (LE) associate with the thermogenic capacity of BAT, suggesting plasticity in diurnal BAT activity.

We [11] and others [12] have shown that plasma lipid concentrations are highly rhythmic independent of food intake behavior, suggesting oscillations in the clearance of lipids by metabolic organs. Given the relevance of BAT function for lipoprotein metabolism [1, 13], we hypothesized that physiological diurnal rhythmicity of BAT activity regulates fasting and postprandial lipid concentrations. The aim of the present study was to unravel the diurnal rhythm of lipid uptake by BAT and its consequence for (postprandial) lipid handling, by performing studies in mice as well as in healthy humans.

METHODS

Animal Husbandry

Local ethics committee approved all animal experiments. Mice were single housed at 22°C room temperature and fed *ad libitum*. Wild-type mice were fed standard laboratory chow (Special Diets Services, UK), APOE*3-Leiden.CETP mice were fed Western-type diet (WTD; 35% energy from fat; supplemented with 0.1% cholesterol; AB Diets, Woerden, The Netherlands).

Wild type mice experiments

12 week old male wild-type mice (C57Bl/6J background; Charles River) were housed on 12h light: 12h dark cycle (normal daily light exposure (LE), 8h light: 16h dark cycle (short daily LE) or a 16h light: 8h dark cycle (long daily LE) (n=24 per group). After five weeks, the uptake of triglyceride (TG)-derived fatty acid (FA) by metabolic organs was assessed (see below) at time points ZT (Zeitgeber Time, time after lights on) 0, 4, 6, 8, 12 and 18h. At the end of

this experiment, mice were killed and organs were collected for gene / protein expression analysis (see below).

In an addition group of male C57Bl/6J mice, 24 h rhythms in food intake, energy expenditure and substrate utilization was determined by means of indirect calorimetry in metabolic cages (PhenoMaster, TSE systems, Bad Homburg, Germany) containing automatized scales placed inside the calorimeters. All mice were first measured at 12h LE and subsequently housed in light tight cabinets and split into two groups which were acclimated to either short or long LE for five weeks. During the last week, mice were again housed in metabolic chambers to assess the effects of LE on energy metabolism.

Dyslipidemic mice experiments

Homozygous human cholesteryl ester transfer protein (CETP) transgenic mice were crossbred with hemizygous APOE*3-Leiden mice at our Institutional animal facility to obtain APOE*3-Leiden.CETP mice (C57Bl/6J background). Female mice were used as these specifically develop high levels of plasma triglycerides and cholesterol. Mice of 9-12 weeks old were fed Western-type diet (WTD; caloric energy: 35% fat, 17% protein, 48% carbohydrates; addition of 0.1% cholesterol; AB Diets, Woerden, the Netherlands). After 3 weeks, mice were matched for body weight and plasma TG and adapted to either short or long daily LE (n=27/group). In a subset of mice (n=5/group) a telemetric transmitter was implanted under isoflurane anesthesia. A small incision was made between the shoulder blades via which a TA-F10 miniature transmitter (Data Sciences International, MN, USA) was inserted subcutaneously in the flank. Data acquisition was performed using Dataquest A.R.T. TM Software (Data Sciences International). In the same subset of mice, after four weeks, seven consecutive blood samples via venous tail bleeding were obtained at time points ZT 0, 4, 8, 12, 16, 20, 24 and one week later, stress-free blood samples were obtained at ZT0, 8 and 16 by drawing blood within one minute of handling the mouse. Fasting and postprandial lipids were determined either at ZT 0, 8 or 16 (see below). After five weeks, the uptake of TG-derived FA by metabolic organs and clearance from the circulation was determined (see below) at the same time points.

For experiments at thermoneutrality, an additional group of APOE*3-Leiden.CETP mice was adapted to normal LE (n=7-8/group), fed a WTD for 3 weeks and switched to an environmental temperature of 30°C. After 2 days, postprandial lipid response experiment was performed and after four days, uptake of TG-derived FA and clearance was determined.

Rev-erbα-/- mice and control littermates were maintained on a 12 h light: 12 h dark cycle at thermoneutrality (30°C). iBAT was collected from 12-14 week old male mice at thermoneutrality at ZT10 or following a 6 hour 4°C cold exposure (ZT4-ZT10) for gene expression analysis.

Postprandial lipid response

To determine the postprandial lipid response, mice were fasted for 4h prior to the start of the experiment, after which a fasting blood sample via tail vein bleeding was drawn. Immediately thereafter, mice received an intragastric bolus of 200 µL olive oil (Carbonell,

Cordoba, Spain). Blood was collected after 1, 2, 4 and 8h to determine plasma lipid concentrations .

TG-derived FA uptake

Glycerol tri[^{3}H]oleate-labeled lipoprotein-like particles (80 nm) were prepared as previously described[2, 14]. Mice were fasted for 4h prior to the start of the experiment, which started with an intravenous injection of radiolabeled particles (1.0 mg TG in 200 µL PBS). Blood was collected after 2, 5, 10 and 15 minutes to determine plasma decay of the radiolabel. After 15 minutes, mice were killed by cervical dislocation, perfused with ice-cold PBS and organs were harvested. The uptake of [^{3}H]oleate by metabolic organs was determined.

Indirect calorimetry and food intake

For the measurements of food intake, energy expenditure and respiratory exchange ratio, male C57Bl/6J mice fed chow diet were previously acclimated to the indirect calorimeters for a 2-day period. All experiments took place at 22°C, while food and water were provided *ad libitum*. Data points were collected at 20-min intervals.

Biochemical analyses

Mouse blood was collected into chilled paraoxon-coated capillaries to prevent *ex vivo* lipolysis. Capillaries were centrifuged at RT and plasma was isolated and stored at -80°C. Human blood samples were kept at RT for 1 h after collection. Serum was isolated and aliquoted into 500 µL tubes and stored at -80°C. Plasma was assayed using a commercially available enzymatic kit for TG (Roche Diagnostics, Mannheim, Germany) and free FA (NEFA-C kit, Wako Diagnostics, Instruchemie, Delfzijl, the Netherlands). Corticosterone measurements were performed in 2 µL blood samples by high sensitivity enzyme immunoassay according to the manufacturers' protocol (Immunodiagnosticsystems, UK, kit reference: Ref AC-15F1).

Gene and protein expression

A part of iBAT was snap frozen and stored at -80°C for gene expression analysis. Total RNA was isolated using TriPure (Roche) according to the manufacturer's instructions. 1 µg of total RNA was reverse-transcribed using M-MLV reverse transcriptase (Promega, Madison, WI, USA). Real-time PCR was carried out on a CFX96 PCR machine using IQ SYBR-Green Supermix (Bio-Rad). Melt curve analysis was included to assure a single PCR product was formed. Expression levels were normalized to *36b4* and *Hprt* housekeeping gene expression. Data was plotted as relative expression to expression in normal 12h daily LE group at ZT0.

To extract proteins, BAT was lysed in RIPA buffer (25 mM Tris-HCl pH 7.6, 150 mM NaCl, 1% NP-40, 1% sodium deoxycholate and 1% SDS; Thermo Fisher-Scientific, Landsmeer, the Netherlands) supplemented with cOmplete protease and phosSTOP phosphatase inhibitors (Roche Diagnostics, Almere, the Netherlands) with the Qiagen Tissuelyser II (Qiagen, Venlo, the Netherlands). Upon homogenization, lysates were placed on ice for

30 minutes and centrifuged 4 times at 13,000 rpm for 10 min at 4˚C to remove fat and cell debris. Protein concentrations were determined by using a bicinchoninic acid (BCA) assay (Thermo Fisher-Scientific). Equal amounts of protein (11.25 µg (LPL/HSP90) or 40 µg (ANGPTL4) protein per lane) were combined with 2x Laemmli sample buffer, boiled at 95˚C for 5 minutes, and loaded onto 8-16% (LPL/HSP90) or 10% (ANGPTL4) Criterion gradient gels (Bio-Rad, Veenendaal, The Netherlands). Next, proteins were transferred onto a PVDF membrane using the Transblot Turbo System (Bio-Rad). Membranes were probed with a goat anti-mouse LPL antibody (kind gift from André Bensadoun); a rabbit anti-mouse HSP90 antibody (Cell Signaling Technology, #4874); or a rat anti-mouse ANGPTL4 antibody (Adipogen, Kairos 142-2) at 1:5000 (LPL), 1:2000 (HSP90) or 1:1000 (ANGPTL4) dilution. Tris-buffered saline, pH 7.5, with 0.1% Tween-20 (TBS-T) and 5% w/v skimmed milk was used to block membranes and for primary and secondary antibody incubations. In between, membranes were washed in TBS-T only. Imaging of western blots was performed with the ChemiDoc MP system (Bio-Rad) and Clarity ECL substrate (Bio-Rad). Western blot quantifications were done with Image Lab software (Bio-Rad).

Mature glycosylated LPL (LPL in the Golgi and on the cell surface) was determined by digesting 40 µg of protein with EndoH (New England BioLabs) according to the manufacturer's instructions. Briefly, BAT protein lysates were combined with glycoprotein denaturing buffer and boiled for 10 minutes at 95˚C. Following the addition of EndoH, the samples were incubated at 37 ˚C for 1h and, subsequently, combined with 5x Laemmli sample buffer, boiled at 95˚C for 5 minutes and loaded onto 10% Criterion gradient gels (Bio-Rad) for analysis by western blotting as described above. EndoH-resistant LPL represents mature glycosylated LPL located in the Golgi or on the cell surface, whereas EndoH-sensitive LPL represents LPL located in the endoplasmic reticulum with oligosaccharide side chains high in mannose residues [15].

Human study

As described in more detail previously, 38 healthy participants were recruited within the Switchbox study for in-depth endocrine and metabolic phenotyping, which included diurnal venous blood sampling as described in more detail earlier [16]. To be included in the Switchbox study, participants had to have a fasting glucose level <7 mM, hemoglobin level <7.1 mM, a body mass index (BMI) between 19 kg/m^2 and 33 kg/m^2 and had to be free of any significant chronic disease. Of the 38 participants, one participant was excluded because of a newly diagnosed hypertriglyceridemia, leaving 37 participants for the present study. After an overnight fast of 10-14 h, a catheter was inserted before start of the study, and blood sampling started at 09:00h. Every 10 min 1.2 mL of blood was collected in a K3-EDTA tube and 2 mL of blood in a serum separator (SST)-tube. Participants received three standardized liquid meals at 09:00h, 12:00h and 18:00h during a day. All meals consisted of 600 kcal Nutridrink, containing a standard percentage of energy derived from fat (35%), carbohydrates (49%) and protein (16%) (Nutricia Advanced Medical Nutrition, Zoetermeer, the Netherlands). All participants were sampled in the same room with standardized ambient conditions, 630 ± 10 lux of light intensity and 22 ± 2 °C. Participants were not allowed to

sleep during the day, and except for lavatory use no physical activity was allowed during the study period. Lights were turned off between 23:00h to 08:00h to allow the participants to sleep.

Statistical analysis

Data are presented as means ± SEM. Statistical analysis was performed using Student's T-test, one-way ANOVA with Tukey's post-hoc test, two-way ANOVA and repeated measure (RM) ANOVA with Dunnett's post-hoc test to compare time points within the series (relative to ZT0). Associations of variables with daily LE (expressed as hours of LE) as independent variable were assessed by linear regression analysis. Differences at $p<0.05$ were considered statistically significant. Analyses were performed using GraphPad v6.0 software (Prism, La Jolla, CA, USA). Differences at $p<0.05$ were considered statistically significant.

RESULTS

The 24h rhythm of fatty acid uptake is most pronounced in BAT

We determined the time-dependent uptake of fatty acids (FA) by BAT and other metabolic organs in male 12-week old C57Bl/6J mice housed under a standard 12:12 light-dark cycle (hereafter referred to as "Normal light exposure (LE)"). Since FA are predominantly transported in plasma as a constituent of triglycerides (TG) within lipoproteins, we assessed the kinetics of intravenously injected glycerol tri[^{3}H]oleate-labeled TG-rich lipoprotein-like particles at six different times of the day (Zeitgeber times (ZT), lights turned on at ZT0) following a 4h fasting period. We found that the time of day during which the experiments took place determined the uptake of [^{3}H]oleate ([^{3}H]FA) in liver, subcutaneous white adipose tissue (sWAT), gonadal WAT (gWAT), heart, muscle, and especially in perivascular adipose tissue (pVAT, representing a mixture of white and brown adipocytes [17]), subscapular BAT (sBAT) and interscapular BAT (iBAT) (all pZT≤ 0.01; Fig. 1a-h, Table 1). The uptake of [^{3}H]FA by sBAT and iBAT reached its peak at the onset of the dark period (ZT12) and was relatively high compared to the other metabolic organs. The difference between the maximum and minimum [^{3}H]FA uptake was 4-, 12- and 15-fold for iBAT, sBAT and pVAT, respectively (Table 1). From these data, we concluded that compared to other metabolic organs BAT depots specifically display a marked 24h rhythmicity regarding TG-derived FA uptake.

The 24h rhythm of fatty acid uptake by BAT adapts to daily light exposure duration

To determine the adaptability of diurnal BAT activity to environmental changes, we compared the diurnal [^{3}H]FA uptake by metabolic organs under normal LE *vs.* the uptake in mice entrained to either a short daily LE (8h light : 16h dark cycle) or a long daily LE (16h light : 8h dark cycle). Interestingly, the duration of LE changed the daily pattern in uptake of [^{3}H]FA by the brown adipocyte depots pVAT (p_{LE} = 0.014), sBAT (p_{LE} =0.009) and iBAT (p_{LE}=0.003) (Fig. 1f-h), but not in other metabolic organs (Fig. 1a-e).

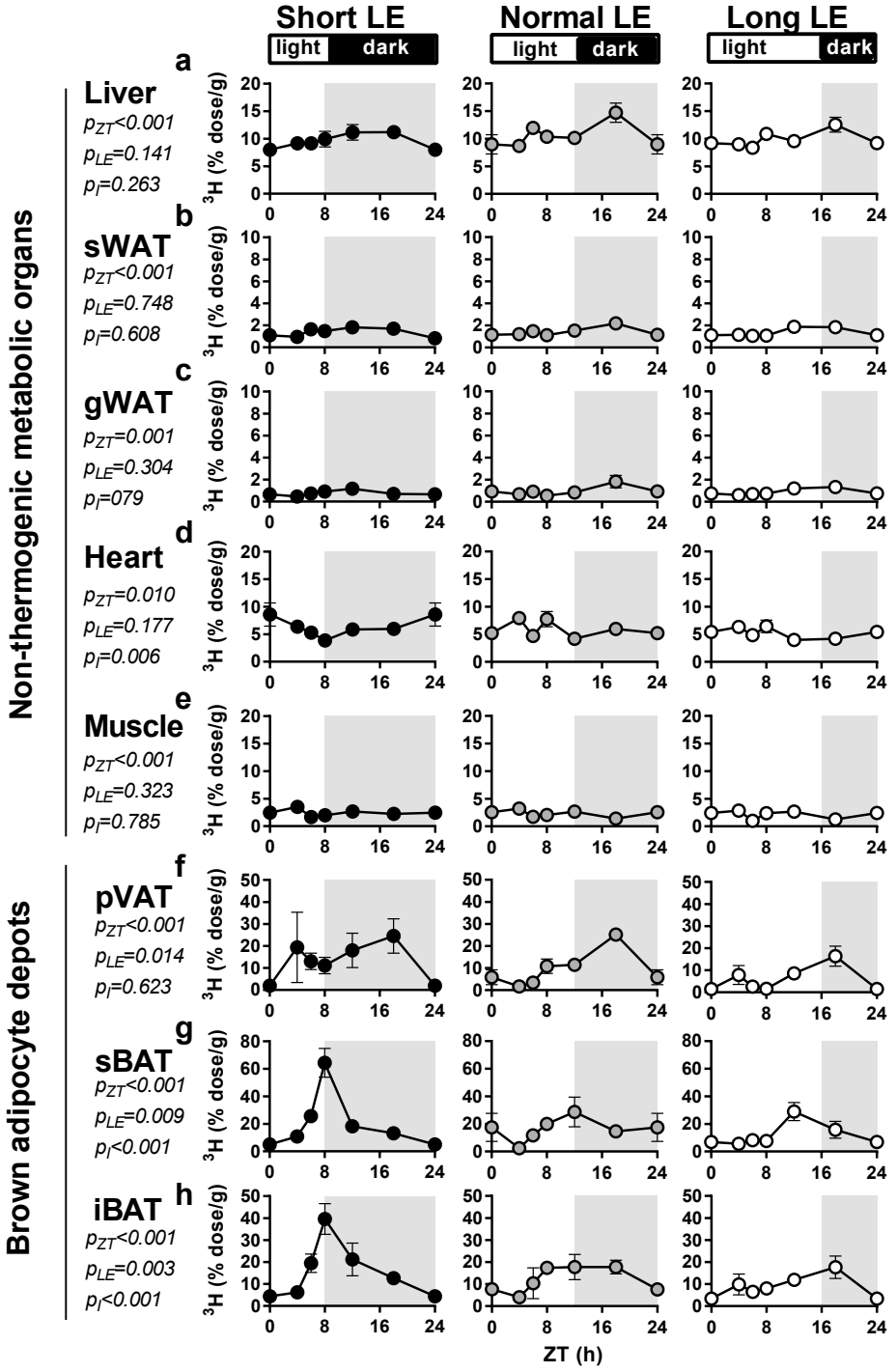
Short LE
Normal LE
Long LE
light
dark
Non-thermogenic metabolic organs
Brown adipocyte depots
a
Liver
p_{ZT}<0.001
p_{LE}=0.141
p_I=0.263
b
sWAT
p_{ZT}<0.001
p_{LE}=0.748
p_I=0.608
c
gWAT
p_{ZT}=0.001
p_{LE}=0.304
p_I=079
d
Heart
p_{ZT}=0.010
p_{LE}=0.177
p_I=0.006
e
Muscle
p_{ZT}<0.001
p_{LE}=0.323
p_I=0.785
f
pVAT
p_{ZT}<0.001
p_{LE}=0.014
p_I=0.623
g
sBAT
p_{ZT}<0.001
p_{LE}=0.009
p_I<0.001
h
iBAT
p_{ZT}<0.001
p_{LE}=0.003
p_I<0.001
^{3}H (% dose/g)
ZT (h)

Irrespective of the daily LE period, highest [^{3}H]FA uptake by iBAT and sBAT was reached around the onset of the dark period (Fig. 1g-h and Table 1). Notably, short daily LE increased the area under the curve for [^{3}H]FA uptake (Supplementary Fig. 1a) and increased the average daily [^{3}H]FA uptake of all time points by iBAT (+90%; p=0.016), sBAT (+107%; p=0.028) and pVAT (+130%; p=0.030) compared to long daily LE (Supplementary Fig. 1b). The LE length negatively correlated with the average [^{3}H]FA uptake by iBAT (p=0.006, R^2=0.11), sBAT (p=0.010, R^2=0.11) and pVAT (p=0.011, R^2=0.10) (Supplementary Fig. 1c-e) but not by other metabolic organs (not shown).

We previously showed that LE duration affects FA uptake by BAT via sympathetic outflow [8]. However, LE can also induce behavioral adaptations in food intake behavior and physical activity patterns [18]. Since we observed that adaptation of behavioral activity patterns to short and long LE (Supplementary Figure 1f-g), we further investigated the adaptations of whole energy metabolism in an additional group of mice housed at normal LE by diurnal measurements of EE, respiratory exchange rate (RER, a surrogate of substrate utilization), food intake, and ambulatory activity. Both calorimetric and behavioral rhythms showed distinct 24h patterns (Fig. 2a, c, e, g), with a sharp rise in food intake and ambulatory activity at the start of the dark period and a secondary peak in the last 4 h of the dark period. During the light period, food intake and ambulatory activity were nearly absent and RER was low, reflecting the resting period of mice. Subsequently, the mice were entrained to either short or long daily LE. Animals adapted to short LE displayed a longer period of wakefulness compared to long LE, as evidenced by the extended ambulatory activity and food intake duration in the dark period, which was accompanied by increased 24h EE (+15%, p=0.050, Fig. 2b), RER (+2%, p=0.012, Fig. 2d) and ambulatory activity (+90%, p<0.001 Fig. 2h). However, despite changes in food intake patterns, total daily food intake was similar between the groups (Fig. 2f). Correlation analysis revealed strong positive correlations between EE and ambulatory activity (R^2=0.91 (short LE), R^2=0.80 (long LE); p<0.001), and to a lesser extent also between EE and food intake (R^2=0.74 (short LE) R^2=0.91 (long LE); p<0.001) in both short and long LE (Supplementary Fig. 2). Together, these data demonstrate that LE duration induces adaptations of diurnal BAT activity and concomitantly in diurnal patterns of ambulatory activity and food intake, which are reflected in the rhythm in total EE. Since these changes occur simultaneously, we cannot conclude whether behavioral and metabolic effects are causally related. FA uptake by BAT was generally determined

Figure 1. (left page) Diurnal rhythm of TG-derived FA uptake by BAT adapts to daily light exposure. *Wild-type mice were entrained to daily light exposure (LE) regimes of 8h (short LE), 12h (normal LE) or 16h (long LE) at standard 22°C ambient temperature for 5 weeks. Mice were injected with glycerol tri[^{3}H]oleate-labeled lipoprotein-like particles at 6 time points (n=4/group) and killed 15 min after the injection. The uptake of [^{3}H]oleate was determined for liver (a), subcutaneous white adipose tissue (sWAT) (b), gonadal WAT (gWAT) (c), heart (d), skeletal muscle (e), perivascular adipose tissue (pVAT) (f), subscapular brown adipose tissue (sBAT) (g) and interscapular BAT (iBAT) (h). Times are given as Zeitgeber times (ZT) in hours with onset of light period at ZT0. Data are presented as means ±SEM and ZT0/ZT24 was double plotted for visualization purposes. p_{ZT}, p_{LE} and p_I represent p-values for the factors Zeitgeber Time, daily LE and interaction, respectively (two-way ANOVA).*

	Minimum FA uptake (% of dose/g)			Maximum FA uptake (% of dose/g)			Range of FA uptake (% of dose/g)			Fold range (max/min)			Peak time (ZT)			Trough time (ZT)		
	Short LE	Normal LE	Long LE	Short LE	Normal LE	Long LE	Short LE	Normal LE	Long LE	Short LE	Normal LE	Long LE	Short LE	Normal LE	Long LE	Short LE	Normal LE	Long LE
Liver	8.0 ±0.8	8.7 ±0.1	8.4 ±0.7	11.2 ±0.3	14.7 ±1.8	12.5 ±1.4	3.2	6.0	4.2	1.4	1.7	1.5	18	18	18	0	4	6
sWAT	0.9 ±0.1	1.1 ±0.1	1.1 ±0.1	1.8 ±0.3	2.2 ±0.5	1.9 ±0.4	0.9	1.1	0.8	1.9	2.0	1.8	12	18	12	4	8	6
gWAT	0.5 ±0.1	0.6 ±0.1	0.6 ±0.1	1.2 ±0.2	1.8 ±0.6	1.3 ±0.4	0.7	1.3	0.7	2.5	3.3	2.2	12	18	18	4	8	4
Heart	3.9 ±0.3	4.2 ±0.7	4.0 ±0.4	8.6 ±2.1	7.9 ±0.6	6.5 ±1.1	4.7	3.8	2.5	2.2	1.9	1.6	0	4	8	8	12	12
Muscle	1.6 ±0.2	1.4 ±0.1	1.0 ±0.2	3.5 ±0.3	3.2 ±0.3	2.9 ±0.2	1.9	1.8	1.9	2.1	2.3	2.8	4	4	4	6	18	6
pVAT	2.0 ±0.5	1.7 ±0.2	1.5 ±0.2	24.5 ±7.8	25.2 ±2.3	16.4 ±4.6	22.5	23.6	14.9	12.4	15.3	11.2	18	18	18	0	4	0
sBAT	4.9 ±3.1	2.4 ±0.5	5.5 ±1.6	64.5 ±10.5	28.6 ±10.8	28.9 ±6.6	59.5	26.3	23.4	13.0	12.0	5.2	8	12	12	0	4	4
iBAT	3.4 ±0.6	4.1 ±0.8	4.4 ±0.9	39.6 ±7.0	17.7 ±5.8	17.6 ±5.1	36.1	13.7	13.2	11.6	4.3	4.0	8	12	18	0	4	0

Table 1. Parameters of [^{3}H]oleate uptake by metabolic organs in mice adapted to short, normal and long daily light exposure. *Wild-type mice were entrained to short (8h), normal (12h) or long (16h) daily light exposure (LE) at an ambient temperature of 22°C for five weeks. Mice were injected with glycerol tri[^{3}H]oleate-containing lipoprotein-like particles at 6 time points (n=4/ group), sacrificed and uptake of [^{3}H]oleate derived activity was determined for liver, subcutaneous white adipose tissue (sWAT), gonadal white adipose tissue (gWAT, heart, muscle, perivascular white adipose tissue (pVAT), subscapular brown adipose tissue (sBAT) and interscapular brown adipose tissue (iBAT). Minimum and maximum fatty acid (FA) uptake (% of injected dose per gram) were taken from observations at two of these 6 time points, the difference being defined as range of FA uptake. Peak and trough times are given as Zeitgeber times (ZT) in hours (ZT0 represents lights on). Data presented as means ± SEM.*

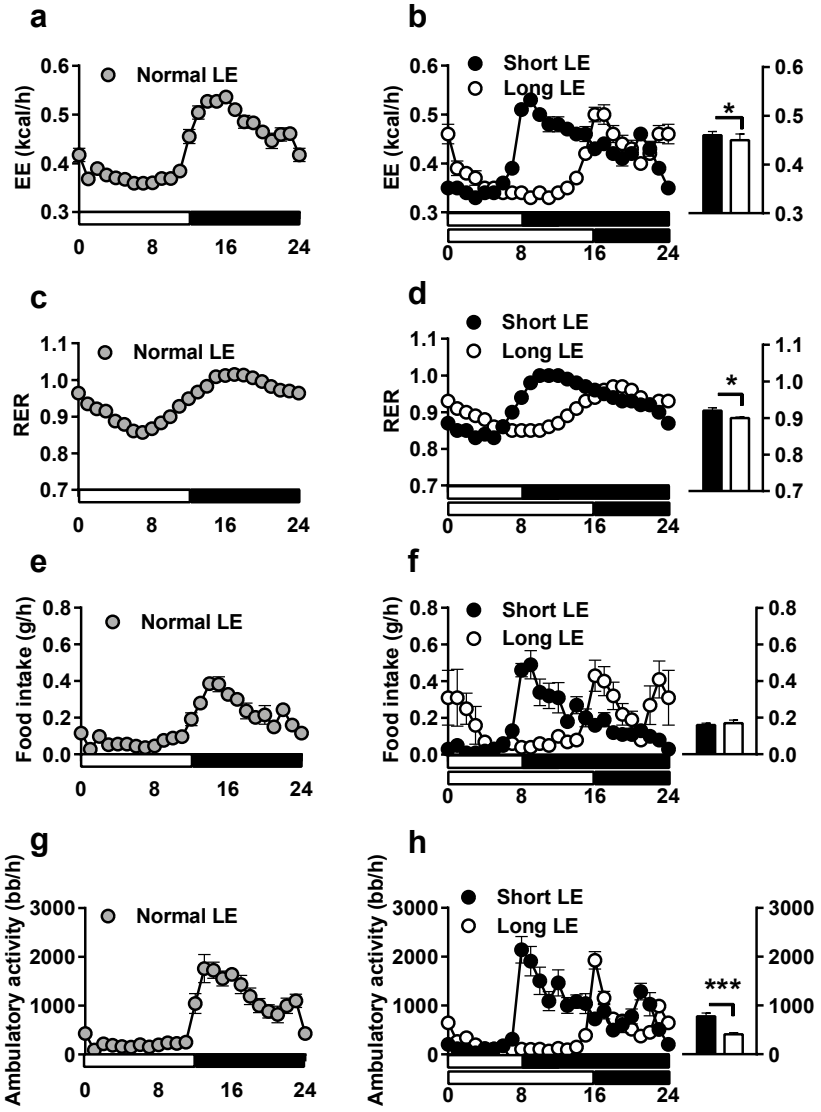

Figure 2. Indirect calorimetry of mice adapted to normal, and short or long daily light exposure. *Indirect calorimetry of mice adapted to normal, and short or long daily light exposure. Wild-type mice were entrained to a daily light exposure (LE) regime of 12h (normal LE) and energy expenditure (EE; a), respiratory exchange ratio (RER; c), food intake (e) and ambulatory activity (g) were determined by means of indirect calorimetry. Subsequently mice were adapted to daily LE regimes of 8h (short LE) or 16h (long LE) and the same factors were measured (b, d, f, h). Data points in the curves represent 1h binned values over a total of three consecutive days. Bars represent the average daily value. Data are presented as means ± SEM of 15-16 mice. *p<0.05, ***p<0.001 (two-tailed independent samples T-tests).*

after a standardized 4h fasting period designed specifically to avoid confounding factors caused by recently ingested food. When experiments were repeated following an 8h fast, the results were similar to 4h of fasting (Supplementary Fig. 3). Therefore, the length of fasting did not determine the difference in FA uptake by BAT between morning and evening.

The 24h rhythm in fatty acid uptake by BAT is reflected by rhythmicity in LPL and ANGPTL4 levels

Since BAT displayed such a remarkable daily rhythm in TG-derived FA uptake and adaptation to light-dark cycles, we investigated possible regulatory pathways in iBAT. At the cellular level, clock proteins drive tissue-specific rhythmic gene expression, which has been extensively studied *in vitro* and *in vivo* for liver tissue [19, 20], but only to a limited extent for BAT [5, 21, 22]. We first confirmed diurnal expression of the clock genes *Rev-erbα* (Fig. 3a) and *Per2* (Fig. 3b), both of which are known to have a role in BAT thermogenesis [3, 4]. Next, we assessed expression of a broad set of genes involved in BAT thermogenesis (Supplementary Figure 3a). We observed marked diurnal rhythms in expression of transcription factors (*Pgc1α* and *Prdm16*) and genes involved in thyroid hormone signaling (*Dio2* and *Thrα1*). To a lesser extent, rhythms were found in the beta-adrenergic receptor (*Adrb3*) and fatty acid transport and metabolism genes (*Fatp1, Elovl3, Hsl, Atgl, Vldlr*), while expression of mitochondrial genes and beige adipose markers were mostly independent of time. Expression of the key thermogenic gene *Ucp1* was found to be rhythmic with an advanced peak in short LE (Fig. 3c). Importantly, the expression pattern of lipoprotein lipase (*Lpl*), an enzyme crucial for the uptake of TG-derived FA [1], was rhythmic (Fig. 3d), correlated with the [^{3}H]FA uptake by iBAT (R^2=0.1833; p<0.001; Supplementary Fig. 3a), and was inverse to its repressor angiopoietin-like 4 (*Angptl4*) [23] (Fig. 3e). Consistent with the gene expression pattern, protein levels of total LPL as well as active LPL were highest at the onset of the dark period and the diurnal pattern adapted to the daily LE. Total LPL levels correlated with the [^{3}H]FA uptake by iBAT (R^2=0.5258; p<0.001; Supplementary Fig. 3b), while ANGPTL4 levels displayed an inverse rhythm reaching a peak at the onset of the light period (Fig. 3f-i). In particular, the levels of mature glycosylated LPL, representing LPL located in the Golgi or on the cell surface sensitive to ANGPTL4 [23], were regulated by the daily LE duration (Fig. 3i). Interestingly, while repression of *Ucp1* expression was previously

Figure 3. (right page) Diurnal rhythm in BAT lipoprotein lipase and angiopoietin-like 4 adapts to daily light exposure. *Wild-type mice were entrained to daily light exposure (LE) regimes of 8h (short LE), 12h (normal LE) or 16h (long LE) at standard 22°C ambient temperature for 5 weeks. Interscapular brown adipose tissue (iBAT) was harvested at six time points (n=4/group). Gene expression was determined by qPCR, calculated relative to 36b4 and Hprt expression, and normalized to mean expression of ZT0 of normal LE group (a-e). Protein levels were determined by Western blot as normalized to HSP90 (f-i). Amount of mature glycosylated LPL protein was determined by EndoH digestion. EndoH-sensitive LPL (ER LPL) is indicated with S; EndoH-resistant LPL (Golgi and cell surface LPL) is indicated with R (i). Data are presented as means ± SEM and ZT0/ZT24 was double plotted for visualization purposes. p_{ZT}, p_{LE} and p_I represent p-values for the factors Zeitgeber Time (ZT), LE and interaction respectively (two-way ANOVA).*

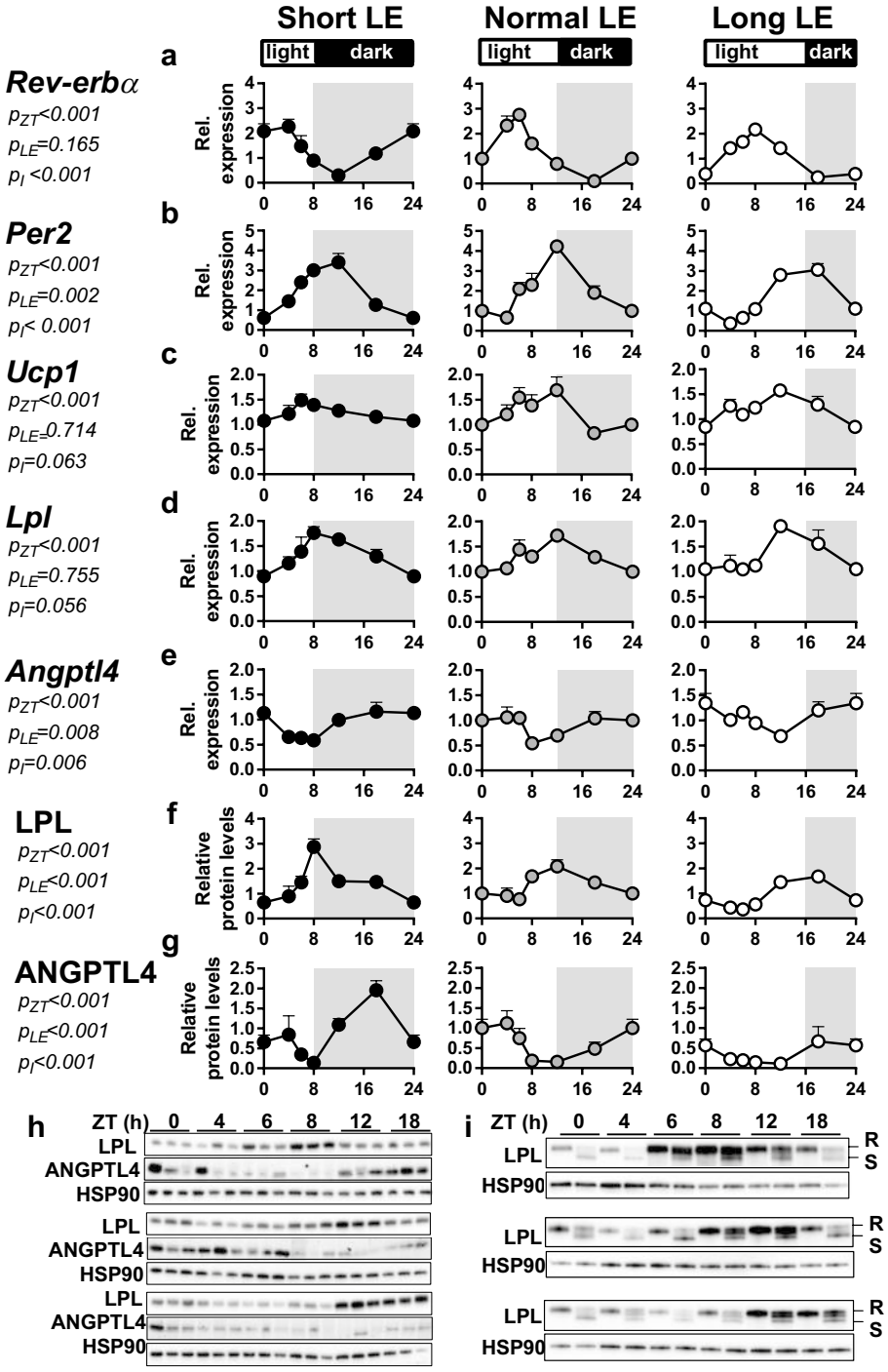
Short LE
Normal LE
Long LE
light
dark
a
b
c
d
e
f
g
Rev-erbα
pZT<0.001
pLE=0.165
pI <0.001
Per2
pZT<0.001
pLE=0.002
pI< 0.001
Ucp1
pZT<0.001
pLE=0.714
pI=0.063
Lpl
pZT<0.001
pLE=0.755
pI=0.056
Angptl4
pZT<0.001
pLE=0.008
pI=0.006
LPL
pZT<0.001
pLE<0.001
pI<0.001
ANGPTL4
pZT<0.001
pLE<0.001
pI<0.001
Rel. expression
Relative protein levels
h
ZT (h) 0 4 6 8 12 18
LPL
ANGPTL4
HSP90
i
R
S

found to be dependent on the rhythmic expression of clock gene *Rev-erbα* [3] this was not the case for expression of *Lpl* and *Angptl4* (Supplementary Fig. 3d).

The diurnal rhythm in FA uptake by BAT determines diurnal variations in plasma lipid levels and postprandial lipid responses in a mouse model of human lipoprotein metabolism

Activation of BAT has been shown to lower plasma TG levels [1, 13, 24]. Therefore, we next investigated the effect of the physiological rhythm in BAT activity on daily plasma TG and FA levels. To this end we used female APOE*3-Leiden.CETP mice, which is a well-established model for human-like lipoprotein metabolism [13, 25]. We first confirmed that these mice adapt to LE regimes in a similar fashion as wild-type mice. Mice were entrained for 5 weeks to short or long daily LE of which a subset was equipped with telemetric transmitters to monitor rhythms in ambulatory activity and in addition core body temperature. In both groups, ambulatory activity and body core temperature displayed a diurnal pattern, with a rise in ambulatory activity at the start of the dark period (Fig. 4a) and a rise in temperature just before the onset of dark period (Fig. 4c). In contrast to the wild-type animals, adaptation to the LE regimes did not affect total 24h ambulatory activity (Fig. 4b). Also the average body temperature remained unaffected (Fig. 4d). These adaptations were accompanied by a peak in corticosterone plasma concentrations at the onset of the dark period (Figure 4e-f). To study body temperature as a function of ambulatory activity a Reitman plot was generated, showing temperature as a function of physical activity [26]. The difference between the light and dark curves represents ambulatory activity-independent heat production, arising from either central modulation of heat loss [27, 28] or thermogenesis [29]. In mice adapted to short daily LE, there was a large light-dark difference (Fig. 4g), most likely reflecting the diurnal amplitude in BAT activity. Interestingly, in line with our observation that BAT activity may be lower in long LE, the difference between the curves for light and dark period disappeared in mice entrained to long LE (Fig. 4h) suggesting partial loss of activity-independent regulation of the body temperature.

Figure 4. (right page) Diurnal rhythms in physiological parameters are present in dyslipidemic APOE*3. Leiden-CETP mice. *APOE*3-Leiden.CETP mice, fed a western type diet, were entrained to daily light exposure (LE) regimes of 8h (short LE) or 16h (long LE) and implanted with telemetric transmitters (n=4-5/group) to measure body temperature and ambulatory activity. Five representative days of ambulatory activity rhythms (a) (black lines = short LE, grey lines = long LE) and body temperature rhythms (c) are shown. Mean 24h ambulatory activity (b) and body temperature (d) were calculated. Stress-free blood samples were obtained at ZT0, 8 and 16 and corticosterone was determined (e-f). The quadratic fit of the body temperature to the ambulatory activity was calculated separately for the dark and light periods for mice adapted short LE (g) or long LE (h). Dotted lines show the 95% confidence intervals of the fitted curves. 7 consecutive blood samples were drawn and TG (i-j) and free FA (k-l) levels were determined. pZT and pI represent p-values for the factors Zeitgeber Time (ZT) and interaction of LE on ZT respectively (two-way RM-ANOVA). Data are presented as means ± SEM. *p<0.05, **p<0.01, ***p<0.001, ****p<0.0001 (compared to ZT0, Dunnett's post-hoc test).*

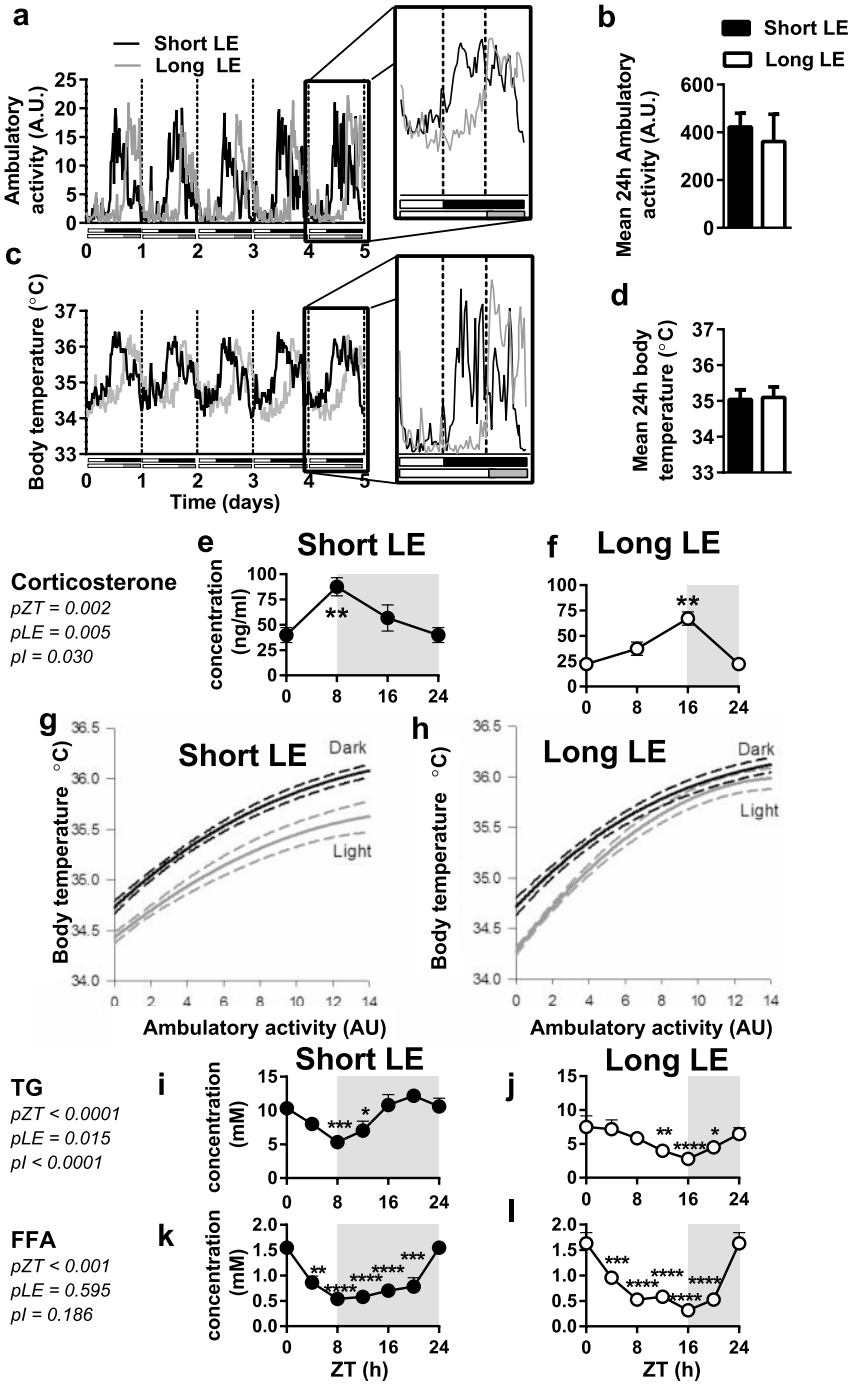
a
Short LE
Long LE
Ambulatory activity (A.U.)
b
Short LE
Long LE
Mean 24h Ambulatory activity (A.U.)
c
Body temperature (°C)
Time (days)
d
Mean 24h body temperature (°C)
Corticosterone
pZT = 0.002
pLE = 0.005
pI = 0.030
e
Short LE
concentration (ng/ml)
f
Long LE
g
Short LE
Dark
Light
Body temperature °C)
Ambulatory activity (AU)
h
Long LE
Dark
Light
Body temperature °C)
Ambulatory activity (AU)
TG
pZT < 0.0001
pLE = 0.015
pI < 0.0001
i
Short LE
concentration (mM)
j
Long LE
FFA
pZT < 0.001
pLE = 0.595
pI = 0.186
k
concentration (mM)
ZT (h)
l
ZT (h)

We measured non-fasted plasma lipid levels every 4h within a single day. Plasma TG and free FA levels were found to be rhythmic and were strongly dependent on LE duration (Fig. 4i-l). Lowest TG and free FA levels were reached at the onset of the dark period (i.e. ZT8 for short day, ZT16 for long day). To evaluate whether these rhythms in plasma lipid levels were determined by the adaptive rhythm in FA uptake by BAT, we assessed the TG-derived FA uptake at three time points to confirm the high morning-evening amplitude of BAT activity. Indeed, like in wild-type mice, the uptake of [^{3}H]FA specifically by the BAT depots was high at the onset of the dark period in APOE*3-Leiden.CETP mice either adapted to a short LE (Fig. 5a) or long LE (Fig. 5b). This coincided with a faster clearance of plasma [^{3}H]FA at the onset of the wakeful period for mice adapted either to a short LE (Fig. 5c-d) or long LE (Fig. 5e-f). As BAT was the only organ found to adapt to changes in LE, these data strongly suggest that diurnal rhythms in BAT activity are responsible for the time-dependent clearance of TG from the circulation.

To further investigate the consequence of the diurnal BAT activity for plasma lipid metabolism, we determined postprandial excursions of TG and free FA following an oral bolus of olive oil given when BAT was active or inactive (Fig. 6a). Comparable to the unfasted state (Fig. 4g-j), baseline 4h fasted plasma TG and free FA levels were low at the start of the dark period (Fig. 6b-c). In the mice adapted to short LE, the time of day at which the oral TG bolus was given clearly determined excursions of both plasma TG (p_{ZT}<0.001) (Fig. 6d) and free FA (p_{ZT}=0.010) (Fig. 6g). In addition, the area under the curve (AUC) was lowest when the oral TG bolus was given at the onset of the dark period (ZT8) for both TG (ZT0/8/16: 64±6 /33±3 /84±5 mM*h, p<0.001 compared to ZT0) (Fig. 6f) and free FA (ZT0/8/16: 11.4±0.9/ 8.7±0.5 /15.0±1.1 mM*h, p<0.001 (ZT0 *vs.* 16)) (Fig. 6i). Similarly, timing of the oral TG bolus in mice adapted to long LE determined the postprandial TG (p_{ZT}<0.001) (Fig. 6e) and free FA (p_{ZT}<0.001) (Fig. 6h) response. The AUC was lowest at the onset of the dark period (ZT16) for both TG (ZT0/8/16: 96±12/ 64 ±5/ 33±3 mM*h, p<0.01 (compared to ZT0)) (Fig. 6f) and free FA (ZT0/8/16: 13.6±1.1/ 9.0±0.5/ 7.3±0.3mM*h, p<0.001 (ZT16 *vs.* ZT8) (Fig. 6i). Short and long LE significantly changed the time of day-dependent postprandial excursion for TG (p_{ZT}<0.001, p_{LE}=0.489, p_I<0.001) (Fig. 6f) and free FA (p_{ZT}<0.001, p_{LE}=0.011, p_I<0.001) (Fig. 6i).

To investigate whether the rhythm in FA uptake by BAT and the effects on (postprandial) lipid levels were dependent on (cold-induced) sympathetic activity, we repeated experiments at thermoneutrality (30°C). At this temperature, FA uptake by BAT still displayed a marked difference in morning-evening TG-derived uptake accompanied by a fast clearance of TG-derived FA at the onset of the dark period (Supplementary Figure 5a-c) and lower fasting concentrations of TG and FFA (Figure 6j, m). Following a bolus of olive oil, postprandial TG excursions were lower at the onset of dark compared to light (Figure 6k-l). In contrast, postprandial FFA excursions were comparable at both time points, suggesting an overall decreased BAT activity, also evident by the observation that the curves do not return to baseline (Figure 6n-o).

Collectively, irrespective of the LE regime, the highest removal rate of oral TG-derived FA from plasma was observed at the start of the dark period when FA uptake by BAT was also highest, both at (30°C) or below (22°C) thermoneutrality. As a consequence, plasma

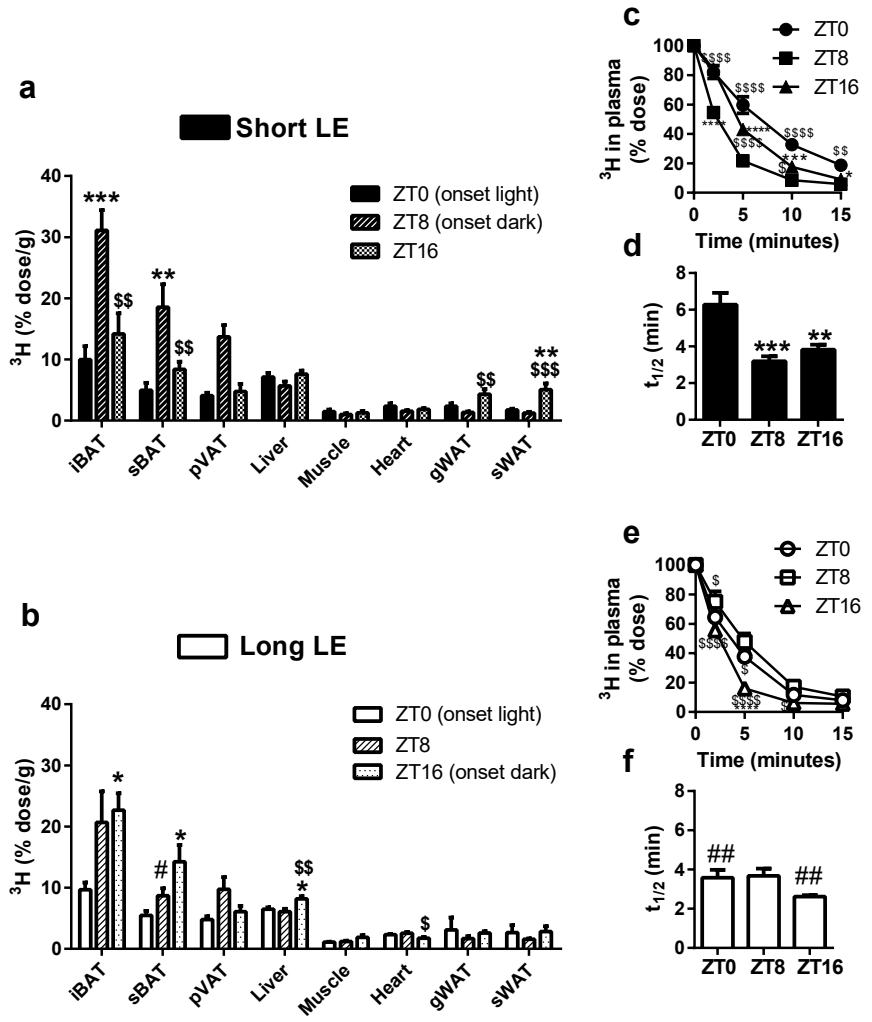

Figure 5. Diurnal rhythm in BAT activity in dyslipidemic mice adapts to daily light exposure. APOE*3-Leiden. *CETP mice, fed a western type diet, were entrained to daily light exposure (LE) regimes of 8h (short LE) or 16h (long LE). After five weeks, mice were injected with glycerol tri[^{3}H]oleate-labeled lipoprotein-like particles at three time points (ZT0, ZT8 or ZT16) (n=7-8/group). Organ uptake of [^{3}H]oleate was determined (a, b). Plasma clearance of [^{3}H]oleate was determined (c, e) and half-life ($t_{1/2}$) was calculated (d, f). Data are presented as means ± SEM. *p<0.05, **p<0.01, ***p<0.001, ****p<0.0001 (compared to ZT0), $$$ p<0.001, $$$$ p<0.0001 (compared to ZT8) (ANOVA, Tukey's post hoc test (a, b, d, f); RM-ANOVA with Dunnett's post hoc test (c, e)). #p<0.05, ##<0.01 (short vs. long LE, Student's T-test). iBAT = interscapular BAT, sBAT= subscapular BAT, pVAT = perivascular adipose tissue; gWAT = gonadal white adipose tissue; sWAT = subcutaneous WAT.*

	All (n=37)	Men (n=19)	Women (n=18)
Age (y)	65.2 ± 0.9	65.7 ± 1.2	64.6 ± 1.2
BMI (kg/m^2)#	25.1 ± 0.6	25.5 ± 0.7	24.6 ± 1.1
Fat mass (%)#	31.5 ± 1.4	24.8 ± 1.0	38.2± 1.2 $^{\$\$\$}$
Current smokers (n)	1	1	0

Table 2. Characteristics of the study population. *Data are presented as means ± SEM or number (current smokers).* $^{\$\$\$}$ *p<0.001 men vs. women.* #*data of 1 person are missing.*

levels of TG and free FA as well as postprandial lipid responses were lowest at the start of the dark period. Although we cannot exclude that the rhythmic uptake of nutrients from the gut may also have contributed to the observed effects, we concluded that lipids consumed at beginning of the active, wakeful period are very efficiently combusted by BAT.

Postprandial lipid response in humans is dependent on the time of the day

To evaluate whether timing of nutrient intake also determines postprandial lipid metabolism in humans, we determined the postprandial lipid response after an isocaloric meal at three time points of the day in a cohort of 37 healthy individuals [16] (characteristics are shown in Table 2). Participants were allowed to sleep from 23.00h to 8.00h, during which lights were off, and consumed a standard liquid test meal at clock time 9.00h, 12.00h and 18.00h. Consistent with our observations in mice, postprandial free FA levels were low at the onset of the wakeful period (at 9.00h) and highest in the evening (Fig. 6j). Postprandial free FA excursions (measured as 3h postprandial area under the curve (AUC) gradually increased from 9.00h (AUC 1.64±0.09 mM*h) via 12.00h (AUC 1.89±0.13 mM*h; p=0.004) to at 18.00h (AUC 2.52±0.17 mM*h; p<0.0001) (Fig. 6k). We previously showed that TG levels of this cohort were highly rhythmic [11]. The postprandial excursions at 9.00h (AUC 3.2±0.2 mM*h) were lower compared to 12.00h (AUC 5.0±0.3 mM*h; p<0.0001) and 18.00h (AUC 4.0±0.2 mM*h; p<0.001) (Supplementary Fig. 5d-e), but in contrast to mice, absolute plasma TG values start to decline after 14.00h. Since clearance of plasma TG via LPL-mediated lipolysis results in FA 'spillover' into plasma that contributes up to 50% of postprandial plasma free FA concentrations in humans [30], FA levels likely inversely reflect the capacity of metabolic organs including BAT to take up TG-derived FA. Collectively these data show the postprandial lipid response to be lowest at the start of the wakeful period in mice as well as humans.

DISCUSSION

In this study, we have shown that BAT in mice displays a strong diurnal rhythm with respect to uptake of TG-derived FA from the circulation, likely regulated through diurnal LPL activity within the tissue. In addition, FA uptake specifically by BAT and not by other organs was found to readily adapt to modulation of the daily LE. The peak in FA uptake by BAT peaked was aligned to the light-dark cycles and consistently occurred at the onset of the dark period. The daily pattern of BAT activity inversely related to daily patterns of plasma TG and FA levels and determined postprandial handling of TG in mice and possibly also in humans.

We first investigated time-dependent differences in the uptake of FA by metabolically active organs. We observed a steep rise in uptake of FA by BAT activity in anticipation of the dark period which corresponded with a rise in the core body temperature and EE. Within the tissue, we identified rhythms in the core clock genes *Rev-erbα* and *Per2* as well as the key thermogenic gene *Ucp1.* In line with a previous report, *Ucp1* expression was in anti-phase with the expression of its transcriptional repressor *Rev-erbα* [3]. Importantly, we identified a diurnal rhythm in mRNA expression and protein levels of LPL, a protein critical for TG-derived FA uptake [2, 31], which correlated with FA uptake by BAT. In addition, mRNA and protein levels of ANGPTL4 were found to be rhythmic and almost undetectable at the onset of the dark period. We previously demonstrated that ANGPTL4 is a potent inhibitor of LPL function [23], therefore we anticipate that the combined effect of high levels of active LPL and low levels of ANGPTL4 causes the peak in FA uptake by BAT before the onset of the dark period.

How diurnal BAT activity is regulated exactly remains to be determined. The central biological clock (located in the suprachiasmatic nucleus of the hypothalamus) orchestrates diurnal anticipatory adaptations of energy metabolism through a complex interplay of endocrine, neuronal and behavioral factors. These oscillating factors can influence metabolic processes either directly or indirectly through synchronization of the cell-autonomous clocks. BAT activity has been shown to be modulated at all of these levels of regulation. Examples include the modulation of BAT activity through food intake, physical activity, hormones such as glucocorticoids [32] and thyroid hormone [33], which are also known to adapt to seasonal cues [34, 35], and the cell-autonomous regulation through Per2 [4] and Rev-erbα [3]. In addition, we previously showed that sympathetic innervation of BAT is affected by prolonged daily LE [8].

We investigated the adaptation of the tissue to changes in the environment, in this case daily LE duration, a physiological signal of the time of year. Interestingly, we observed a specific adaptation in activity of BAT with respect to FA uptake, and not in that of other metabolic organs. It is tempting to speculate on the reasons why BAT is relatively more sensitive to changes in daily LE. BAT has evolved as a natural defense system against hypothermia and the physiological importance of a seasonal and diurnal rhythm in BAT activity likely relates to this. From an evolutionary perspective, it would be waste of energy to have BAT constitutively active. Our data indicates that diurnal BAT activity is aligned with wakening, before which body temperatures are generally low and the body potentially will

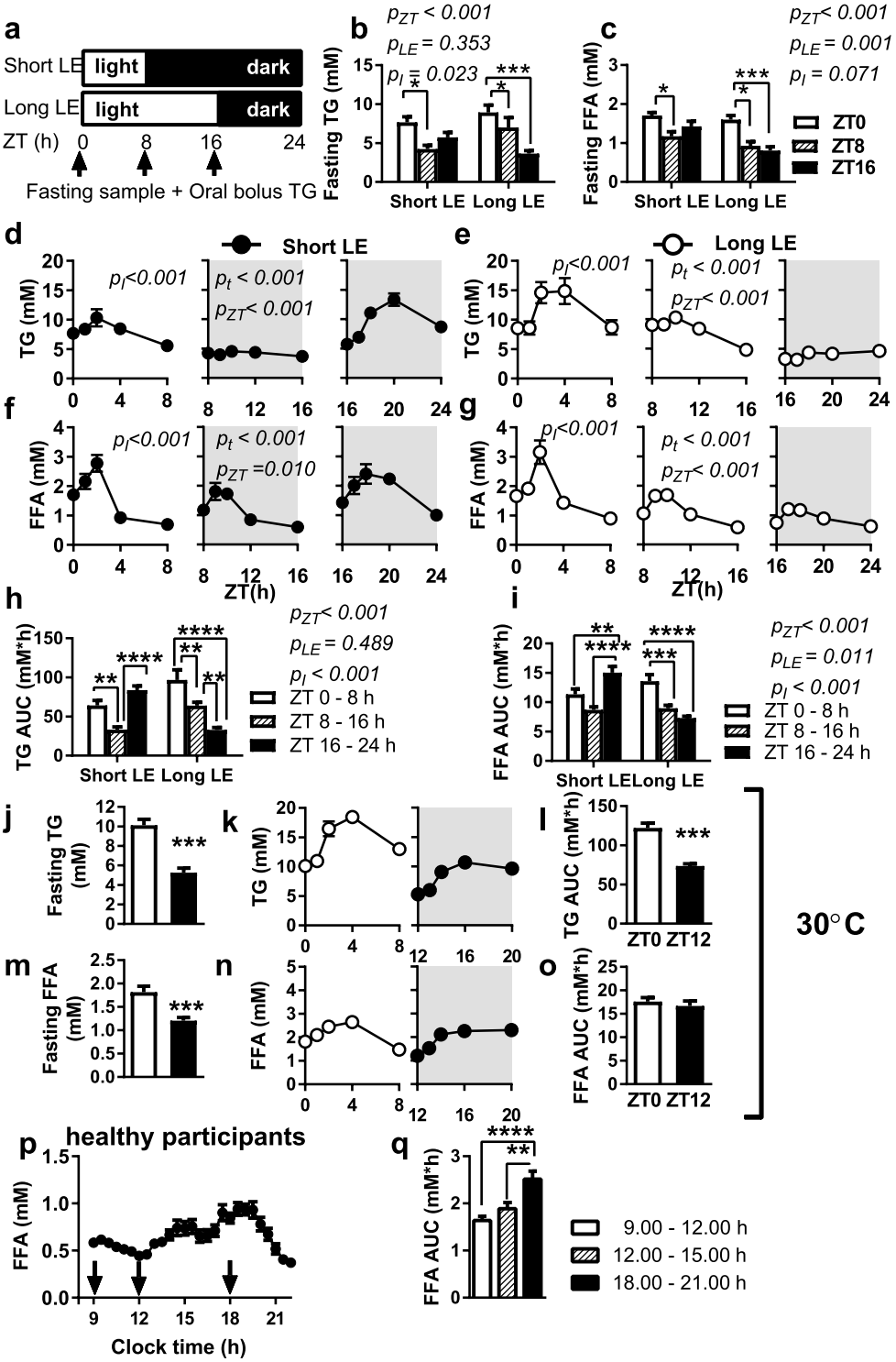
a
Short LE
light
dark
Long LE
light
dark
ZT (h) 0 8 16 24
Fasting sample + Oral bolus TG
b
p_{ZT} < 0.001
p_{LE} = 0.353
p_I = 0.023
Fasting TG (mM)
Short LE Long LE
c
p_{ZT}< 0.001
p_{LE} = 0.001
p_I = 0.071
Fasting FFA (mM)
ZT0
ZT8
ZT16
Short LE Long LE
d
Short LE
TG (mM)
p_I<0.001
p_t < 0.001
p_{ZT}< 0.001
e
Long LE
TG (mM)
p_I<0.001
p_t < 0.001
p_{ZT}< 0.001
f
FFA (mM)
p_I<0.001
p_t < 0.001
p_{ZT} =0.010
ZT(h)
g
FFA (mM)
p_I<0.001
p_t < 0.001
p_{ZT}< 0.001
ZT(h)
h
TG AUC (mM*h)
p_{ZT}< 0.001
p_{LE} = 0.489
p_I < 0.001
ZT 0 - 8 h
ZT 8 - 16 h
ZT 16 - 24 h
Short LE Long LE
i
FFA AUC (mM*h)
p_{ZT}< 0.001
p_{LE} = 0.011
p_I < 0.001
ZT 0 - 8 h
ZT 8 - 16 h
ZT 16 - 24 h
Short LE Long LE
j
Fasting TG (mM)
k
TG (mM)
l
TG AUC (mM*h)
ZT0 ZT12
30°C
m
Fasting FFA (mM)
n
FFA (mM)
o
FFA AUC (mM*h)
ZT0 ZT12
p
healthy participants
FFA (mM)
Clock time (h)
q
FFA AUC (mM*h)
9.00 - 12.00 h
12.00 - 15.00 h
18.00 - 21.00 h

be exposed to cold environmental conditions. This observation could be analogous to the indispensable rise in BAT activity during arousal in hibernating mammals [36, 37]. Consistent with these data, previous studies demonstrated a stronger increase in oxygen consumption in response to cold at the start of the wakeful period in mice [3] and an enhanced insulin-stimulated glucose uptake by human BAT explant in the morning[7]. Furthermore, mice with dysfunctional BAT through genetic modification or denervation display an aberrant sleep phenotype [38]. Since short LE signals winter, which is accompanied by lower temperatures, it stands to reason that short LE is an anticipatory signal to increase overall thermogenesis while long LE results in diminished heat production.

Importantly, changes in daily LE duration are pertinent to metabolic health. Human studies have shown that exposure to light at night correlates to a higher body weight [39, 40] and prolonged duration of environmental light exposure predicts increased weight gain in children [41]. We previously identified impaired BAT activity as the potential missing link in the established association between perturbations in diurnal rhythms and metabolic disorders, by demonstrating that prolonged daily light exposure reduces BAT activity and induces adiposity in mice [8]. Moreover, we anticipate that diurnal BAT activity can be exploited to our benefit. We showed that postprandial lipids are lower in the morning than in the afternoon and propose that diurnal BAT activity is responsible for this phenomenon. In favor of this hypothesis and in line with our data, others have demonstrated that postprandial thermogenesis in humans is higher in the morning than in the evening [42] and that supraclavicular temperature, which was shown to associate with cold-induced glucose uptake by BAT [43] rises in the early morning [7].

Our data help to explain previous findings that time-restricted feeding contributes to metabolic phenotypes. Feeding mice at the biological 'wrong' time (i.e. the resting phase) increases body weight [44], while feeding at the 'right' time (i.e. the active phase) prevents diet-induced obesity and related health problems [45]. Humans eat virtually whenever they are awake [46]. Early eaters were shown to be more successful at weight-loss therapy than late eaters independent of caloric intake [47] and limited caloric intake in the evening has

Figure 6. (left page) Postprandial lipid response depends on time of day in mice and humans. *APOE*3-Leiden.CETP mice, fed a western type diet, were entrained to daily light exposure (LE) regimes of 8h (short LE) or 16h (long LE) at 22°C (a-i) and an additional group was entrained to normal 12h LE and housed at 30°C 2 days prior to experiments (j-o). After four weeks, mice were fasted for 4h, blood was drawn and oral TG bolus was administered at three time points (ZT0, ZT8 or ZT16) (n=7-8/group) (a). Fasting TG (b, j) and FFA (c, m) were determined. Postprandial plasma TG excursion (d, e, j, k) and FFA (g, h, m, n) were determined at t = 1, 2, 4, and 8h after oral TG bolus. Postprandial AUC was calculated for TG (f,l) and FFA (i,p). 37 healthy individuals were fasted overnight before a diurnal venous blood sampling. At 9.00h, 12.00h, 18.00h a standard liquid meal was consumed. FFA levels were determined every 30 minutes (p) and postprandial AUC was calculated 3h after ingestion of isocaloric meal (q). Data presented as means ±SEM. *p<0.05, **,$$p<0.01, ***p<0.001, ****,$$$$p<0.0001. p_t, p_{ZT} p_i represent p-values for the factors postprandial time point and for ZT (time of day of oral gavage) and the interaction respectively, based on two-way RM-ANOVA (d,e,g,h) or two-way ANOVA, Tukey's post-hoc test (B,C,F,I). Arrows indicate oral TG bolus (a,d/g,e/h,n,o) or standard meal (p).*

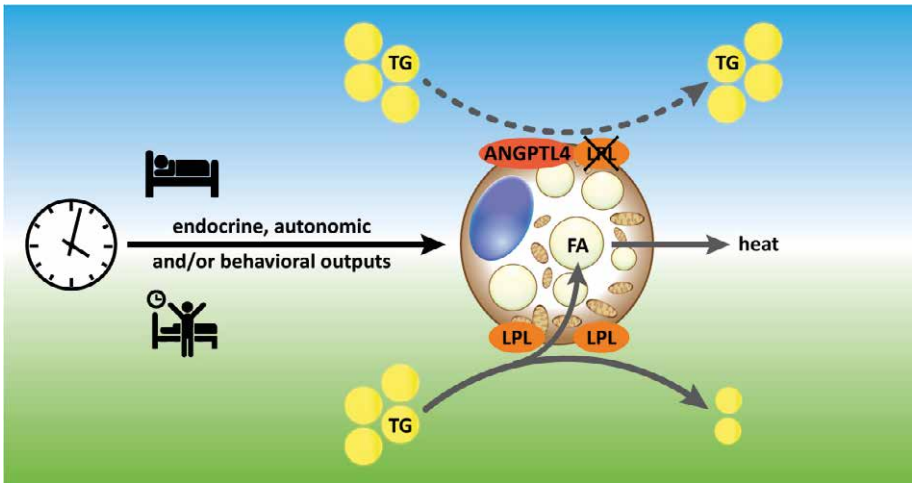

Figure 7. Graphical summary. *See text for explanation. ANGPTL4 = Angioprotein-like 4, FA = fatty acids, LPL = lipoprotein lipase, TG= triglycerides.*

been associated with lower body mass index [48, 49]. Indeed, when overweight individuals were asked to limit the duration of food intake to a maximum of 11 h daily [46] they were metabolically healthier and more energetic. Taken together, these data strongly suggest that timing of food intake defines the fate of consumed calories and imply that BAT has a higher capacity to take up FA and combust calories in the morning than in the evening (Figure 7). This might be a mechanistic basis for early timing of food intake as a potential strategy to improve metabolic health.

ACKNOWLEDGMENTS

The authors thank Janny P. van der Elst, Hetty C.M. Sips and Trea C.M. Streefland for excellent technical support, Steffy W. Jansen and Abimbola A. Akintola for inclusion of study participants and collection of biomaterials in the Switchbox study, and Mitch Lazar for the kind gift of the Rev-erbα$^{-/-}$ mice. **Funding**: This work was supported by the European Foundation for the Study of Diabetes (EFSD Rising Star Fellowship Programme to S Kooijman), the Netherlands Organization for Scientific Research (NWO-VENI grant 016.136.125 to NR Biermasz), the European Foundation for the Study of Diabetes and the Programme Partner Novo Nordisk (grant 94802 to CP Coomans, JH Meijer and PCN Rensen), the Dutch Diabetes Research Foundation (grant 2013.81.1663 to CP Coomans), the European funded projects Switchbox (FP7, Health-2010-259772), HUMAN (FP7, Health-2013-INNOVATION-1-602757) and aCROBAT (ERC Starting Grant 639382 to Z Gerhart-Hines), and 'the Netherlands CardioVascular Research Initiative: the Dutch Heart Foundation, Dutch Federation of University Medical Centers, the Netherlands Organisation

for Health Research and Development and the Royal Netherlands Academy of Sciences' for the GENIUS project 'Generating the best evidence-based pharmaceutical targets for atherosclerosis' (CVON2011-9) and the ENERGISE project 'Targeting energy metabolism to combat cardiovascular disease' (CVON2014-2). PCN Rensen is an Established Investigator of the Dutch Heart Foundation (grant 2009T038). **Author Contributions:** Conceptualization, RvdB, SK, NRB and PCNR; Methodology, RvdB, SK, NRB and PCNR; Investigation, RvdB, SK, AR, GAV, IMM, BK, WD, LT, RC, LSP, EdR and CPC; Resources, RN, CC, LWMvK, FK, SK, ZGH, Data Curation, RN and GAV; Writing – Original draft, RvdB and SK; Writing Review & Editing, NRB and PCNR; Supervision, JHM, DvH, NRB and PCNR; Funding Acquisition, CPC, ZGH, JHM, DvH, NRB and PCNR.

REFERENCES

1. Bartelt, A., *et al., Brown adipose tissue activity controls triglyceride clearance.* Nat. Med, 2011. **17**(2): p. 200-205.
2. Khedoe, P.P., *et al., Brown adipose tissue takes up plasma triglycerides mostly after lipolysis.* J. Lipid Res, 2015. **56**(1): p. 51-59.
3. Gerhart-Hines, Z., *et al., The nuclear receptor Rev-erbalpha controls circadian thermogenic plasticity.* Nature, 2013. **503**(7476): p. 410-413.
4. Chappuis, S., *et al., Role of the circadian clock gene Per2 in adaptation to cold temperature.* Mol. Metab, 2013. **2**(3): p. 184-193.
5. Zvonic, S., *et al., Characterization of peripheral circadian clocks in adipose tissues.* Diabetes, 2006. **55**(4): p. 962-970.
6. van der Veen, D.R., *et al., A diurnal rhythm in glucose uptake in brown adipose tissue revealed by in vivo PET-FDG imaging.* Obesity. (Silver. Spring), 2012. **20**(7): p. 1527-1529.
7. Lee, P., *et al., Brown Adipose Tissue Exhibits a Glucose-Responsive Thermogenic Biorhythm in Humans.* Cell Metab, 2016.
8. Kooijman, S., *et al., Prolonged daily light exposure increases body fat mass through attenuation of brown adipose tissue activity.* Proc. Natl Acad. Sci. U. S. A, 2015. **112**(21): p. 6748-6753.
9. Au-Yong, I.T., *et al., Brown adipose tissue and seasonal variation in humans.* Diabetes, 2009. **58**(11): p. 2583-2587.
10. Yoneshiro, T., *et al., Brown adipose tissue is involved in the seasonal variation of cold-induced thermogenesis in humans.* Am J Physiol Regul Integr Comp Physiol, 2016: p. ajpregu.00057.2015.
11. van den Berg, R., *et al., Familial longevity is characterized by high circadian rhythmicity of serum cholesterol in healthy elderly individuals.* Aging Cell, 2016: p. n/a-n/a.
12. Chua, E.C., *et al., Extensive diversity in circadian regulation of plasma lipids and evidence for different circadian metabolic phenotypes in humans.* Proc. Natl Acad. Sci. U. S. A, 2013. **110**(35): p. 14468-14473.
13. Berbee, J.F., *et al., Brown fat activation reduces hypercholesterolaemia and protects from atherosclerosis development.* Nat Commun, 2015. **6**: p. 6356.
14. Rensen, P.C., *et al., Selective liver targeting of antivirals by recombinant chylomicrons--a new*

therapeutic approach to hepatitis B. Nat Med, 1995. **1**(3): p. 221-225.

15. Davies, R.W., *et al.*, *Proteinuria, not altered albumin metabolism, affects hyperlipidemia in the nephrotic rat.* J Clin Invest, 1990. **86**(2): p. 600-5.
16. Jansen, S.W., *et al.*, *Human longevity is characterised by high thyroid stimulating hormone secretion without altered energy metabolism.* Sci. Rep, 2015. **5**: p. 11525.
17. Brown, N.K., *et al.*, *Perivascular adipose tissue in vascular function and disease: a review of current research and animal models.* Arterioscler. Thromb. Vasc. Biol, 2014. **34**(8): p. 1621-1630.
18. Warner, A., *et al.*, *Effects of photoperiod on daily locomotor activity, energy expenditure, and feeding behavior in a seasonal mammal.* Am J Physiol Regul Integr Comp Physiol, 2010. **298**(5): p. R1409-16.
19. Zheng, B., *Nonredundant roles of the mPer1 and mPer2 genes in the mammalian circadian clock.* Cell, 2001. **105**: p. 683-694.
20. Koike, N., *et al.*, *Transcriptional architecture and chromatin landscape of the core circadian clock in mammals.* Science, 2012. **338**(6105): p. 349-354.
21. Orozco-Solis, R., *et al.*, *The Circadian Clock in the Ventromedial Hypothalamus Controls Cyclic Energy Expenditure.* Cell Metab, 2016. **23**(3): p. 467-478.
22. Yang, X., *et al.*, *Nuclear receptor expression links the circadian clock to metabolism.* Cell, 2006. **126**(4): p. 801-810.
23. Dijk, W., *et al.*, *ANGPTL4 mediates shuttling of lipid fuel to brown adipose tissue during sustained cold exposure.* Elife, 2015. **4**.
24. Hoeke, G., *et al.*, *Role of Brown Fat in Lipoprotein Metabolism and Atherosclerosis.* Circ. Res, 2016. **118**(1): p. 173-182.
25. Kuhnast, S., *et al.*, *Anacetrapib reduces progression of atherosclerosis, mainly by reducing non-HDL-cholesterol, improves lesion stability and adds to the beneficial effects of atorvastatin.* Eur. Heart J, 2015. **36**(1): p. 39-48.
26. Lateef, D.M., *et al.*, *Regulation of body temperature and brown adipose tissue thermogenesis by bombesin receptor subtype-3.* Am. J Physiol Endocrinol. Metab, 2014. **306**(6): p. E681-E687.
27. Warner, A., *et al.*, *Inappropriate heat dissipation ignites brown fat thermogenesis in mice with a mutant thyroid hormone receptor alpha1.* Proc. Natl Acad. Sci. U. S. A, 2013. **110**(40): p. 16241-16246.
28. Fischer, A.W., *et al.*, *Leptin Raises Defended Body Temperature without Activating Thermogenesis.* Cell Rep, 2016. **14**(7): p. 1621-1631.
29. Abreu-Vieira, G., *et al.*, *Integration of body temperature into the analysis of energy expenditure in the mouse.* Mol Metab, 2015. **4**(6): p. 461-470.
30. Fielding, B., *Tracing the fate of dietary fatty acids: metabolic studies of postprandial lipaemia in human subjects.* Proc. Nutr. Soc, 2011. **70**(3): p. 342-350.
31. Olivecrona, T., *et al.*, *Lipoprotein lipase: regulation and role in lipoprotein metabolism.* Proceedings of the Nutrition Society, 1997. **56**(2): p. 723-729.
32. van den Beukel, J.C., *et al.*, *Direct activating effects of adrenocorticotropic hormone (ACTH) on brown adipose tissue are attenuated by corticosterone.* Faseb j, 2014. **28**(11): p. 4857-67.
33. Weiner, J., *et al.*, *Thyroid hormone status defines brown adipose tissue activity and browning of white adipose tissues in mice.* Sci Rep, 2016. **6**: p. 38124.
34. Otsuka, T., *et al.*, *Photoperiod regulates corticosterone rhythms by altered adrenal sensitivity via melatonin-independent mechanisms in Fischer 344 rats and C57BL/6J mice.* PLoS One, 2012. **7**(6): p. e39090.
35. Ono, H., *et al.*, *Involvement of thyrotropin in photoperiodic signal transduction in mice.* Proc Natl Acad Sci U S A, 2008. **105**(47): p. 18238-42.
36. Oelkrug, R., G. Heldmaier, and C.W. Meyer, *Torpor patterns, arousal rates, and temporal organization of torpor entry in wildtype and UCP1-ablated*

mice. J Comp Physiol B, 2011. **181**(1): p. 137-145.

37. Kitao, N. and M. Hashimoto, *Increased thermogenic capacity of brown adipose tissue under low temperature and its contribution to arousal from hibernation in Syrian hamsters.* Am. J Physiol Regul. Integr. Comp Physiol, 2012. **302**(1): p. R118-R125.
38. Szentirmai, E. and L. Kapas, *Intact brown adipose tissue thermogenesis is required for restorative sleep responses after sleep loss.* Eur. J Neurosci, 2014. **39**(6): p. 984-998.
39. McFadden, E., *et al.*, *The Relationship Between Obesity and Exposure to Light at Night: Cross-Sectional Analyses of Over 100,000 Women in the Breakthrough Generations Study.* Am. J Epidemiol, 2014.
40. Rybnikova, N.A., A. Haim, and B.A. Portnov, *Does artificial light-at-night exposure contribute to the worldwide obesity pandemic?* Int J Obes. (Lond), 2016.
41. Pattinson, C.L., *et al.*, *Environmental Light Exposure Is Associated with Increased Body Mass in Children.* PLoS One, 2016. **11**(1): p. e0143578.
42. Morris, C.J., *et al.*, *The Human Circadian System Has a Dominating Role in Causing the Morning/Evening Difference in Diet-Induced Thermogenesis.* Obesity. (Silver. Spring), 2015. **23**(10): p. 2053-2058.
43. Boon, M.R., *et al.*, *Supraclavicular skin temperature as a measure of 18F-FDG uptake by BAT in human subjects.* PLoS One, 2014. **9**(6): p. e98822.
44. Arble, D.M., *et al.*, *Circadian timing of food intake contributes to weight gain.* Obesity. (Silver. Spring), 2009. **17**(11): p. 2100-2102.
45. Hatori, M., *et al.*, *Time-restricted feeding without reducing caloric intake prevents metabolic diseases in mice fed a high-fat diet.* Cell Metab, 2012. **15**(6): p. 848-860.
46. Gill, S. and S. Panda, *A Smartphone App Reveals Erratic Diurnal Eating Patterns in Humans that Can Be Modulated for Health Benefits.* Cell Metab, 2015. **22**(5): p. 789-798.
47. Garaulet, M., *et al.*, *Timing of food intake predicts weight loss effectiveness.* Int J Obes. (Lond), 2013. **37**(4): p. 604-611.
48. Baron, K.G., *et al.*, *Role of sleep timing in caloric intake and BMI.* Obesity. (Silver. Spring), 2011. **19**(7): p. 1374-1381.
49. Jakubowicz, D., *et al.*, *High caloric intake at breakfast vs. dinner differentially influences weight loss of overweight and obese women.* Obesity. (Silver. Spring), 2013. **21**(12): p. 2504-2512.

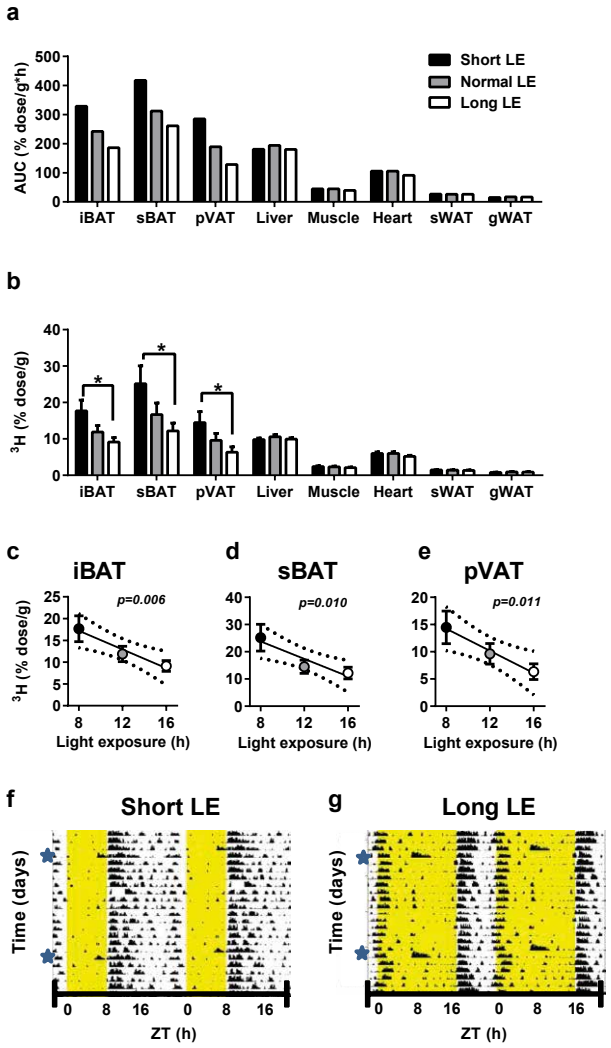

Supplementary Figure 1. Effect of light exposure on overall FA uptake and behavioral rhythms. *Wild-type mice were entrained to daily light exposure (LE) regimes of 8h (short LE), 12h (normal LE) or 16h (long LE) at standard 22°C ambient temperature for 5 weeks. Mice were injected with glycerol tri[^{3}H]oleate-labeled particles at 6 time points (n=4/group) and killed after 15 min of injection. AUC (a) and the average daily uptake of [^{3}H]oleate was determined per organ (b). Correlations were made between light exposure duration in hours and uptake of [^{3}H]oleate by iBAT (c), sBAT (d) and pVAT (e). Data are presented as means ±SEM. * p<0.05 (one-way ANOVA, Tukey's post-hoc test). Correlations were analyzed by linear regression (dotted line represents 95%-confidence band). Abbreviations: AUC = area under the curve, iBAT = interscapular BAT; sBAT = subscapular BAT; pVAT = perivascular adipose tissue, sWAT = subcutaneous white adipose tissue; gWAT = gonadal white adipose tissue. Passive infrared monitors were fitted on the lid to monitor spontaneous ambulatry activity patterns. Representative actograms for mice adapted to short LE (f) and long LE (g) are shown. Stars indicate opening of cabinets for feeding. Actogram represent double-plotted activity data into 10-min bins.*

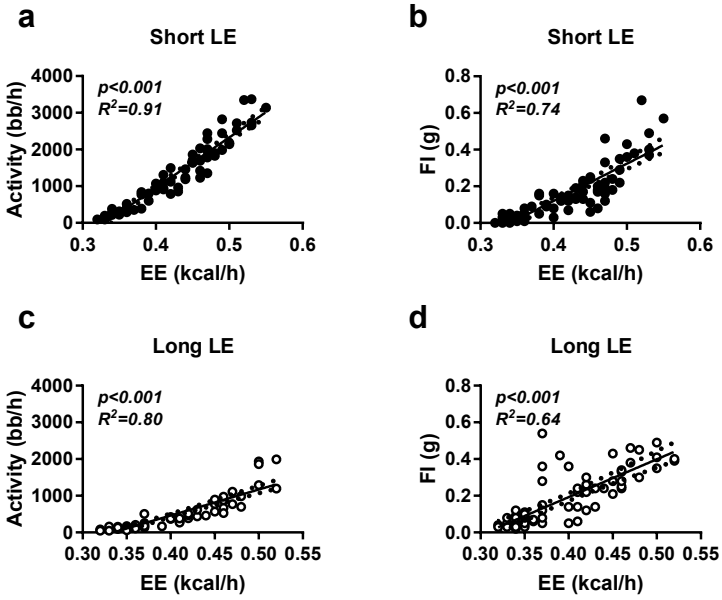

Supplementary Figure 2. Energy expenditure aligns with activity and food intake behavior under short and long LE. *Wild-type mice were entrained to daily light exposure (LE) regimes of 8h (short LE) or 16h (long LE) at standard 22°C ambient temperature for 5 weeks and placed in metabolic cages to determine whole body energy metabolism by means of indirect calorimetry. Energy expenditure was correlated to ambulatory activity in beam breaks/h (bb/h) (a, c) and food intake (b, d). Data points in the curves represent 1h binned values over a total of three consecutive days. Data are presented as means of 15-16 mice. Correlation was performed by linear regression analysis.*

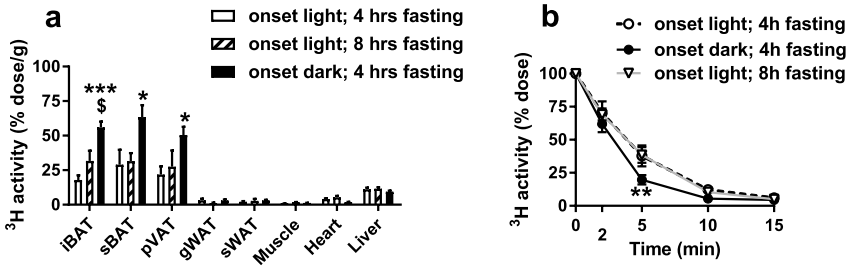

Supplementary Figure 3. (left page) Effect of fasting on FA uptake. *Wild-type mice were entrained to short daily light exposure (LE) regimes of 8h at standard 22°C ambient temperature for 5 weeks. Mice were injected with glycerol tri[³H]oleate-labeled particles either at the onset of light or the onset of the dark period. At onset of light, food was removed either 4 or 8 hours prior to injection to mimic physiological diurnal fasting period (n=4-5/group) and killed after 15 min of injection. The uptake of [³H]oleate was determined for interscapular and subscapular brown adipose tissue (iBAT, sBAT), perivascular adipose tissue (pVAT), liver, muscle, heart, gonadal and subcutaneous white adipose tissue (gWAT, sWAT) (a). Plasma clearance of [³H]oleate was determined (b). Data presented as means ±SEM. *p<0.05, **p<0.01, ***p<0.001 (compared to onset light/4h fasting), $p<0.05 (compared to onset light/8h fasting), (1-way ANOVA; a, two-way repeated measure-ANOVA with Tukey's post hoc test; b).*

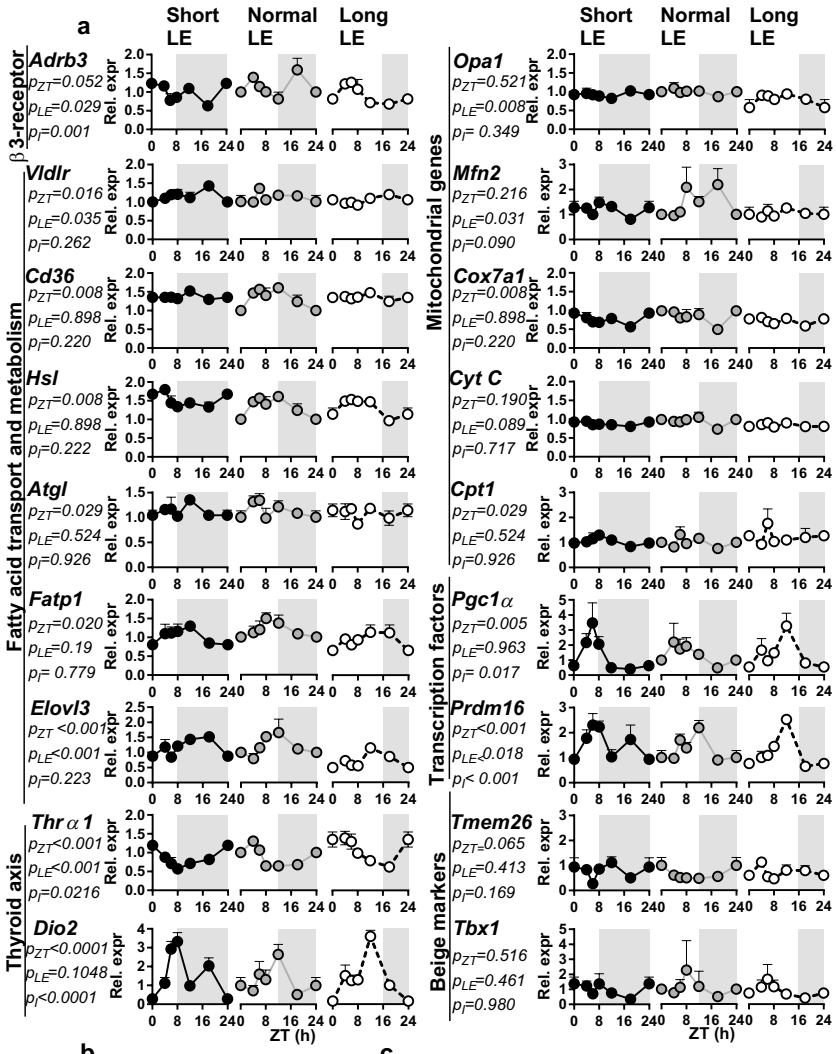
a
Short LE
Normal LE
Long LE
β3-receptor
Adrb3
pZT=0.052
pLE=0.029
pI=0.001
Fatty acid transport and metabolism
Vldlr
pZT=0.016
pLE=0.035
pI=0.262
Cd36
pZT=0.008
pLE=0.898
pI=0.220
Hsl
pZT=0.008
pLE=0.898
pI=0.222
Atgl
pZT=0.029
pLE=0.524
pI=0.926
Fatp1
pZT=0.020
pLE=0.19
pI= 0.779
Elovl3
pZT <0.001
pLE<0.001
pI=0.223
Thyroid axis
Thrα1
pZT<0.001
pLE<0.001
pI=0.0216
Dio2
pZT<0.0001
pLE=0.1048
pI<0.0001
Mitochondrial genes
Opa1
pZT=0.521
pLE=0.008
pI= 0.349
Mfn2
pZT=0.216
pLE=0.031
pI=0.090
Cox7a1
pZT=0.008
pLE=0.898
pI=0.220
Cyt C
pZT=0.190
pLE=0.089
pI=0.717
Cpt1
pZT=0.029
pLE=0.524
pI=0.926
Transcription factors
Pgc1α
pZT=0.005
pLE=0.963
pI= 0.017
Prdm16
pZT<0.001
pLE<0.018
pI< 0.001
Beige markers
Tmem26
pZT=0.065
pLE=0.413
pI=0.169
Tbx1
pZT=0.516
pLE=0.461
pI=0.980
Rel. expr
ZT (h)
b
Lpl mRNA (relative expression)
R2=0.1833
p<0.001
3H (% dose / g iBAT)
c
LPL protein (relative quantity)
R2=0.5258
p<0.001
3H (% dose / g iBAT)
Short LE
Normal LE
Long LE
d
WT 30°C
WT 4°C
Rev-erbα -/- 30°C
Rev-erbα -/- 4°C
Rel. expression
nd
0.059
Rev-erbα
Ucp1
Lpl
Angptl4

Supplementary Figure 4. (left page) 24-h rhythm in BAT gene expression adapts to daily light exposure. *Wild-type mice were entrained to daily light exposure (LE) regimes of 8h (short LE), 12h (normal LE) or 16h (long LE) at standard 22°C ambient temperature for 5 weeks. Interscapular brown adipose tissue (iBAT) was harvested at six time points (n=4/ group) and gene expression was determined by qPCR (a). Lpl gene expression (qPCR) (b) and LPL protein levels (Western blot) (c) were determined and correlation to FA uptake by iBAT was performed by linear regression analysis. Gene expression is relative to 36B4 or Hprt expression and normalized to mean expression of ZT0 of normal LE group. Rev-erbα-/- and control littermates were maintained on a normal 12h LE at 30°C. BAT was collected at ZT10 or following a 6h 4°C cold exposure (ZT4-ZT10) for gene expression analysis. Data are presented as means ±SEM and ZT0/ZT24 was double plotted for visualization purposes.* p_{ZT}, p_{LE} *and* p_{I} *represent p-values for the factors Zeitgeber Time (ZT), LE and interaction respectively (two-way ANOVA)(a).*p<0.05, **p<0.01, ***p<0.001 (4 vs. 30°C), $p<p0.05, $$p<0.01 (WT vs. knock-out) (d).*

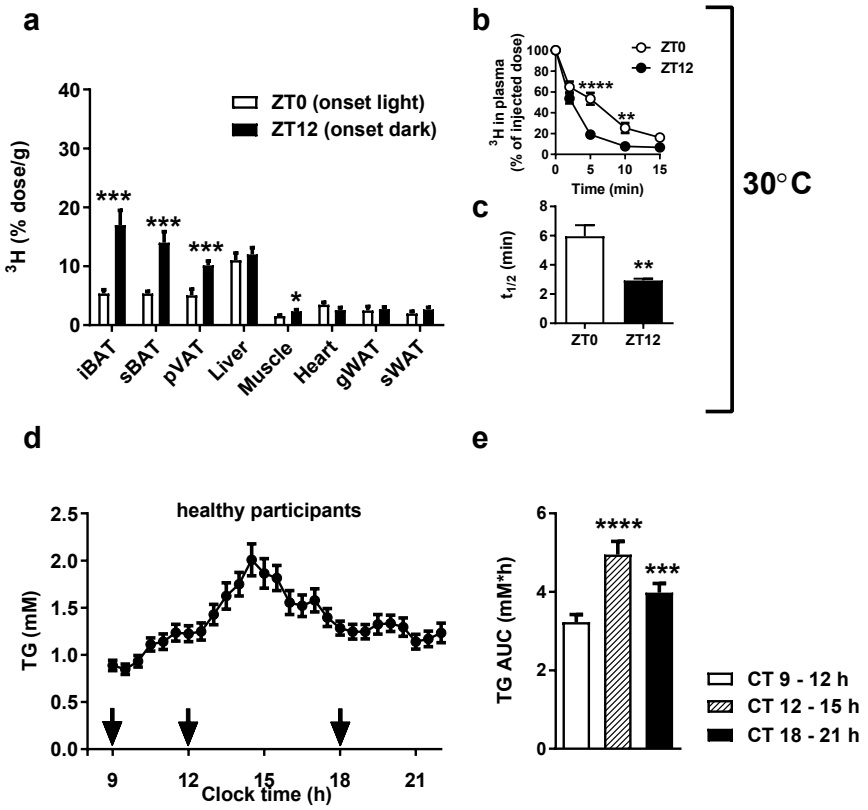

Supplementary Figure 5. Rhythmicity is present in TG-derived FA uptake by BAT in mice at thermoneutrality and postprandial TG concentrations in humans. *APOE*3-Leiden.CETP mice, fed a western type diet and entrained to 12h daily light exposure, were housed at thermoneutrality (30°C) for four days. Mice were injected with glycerol tri[^{3}H]oleate-labeled particles at 2 time points (ZT0 or ZT12) (n=7/group) and killed after 15 min of injection. Uptake of [^{3}H]oleate was determined for interscapular and subscapular brown adipose tissue (iBAT, sBAT), perivascular adipose tissue (pVAT), liver, muscle, heart, gonadal and subcutaneous white adipose tissue (gWAT, sWAT) (a). Plasma clearance of [^{3}H]oleate was determined 2, 5, 10 and 15 minutes after injection (b) and half-life ($t_{1/2}$) was calculated (c). 37 healthy individuals were fasted overnight and diurnal venous blood sampling was started, at clock time 9.00h. At 9.00h, 12.00h, 18.00h a standard liquid meal was consumed (arrows). TG levels were determined every 30 minutes (A) and postprandial AUC was calculated 3h after ingestion of an isocaloric meal (d). Abbreviations: AUC = area under the curve, CT = clock time, TG = triglycerides. Data are presented as means ±SEM. *p<0.05, **p<0.01, ***p<0.001, ****p<0.0001 (Student's T-test/ one-way ANOVA.*

Chapter 4

Glucocorticoid rhythm regulates the diurnal activity of brown adipose tissue

Rosa van den Berg, Maaike Schilperoort, Jan Kroon, Sander Kooijman,
Isabel M. Mol, Nikki van Trigt, Eveline Gart, Onno C. Meijer
Nienke R. Biermasz, Patrick C.N. Rensen,

In preparation

ABSTRACT

The biological clock regulates brown adipose tissue (BAT) activity. However, how the timing signal is conferred is poorly understood. We hypothesize that the diurnal rhythm in glucocorticoid levels (corticosterone in rodents) plays a crucial role. To address this hypothesis mice received subcutaneous pellets containing a low-dose of corticosterone, which markedly dampened the rhythm of endogenous circulating corticosterone concentrations. After one week the ability of BAT to take up triglyceride-derived fatty acids from the circulation was determined at AM and PM. In control mice fatty acid uptake by BAT displayed a large AM-PM fluctuation. In mice with dampened corticosterone rhythm this AM-PM fluctuation was abolished due to lowered PM uptake of fatty acids by BAT. This was accompanied by dampened AM-PM differences in the expression of *Lpl* and the phosphorylation of CREB, a downstream β3-receptor signaling target. Unexpectedly, known glucocorticoid-responsive element-controlled genes retained a rhythmic expression, suggesting that glucocorticoids did not directly act on the brown adipocyte. We conclude that short-term dampening of corticosterone rhythm in mice dampens the rhythmicity of BAT activity with respect to the uptake of triglyceride-derived fatty acids. Our data suggest that glucocorticoid rhythms may act as a signal from the biological clock to regulate diurnal rhythm of BAT activity via a yet to be identified mechanism.

INTRODUCTION

Brown adipose tissue (BAT) is currently viewed as a promising therapeutic target to combat metabolic disease due to its ability to dissipate energy into heat [1]. Brown adipocytes contain large amounts of mitochondria that uniquely contain uncoupling protein 1 (UCP-1). UCP-1 uncouples electron transport from ATP synthesis, resulting in heat production [2]. To fuel thermogenesis, intracellular triglyceride (TG) stores are used, which are replenished by LPL-mediated uptake of TG-derived fatty acids (FA) from the circulation [3]. Activation of BAT increases energy expenditure and reduces plasma TG levels; in mice this prevents obesity and reduces dyslipidemia [4]. Low temperature is the physiological stimulus for BAT activity. Cold is perceived by skin; the signal is transmitted to the hypothalamus, which increases sympathetic nervous system output and increases peripheral release of noradrenaline that activates the β3-adrenergic receptor on the brown adipocyte [5]. In addition to adrenergic input, BAT activity is controlled by the endocrine system [6]. It is becoming increasingly clear that the biological clock regulates BAT function.

The mammalian biological clock system generates circadian (i.e. 24 h) rhythms in physiological and behavioral functions. It consists of a central pacemaker located in the suprachiasmatic nucleus (SCN) of the hypothalamus and peripheral clocks within organs, which regulate rhythmicity within the different tissues. Light-dark information is processed by the SCN, which synchronizes peripheral clocks via sympathetic and endocrine output [7]. Disturbances of day-night rhythms in humans, *e.g.* through shift work and artificial light exposure, are associated with an increased risk for obesity, type 2 diabetes and dyslipidemia [8-10]. Studies in rodents demonstrated a causal relationship between a disturbed biological clock and the development of metabolic disease [11-13]. We recently showed that BAT may be the missing link in this causal relationship. Prolonged light exposure duration specifically reduced the uptake of TG-derived FA by BAT resulting in increased adiposity in mice, without affecting food intake [14]. Furthermore, we demonstrated that BAT activity is not only regulated by light exposure duration but also displays a strong diurnal rhythm (Chapter 3). Although we showed that fatty acid uptake by BAT is highly rhythmic, the exact mechanism by which the SCN transfers diurnal information to BAT is not fully understood.

Besides noradrenalin, glucocorticoids are likely candidates for transferring the circadian time-keeping signal to BAT. The release of glucocorticoids, cortisol in humans and corticosterone in rodents, shows a pronounced diurnal rhythm. Glucocorticoids peak before wakening and show a trough before sleeping [15]. The diurnal profile of plasma corticosterone concentrations and FA uptake by BAT are strikingly similar, with a peak just before wakening and a through at the end of the waking period. Moreover, prolonged light exposure duration, which directly affects SCN output [16], shifts the peak time and decreases the amplitude in the diurnal rhythm of both plasma corticosterone concentrations and FA uptake by BAT, as shown by others [17] and us (Chapter 3). Therefore, we hypothesized that the diurnal rhythm of plasma corticosterone confers the diurnal timing signal of the SCN towards BAT. To investigate this hypothesis, we dampened the endogenous diurnal rhythm of corticosterone by implantation of a low dose corticosterone-containing pellet in

mice and evaluated the effects on rhythmicity of whole-body metabolism and BAT activity. The subcutaneously implanted pellets release a continuous dose of corticosterone, which inhibits production of CRH and ACTH through negative feedback on the hypothalamus and the pituitary [18]. In this study, we demonstrate that dampening of the corticosterone rhythm did not flatten whole-body energy metabolism rhythms, but did reduce the evening peak in FA uptake by BAT.

METHODS

Animal husbandry

All animal experiments were performed in accordance with the local ethics committee. Male 8-week-old C57Bl/6J mice (Charles River) were single-housed in clear plastic cages within light-tight cabinets on a 12h:12h light:dark cycle (lights on 9.00h) at constant ambient temperature of 22°C with *ad libitum* access to food (standard chow, Special Diet Services) and water.

Experimental design

Mice (n=32) were housed in metabolic cages (Phenomaster, TSE systems) one day prior to the experiment. Mice (n=16/group) were implanted with a subcutaneous pellet containing 2.5% w/w corticosterone (2.5 mg corticosterone, 97.5 mg cholesterol) or 100 mg cholesterol as placebo. After 6 days, stress-free AM and PM blood samples were drawn at Zeitgeber Time (ZT) 1 and ZT11. After 7 days, a TG clearance experiment was performed at either AM (ZT0) or at PM (ZT12). An additional group of 10 animals were also implanted with a corticosterone-containing or placebo pellet (n=5/group) as well as a telemetric system to continuously measure body temperature and activity rhythms.

Surgical procedures

Implantation of the corticosterone pellets was performed under 2.5% isoflurane anesthesia. A small incision was made between the shoulder blades and a subcutaneous pocket was created by blunt end of a scissor. The pellet was inserted subcutaneously in the flank. Mice which also received a telemetric system were implanted with a TA-F10 miniature transmitter (Data Sciences International, MN, USA, kindly provided by Linda van Kerkhof, RIVM) through the same incision in the contralateral flank.

Indirect calorimetry and body composition

Mice were housed in automated metabolic cages to measure oxygen consumption (volume O_2; mL/h), carbon dioxide production (volume CO_2; mL/h), respiratory exchange ratio (RER; VCO_2/VO_2), physical activity via infra-red beam breaks and food intake during 7 days. Means were calculated over 7 days. Mice were weighed and body composition was determined by echoNMR (EchoMRI-100, Houston, TX, USA) the day before acclimatization to metabolic cages and at day 6.

Blood biochemistry

To determine the effects of a corticosterone pellet on circulating corticosterone levels, stress-free (i.e. within 2 minutes of handling the cage) blood samples were taken after the onset of light (AM; ZT 1) and before the onset of dark (PM; ZT11) via tail vein bleeding. To evaluate possible effects of acute stress of the final experiment, blood samples were taken right before the start of TG-clearance experiment from the tail vein into EDTA-coated Eppendorf tubes. Total plasma corticosterone concentrations were determined using ^{125}I-RIA ELISA kit (MP Biomedicals, Orangeburg, NY, USA).

TG clearance experiment

After 7 days of corticosterone or placebo treatment, the kinetics of triglyceride (TG) and cholesterol clearance from plasma and uptake by organs were assessed at AM (ZT0) and PM (ZT12). TG-rich lipoprotein (TRL)-like emulsion particles (80 nm), radiolabeled with glycerol tri[^{3}H]oleate ([^{3}H]TO) and [^{14}C]cholesteryl oleate ([^{14}C]CO), were prepared as previously described [19]. Mice were fasted for 4h and received an intravenous injection of particles (1 mg TG in total volume of 200 µl) via the tail vein. After 15 minutes, mice were euthanized by cervical dislocation and perfused with ice-cold PBS for 5 min. Organs were harvested, weighed, and ^{3}H and ^{14}C radioactivity was determined by liquid scintillation.

Gene expression analysis

Interscapular brown adipose tissue (iBAT) was snap frozen and stored at -80°C. Total RNA was isolated using TriPure (Roche) and cDNA was reverse-transcribed starting with 1 µg of RNA using M-MLV reverse transcriptase (Promega, Madison, WI, USA). Quantitative real-time PCR was performed in triplicate using SYBR-Green (Bio-Rad) on a CFX96 PCR machine (Bio-Rad). Expression levels were normalized to *36b4* housekeeping gene expression.

Protein isolation and Western blot

The iBAT samples stored at -80°C were homogenized and diluted in lysis buffer. The homogenates were centrifuged at 6.5 m/sec for 20 sec (FastPrep-24™ 5G, MP Biomedicals, California, USA) and the protein content was determined using a BCA protein assay kit (Thermo Scientific). Subsequently, after adding Laemmli Sample buffer (1:1 vol/vol; Serva, Heidelberg, Germany), the samples were denatured for 5 min at 95°C. Proteins within homogenates (20 µg) were separated on a 10% SDS-page gel and subsequently transferred onto nitrocellulose blotting membranes. The blotting membranes were blocked with 5% milk powder and incubated overnight at 4°C with the primary antibody rabbit pCREB (Cell Signalling; 1:1000) or mouse β-actin (Sigma; 1:1000). Subsequently, the membranes were incubated for 1 hour with secondary antibodies (anti-rabbit or anti-mouse IgG HRP conjugate; 1:5000; Promega, Madison, WI, USA), after which the protein bands were visualized with SuperSignal Western blot Enhancer (Thermo Scientific, Rockford, IL, USA). The Blots were analyzed with ChemiDoc Touch Imaging System (Bio-Rad) and normalized to β-actin expression levels.

Histology

To assess lipid fraction within BAT the lipid-containing area was determined on Mayer's hematoxylin and eosin (HE) stained formalin-fixed paraffin-embedded iBAT tissue sections (5 µm), using standard protocols. The lipid areas were quantified (as percentage of total area) using ImageJ.

Statistical analysis

Data are presented as means ± SEM. Differences between two groups were determined by T-tests and between more than two groups with a one-way ANOVA. To test for differences between AM-PM groups, post hoc Sidaks for multiple comparisons was used. For repeated measures, repeated measure ANOVA was used. Associations of variables with time were assessed by linear regression analysis. Graphpad Prism v6.0 was used for all analyses. P values < 0.05 were considered statistically significant.

RESULTS

Subcutaneous corticosterone-containing pellets dampen corticosterone rhythm

Mice were implanted with subcutaneous pellets containing vehicle or 2.5% corticosterone, aimed to flatten the endogenous diurnal corticosterone rhythm. To confirm this, we determined plasma corticosterone levels at AM (ZT1) and PM (ZT11). Mice implanted with placebo pellets showed a 29-fold difference between AM and PM plasma corticosterone levels (4.5 ± 1.2 *vs.* 129.9 ± 9.1 ng/ml, P < 0.0001) (Fig. 1a). In contrast, mice implanted with corticosterone pellets displayed similar plasma corticosterone levels at AM and PM (39.3 ± 3.3 *vs.* 46.9 ± 3.0 ng/ml, P = 0.408) (Fig. 1a). Moreover, corticosterone levels did not reach the physiological trough and peak values at either AM or PM. To further explore whether mice had been exposed to supraphysiological levels of corticosterone during the treatment, the thymus and adrenals were weighted after 7 days of implantation. The thymus and adrenals are sensitive to chronic hypercorticosteronemia and decrease in weight due to apoptosis of thymocytes [20] and lack of trophic effect of ACTH on adrenals. Thymus weight decreased by 34% in the corticosterone-treated group compared to the placebo group (43 ± 2 *vs.* 28 ± 2 mg, P < 0.001) (Fig. 1b). Adrenal weight also decreased by 20% in the corticosterone treated mice compared to placebo (1.4 ± 0.1 *vs.* 1.8 ± 0. 1 mg, P = 0.038) (Fig. 1c). These data indicate that corticosterone pellets may have raised the total corticosterone exposure in treated mice. Therefore, we conclude that corticosterone pellets dampened the diurnal rhythm of endogenous corticosterone treatment, with a possible elevation of total 24h corticosterone exposure.

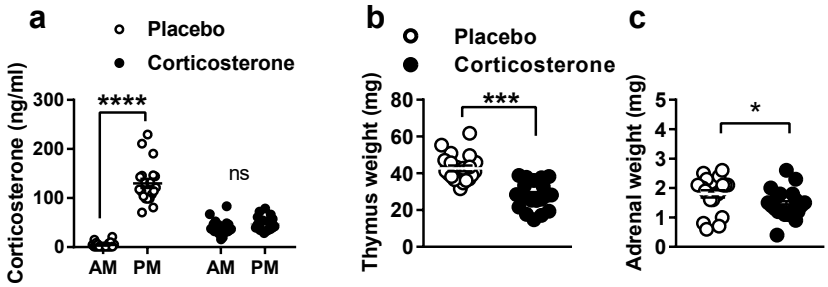

Figure 1. Implantation of corticosterone pellet flattens endogenous glucocorticoid rhythm. *C57BL6/J mice were implanted with placebo pellets (n=16) or low-dose corticosterone pellets (n=16). After 6 days, corticosterone plasma levels were determined at AM (ZT1) and PM (ZT11) (a). After 7 days, mice were sacrificed at AM (ZT0) or PM (ZT12) and thymus (b) and an adrenal (left-sided) (c) were weighed. Data are presented as individual values and the mean ± SEM. *P < 0.05, ***P < 0.001, ****P < 0.0001 (repeated measure ANOVA (a); Student's T-test (b-c)).*

Dampened rhythm of corticosterone levels does not affect body composition and diurnal energy expenditure

To investigate the effects of a dampened corticosterone rhythm on energy metabolism, we measured body composition before and after 7 days of treatment, and performed indirect calorimetric analysis. Corticosterone treatment did not affect fat mass (corticosterone vs placebo; 1.1 ± 0.1 *vs*. 1.3 ± 0.1 g, P = 0.122) (Fig. 2a), lean mass (22.5 ± 0.2 *vs*. 23.2 ± 0.3 g, P = 0.083) (Fig. 2b), or total body weight (23.8 ± 0.3 *vs*. 24.5 ± 0.2 g, P = 0.135) (Fig. 2c). Also, flattening of the rhythm in corticosterone concentrations did not change the diurnal pattern of fat oxidation, carbohydrate (CH) oxidation, energy expenditure (EE), respiratory exchange ratio (RER), physical activity or food intake obtained over a period of 7 days (Fig. 2d-i). Average values were different between light and dark period, but unaffected by a dampened corticosterone rhythm (Fig. 2d-i). In an additional group of mice equipped with telemetric systems, 24h body temperature (Fig. 2j) and activity (Fig. 2k) were simultaneously recorded. Overall, the diurnal rhythm of metabolic parameters as well as body temperature rhythms were similar between the placebo and corticosterone-treated mice.

Dampened rhythm of corticosterone levels flattens the rhythm of TG-derived FA-uptake specifically by BAT

To investigate the effect of a dampened diurnal corticosterone rhythm on BAT activity, we assessed the ability of BAT to take up TG-derived FA from plasma at two time points. To this end, mice were injected with double-labeled TRL-mimicking particles either at AM (ZT0) or PM (ZT12). The AM and PM uptake of [^{3}H]oleate by interscapular BAT (iBAT) and subscapular BAT (sBAT) was higher than the uptake by subcutaneous white adipose tissue (sWAT), liver, gonadal WAT (gWAT), heart, spleen and muscle, indicating that iBAT and sBAT are highly metabolically active compared to other metabolic organs. The PM uptake of [^{3}H]oleate by

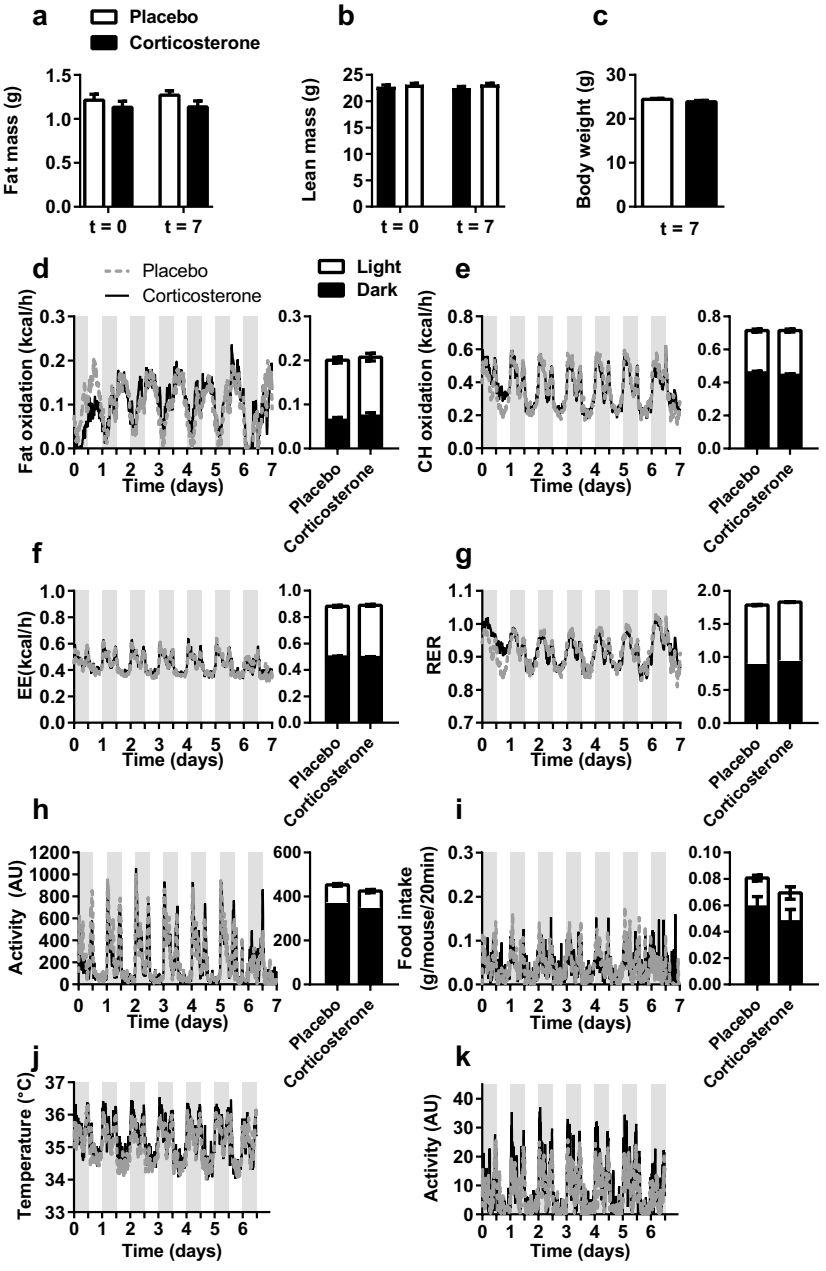
a
Placebo
Corticosterone
Fat mass (g)
t = 0
t = 7
b
Lean mass (g)
t = 0
t = 7
c
Body weight (g)
t = 7
d
Placebo
Corticosterone
Light
Dark
Fat oxidation (kcal/h)
Time (days)
Placebo
Corticosterone
e
CH oxidation (kcal/h)
Time (days)
Placebo
Corticosterone
f
EE(kcal/h)
Time (days)
Placebo
Corticosterone
g
RER
Time (days)
Placebo
Corticosterone
h
Activity (AU)
Time (days)
Placebo
Corticosterone
i
Food intake (g/mouse/20min)
Time (days)
Placebo
Corticosterone
j
Temperature (°C)
Time (days)
k
Activity (AU)
Time (days)

iBAT, sBAT and perivascular adipose tissue (pVAT) was higher compared to AM (iBAT: 35.2 ± 6.4 *vs.* 20.8 ± 2.6 % dose/g, P = 0.029; sBAT: 41.7 ± 6.4 *vs.* 21.0 ± 2.7 % dose/g, P = 0.004; pVAT: 24.1 ± 3.0 *vs.* 14.8 ± 1.8 % dose/g, P = 0.023) (Fig. 3a). Remarkably, corticosterone treatment abolished this difference between AM and PM in iBAT (22.0 ± 2.9 *vs*. 22.8 ± 2.0 % dose/g, P = 0.985), sBAT (23.9 ± 2.7 *vs*. 24.5 ± 3.4 % dose/g, P = 0.993) and pVAT (17.5 ± 2.1 *vs*. 18.1 ± 2.3 % dose/g, P = 0.982). Since the AM uptake decreased and the PM uptake remained the same, the average total uptake of [^{3}H]oleate by brown adipocyte depots was decreased by corticosterone treatment. In placebo treated mice, the liver showed the highest uptake of [^{14}C]CO, reflecting the clearance of cholesterol-rich remnant particles, when compared to all other organs (Fig. 3b). Remnant uptake by the liver was significantly higher PM versus AM in placebo treated mice (61 ± 3 *vs.* 46 ± 2 % dose/g, P=0.002), while in corticosterone treated mice, the PM and AM uptake of remnants was equal (58 ± 3 *vs.* 57 ± 3 % dose/g, P=0.958). In conclusion, corticosterone pellet implantation dampened the diurnal rhythm in TRL clearance with respect to TG-derived FA uptake by BAT depots, as well as the rhythm in remnant uptake by the liver.

Dampened rhythm of corticosterone levels flattens the rhythm in clock gene expression in BAT

Corticosterone-containing pellets dampened both the rhythm in endogenous corticosterone levels and the rhythm in BAT activity with respect to TG-derived FA uptake. We aimed to further investigate the underlying mechanism by which corticosterone levels influence FA uptake by BAT. Corticosterone can act through binding of the mineralocorticoid receptor (MR) as well as the glucocorticoid receptor (GR). To investigate whether corticosterone directly acts on brown adipocytes, we determined the gene expression in iBAT of the known MR and GR responsive genes *Fkbp5* (Fig. 4a), *Gilz* (Fig. 4b) and *Hsd11b1* (Fig. 4c). Corticosterone pellets did not influence the AM-PM difference in expression of these responsive genes, showing that the corticosterone-containing pellets do not universally flatten GR and MR dependent gene expression within the brown adipocytes.

We previously demonstrated that diurnal FA-uptake by BAT is accompanied by diurnal clock gene expression (Chapter 3). We hypothesize that corticosterone may act on the cell autonomous clock to regulate diurnal FA-uptake. We studied genes in both the forward and negative feedback loop of the clock machinery. The expression levels of the genes in the positive loop, namely *Clock* (Fig. 4d) and *Bmal1* (Fig. 4e) showed no rhythmicity in

Figure 2. (left page) Dampened rhythm of corticosterone levels does not affect body composition and diurnal energy metabolism pattern. *C57BL6/J mice were implanted with placebo pellets (n=16) or low-dose corticosterone pellets (n=16). Fat mass (a) and lean mass (b) were determined by EchoMRI at baseline and after 7 days and total body mass was determined after 7 days (c). Indirect calorimetry was used to determine fat oxidation (d), carbohydrate oxidation (e), energy expenditure (EE) (f), respiratory exchange ratio (RER) (g), physical activity (h) and food intake (i). Bars show mean value over 7 days. Body temperatures (j) and activity (k) measured every 10 minutes from subcutaneously implanted thermometers in placebo (n=5) and corticosterone pellet treated (n=5) mice. Grey dotted line represents placebo, black line represents corticosterone. Data are presented as spline curve (d-l) or means ± SEM (a-c).*

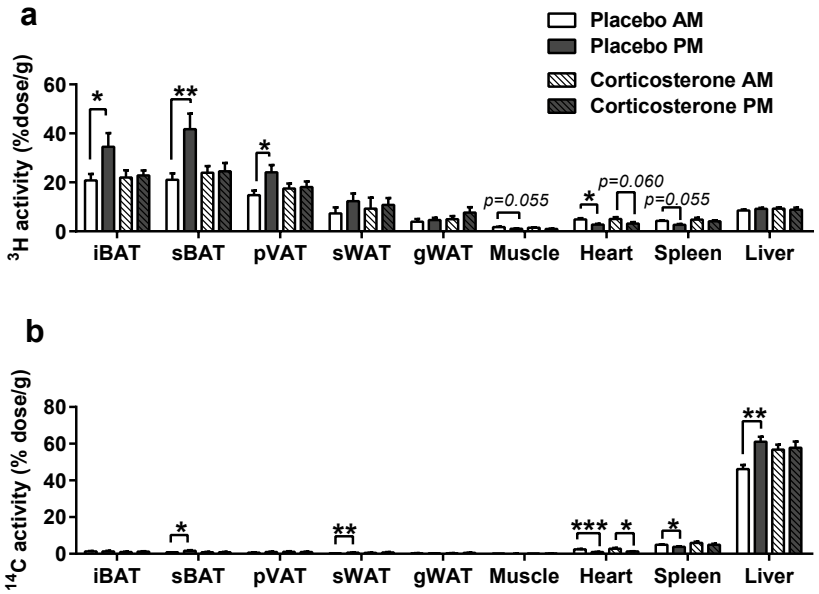

Figure 3. Dampened rhythm of corticosterone levels dampens rhythmicity of TG-derived FA-uptake specifically by BAT. *C57BL6/J mice were implanted with placebo pellets (n=16) or low-dose corticosterone pellets (n=16) and the VLDL-TG uptake was assessed after 7 days by injection of glycerol tri[^{3}H]oleate ([^{3}H]TO) and [^{14}C]cholesteryl oleate ([^{14}C]CO)-labeled emulsion particles. Uptake of [^{3}H]TO-derived (a) and [^{14}C]CO-derived activity (b) by the various organs was determined. Open bars = placebo, hatched bars = corticosterone; grey bars = PM, white bars = AM. Data are presented as means ± SEM. *P < 0.05, **P < 0.01, ***P < 0.001*

Figure 4. (right page) Dampened rhythm of corticosterone levels dampens clock gene expression rhythmicity within BAT C57BL6/J mice were implanted with placebo pellets (n=16) or low-dose corticosterone pellets (n=16). *After 7 days, mice were sacrificed at AM (ZT0) or PM (ZT12) and interscapular BAT was isolated. Gene expression was determined by qPCR (a-l, o-u). Histological sections were stained with HE were analyzed for lipid content (m, n). Protein expression was determined by Western blot and quantified (normalized to actin levels, not shown) (v, w, x). Open bars = placebo, hatched bars = corticosterone, grey bars = PM, white bars = AM. Data are presented as means ± SEM. Relative expression was calculated normalized to AM-placebo values. Ns= not significant (P>0.05). *P < 0.05, **P < 0.01, ***P < 0.001 (one-way ANOVA, post hoc Sidaks multiple comparisons AM vs. PM).*

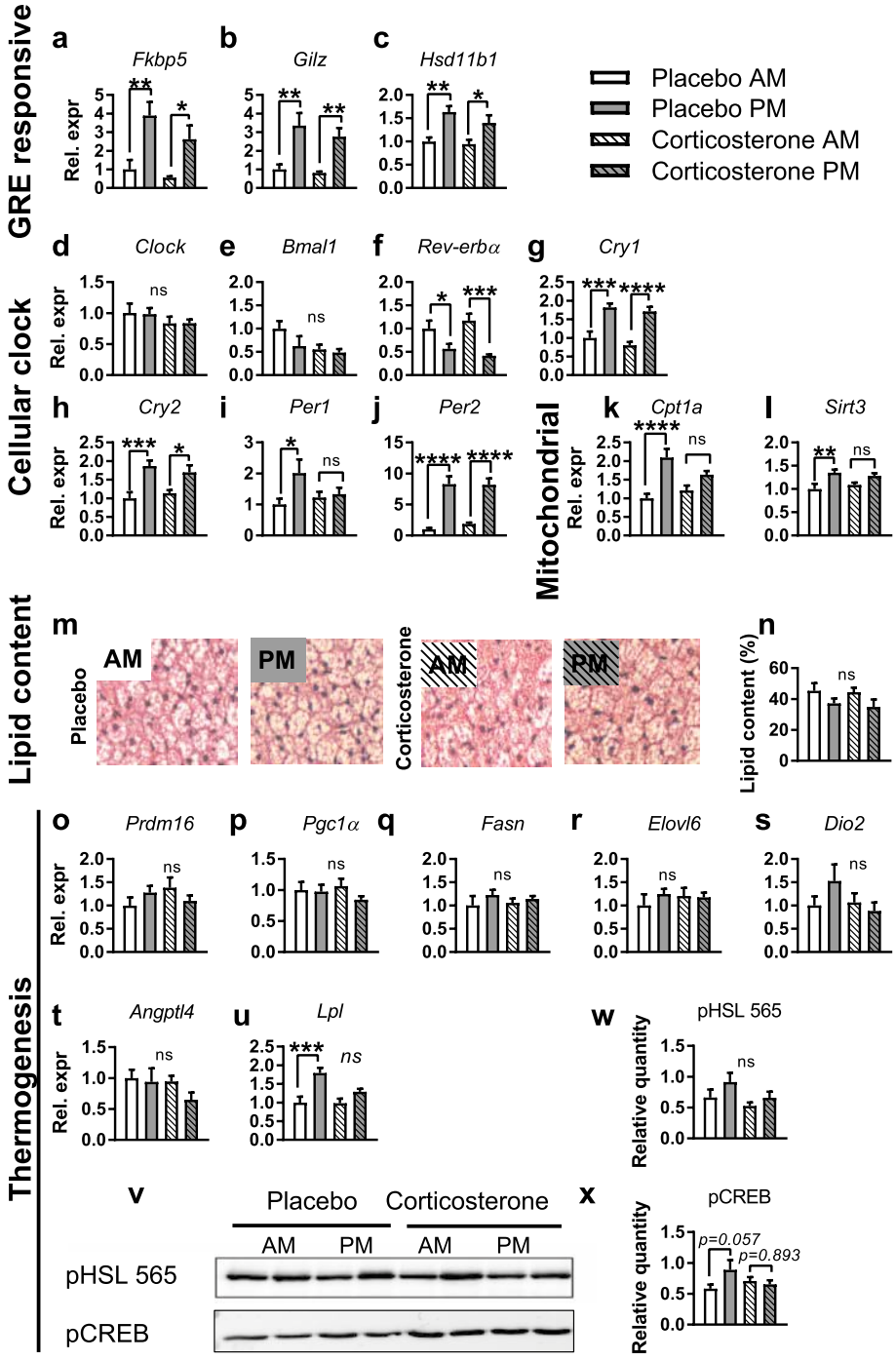
GRE responsive
Cellular clock
Mitochondrial
Lipid content
Thermogenesis
Placebo AM
Placebo PM
Corticosterone AM
Corticosterone PM
Rel. expr
Fkbp5
Gilz
Hsd11b1
Clock
Bmal1
Rev-erbα
Cry1
Cry2
Per1
Per2
Cpt1a
Sirt3
AM
PM
Placebo
Corticosterone
Lipid content (%)
Prdm16
Pgc1α
Fasn
Elovl6
Dio2
Angptl4
Lpl
pHSL 565
Relative quantity
Placebo
Corticosterone
pCREB
p=0.057
p=0.893
ns

both the placebo and corticosterone treated groups. *Rev-erbα* displayed a significant AM-PM difference with highest expression at AM (Fig. 4f) in the placebo group ($P<0.05$) and after corticosterone intervention ($P < 0.001$). For the other clock genes, gene expression was highest at PM. The preservation of AM-PM difference in the corticosterone treated groups, was also observed for gene expression of *Per2* (Fig. 4j), *Cry1* (Fig. 4g), *Cry2* (Fig. 4h). Interestingly, the AM-PM difference in gene expression of *Per1* (Fig. 4i) was blunted by corticosterone treatment. Therefore, we conclude that flattening of the plasma corticosterone rhythm specifically dampens the clock gene expression of *Per1*.

Next we investigated which thermogenic pathways within the brown adipocyte may be rhythmic and therefore blunted upon corticosterone rhythm flattening. Since intracellular TG stores are burned upon activation of BAT, the intracellular lipid content of BAT is an indirect measure of its activity. Histologic analysis. of BAT demonstrated that although not significant, BAT tended to contain less lipids at PM than AM, which would be consistent with a higher thermogenic activity at PM (Fig. 4m). However, the same trend was apparent in corticosterone-treated mice (Fig. 4n). Subsequently, we examined the possibility that corticosterone rhythm flattening reduces mitochondrial function which could eventually reduce FA uptake by brown adipocytes. The rhythmic expression of carnitine palmitoyltransferase 1a (*Cpt1a*) (Fig. 4k), which facilitates the transfer of FA into the mitochondrial matrix for oxidation, was blunted in corticosterone-treated mice. Likewise, gene expression of NAD-dependent deacetylase sirtuin-3 (*Sirt3*) (Fig. 4l), which regulates several mitochondrial metabolic enzymes, showed an AM-PM difference in the placebo treated mice, which lost significance in corticosterone treated mice. In contrast, thermogenic genes *Prdm16*, *Pgc1α*, *Fasn* and *Elovl6, Dio2* (Fig 4o-s) did not display any AM-PM difference. LPL is crucial for hydrolysis of TG within TRL and subsequent uptake FA by BAT. We previously found that expression of *Angptl4*, which encodes for the inhibitor of LPL activity, displays a diurnal rhythm within BAT (chapter 3). Although *Angptl4* did not show a AM-PM difference (Fig 4t), *Lpl* expression was rhythmic, and this rhythmicity was dampened after corticosterone treatment (Fig. 4u). Thus, our data suggest that corticosterone rhythms may regulate BAT activity at the level of expression of genes involved in both cellular FA uptake (*Lpl*) and FA oxidation (*Cpt1a*, *Sirt3*).

Since expression of direct GR and MR targets retained their rhythmicity, we hypothesized that corticosterone affects BAT indirectly, *e.g.* via sympathetic output. We studied phosphorylated protein levels of hormone sensitive lipase (HSL), involved in TG hydrolysis, as well as CREB, a downstream target of adrenergic signaling. While HSL phosphorylation was not different between AM and PM (Figs. 4v,w), we found that near-significant rhythmic levels of phosphorylated CREB (pCREB) was dampened upon corticosterone treatment (Fig 4v, x).

DISCUSSION

The uptake of FA uptake by BAT is higher at the onset of the active period (i.e. the dark period for mice, at PM) than at the onset of the resting period (the light period, AM). These data support our recent observations, demonstrating a pronounced diurnal rhythm in TG-derived FA uptake by BAT (Chapter 3). The diurnal rhythmicity of TG-derived FA uptake parallels that of glucose uptake by BAT in mice [21] and supraclavicular temperature in humans [22] (a measure for human BAT activity since it highly correlates to glucose uptake [23]). We showed that implantation of a low dose corticosterone-containing pellet dampens the endogenous diurnal rhythm in plasma corticosterone concentrations in mice; corticosterone plasma levels increased at AM and decreased at PM. Together with the dampened corticosterone rhythm, BAT depots decreased TG-derived FA uptake at PM. Whole body energy expenditure retained a diurnal rhythm and body composition was maintained.

Dampened corticosterone rhythm may act on BAT activity either directly in the brown adipocyte by binding MR and GR, or indirectly, via the central nervous system (CNS). We examined effects on genes with a known high affinity GR-response element (GRE) [24]. Expression of *Fkbp5* and *Gilz* retained rhythmicity, dismissing a direct effect of corticosterone rhythm via GRE-induced expression. Nevertheless, we observed a dampened rhythm in expression of *Per1*, which also has a known high affinity GRE. This phenomenon is in line with recent study in zebrafish with a genetic disturbance of diurnal cortisol levels. In that study, transcriptomic analysis showed a disturbance in rhythmic expression in many metabolic genes. Supplementation with a continuous dose of dexamethasone restored rhythmic expression in part of the arrhythmic genes [25]. In other words, constant glucocorticoid levels restore are sufficient to restore rhythmic gene expression of some genes, but for other genes, the rhythmicity of glucocorticoid levels is necessary to restore the rhythmic expression. The intracellular mechanisms remain obscure, but likely involve non-genomic effects of the GR, such as the interaction with clock proteins.

Implantation of low-dose corticosterone pellet resulted in decreased phosphorylation of CREB at PM. Adrenergic stimulation of BAT increases CREB phosphorylation [26]. Therefore, corticosterone rhythm may centrally regulate BAT activity via modulating the sympathetic outflow. No studies have yet demonstrated a diurnal sympathetic outflow towards BAT. Corticosterone is able to pass the blood-brain barrier, and can bind MR and GR present in the CNS. MR activation in the CNS increases hypertension and sympathetic outflow [27], which represents a possible pathway by which glucocorticoids may affect sympathetic outflow towards BAT.

The difference in AM and PM nutrient uptake by BAT was accompanied by a marked AM-PM difference in *Lpl* expression, which is in line with our previous finding that *Lpl* gene expression and protein levels are highly rhythmic and coincide with FA uptake rhythms by BAT (Chapter 3). Furthermore expression of *Cpt1a* and *Sirt3* was dampened after implantation of low-dose corticosterone pellets. Cold-induced adrenergic stimulation

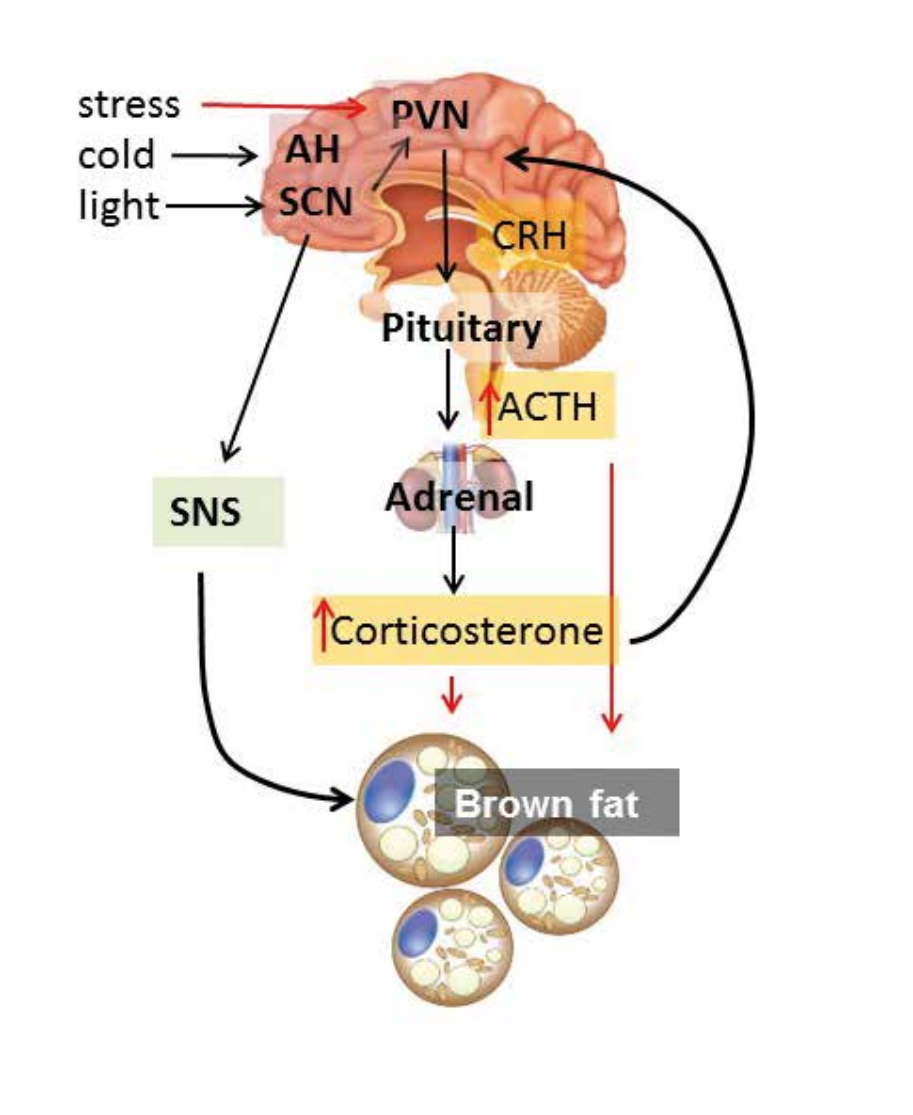

Figure 5. Hypothetical model. *Light information is processed by the SCN, which regulates rhythmic output of the HPA axis via the PVN. Under physiological circumstances, peak corticosterone levels do not directly regulate brown fat rhythm but rather feed back to the brain (possibly via the AH) and via the SNS, BAT rhythmicity is regulated. If a stressor is perceived, the PVN is activated, high levels of ACTH and corticosterone are reached in the circulation, which directly affect BAT activity. AH = anterior hypothalamus, SNS = sympathetic nervous system, PVN = paraventricular nucleus, SCN = suprachiasmatic nucleus.*

increases expression of these genes [28]. Therefore, the dampened expression support the hypothesis that glucocorticoid act indirectly via the CNS to modulate sympathetic outflow.

A few publications reported on the role of glucocorticoids on BAT activity. Increased glucocorticoid levels have been shown to inhibit thermogenic BAT activity *in vitro* in murine brown adipocytes [29]. On the other hand, elimination of endogenous glucocorticoids by adrenalectomy increases UCP-1 protein content and mitochondrial content in BAT in rats, which again decreases with increasing substitution dosages of corticosterone [30]. However, due to the ablation of negative feedback in these models, they are also characterized by increased ACTH levels, which has recently been demonstrated to activate BAT [31, 32]. Therefore, the question remains whether adrenalectomy increases BAT activity due to reduced glucocorticoid levels or because of increased ACTH levels. Furthermore, flattened glucocorticoid levels could affect BAT activity by lack of peak levels or by an increase of the through levels. *In vitro* experiments have demonstrated that GR agonism inhibits *Ucp1* expression in murine brown adipocytes [33, 34]. In these studies, supraphysiological doses of glucocorticoids or dexamethasone were administered. Gene expression responses as well as behavioral responses to glucocorticoids are context and dose dependent [35, 36]. Notably, two human studies recently demonstrated that infusion of glucocorticoids increased BAT thermogenesis, as measured by supraclavicular skin temperature [29, 37]. Taken these data together, we propose that glucocorticoids may serve both as a signal for diurnal BAT activity and as a signal for stress, depending on the plasma levels.

A limitation of the current study is the use of only two time points to determine rhythmicity. Although our study confirmed previous finding of a large amplitude between AM and PM corticosterone rhythm as well as FA uptake by BAT, the detection of rhythms in *e.g.* expression of genes that have other peak and trough times may be missed. It has been previously shown that diurnal oscillations in gene expression in many of the peripheral circadian clocks can be shifted by the administration of glucocorticoids or by adrenalectomy [38]. Additionally, we cannot exclude that total 24h corticosterone plasma levels may be different between the groups only based on AM and PM corticosterone levels. Indeed, adrenal and thymus weight were slightly lowered upon corticosterone treatment. However, we did not observe metabolic effects associated with hypercorticosteronemia such as decreased lean mass [39].

In conclusion, we show that dampening of glucocorticoid levels specifically dampens FA uptake rhythm by BAT. Our study may help to understand how disturbed circadian rhythms can cause metabolic disorders. Chronic disruption of circadian rhythm in BAT may be such a mediator, as lower BAT activity is associated with lower energy expenditure, dyslipidemia and obesity in rodents [40]. Disturbed day-night rhythms, such as through shift work, may disturb circadian BAT function. Glucocorticoid administration may help to restore disturbed circadian BAT function and thereby treating metabolic disease.

Acknowledgments

The authors thank Trea Streefland and Hetty Sips for excellent technical assistance and José van den Heuvel for consultation on design of experiments. **Conflict of Interest**: none. **Funding**: This research was supported by the Netherlands Organization for Scientific Research (NWO-VENI grants 016.136.125 to NR Biermasz). We also acknowledge the support from the Netherlands Cardiovascular Research Initiative: an initiative with support of the Dutch Heart Foundation (CVON2014-02 ENERGISE). PCN Rensen is an Established Investigator of the Dutch Heart Foundation (grant 2009T038). **Author contributions:** RvdB designed and performed experiments, analyzed data and wrote manuscript; SK designed and performed experiments and analyzed data; MS and JK and analyzed data and wrote manuscript; IMM, NvT and EG performed experiments and analyzed data; OCM, NRB and PCNR supervised the study.

References

1. Lidell, M.E., M.J. Betz, and S. Enerback, *Brown adipose tissue and its therapeutic potential.* J Intern Med, 2014. **276**(4): p. 364-77.
2. Golozoubova, V., *et al., Only UCP1 can mediate adaptive nonshivering thermogenesis in the cold.* FASEB J, 2001. **15**(11): p. 2048-50.
3. Khedoe, P.P., *et al., Brown adipose tissue takes up plasma triglycerides mostly after lipolysis.* J. Lipid Res, 2015. **56**(1): p. 51-59.
4. Bartelt, A., *et al., Brown adipose tissue activity controls triglyceride clearance.* Nat. Med, 2011. **17**(2): p. 200-205.
5. Cannon, B. and J. Nedergaard, *Brown adipose tissue: function and physiological significance.* Physiol Rev, 2004. **84**(1): p. 277-359.
6. Cereijo, R., J. Villarroya, and F. Villarroya, *Non-sympathetic control of brown adipose tissue.* Int J Obes Suppl, 2015. **5**(Suppl 1): p. S40-4.
7. Reppert, S.M. and D.R. Weaver, *Coordination of circadian timing in mammals.* Nature, 2002. **418**(6901): p. 935-941.
8. Maury, E., K.M. Ramsey, and J. Bass, *Circadian rhythms and metabolic syndrome: from experimental genetics to human disease.* Circ Res, 2010. **106**(3): p. 447-62.
9. Esquirol, Y., *et al., Shift work and cardiovascular risk factors: New knowledge from the past decade.* Archives of Cardiovascular Diseases, 2011. **104**(12): p. 636-668.
10. McFadden, E., *et al., The Relationship Between Obesity and Exposure to Light at Night: Cross-Sectional Analyses of Over 100,000 Women in the Breakthrough Generations Study.* Am. J Epidemiol, 2014.
11. Turek, F.W., *et al., Obesity and metabolic syndrome in circadian Clock mutant mice.* Science, 2005. **308**(5724): p. 1043-1045.
12. Shi, S.Q., *et al., Circadian disruption leads to insulin resistance and obesity.* Curr. Biol, 2013. **23**(5): p. 372-381.
13. Coomans, C.P., *et al., Detrimental effects of constant light exposure and high-fat diet on circadian energy metabolism and insulin sensitivity.* FASEB J, 2013. **27**(4): p. 1721-1732.
14. Kooijman, S., *et al., Prolonged daily light exposure increases body fat mass through attenuation of brown adipose tissue activity.* Proc. Natl Acad. Sci. U. S. A, 2015. **112**(21): p. 6748-6753.
15. Kalsbeek, A., *et al., SCN outputs and the hypothalamic balance of life.* J. Biol. Rhythms, 2006. **21**(6): p. 458-469.
16. VanderLeest, H.T., *et al., Seasonal encoding by the circadian pacemaker of the SCN.* Curr. Biol, 2007. **17**(5): p. 468-473.

17. Otsuka, T., *et al.*, *Photoperiod regulates corticosterone rhythms by altered adrenal sensitivity via melatonin-independent mechanisms in Fischer 344 rats and C57BL/6J mice.* PLoS One, 2012. **7**(6): p. e39090.
18. Brinks, V., *et al.*, *Differential MR/GR activation in mice results in emotional states beneficial or impairing for cognition.* Neural Plast, 2007. **2007**: p. 90163.
19. Rensen, P.C., *et al.*, *Selective liver targeting of antivirals by recombinant chylomicrons--a new therapeutic approach to hepatitis B.* Nat Med, 1995. **1**(3): p. 221-225.
20. Compton, M.M. and J.A. Cidlowski, *Rapid in vivo effects of glucocorticoids on the integrity of rat lymphocyte genomic deoxyribonucleic acid.* Endocrinology, 1986. **118**(1): p. 38-45.
21. van der Veen, D.R., *et al.*, *A diurnal rhythm in glucose uptake in brown adipose tissue revealed by in vivo PET-FDG imaging.* Obesity. (Silver. Spring), 2012. **20**(7): p. 1527-1529.
22. Lee, P., *et al.*, *Brown Adipose Tissue Exhibits a Glucose-Responsive Thermogenic Biorhythm in Humans.* Cell Metab, 2016.
23. Boon, M.R., *et al.*, *Supraclavicular skin temperature as a measure of 18F-FDG uptake by BAT in human subjects.* PLoS One, 2014. **9**(6): p. e98822.
24. Mifsud, K.R. and J.M. Reul, *Acute stress enhances heterodimerization and binding of corticosteroid receptors at glucocorticoid target genes in the hippocampus.* Proc Natl Acad Sci U S A, 2016. **113**(40): p. 11336-11341.
25. Weger, B.D., *et al.*, *Extensive Regulation of Diurnal Transcription and Metabolism by Glucocorticoids.* PLoS Genet, 2016. **12**(12): p. e1006512.
26. Morrison, S.F., *Central neural control of thermoregulation and brown adipose tissue.* Auton Neurosci, 2016. **196**: p. 14-24.
27. Geerling, J.C. and A.D. Loewy, *Aldosterone in the brain.* Am J Physiol Renal Physiol, 2009. **297**(3): p. F559-76.
28. Shore, A.M., *et al.*, *Cold-induced changes in gene expression in brown adipose tissue, white adipose tissue and liver.* PLoS. One, 2013. **8**(7): p. e68933.
29. Ramage, L.E., *et al.*, *Glucocorticoids Acutely Increase Brown Adipose Tissue Activity in Humans, Revealing Species-Specific Differences in UCP-1 Regulation.* Cell Metab, 2016. **24**(1): p. 130-41.
30. Strack, A.M., M.J. Bradbury, and M.F. Dallman, *Corticosterone decreases nonshivering thermogenesis and increases lipid storage in brown adipose tissue.* Am J Physiol, 1995. **268**(1 Pt 2): p. R183-91.
31. van den Beukel, J.C., *et al.*, *Cold Exposure Partially Corrects Disturbances in Lipid Metabolism in a Male Mouse Model of Glucocorticoid Excess.* Endocrinology, 2015. **156**(11): p. 4115-28.
32. van den Beukel, J.C., *et al.*, *Direct activating effects of adrenocorticotropic hormone (ACTH) on brown adipose tissue are attenuated by corticosterone.* Faseb j, 2014. **28**(11): p. 4857-67.
33. Soumano, K., *et al.*, *Glucocorticoids inhibit the transcriptional response of the uncoupling protein-1 gene to adrenergic stimulation in a brown adipose cell line.* Mol Cell Endocrinol, 2000. **165**(1-2): p. 7-15.
34. Armengol, J., *et al.*, *Pref-1 in brown adipose tissue: specific involvement in brown adipocyte differentiation and regulatory role of C/EBPdelta.* Biochem J, 2012. **443**(3): p. 799-810.
35. Polman, J.A., E.R. de Kloet, and N.A. Datson, *Two populations of glucocorticoid receptor-binding sites in the male rat hippocampal genome.* Endocrinology, 2013. **154**(5): p. 1832-44.
36. Roozendaal, B., *et al.*, *Glucocorticoid enhancement of memory requires arousal-induced noradrenergic activation in the basolateral amygdala.* Proc Natl Acad Sci U S A, 2006. **103**(17): p. 6741-6.

37. Scotney, H., *et al.*, *Glucocorticoids modulate human brown adipose tissue thermogenesis in vivo.* Metabolism, 2017. **70**: p. 125-132.
38. Sotak, M., *et al.*, *Peripheral circadian clocks are diversely affected by adrenalectomy.* Chronobiol Int, 2016. **33**(5): p. 520-9.
39. Depke, M., *et al.*, *Hypermetabolic syndrome as a consequence of repeated psychological stress in mice.* Endocrinology, 2008. **149**(6): p. 2714-23.
40. Berbee, J.F., *et al.*, *Brown fat activation reduces hypercholesterolaemia and protects from atherosclerosis development.* Nat Commun, 2015. **6**: p. 6356.

Chapter 5

Effects of mistimed light exposure on atherosclerosis development in APOE*3-Leiden.CETP mice

Rosa van den Berg, Maaike Schilperoort, Sander Kooijman, Ashna Ramkisoensing, Padmini P.S.J. Khedoe, Lianne Wee-Pals, Sanne Boekestijn, Karina Wagner, Johanna H. Meijer, Claudia P. Coomans, Jimmy F.P. Berbée, Patrick C.N. Rensen, Nienke R. Biermasz

In preparation

ABSTRACT

Shift work is a risk factor for atherosclerotic disease in humans. However, whether shift work is causally involved in atherosclerosis and which facet of shift work is responsible are unknown. Here, we investigated the hypothesis that mistimed light exposure may causally contribute to atherosclerosis by performing studies in APOE*3-Leiden.CETP mice, a well-established model for human-like lipoprotein metabolism and atherosclerosis. In two separate experiments, female mice were either subjected to constant light (LL) or to three different rotating light schedules, compared to control 12h light-dark (LD) schedule. While LL disturbed the circadian rhythm to some extent, it did not affect atherosclerotic lesion development. In contrast, a weekly 6 h advance light schedule increased plaque severity. Moreover, weekly reversal of LD schedule increased plaque severity as well as plaque size. Increased atherosclerotic development could not be attributed to higher plasma cholesterol levels. In conclusion, mistimed light exposure per se aggravates atherosclerotic development in mice, which may at least partly explain the association between shift work and cardiovascular disease in humans. Future studies should focus on underlying mechanisms.

INTRODUCTION

Cardiovascular diseases (CVD) are currently the leading cause of death world-wide [1]. The main cause of CVD is atherosclerosis, to which a pro-inflammatory state and dyslipidemia are key contributors [2]. Dyslipidemia is characterized by increased levels of plasma triglycerides (TG) and LDL-cholesterol and decreased HDL-cholesterol [3]. Plasma levels of lipids display day-night variations independent of food intake [4], suggesting that the biological clock is an important determinant of lipid levels. Consequently, disturbed biological clock function may contribute to dyslipidemia and thereby increase the risk for CVD.

Epidemiological studies have repeatedly shown associations between disturbance of biological clock function, responsible for generating circadian (i.e. ~24 h) rhythms, and metabolic disorders such as obesity, type 2 diabetes and CVD [5-7]. Already in 1949 a Scandinavian observational study among factory workers reported an association between shift work and cardiovascular mortality [8]. Longitudinal studies indicate that shift work is indeed a causal risk factor for cardiovascular events, including hard end-points like ischemic stroke and myocardial infarction [9, 10]. However, the underlying mechanisms remained elusive. Meanwhile, the behavioral patterns of human activity, especially in industrialized countries, have undergone dramatic changes with respect to adherence to day and night rhythms. The use of electrical light has uncoupled the behavioral active period from the natural occurring day, social activities are shifted and the 24-hour economy necessitates working at night. Of note, in Europe approximately 20% of the working population is involved in some form of shift work [11].

Shift work likely contributes to adverse health outcomes via multifactorial pathways, including psychosocial factors, sleep loss, a decrease in physical activity, altered food intake quantity (i.e. an increase in caloric intake) and quality (i.e. changes in timing and choice of food) and lack of sun light exposure. An undervalued aspect is the contributing factor of mistimed light exposure itself. Prolonged light exposure is associated with obesity in humans [12-16]. Recently, we were able to show in mice that prolonged light exposure increases adiposity by attenuation of brown adipose tissue (BAT) activity, independent of food intake [17]. Upon activation, BAT takes up fatty acids from TG-rich lipoproteins to burn into heat, resulting in accelerated hepatic clearance of TG-rich lipoprotein remnants [18]. In fact, pharmacological activation of BAT in mice decreases plasma TG and cholesterol, accompanied with attenuation of atherosclerosis formation [19]. It is thus conceivable to reason that mistimed light exposure could reduce BAT activity, thereby increasing plasma cholesterol and accelerating atherosclerosis.

Although it has been established that mistimed light exposure by rotating light shifts increases breast cancer development in mice [20] and shift advance increases mortality [21], the effects of mistimed light exposure on lipid metabolism and atherosclerosis development are currently unknown. Therefore, the aim of the present study was to investigate the role of mistimed light exposure on atherosclerosis development. To investigate this, we subjected APOE*3-Leiden.CETP female mice, which have a humanized

lipoprotein metabolism and develop human-like atherosclerosis, to different light regimes and determined the effect on atherosclerosis development.

MATERIAL AND METHODS

Animal Husbandry

All animal experiments were approved by the Institutional Ethics Committee on Animal Care and Experimentation (Leiden University Medical Center). Mice heterozygous for the APOE*3-Leiden gene were crossbred at our own facility with mice expressing human cholesteryl ester transfer protein (CETP) to yield APOE*3-Leiden.CETP (E3L.CETP) transgenic mice [22], a mouse model with a human-like lipoprotein metabolism [23]. Female E3L.CETP mice of 8-12 weeks old were fed *ad libitum* with Western-type diet (WTD) containing 15% fat from cocoa butter, 1% fat from corn oil (diet T, HopeFarms, Aldrich, Zwijndrecht, the Netherlands), enriched with 0.1% cholesterol. During a run-in period of three weeks mice were housed under standard 12h:12h light:dark (LD) conditions. Afterwards, mice were randomized based on fasting plasma total cholesterol (TC), TG, body weight and age to experimental groups described below. Mice were group-housed (n=3/cage) in clear plastic cages, placed in light-tight cabinets fitted with diffuse white fluorescent light with an intensity of approximately 85 μW/cm^2. In the last two weeks of the experiment, behavioral activity patterns were assessed by housing mice individually in cages fitted with passive infrared detectors.

Experimental Design

In two separate atherosclerosis experiments, the effects of prolonged light exposure and of mistimed light exposure on atherosclerosis development were investigated. Blood drawing and final experiments started at ZT4 (ZT = Zeitgeber time in hours where ZT0 represents lights on) and groups were alternated. In the first experiment, mice were randomized to either a regular 12h:12h LD cycle or to constant light exposure (LL) (n=18/group) for the total duration of 14 weeks. In week 2, 4, 8 and 12 after start of light exposure intervention unfasted blood samples were obtained. At the same time, body weight was measured and food intake was determined by weighing food on the lid of the cage. After 14 weeks, body composition was assessed by EchoMRI-100 (EchoMRI, Houston, Texas), mice were anesthetized by intraperitoneal injection of acepromazin (6.25 mg/kg; Sanofi Sant Nutrition Animale, Libourne Cedex, France), midazolam (6.25 mg/kg; Roche, Mijdrecht, the Netherlands), and fentanyl (0.31 mg/kg; Janssen-Cilag, Tilburg, the Netherlands), and blood was drawn retro-orbitally into EDTA coated cups for immune cell analysis. Afterwards, mice were killed by cervical dislocation and organs were harvested for further analysis.

In the second experiment, mice were randomized to either LD, a 6-h phase advance every week (advance), a 6-h phase delay every week (delay) or a weekly reversal of the 12h light-dark cycle (LD-DL) (n=15/group) for the total duration of 15 weeks. In week 3, 7, 11 and 15 after start of the light regime, when light regimes were aligned among the groups,

unfasted blood was drawn at ZT4 on the 2nd day and also on the 6th day after a shift where indicated. At the same time, body weight and food intake were measured as described above. At week 11, blood was collected into EDTA-coated cups and used for immune cell analysis. After 15 weeks, mice were killed by CO_2 inhalation, blood was drawn into EDTA-coated cups and organs were harvested for further analysis.

Biochemistry

Blood was drawn via the tail vein into paraoxon coated capillaries. Plasma was isolated by centrifugation, snap frozen into liquid nitrogen and stored at -80°C until further analyses. Plasma TC and TG were analysed by commercially available enzymatic kits according to manufacturer's protocols (Roche Molecular Biochemicals, IN, USA). HDL was isolated by precipitation of ApoB-containing lipoproteins. Hereto, 20% polyethylene glycol (Sigma Aldrich) in 200 mM glycine-buffered saline (pH 10) was added to plasma, centrifuged for 30 minutes at 6,000 rpm, and HDL-C was determined in the supernatant. Non-HDL-C was calculated by subtracting HDL-C from TC.

Immune cell composition

Immune cell composition of freshly isolated whole blood (100 µl) was determined using Sysmex using a XT-2000i hematology analyzer (Sysmex Corporation, Japan).

Histological analysis of the heart

Hearts were fixated in phosphate buffered 4% paraformaldehyde and embedded in paraffin and cross-sections of 5 µm were made in the aortic valve region. Sections were stained with haematoxylin-phloxine-saffron for histological analysis. Per mouse, lesion area was quantified in the aortic root starting from the appearance of open aortic valve leaflets in four subsequent sections with 50 µm intervals. Lesion area was determined by analysis using Image J software. Lesion severity was scored according to the guidelines of the American Heart Association adapted for mice [24].

Histological analysis of adipose tissue

Interscapular brown adipose tissue (iBAT) was fixated in phosphate buffered 4% paraformaldehyde, embedded in paraffin and cross-sections of 5 µm were made. Sections were stained with Mayer's haematoxylin and eosin. BAT lipid droplet content was quantified using ImageJ software.

Gene expression analysis

A part of iBAT was snap frozen and stored at -80°C for gene expression analysis and protein analysis (see below). Total RNA was isolated using TriPure (Roche) according to the manufacturer's instructions. 1 µg of total RNA was reverse-transcribed using M-MLV reverse transcriptase (Promega, Madison, WI, USA). Real-time PCR was carried out on a CFX96 PCR machine (Bio-Rad) using IQ SYBR-Green Supermix (Bio-Rad). Expression levels were normalized to 36B4 as housekeeping gene.

Behavioral analysis

Behavioral patterns were analysed by plotting actograms using Clock lab (Actimetrics, Wilmette, IL, USA). F-periodogram analysis was performed on activity binned into 10 minutes interval of the last 10 consecutively recorded experimental days according to the algorithm of Dörrscheidt and Beck [25].

Statistical analysis

Comparisons between group averages were performed using Student's T-test or ANOVA with Fisher LSD post-hoc test (compared to LD light schedule), where appropriate (Graphpad Prism v.6). Correlations between two dependent variables were made using Pearson's correlation analysis. Data are presented as means ± SEM. Differences at P values < 0.05 were considered statistically significant.

5

RESULTS

Constant light attenuates circadian rhythm strength in APOE*3-Leiden.CETP mice

Dyslipidemic APOE*3-Leiden.CETP female mice were subjected to 14 weeks of either constant light (LL) or normal light dark cycles (LD). The effect of light intervention on the circadian behavior was assessed by monitoring spontaneous physical activity rhythms via passive infrared detectors. Periodogram analysis demonstrated that LL lengthened the period of physical activity rhythmicity, compared to the LD mice (26.29 ± 0.14 *vs.* 24.02 ± 0.03 h; p<0.0001) (Fig. 1a). In addition, average rhythm strength was decreased in LL mice compared to LD mice (0.59 ± 0.02 *vs.* 0.66 ± 0.01; p=0.038) (Fig. 1b). LL mice showed considerably higher variation compared to LD mice (CV 16% *vs.* 5%) and between various LL mice we observed different physical activity patterns between high and low amplitude actograms (Fig. 1c-h). These data indicate that, while chronic LL exposure does not render all mice arrhythmic as determined by physical activity patterns, LL clearly attenuates the rhythmic circadian clock output.

Figure 1. (right page) Constant light attenuates circadian rhythm strength in APOE*3-Leiden.CETP mice. *APOE*3-Leiden.CETP mice fed WTD were exposed to LD or LL (n=18/group) for 14 weeks. During the last 10 days, mice were individually housed and behavioral activity was monitored by passive infrared monitors (n=8 LD, n=18 LL). Rhythm length (a) and rhythm strength (b) was calculated using F periodogram analysis. Representative double-plotted actogram (c) and periodogram (d) is shown for 1 LD mouse. Double-plotted actograms (e, g) and periodograms (f, h) are shown for 2 LL mice. Gray dotted line represents significance threshold. * = p<0.05; **** = p<0.0001 (unpaired T-test). Data is presented as individual data points including means ± SEM.*

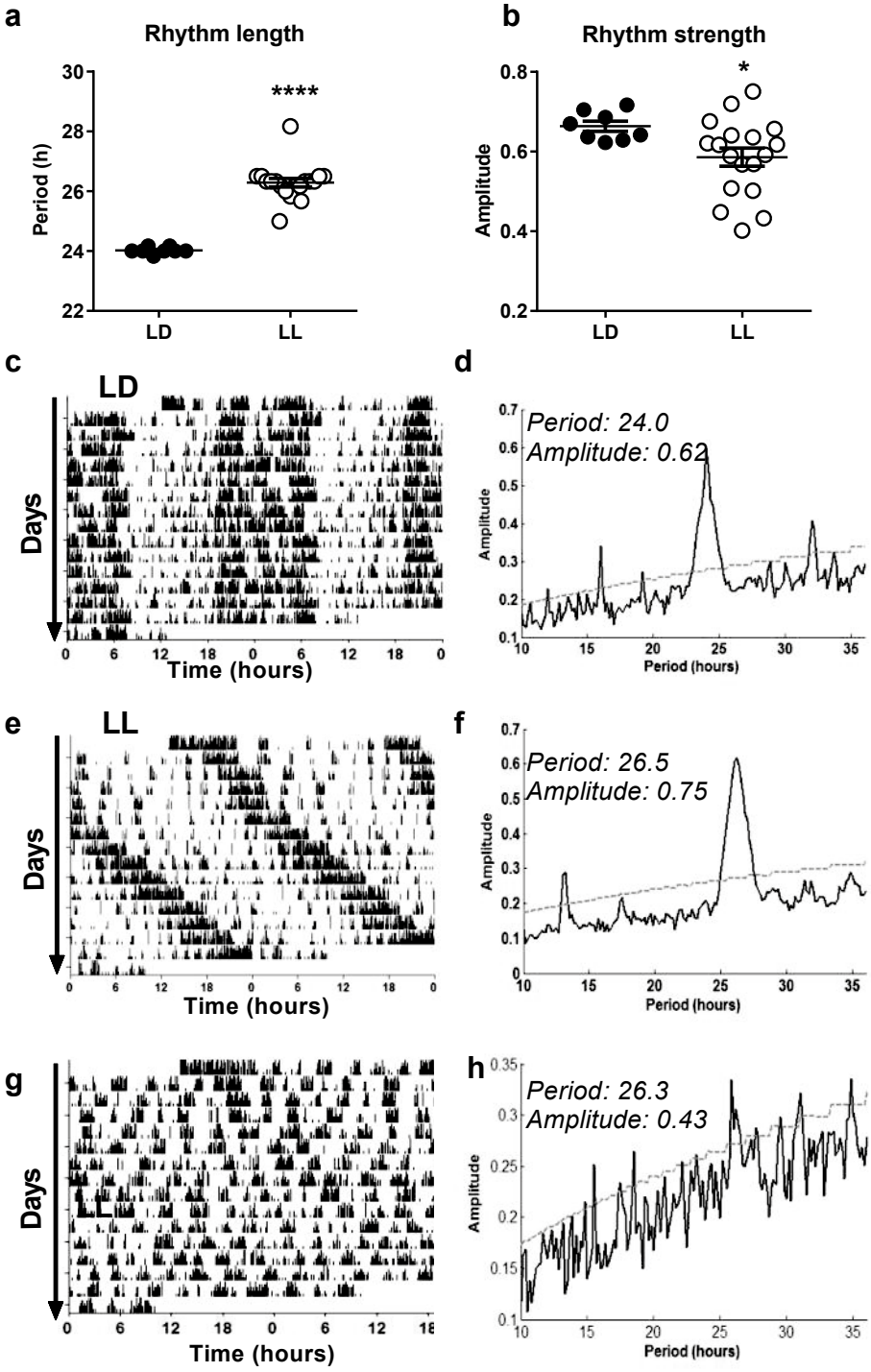
a
Rhythm length
Period (h)
30
28
26
24
22
****
LD
LL
b
Rhythm strength
Amplitude
0.8
0.6
0.4
0.2
*
LD
LL
c
LD
Days
0 6 12 18 0 6 12 18 0
Time (hours)
d
Period: 24.0
Amplitude: 0.62
Amplitude
Period (hours)
e
LL
Days
Time (hours)
f
Period: 26.5
Amplitude: 0.75
Amplitude
Period (hours)
g
Days
Time (hours)
h
Period: 26.3
Amplitude: 0.43
Amplitude
Period (hours)

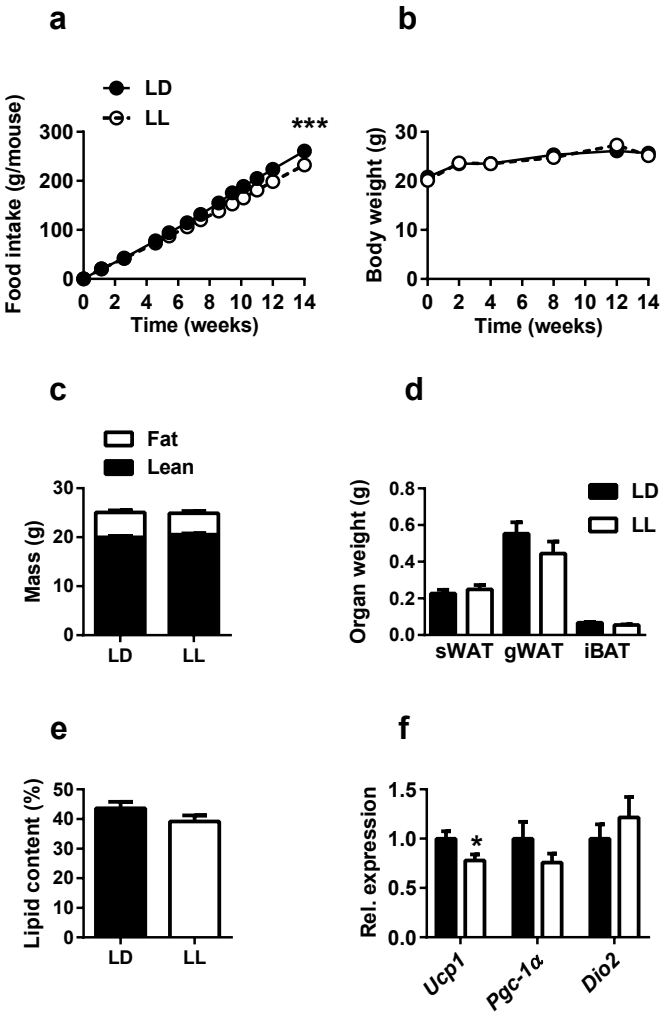

Figure 2. Constant light decreases food intake without increasing body weight or adiposity in APOE*3-Leiden.CETP-mice. *APOE*3-Leiden.CETP mice fed WTD were exposed to LD or LL (n=18/group) for 14 weeks. Food intake (a) and body weight (b) were determined at regular intervals. After 14 weeks, body composition (fat mass versus lean mass) was determined by EchoMRI (c) and subcutaneous white adipose tissue (sWAT), gonadal WAT (gWAT) and interscapular brown adipose tissue (iBAT) were weighed (d). Part of iBAT was stained with H&E for lipid content quantification (e) and in part used for gene expression analysis by qPCR (f). Expression is normalized for 36b4 and relative to mean LD expression. * = p<0.05; *** = p<0.001 (unpaired T-test). Data is presented as means ± SEM.*

Constant light decreases food intake without altering body weight or adiposity in APOE*3-Leiden.CETP mice

Body weight and food intake were measured throughout the study and fat mass was determined after 14 weeks of light intervention. We observed a small but consistent decrease in food intake in mice subjected to LL (Fig. 2a), which resulted in a lower cumulative food intake in LL mice compared to LD mice over 14 days (232 ± 4 *vs*. 260 ± 5 g/mouse; p<0.0001). This difference in food intake did not result in differences in body weight of the mice over time (at 14 weeks 25.2 ± 0.6 *vs*. 25.7 ± 0.7 g; p=0.608) (Fig. 2b), nor in fat mass as measured by EchoMRI (4.3 ± 0.5 *vs.* 5.1 ± 0.5 g; p=0.301) (Fig. 2c). Also, wet tissue weights of subcutaneous and gonadal white adipose tissue (sWAT; gWAT) depots were similar in LL mice compared to LD mice after 14 weeks (sWAT 0.25 ± 0.02 *vs.* 0.23 ± 0.02 g; p=0.460) (gWAT 0.45 ± 0.07 *vs.* 0.55 ± 0.06 g; p=0.242) (Fig. 2d). BAT activation leads to increased delipidation of BAT, which is reflected by the weight and lipid content [26]. BAT weight did not decrease due to LL (iBAT 0.054 ± 0.004 *vs.* 0.067 ± 0.005 g; p=0.064) (Fig. 2d), which was in line with the lipid content, which was equal between mice exposed to LL and LD (39 ± 2 *vs.* 44 ± 2%; p=0.149) (Fig. 2e). Thermogenic gene *Ucp1* showed a decreased relative expression in LL compared to LD (0.78 ± 0.06 *vs.* 1.00 ± 0.07 fold change; p=0.028) (Fig. 2f), however this was not accompanied by a lower expression of thermogenic genes *Pgc1α* (p=0.221) and *Dio2* (p=0.400) (Fig. 2f).

Constant light increases total cholesterol exposure without increasing atherosclerosis

Compared to LD, LL exposure raised TC plasma levels after 4 weeks (+3.6 ± 1.5 mM; p=0.025), 8 weeks (+3.0 ± 1.5 mM; p=0.056) and after 12 weeks (+4.5 ± 1.9 mM; p=0.025) of light intervention (Fig. 3a). This increase in TC was accompanied by a slightly lower TG level after 4 weeks (-1.1 ± 0.5 mM; p=0.013) and 14 weeks (-1.1 ± 0.5 mM; p=0.044) (Fig. 3b), but not at the other time points. Determination of cholesterol in lipoprotein subfractions showed that TC levels were increased due to a selective increase in non-HDL-cholesterol levels, i.e. (V)LDL-cholesterol (Fig. 3c-d). We therefore calculated TC exposure for the duration of light intervention, which was elevated in LL mice compared to LD mice (288 ± 12 *vs.* 251 ± 11 mM*week; p=0.038) (Fig. 3e). Since atherosclerosis development depends on both dyslipidemia and inflammation, we explored whether light interventions may have altered immune cell composition by measuring white blood count in peripheral blood. Interestingly, we observed a decrease in white blood cell (2.8 ± 0.2 $*10^9$ *vs.* 4.7 ± 0.4$*10^9$ cells/l; p<0.001) and platelet counts (1.8 ± 0.2 $*10^{12}$ *vs.* 1.4 ± 0.1$*10^{12}$ cells/l; p=0.013) due to LL exposure (Fig. 3f).

We next determined atherosclerotic lesion formation by assessing atherosclerosis plaque size and severity in the aortic root. Despite the raised TC exposure in LL mice, we observed no difference in atherosclerotic lesion size between LL and LD exposed mice (11.3 ± 1.0$*10^4$ *vs.* 12.0 ± 1.2$*10^4$ mm^2; p=0.540) (Fig. 3g). Likewise, lesion severity was not different (66 ± 5 *vs*. 62 ± 4% mild lesions; p=0.579) (37 ± 4 *vs*. 34 ± 5 % severe lesions; p=0.580) (Fig. 3h). Since rhythm strength varied in the LL group, we explored whether

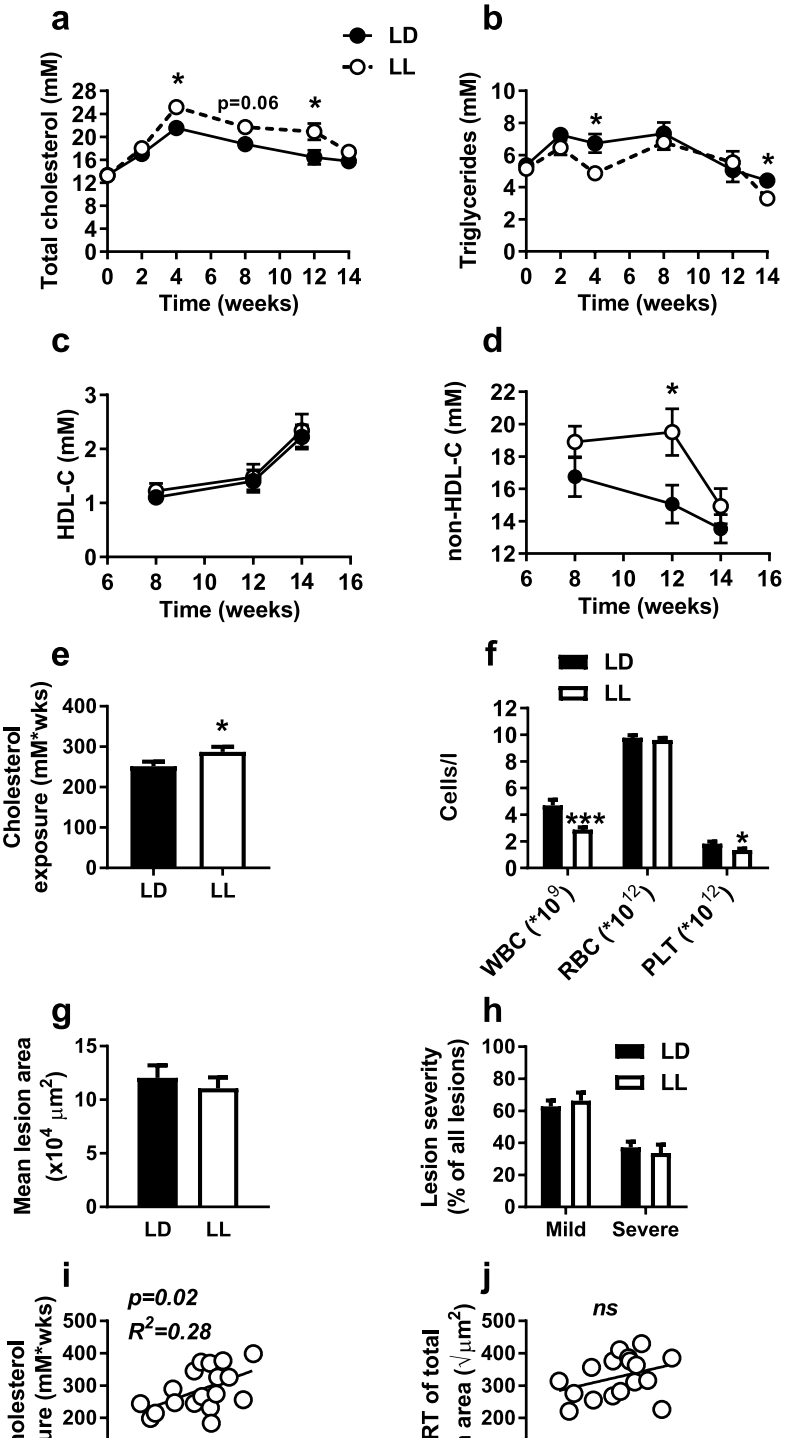
a
LD
LL
Total cholesterol (mM)
p=0.06
Time (weeks)
b
Triglycerides (mM)
Time (weeks)
c
HDL-C (mM)
Time (weeks)
d
non-HDL-C (mM)
Time (weeks)
e
Cholesterol exposure (mM*wks)
LD
LL
f
LD
LL
Cells/l
WBC (*10^9)
RBC (*10^12)
PLT (*10^12)
g
Mean lesion area (x10^4 µm^2)
LD
LL
h
Lesion severity (% of all lesions)
LD
LL
Mild
Severe
i
p=0.02
R^2=0.28
j
ns

Figure 3. (left page) Constant light increases total cholesterol exposure without increasing atherosclerosis. *APOE*3-Leiden.CETP mice fed WTD were exposed to LD or LL (n=18/group) for 14 weeks. Plasma total cholesterol (a) and triglycerides (b) was determined at regular intervals, HDL-cholesterol (c) and non-HDL-cholesterol (d) was determined after 8, 12 and 14 weeks. Total cholesterol exposure was calculated (e). After 14 weeks, mice were sacrificed and whole blood was collected and pooled (n=4-5/group) for cell count using Sysmex (f). Hearts were isolated and, at the aortic root, atherosclerotic lesion size (g) and severity (h) was determined. Rhythm strength was correlated to total cholesterol exposure (i) and atherosclerotic plaque area (j) for mice exposed to LL (Pearson correlation). * = p<0.05 (unpaired T-test). Data is presented as means ± SEM. WBC= white blood cells, RBC=red blood cells, PLT=platelets.*

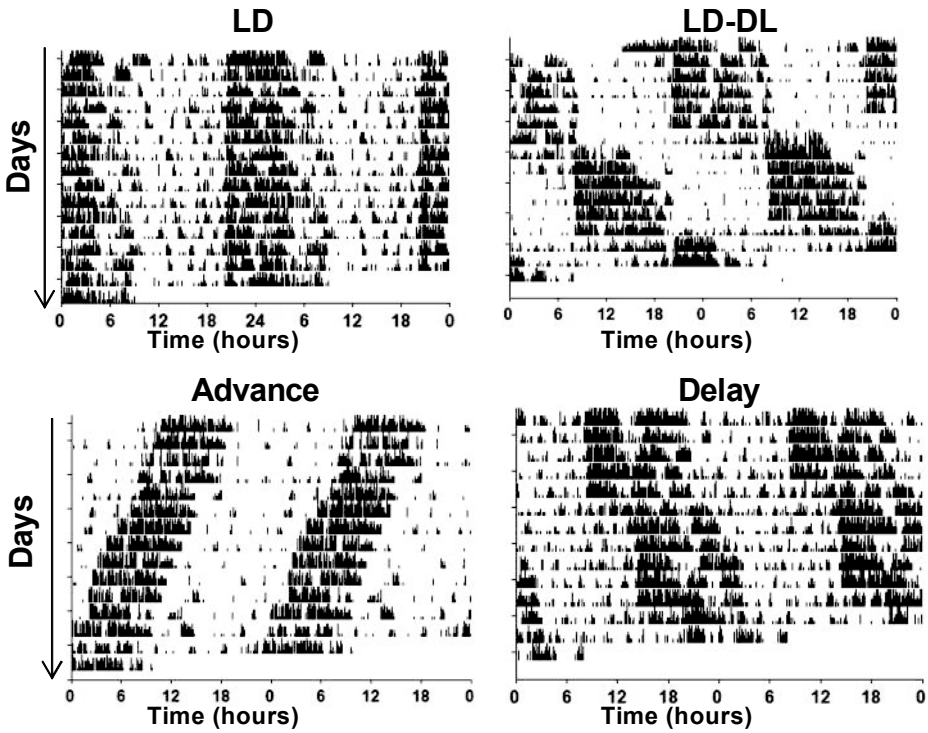

Figure 4. Representative actograms of mistimed light exposure. *APOE*3-Leiden.CETP mice fed WTD were exposed to LD, weekly 12 h reversal (LD-DL), weekly 6h advance or weekly 6h delay. During the last 10 days, mice were individually housed and behavioral activity was monitored by passive infrared monitors. Representative double-plotted actograms for 1 mouse per group are shown. Gray shading indicates dark period.*

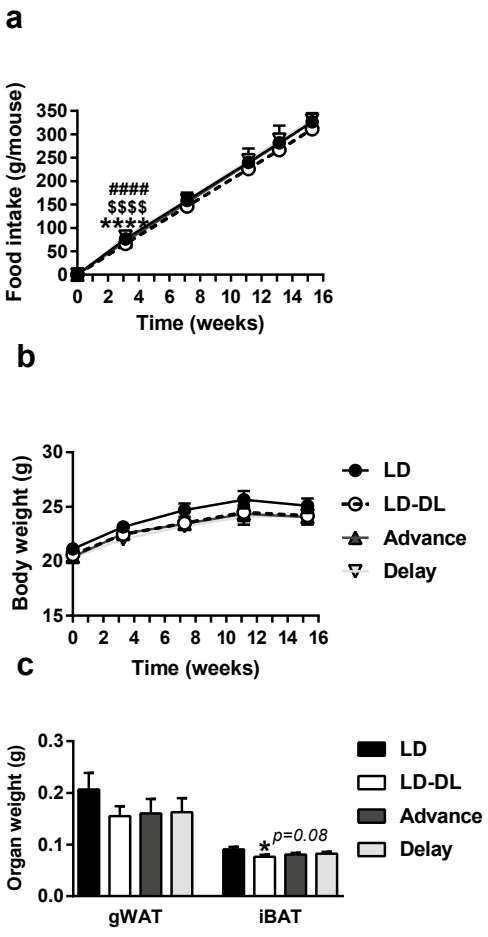

Figure 5. Weekly phase shift does not increase body weight or food intake. *APOE*3-Leiden.CETP mice fed WTD were exposed to LD, weekly 12 h reversal (LD-DL), weekly 6h advance or weekly 6h delay (n=15/group). Food intake (a) and body weight (b) were determined at regular intervals. After 14 weeks, subcutaneous gonadal white adipose tissue (gWAT) and interscapular brown adipose tissue (iBAT) were weighed (c). Data is presented as means ± SEM. * (LD-DL vs LD), $ (Delay vs LD); ANOVA, Fischer LSD post-hoc) = p<0.05, **,$$ = p<0.01. Data is presented as means ± SEM.*

Figure 6. (right page) Weekly phase shift increases atherosclerotic development independent of cholesterol levels. *APOE*3-Leiden.CETP mice fed WTD were exposed to LD, weekly 12 h reversal (LD-DL), weekly 6h advance or weekly 6h delay (n=15/group). Plasma total cholesterol (a) was determined at regular intervals. Total cholesterol exposure was calculated (b). After 11 weeks, whole blood was collected and pooled (n=3/group) for cell count using Sysmex (c). After 15 weeks, mice were sacrificed, hearts were isolated and atherosclerotic lesion size was determined at the aortic root (d) as well as lesion severity (e). Representative histological slides are shown for each group (f). Data is presented as means ± SEM. * (LD-DL vs. LD), $ (delay vs. LD), # advance vs. LD; ANOVA, Fischer LSD post-hoc) = p<0.05, ** = p<0.01. Data is presented as means ± SEM. WBC= white blood cells, RBC=red blood cells, PLT=platelets. Arrows indicate first day of light shift.*

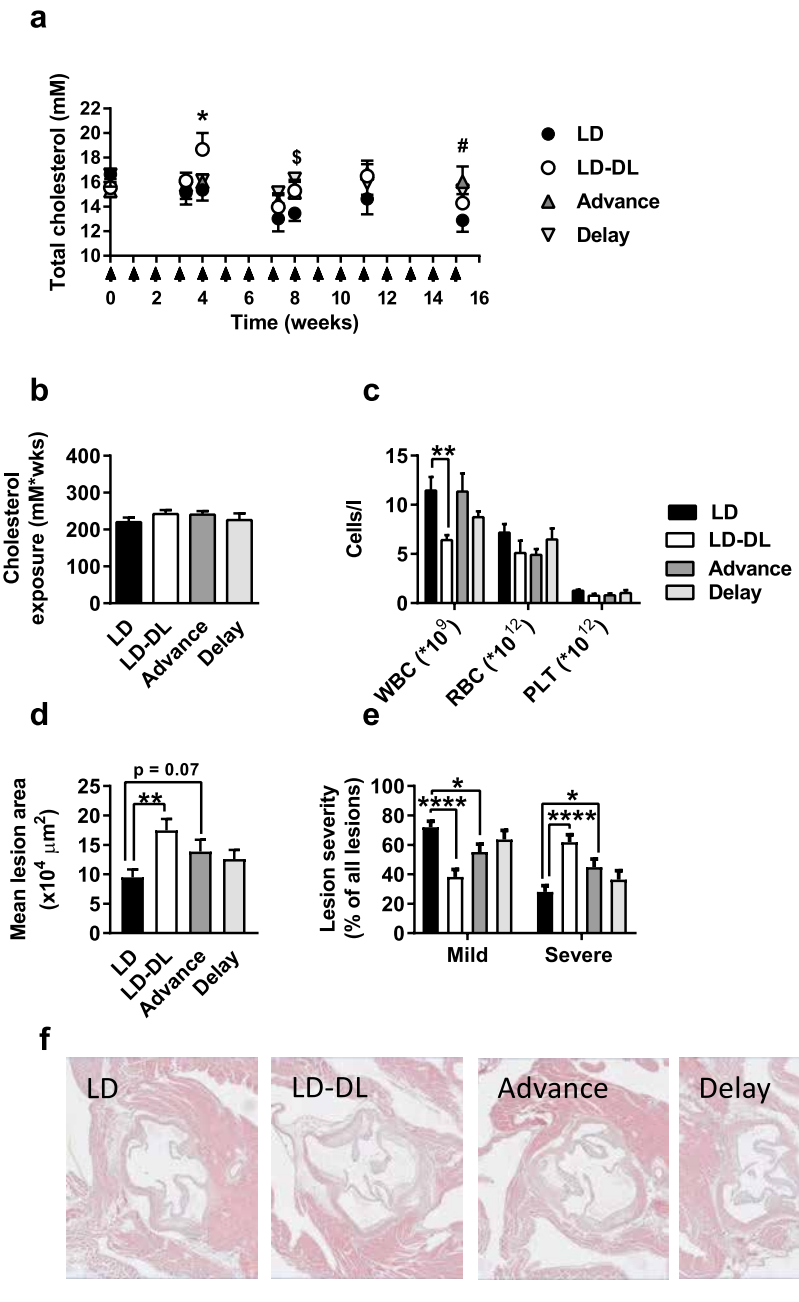
a
Total cholesterol (mM)
Time (weeks)
LD
LD-DL
Advance
Delay
b
Cholesterol exposure (mM*wks)
c
Cells/l
WBC (*10^9)
RBC (*10^12)
PLT (*10^12)
d
Mean lesion area (x10^4 µm^2)
p = 0.07
e
Lesion severity (% of all lesions)
Mild
Severe
f
LD
LD-DL
Advance
Delay

rhythm strength associated to either TC exposure or atherosclerotic lesion size. We found a weak positive correlation between rhythm strength and TC exposure ($p=0.02$, $R^2=0.28$) and not with atherosclerotic lesion area (Fig. 3i-j). In summary, as compared to LD exposure, 14 weeks of LL exposure attenuated circadian rhythm without increasing atherosclerosis development in dyslipidemic mice, despite raised TC exposure.

Weekly light shifts do not affect total food intake nor body weight

Previously, we showed that 5 weeks of LL exposure severely decreases rhythm strength in mice [27]. In the present experiment, we observed that after 14 weeks of LL a large subset of mice retained a strong rhythmicity, albeit with increased period length (Fig. 1). We reasoned that chronic LL exposure may have led to adaptation of mice to the light schedule. Additionally, constant light does not model human shift work, as in shift work light-dark cycles are maintained but shifted repeatedly depending on the shift rotation. This induces a repeated stress on the biological clock system, as the internal clocks need to adapt to the environmental light condition with every shift. For these reasons, we conducted a second experiment in which mice were subjected to either a weekly changing schedule of 6 h advance (advance), 6 h delay (delay) or 12 h light-dark reversal (LD-DL), compared to regular 12h light-dark (LD) cycles. Typical physical activity patterns are shown in (Fig. 4).

Similar to LL exposure, weekly shifted schedules transiently affected food intake of the mice in the first 3 weeks of the intervention. Compared to LD (76.1 ± 0.7 g/mouse), cumulative food intake measured during the first three weeks was lower in LD-DL (66.1 ± 0.7 g/mouse; $p<0.0001$) and advance (71.1 ± 0.7 g/mouse; $p=0.0001$) groups and higher in the delay group (81.1 ± 0.7 g/mouse; $p=0.0001$) (Fig. 5a). However, at subsequent time points, these differences did not persist. Also, body weight (Fig. 5b) and gonadal white adipose tissue mass did not differ between the different light schedules (Fig. 5c). Interestingly, compared to LD, iBAT weight decreased in LD-DL (0.076 ± 0.004 *vs.* 0.090 ± 0.005 g; $p=0.015$) and tended to decrease in the advance group (0.080 ± 0.003 g; $p=0.084$) (Fig. 5c).

Weekly light shifts increase atherosclerotic development independent of cholesterol levels

TC plasma levels were determined every 3-4 weeks. We did not observe consistent differences between the different groups with respect to TC levels (Fig. 6a), which was reflected by similar TC exposure between groups (Fig. 6b). After 11 weeks of light shifts, white blood count in peripheral blood was measured. In line with the decrease in white blood cells due to LL exposure, we observed also a decrease in white blood cell count due to LD-DL exposure ($6.4 \pm 1.5*10^9$ *vs.* $11.5 \pm 1.4*10^9$ cells/l; $p=0.010$). However, advance or delay did not change immune cell counts in peripheral blood and platelet count was not affected (Fig. 6c).

After 15 weeks of light schedule intervention, we determined atherosclerosis development. Compared to LD mice ($9.5 \pm 1.3*10^4$ mm^2), the delay group did not show differences in atherosclerotic plaque size in the aortic root ($12.6 \pm 1.5*10^4$ mm^2; $p=0.207$).

In contrast, 6h advance light schedule tended to increase atherosclerotic plaque size (13.9 ± 1.9*10^4 mm^2; p=0.074). Strikingly, LD-DL increased plaque size by 1.8-fold compared to LD mice (17.5 ± 1.9*10^4 mm^2; p=0.002) (Fig. 6d, f). The increased plaque size in LD-DL group and 6h advance group was accompanied by a shift of plaque severity, as LD-DL and 6h advance group displayed a decrease in mild plaques and an increase of severe plaques compared to LD (Fig. 6e).

DISCUSSION

This is the first study to demonstrate that mistimed light exposure aggravates atherosclerosis development. Specifically, we show that a weekly reversal of LD cycle, and to a lesser extent 6 h phase advance, increases atherosclerotic lesion size and lesion severity without considerable changes in plasma cholesterol levels. We therefore conclude that pro-atherogenic effects of disturbed rhythms may be due to mistimed light exposure, but are dependent on the timing of the light shift.

Constant light exposure of APOE*3-Leiden.CETP mice induced lengthening of the period of circadian physical activity rhythms in all mice, while only in a subset of mice it weakened the rhythm strength. We previously observed that 5 weeks of constant light exposure of male wild type mice induced a decrease in amplitude of the output of the central biological clock in the hypothalamus, the suprachiasmatic nuclei (SCN) [27]. Also, constant light induced an analogous decrease in rhythm strength in physical activity rhythms [17, 27]. Gender differences between these studies may have contributed to a different effect of light regime on rhythm strength. The SCN is sensitive to sex hormones, and gonadectomy experiments have demonstrated that sex hormones change circadian rhythms [28].

In our study, we did not observe an effect on body weight and adiposity. This is contrast with previous reports showing that constant light exposure increases body weight [29] and adiposity [17]. Most likely, this is due to use of different mouse models and gender. In our study, we used female APOE*3-Leiden.CETP mice on a C57Bl/6J background. It is known that female C57Bl/6J mice are less prone to diet-induced weight gain and development of insulin resistance than male C57Bl/6J mice [30] [31].

We did show that constant light exposure increased plasma TC levels, due to an increase in non-HDL-cholesterol. This effect could be explained by decreased BAT activity, since we previously observed that BAT activation increases hepatic uptake of remnants and thereby decreases TC levels in APOE*3-Leiden.CETP mice [19]. Short term LL exposure indeed decreased BAT activity [17]. In this study, we explored whether BAT was affected by long term LL but found only a lower *Ucp1* gene expression to support this hypothesis. Further studies are needed to investigate whether chronic LL exposure also decreases FA uptake by BAT. The increased plasma TC may also be a result of increased cholesterol absorption in the intestine. *Clockmt*$^{/mt}$ mice, which have a genetic disturbance of the biological clock, display increased enteric uptake of cholesterol. Consequently, these mice have

increased plasma TC levels and, when crossbred with *Ldlr-/-* mice, also display enhanced atherosclerosis development [32, 33].

Weekly reversal of light exposure aggravated atherosclerosis development without detectable changes in plasma cholesterol levels. This is striking, as previous studies in APOE*3.Leiden-CETP mice consistently showed a strong correlation between TC exposure and atherosclerosis development [34, 35]. Possibly, activation of pro-inflammatory pathways may be more important in the atherogenic effects of LD-DL exposure. We observed a decrease in total white blood cell count, which traditionally is associated with anti-atherogenic phenotype [36]. Alternatively, it may indicate more clearance of white blood cells, *e.g.* into the arterial wall. Additionally, inflammatory cells may be more polarized towards a pro-inflammatory status. In line with this hypothesis, it was previously shown that macrophages derived from *Clockmt/mt* mice have increased expression of pro-inflammatory cytokines [33]. Also, selective hematopoietic overexpression of clock gene *Rev-erbα* in *Ldlr*$^{-/-}$ mice skewed macrophages towards an M1 phenotype, thereby aggravating atherosclerotic development [37]. Lastly, phase shift increased LPS-induced mortality in mice and heightened LPS response in macrophages [38]. Together, these data strongly suggest that disturbed biological clock function induces a pro-inflammatory status, which may underlie the pro-atherogenic effect of LD-DL. The various light conditions had different effects on atherosclerosis formation. A weekly 6 h advance induced more severe lesions and tended to increase lesion size, while delay did not. This is in line with a study showing that in aged mice, advance but not delay light schedule increases mortality [21]. Adaptation to phase advance is more disturbing for the biological clock function. Moreover, 12h shifts induced more atherosclerosis than a 6 h shift. Therefore, there seems to be a correlation between the extent of disturbance to the biological clock function and atherosclerosis development.

We conclude that severe disturbance of circadian rhythm by advance light schedules and alternating LD-DL schedules accelerates atherosclerosis formation independent of plasma cholesterol levels. In human shift work, it has been shown that rotating shift work has a higher risk for CVD than fixed schedules [39]. Also, the duration of shift work has been shown to correlate to increase risk for CVD [10, 40, 41]. Our study supports a dose-dependent relationship between disturbance to the biological clock through mistimed light exposure and atherosclerosis. Together, these studies imply that employers and governments may need to rethink work schedules to minimize health risks.

ACKNOWLEDGMENTS

The authors thank M. Hoekstra and M. van Eck for use of hematology analyzer and EM de Ruiter and TCM Streefland for excellent technical assistance. **Conflict of Interest**: none. **Funding**: This research was supported by the Netherlands Organization for Scientific Research (NWO-VENI grant 016.136.125 to NR Biermasz), the European Foundation for the Study of Diabetes and the Programme Partner Novo Nordisk (grant 94802 to CP Coomans, JH Meijer and PCN Rensen), and the Dutch Diabetes Research Foundation (grant 2013.81.1663 to CP Coomans). PCN Rensen is an Established Investigator of the Dutch Heart Foundation (grant 2009T038). **Author contributions**: RB designed the study, wrote manuscript, performed experiments and analysed data; MS, SK performed experiments and analysed data; AR, PPSJ, LWP, SB, KW, CPC; performed experiments, NRB, JHM, PCN supervised the study.

REFERENCES

1. Alwan, A., *Global status report on noncommunicable diseases 2010*. 2011: World Health Organization.
2. Steinberg, D., *Atherogenesis in perspective: hypercholesterolemia and inflammation as partners in crime.* Nat Med, 2002. **8**(11): p. 1211-7.
3. Anderson, K.M., W.P. Castelli, and D. Levy, *Cholesterol and mortality. 30 years of follow-up from the Framingham study.* JAMA, 1987. **257**(16): p. 2176-2180.
4. Chua, E.C., *et al.*, *Extensive diversity in circadian regulation of plasma lipids and evidence for different circadian metabolic phenotypes in humans.* Proc. Natl Acad. Sci. U. S. A, 2013. **110**(35): p. 14468-14473.
5. Reutrakul, S. and K.L. Knutson, *Consequences of Circadian Disruption on Cardiometabolic Health.* Sleep Med Clin, 2015. **10**(4): p. 455-68.
6. Reutrakul, S. and C.E. Van, *Interactions between sleep, circadian function, and glucose metabolism: implications for risk and severity of diabetes.* Ann. N. Y. Acad. Sci, 2014. **1311**: p. 151-173.
7. Laermans, J. and I. Depoortere, *Chronobesity: role of the circadian system in the obesity epidemic.* Obes Rev, 2016. **17**(2): p. 108-25.
8. Eyv, T.-E., *Skiftwarbeid og helse (Shift work and health): en undersøkelse av mortalitet og morbiditet hos arbeidere i en kjemisk fabrik.* 1949: Porsgrunn; Jacobsen.
9. Brown, D.L., *et al.*, *Rotating night shift work and the risk of ischemic stroke.* Am J Epidemiol, 2009. **169**(11): p. 1370-7.
10. Vetter, C., *et al.*, *Association Between Rotating Night Shift Work and Risk of Coronary Heart Disease Among Women.* Jama, 2016. **315**(16): p. 1726-34.
11. Parent-Thirion, A.M., EnriqueHurley, JohnVermeylen, Greet, *Fourth European Working Conditions Survey*. 2007, EurWORK: Dublin: European Foundation for the Improvement of Living and Working Conditions.
12. McFadden, E., *et al.*, *The Relationship Between Obesity and Exposure to Light at Night: Cross-Sectional Analyses of Over 100,000 Women in the Breakthrough Generations Study.* Am. J Epidemiol, 2014.
13. Pattinson, C.L., *et al.*, *Environmental Light Exposure Is Associated with Increased Body Mass in Children.* PLoS One, 2016. **11**(1): p. e0143578.
14. Rybnikova, N.A., A. Haim, and B.A. Portnov, *Does*

artificial light-at-night exposure contribute to the worldwide obesity pandemic? Int J Obes. (Lond), 2016.

15. Koo, Y.S., *et al.*, *Outdoor artificial light at night, obesity, and sleep health: Cross-sectional analysis in the KoGES study.* Chronobiol Int, 2016. **33**(3): p. 301-14.
16. Obayashi, K., *et al.*, *Exposure to light at night, nocturnal urinary melatonin excretion, and obesity/dyslipidemia in the elderly: a cross-sectional analysis of the HEIJO-KYO study.* J Clin Endocrinol. Metab, 2013. **98**(1): p. 337-344.
17. Kooijman, S., *et al.*, *Prolonged daily light exposure increases body fat mass through attenuation of brown adipose tissue activity.* Proc. Natl Acad. Sci. U. S. A, 2015. **112**(21): p. 6748-6753.
18. Khedoe, P.P., *et al.*, *Brown adipose tissue takes up plasma triglycerides mostly after lipolysis.* J. Lipid Res, 2015. **56**(1): p. 51-59.
19. Berbee, J.F., *et al.*, *Brown fat activation reduces hypercholesterolaemia and protects from atherosclerosis development.* Nat Commun, 2015. **6**: p. 6356.
20. Van Dycke, K.C., *et al.*, *Chronically Alternating Light Cycles Increase Breast Cancer Risk in Mice.* Curr Biol, 2015. **25**(14): p. 1932-7.
21. Davidson, A.J., *et al.*, *Chronic jet-lag increases mortality in aged mice.* Curr Biol, 2006. **16**(21): p. R914-6.
22. Westerterp, M., *et al.*, *Cholesteryl ester transfer protein decreases high-density lipoprotein and severely aggravates atherosclerosis in APOE*3-Leiden mice.* Arterioscler Thromb Vasc Biol, 2006. **26**(11): p. 2552-9.
23. van den Maagdenberg, A.M., *et al.*, *Transgenic mice carrying the apolipoprotein E3-Leiden gene exhibit hyperlipoproteinemia.* J. Biol. Chem, 1993. **268**(14): p. 10540-10545.
24. Zadelaar, S., *et al.*, *Mouse models for atherosclerosis and pharmaceutical modifiers.* Arterioscler. Thromb. Vasc. Biol, 2007. **27**(8): p. 1706-1721.
25. Dörrscheidt GL and B. L., *Advanced methods for evaluating characteristic parameters of circadian rhythms.* J Mathemat Biol, 1975. **2**: p. 107-121.
26. Virtue, S. and A. Vidal-Puig, *Assessment of brown adipose tissue function.* Front Physiol, 2013. **4**: p. 128.
27. Coomans, C.P., *et al.*, *Detrimental effects of constant light exposure and high-fat diet on circadian energy metabolism and insulin sensitivity.* FASEB J, 2013. **27**(4): p. 1721-1732.
28. Yan, L. and R. Silver, *Neuroendocrine underpinnings of sex differences in circadian timing systems.* J Steroid Biochem Mol Biol, 2016. **160**: p. 118-26.
29. Fonken, L.K., *et al.*, *Dim light at night disrupts molecular circadian rhythms and increases body weight.* J. Biol. Rhythms, 2013. **28**(4): p. 262-271.
30. Montgomery, M.K., *et al.*, *Mouse strain-dependent variation in obesity and glucose homeostasis in response to high-fat feeding.* Diabetologia, 2013. **56**(5): p. 1129-39.
31. Yang, Y., *et al.*, *Variations in body weight, food intake and body composition after long-term high-fat diet feeding in C57BL/6J mice.* Obesity (Silver Spring), 2014. **22**(10): p. 2147-55.
32. Pan, X., *et al.*, *Diurnal regulation of MTP and plasma triglyceride by CLOCK is mediated by SHP.* Cell Metab, 2010. **12**(2): p. 174-186.
33. Pan, X., X.C. Jiang, and M.M. Hussain, *Impaired Cholesterol Metabolism and Enhanced Atherosclerosis in Clock Mutant Mice.* Circulation, 2013.
34. Kühnast, S., *et al.*, *Niacin Reduces Atherosclerosis Development in APOE*3Leiden.CETP Mice Mainly by Reducing NonHDL-Cholesterol.* PLoS One, 2013. **8**(6).
35. Kuhnast, S., *et al.*, *Anacetrapib reduces progression of atherosclerosis, mainly by reducing non-HDL-cholesterol, improves lesion stability and adds to the beneficial effects of atorvastatin.* Eur. Heart J, 2015. **36**(1): p. 39-48.
36. Kounis, N.G., *et al.*, *White Blood Cell Counts, Leukocyte Ratios, and Eosinophils as*

Inflammatory Markers in Patients With Coronary Artery Disease. Clinical and Applied Thrombosis/ Hemostasis, 2015. **21**(2): p. 139-143.

37. Ma, H., *et al.*, *Increased Atherosclerotic Lesions in LDL Receptor Deficient Mice With Hematopoietic Nuclear Receptor Rev-erbalpha Knock- Down.* J. Am. Heart Assoc, 2013. **2**(4): p. e000235.
38. Castanon-Cervantes, O., *et al., Dysregulation of inflammatory responses by chronic circadian disruption.* J Immunol, 2010. **185**(10): p. 5796-805.
39. Fujino, Y., *et al., A prospective cohort study of shift work and risk of ischemic heart disease in Japanese male workers.* Am. J. Epidemiol, 2006. **164**(2): p. 128-135.
40. Kawachi, I., *et al.*, *Prospective study of shift work and risk of coronary heart disease in women.* Circulation, 1995. **92**(11): p. 3178-3182.
41. Haupt, C.M., *et al., The relation of exposure to shift work with atherosclerosis and myocardial infarction in a general population.* Atherosclerosis, 2008. **201**(1): p. 205-211.

PART II

Circadian rhythms in human studies: implications for metabolic health

Chapter 6

A single night of sleep curtailment increases plasma acylcarnitines: novel insights in the relationship between sleep and insulin resistance

Rosa van den Berg, Dennis O. Mook-Kanamori, Esther Donga, Marieke van Dijk, J. Gert van Dijk, Gert-Jan Lammers, Klaas W. van Kralingen, Cornelia Prehn, Jerzy Adamski, Johannes A. Romijn, Ko Willems van Dijk, Eleonora P. M. Corssmit, Patrick C.N. Rensen, Nienke R. Biermasz

Arch Biochem Biophys 2016; 589: 145-51

ABSTRACT

We have previously shown that acute sleep curtailment induces insulin resistance, both in healthy individuals as well as in patients with type 1 diabetes, suggesting a causal role for sleep disturbances in pathogenesis of insulin resistance, independent of endogenous insulin production. However, the underlying mechanisms remain unclear. This study aimed to explore the metabolic pathways affected by sleep loss using targeted metabolomics in human fasting plasma samples. Healthy individuals (n = 9) and patients with type 1 diabetes (n = 7) were studied after a single night of short sleep (4 hours) versus normal sleep (8 hours) in a cross-over design. Strikingly, one night of short sleep specifically increased the plasma levels of acylcarnitines, essential intermediates in mitochondrial fatty acid oxidation (FAO). Specifically, short sleep increased plasma levels of tetradecenoyl-L-carnitine (C14:1) (+32%, $p=2.67*10^{-4}$), octadecanoyl-L-carnitine (C18:1) (+22%, $p=1.92*10^{-4}$) and octadecadienyl-L-carnitine (C18:2) (+27%, $p=1.32*10^{-4}$). Since increased plasma acylcarnitine levels could be a sign of disturbed FAO, it is possible that sleep curtailment acutely induces inefficient mitochondrial function. Our observations provide a basis for further research into the role of acylcarnitines as a potential mechanistic pathway by which sleep deprivation – even short term – causes adverse metabolic effects, such as insulin resistance.

INTRODUCTION

Diabetes mellitus (DM) is characterized by either an absolute (type 1; DM1) or relative (type 2; DM2) deficiency of insulin. Both DM1 and DM2 are associated by increased morbidity and increased cardiovascular risk [1, 2]. Peripheral insulin resistance precedes the development of DM2 and recently it has been recognized that a certain degree of insulin resistance is also present in DM1 [3]. Therefore, uncovering modifiable risk factors in an early stage of insulin resistance development is of crucial importance to reduce the number of patients with DM2 and improve glycemic control in DM1. Interestingly, the DM2 epidemic coincides with a reduction in the average sleep duration, which has gradually declined with ~1.5 hours per night [4] over the past decades. In fact, large epidemiological cohorts have documented an association between sleep duration and increased insulin resistance [5]. Furthermore, short sleep has been associated with poor glycemic control in DM1 [6]. Both short and long duration of sleep are associated with an increased risk for insulin resistance, implying that there might be an optimal sleep duration of approximately 8 hours [7-10]. Several human intervention studies showed that decreased sleep duration causes insulin resistance. Repeated sleep curtailment during more than 6 nights increased insulin resistance in healthy individuals [11-13]. Moreover, we previously published that even one single night with partial sleep loss, i.e. 4 hours sleep allowed, a condition representative for incidental daily life sleep habits, is sufficient to induce peripheral insulin resistance in both healthy young individuals [14] as well as patients with DM1 [15].

The mechanism by which acute sleep curtailment induces insulin resistance has not been fully elucidated. Plasma metabolomics is considered a valuable approach to assess underlying biological processes, complementary to genomics and transcriptomics. Strikingly, metabolite levels reflect biological activity of the encoded proteins and are thus closer to the clinical endpoints [16]. Indeed, metabolomics has previously been demonstrated to be a powerful tool in investigating insulin resistance and DM2 [17]. Thus far, the effects of sleep loss on the human metabolome are poorly characterized. Prolonged sleep deprivation during 5 days has been shown to induce metabolite changes in lipid, carbohydrate, amino acid and protein pathways [18, 19]. In contrast, Davies *et al.* [20] subjected healthy individuals to complete sleep restriction of 24 hours. This extreme sleep deprivation resulted in increased plasma levels of glycerophospholipids, acylcarnitines, sphingolipids and amino acids. However, the sleep intervention and control sleep occurred on consecutive days in all individuals. Differences between metabolite levels were also observed between the wake periods, suggesting that the study conditions were not fully comparable. In addition, none of these previous studies included measurements of insulin resistance. Therefore, the aim of the present study was to use metabolomics to explore pathways involved in the relationship between sleep and insulin resistance in a cohort with proven insulin resistance upon short sleep duration [14, 15]. To this end, we examined 163 metabolites in 16 individuals (healthy individuals and individuals with DM1) subjected to a night of normal sleep duration (8 hours) and one night of short sleep duration (4 hours). Here, we report that one night of sleep curtailment specifically increases the metabolic class of

acylcarnitines in plasma, suggesting that increased acylcarnitines are associated with the observed relationship between sleep curtailment and induction of insulin resistance.

MATERIALS AND METHODS

Protocol

Two studies were previously performed, to study the effect of one night of short sleep duration (4 hours) compared to normal sleep duration (8 hours) on peripheral insulin resistance [14, 15]. The studies applied the same study design in two different populations, namely healthy individuals and patients [14] with type 1 diabetes (DM1) [15]. Healthy individuals were studied to determine the effects of a single night of short sleep duration on insulin resistance. The second study assessed the effects of short sleep duration on insulin resistance in DM1 patients on stable insulin pump therapy. DM1 patients do not have endogenous insulin production and therefore cannot compensate for fluctuations in insulin resistance. We hypothesized that variations in sleep duration could contribute the intra-individual variations in glucoregulation. In both healthy individuals and individuals with DM1, decreased sleep duration induced insulin resistance. Therefore, we reasoned that a single night of short sleep duration may increase peripheral insulin resistance via a common metabolic pathway. To investigate which pathways could be involved, we analyzed metabolites from both studies and pooled the data.

Subjects

The study was approved by the medical ethical committee of the Leiden University Medical Center and all subjects gave written informed consent. We recruited a total of 18 individuals. Briefly, nine healthy individuals were recruited by advertisement and nine individuals with DM1 with stable continuous subcutaneous insulin pump therapy were included from our outpatient clinic. Exclusion criteria for all individuals were BMI>26 kg/m^2, history of sleep disorders, psychiatric disorders and use of sleep medication, β-blocking drugs and prokinetic drugs. All individuals had a stable weight in the past 3 months and had regular and non-extreme sleeping habits. Habitual sleep duration was assessed by 7 days of actigraphy (Actiwatch AW7; Cambridge Neurotechnology, Cambridge, UK) prior to both study days and sleep questionnaires (Epworth Sleepiness Scale, Pittsburg Sleep Quality Index and Berlin Questionnaire). Subjects were instructed to maintain a regular dietary, activity and sleep regiments 3 days prior to both study days, fitting their habits, which they recorded in a diary. DM1 patients were instructed to keep a stable insulin pump setting. Of the 18 recruited individuals, 2 individuals with DM1 were excluded from all analyses, one due to previously undiagnosed sleep apnea and one due to nocturnal hypoglycemia.

Experimental design

Subjects were subjected to in-hospital sleep registration for 3 days, of which study day 1 was for basal measurements and habituation to hospital conditions. Sleep duration and quality (of parameters) was assessed by polysomnography as described previously [14, 15]. All subjects underwent both a normal sleep night of at least 8 hours and one night of 4 hours sleep, the order of which was determined by balanced assignment, in a cross-over design with at least 3 weeks interval between measurements. In both sleep conditions, subjects spent 8.5 hours (from 23:00 to 7:30) in bed and were fasting from 22:00 onwards. During sleep curtailment, subjects were allowed to sleep from 01:00 to 05:00, the remaining time they were allowed to read or watch movies in upward position in dim light. Their wakefulness was monitored. After the night of normal or short sleep, a fasting plasma sample was obtained at 8:30 am, after which a hyperinsulinemic euglycemic clamp was performed as described in detail previously [15] to establish peripheral insulin sensitivity, endogenous glucose production and hepatic insulin sensitivity. Briefly, a primed (17.6 µmol*kg^{-1}) continuous (0.22 µmol*kg^{-1}*min^{-1}) infusion of [6,6-$^{2}H_{2}$]glucose (Cambridge Isotope laboratory, Andover, MA) was administered via a catheter. Infusion of insulin (Actrapid, Novo Nordisk, Alphen a/d Rijn) occurred simultaneously according to DeFronzo [21]. Blood samples were obtained every 5 minutes from the contralateral arm for glucose measurements to adjust variable infusion of 20% glucose with 3% [6,6-$^{2}H_{2}$]glucose to maintain euglycemia (i.e. 5.0 mM), which was started 4 min after start of insulin infusion. Free fatty acids were determined in basal fasting plasma samples as by enzymatic colorimetric assay [14, 15].

Metabolomics

Metabolomics analysis was performed on fasting plasma samples in all individuals using the Biocrates Absolute*IDQ*™ p150 kit (Biocrates, Life Science AG, Innsbruck, Austria) in the Genome Analysis Center at the Helmholtz Zentrum, Munich, Germany. The assay procedures of the Absolute*IDQ*™ p150 kit as well as the metabolite nomenclature have been described in detail previously [22, 23]. Briefly, 10 µL of each plasma sample was pipetted into a 96 well sandwich plate containing an inserted filter with previously applied stable isotope labeled internal standards. The filters in the wells were dried using a stream of nitrogen. Amino acids were derivatized with 5% phenylisothiocyanate reagent (PITC) and the filters were dried again. Metabolites as well as internal standards were extracted with 5 mM ammonium acetate in methanol and the solutions were centrifuged through the filter membrane into the lower deep well plate. The extracts were diluted with MS running solvent and analyzed. Flow injection analysis (FIA) tandem mass spectrometry (MS/MS) method was used to quantify 163 metabolites, including free carnitine, 40 acylcarnitines, 14 amino acids (13 proteinogenic + ornithine), hexoses (sum of hexoses), 92 glycerophospholipids (15 lysophosphatidylcholines (lysoPC) and 77 phosphatidylcholines (PC), and 15 sphingolipids. Internal standards served as reference for the calculation of metabolite concentrations (µM). The complete list of analyzed metabolites grouped by metabolite class is presented in supplementary material (Table S3).

Statistical analysis

For all metabolites, differences between short and normal sleep were calculated by subtracting plasma levels obtained after short sleep from those obtained after normal sleep. Paired Students T-tests for were performed comparing normal and short sleep (SPSS statistical package edition 20) with Bonferroni post-hoc correction for multiple testing. $P< 3.07*10^{-4}$ (=0.05/163; after correction) was considered statistically significant. Calculations for hyperinsulinemic euglycemic clamp analysis were described previously [14, 15]. Since we aimed to investigate the effect of short sleep on metabolite levels, individuals of both groups (healthy individuals and individuals with DM1) were pooled to determine effects of sleep duration. Two way repeated measure ANOVA was performed to analyze interaction effects of subgroup (healthy *vs.* DM1) with sleep duration. Data are presented as means ± SD. Since baseline characteristics and insulin sensitivity data were published for healthy individuals and individuals with DM1 separately, in this paper these data are shown for the two groups together. To allow comparison between subgroups, the baseline characteristics, sleep indices and insulin sensitivity data are included in the supplemental tables and were compared using Student's t-test.

RESULTS

Basal clinical characteristics

Metabolites were measured in sixteen individuals after a night of short sleep (4 hours) versus after a night of normal sleep (8 hours) duration. Subjects had a mean age of 44 ± 14 years and included 8 women. Individuals were lean, with an average BMI of 23.7 ± 2.2 kg/m^2 and a waist hip ratio of 0.85 ± 0.08 (Table 1). The study population consisted of nine healthy individuals (56%) and seven individuals with type 1 diabetes mellitus (DM1) (44%). Sleep duration prior to the study days did not differ healthy individuals (mean recorded sleep duration prior to study day 1 and 2: 420 ± 20 min *vs.* 476 ± 11 min; p=0.19) nor in individuals with DM1 (mean recorded sleep duration prior to study day 1 and 2: 475 ± 8 min *vs.* 490 ± 7 min; p=0.12). Results of healthy individuals and individuals with DM1 were reported previously separately [14, 15]. Age, sex distribution, BMI and waist-hip ratio were comparable between these two subgroups (Table S1).

	Subjects (n = 16)
Females (%)	8 (50%)
Age (years)	44 ± 14
BMI (kg/m^2)	23.7 ± 2.2
WHR	0.85 ± 0.08

Table 1: Study population characteristics[1]. *BMI = body mass index. WHR = waist hip ratio. Data is presented as mean (SD or percentage). [1]Data are pooled from two previously published studies [14;15].*

	Subjects (n = 16)		
Sleep parameters	**Normal sleep**	**Short sleep**	**p**
TST (min)	461 ± 25	225 ± 24	**<0.001**
Stage 1 (% of TST)	10 ± 3	10 ± 6	0.798
Stage 2 (% of TST)	43 ± 7	37 ± 9	**0.002**
Stage 3 (% of TST) (SWS)	24 ± 7	34 ± 10	**<0.001**
REM sleep (% of TST)	23 ± 4	18 ± 8	**0.025**
Sleep efficiency (%)	93 ± 4	91 ± 7	0.418
Plasma parameter			
Free fatty acids (mmol/l)	0.65 ± 0.24	0.61 ± 0.19	0.24
Insulin sensitivity parameters			
EGP (µmol * kg LBM^{-1} * min^{-1})	4.7 ± 1.9	5.5 ± 1.7	0.087
GDR (µmol * kg LBM^{-1} * min^{-1})	34.1 ± 13.8	27.9 ± 9.8	**0.001**
GIR (µmol * kg LBM^{-1} * min^{-1})	29.0 ± 14.7	22.1 ± 10.7	**0.001**

Table 2: Effects of short sleep on sleep parameters and insulin sensitivity[1]. *Insulin sensitivity parameters were determined by hyperinsulinemic euglycemic clamp. EGP = endogenous glucose production, GDR = glucose disposal rate (glucose Rd), GIR = glucose infusion rate. LBM = lean body mass. Sleep characteristics were determined by polysomnography. TST = total sleep time. SWS = slow wave sleep. Data is presented as means (SD). Effect of sleep intervention was tested with paired Students T-test, significant differences shown in bold. [1] Data are pooled from two previously published studies [14;15].*

Short sleep increases insulin resistance

Short sleep intervention was effective in reducing total sleep time (TST) by -51% (461 ± 25 *vs* 225 ± 26 min, p < 0.001). The reduction of sleep duration was due to decreased sleep duration of both non-REM (stage 2 and stage 3) and REM sleep (Table 2). Fasting plasma free fatty acids did not differ between sleep conditions (Table 2) or between subgroups (Table S2). Next, the effect of short sleep on insulin resistance was investigated by hyperinsulinemic euglycemic clamp studies. Interestingly, a single night of short sleep increased peripheral insulin resistance, as indicated by a decreased glucose disposal rate (GDR) (34.1 ± 13.8 *vs* 27.9 ± 9.8 µmol*kg LBM^{-1}*min^{-1}, p = 0.001) and decreased glucose infusion rate (GIR) (29.0 ± 14.7 *vs* 22.1 ± 10.7 µmol*kg LBM^{-1}*min^{-1}, p=0.001). Short sleep tended to increase endogenous glucose production (EGP) by the liver in all subjects (4.7 ± 1.9 vs 5.5 ± 1.6 µmol*kg LBM^{-1}*min^{-1}, p=0.08; Table 2). This was mainly due to increased endogenous glucose production in the subset of healthy individuals (Table S2; previously published in [14]). Expectedly, individuals with DM1 displayed higher baseline insulin resistance than in healthy individuals [3] (EGP 6.2 ± 1.9 *vs*. 3.6 ± 0.6, p=0.003; GDR 25.5 ± 6.4 *vs.* 40.7 ± 14.3, p=0.028; GIR 19.0 ± 7.0 *vs*. 36.9 ± 14.4, p=0.014, Table S2). Moreover, short sleep increased peripheral insulin resistance irrespective of this difference in baseline insulin sensitivity, suggesting a that short sleep may induce insulin resistance in healthy individuals and individuals with DM1 via a common pathway. Therefore, the effect of short sleep was investigated for healthy individuals and individuals with DM1 together.

	All subjects			*Healthy*			*DM1*		
Metabolite	**Mean Difference[1]**	**Change (%)[2]**	**P-Value**	**Mean Difference[1]**	**Change (%)[2]**	**P-Value**	**Mean Difference[1]**	**Change (%)[2]**	**P-Value**
C0	0.191	0.7%	$8.81*10^{-1}$	0.398	1.3%	$8.47*10^{-1}$	-0.075	-0.3%	$9.61*10^{-1}$
C2	**0.662$**	**16.8%**	**2.28*10-2**	**0.184**	**4.4%**	**5.40*10-1**	**1.276$**	**35.6%**	**1.33*10-2**
C3	-0.006	-2.6%	$6.76*10^{-1}$	-0.002	-0.7%	$9.33*10^{-1}$	-0.012	-6.2%	$6.03*10^{-1}$
C3:1	-0.001	-5.9%	$4.16*10^{-1}$	0.000	-0.1%	$9.93*10^{-1}$	-0.001	-12.3%	$1.58*10^{-1}$
C3-DC (C4-OH)	0.007	11.3%	$4.55*10^{-1}$	0.006	8.0%	$7.20*10^{-1}$	0.009	17.7%	$2.87*10^{-1}$
C3-OH	0.001	3.3%	$5.03*10^{-1}$	0.002	8.5%	$5.91*10^{-2}$	-0.001	-2.1%	$8.24*10^{-1}$
C4	0.011	10.3%	$1.22*10^{-1}$	0.008	7.2%	$4.95*10^{-1}$	0.015	14.4%	$8.68*10^{-2}$
C4:1	0.002	6.7%	$2.90*10^{-1}$	0.002	8.7%	$2.55*10^{-1}$	0.001	4.8%	$6.58*10^{-1}$
C5	0.011	10.2%	$2.80*10^{-1}$	0.012	10.4%	$4.59*10^{-1}$	0.010	9.8%	$4.30*10^{-1}$
C5:1	0.000	1.0%	$8.74*10^{-1}$	-0.001	-2.5%	$7.86*10^{-1}$	0.001	5.0%	$6.20*10^{-1}$
C5:1-DC	0.000	2.6%	$6.75*10^{-1}$	-0.001	-4.8%	$5.96*10^{-1}$	0.002	12.5%	$1.27*10^{-1}$
C5-DC (C6-OH)	-0.001	-4.1%	$4.87*10^{-1}$	-0.001	-8.3%	$2.56*10^{-1}$	0.000	0.7%	$9.45*10^{-1}$
C5-M-DC	0.000	0.3%	$9.32*10^{-1}$	0.000	-1.1%	$8.45*10^{-1}$	0.001	1.9%	$7.11*10^{-1}$
C5-OH (C3-DC-M)	0.000	0.3%	$9.40*10^{-1}$	0.000	-1.5%	$6.89*10^{-1}$	0.001	2.4%	$7.40*10^{-1}$
C6 (C4:1-DC)	0.005	8.7%	$1.22*10^{-1}$	0.001	1.9%	$7.82*10^{-1}$	0.011	18.8%	$6.20*10^{-2}$
C6:1	0.001	2.6%	$3.99*10^{-1}$	0.001	3.5%	$3.35*10^{-1}$	0.000	1.5%	$8.05*10^{-1}$
C7-DC	**0.005$**	**20.0%**	**5.41*10-4**	**0.002**	**8.4%**	**8.50*10-2**	**0.008$**	**34.8%**	**3.21*10-4**
C8	0.003	1.9%	$6.06*10^{-1}$	-0.005	-3.1%	$5.56*10^{-1}$	0.013$	11.0%	$4.38*10^{-3}$
C8:1	0.012	15.4%	$1.62*10^{-1}$	0.008	11.8%	$3.93*10^{-1}$	0.017	18.9%	$3.09*10^{-1}$
C9	0.000	-0.4%	$9.47*10^{-1}$	-0.001	-4.7%	$5.73*10^{-1}$	0.001	5.4%	$5.51*10^{-1}$
C10	0.014	5.8%	$1.84*10^{-1}$	0.003	1.1%	$8.62*10^{-1}$	0.027*	15.1%	$4.54*10^{-3}$
C10:1	0.008	6.9%	$2.68*10^{-1}$	-0.004	-3.1%	$6.68*10^{-1}$	0.022*	23.9%	$2.72*10^{-2}$
C10:2	0.000	-0.7%	$8.65*10^{-1}$	0.000	-0.1%	$9.79*10^{-1}$	0.000	-1.3%	$8.51*10^{-1}$

	All subjects			*Healthy*			*DM1*		
Metabolite	**Mean Difference[1]**	**Change (%)[2]**	**P-Value**	**Mean Difference[1]**	**Change (%)[2]**	**P-Value**	**Mean Difference[1]**	**Change (%)[2]**	**P-Value**
C12	**0.012$**	**17.2%**	**1.70*10-3**	**0.010**	**12.0%**	**9.00*10-2**	**0.015$**	**27.5%**	**3.30*10-3**
C12:1	**0.017$**	**23.6%**	**1.74*10-3**	**0.014**	**17.0%**	**8.32*10-2**	**0.021$**	**35.2%**	**5.85*10-3**
C12-DC	0.002	2.4%	$1.53*10^{-1}$	0.002	2.1%	$3.78*10^{-1}$	0.003	2.8%	$3.01*10^{-1}$
C14	**0.004$**	**15.6%**	**1.21*10-2**	**0.002**	**8.5%**	**2.42*10-1**	**0.006$**	**28.0%**	**1.97*10-2**
C14:1	**0.020#**	**32.4%**	**2.67*10-4**	**0.017$**	**23.5%**	**2.34*10-2**	**0.024$**	**49.1%**	**6.55*10-3**
C14:1-OH	0.001	6.2%	$3.79*10^{-1}$	0.000	-1.7%	$8.10*10^{-1}$	0.001	16.9%	$2.36*10^{-1}$
C14:2	**0.006$**	**26.1%**	**5.48*10-4**	**0.005**	**17.3%**	**5.01*10-2**	**0.008$**	**41.5%**	**4.17*10-3**
C14:2-OH	0.000	5.0%	$3.64*10^{-1}$	0.000	6.4%	$2.91*10^{-1}$	0.000	3.3%	$7.48*10^{-1}$
C16	**0.007$**	**10.8%**	**1.94*10-2**	**0.005**	**6.7%**	**2.05*10-1**	**0.010**	**17.1%**	**5.91*10-2**
C16:1	**0.005$**	**8.8%**	**9.60*10-3**	**0.005$**	**8.3%**	**3.06*10-2**	**0.005**	**9.6%**	**1.55*10-1**
C16:1-OH	**0.001$**	**20.8%**	**5.71*10-3**	**0.001**	**11.8%**	**1.90*10-1**	**0.002$**	**33.8%**	**1.10*10-2**
C16:2	**0.001$**	**21.3%**	**9.72*10-3**	**0.001**	**9.6%**	**2.39*10-1**	**0.002$**	**39.5%**	**1.91*10-2**
C16:2-OH	0.000	2.1%	$6.29*10^{-1}$	0.000	3.8%	$5.45*10^{-1}$	0.000	-0.1%	$9.83*10^{-1}$
C16-OH	0.000	0.9%	$8.89*10^{-1}$	0.000	-3.4%	$5.84*10^{-1}$	0.000	6.1%	$6.49*10^{-1}$
C18	0.003	10.8%	$7.34*10^{-2}$	0.002	9.6%	$3.04*10^{-1}$	0.003	12.5%	$1.18*10^{-1}$
C18:1	**0.016#**	**22.3%**	**1.92*10-4**	**0.015***	**20.1%**	**2.96*10-3**	**0.019$**	**25.1%**	**2.84*10-2**
C18:1-OH	0.001	12.8%	$6.02*10^{-2}$	0.001	5.7%	$3.93*10^{-1}$	0.002	22.3%	$1.07*10^{-1}$
C18:2	**0.007#**	**27.0%**	**1.32*10-4**	**0.005$**	**20.7%**	**9.01*10-4**	**0.010$**	**34.4%**	**1.38*10-2**

Table 3: (caption on next page).

Table 3: (previous pages) Difference between short sleep and normal sleep duration in acylcarnitine levels.

[1]Difference in metabolite levels (μM) as measured by BiocratesIDQTM p150 kit between short and normal sleep duration. Positive mean difference indicates an increase after short sleep duration. Negative mean difference indicates a decrease after short sleep duration.

[2]Change (%) represents percentage of change in metabolite level in short compared to normal sleep (metabolite level (short sleep) – metabolite level (normal sleep)) / metabolite level (normal sleep).

DM1 = individuals with type 1 diabetes. P-values are based on paired Students t-tests. N= 16 (healthy: n=9, DM1: n=7). Full results table is shown in Supplemental Table S2. Abbreviations of acylcarnitines are shown in Supplemental Table S3.

*$: Significant difference (p<0.05). #: Significant difference after Bonferroni correction ($p<3.0*10^{-4}$ (=0.05/163)). Significant differences metabolites in all subjects are displayed in bold.*

Short sleep specifically increases plasma acylcarnitines

To investigate possible pathways which could be involved in the increased of insulin resistance by short sleep duration, we performed metabolomics analysis on fasting morning plasma samples. A total of 163 metabolites representing 5 different classes were measured (Table S3). Short sleep increased thirteen metabolites ($p<0.05$) (Table 3). Strikingly, all of these are acylcarnitines. After stringent post-hoc correction, short sleep significantly increased plasma levels of tetradecenoyl-L-carnitine (C14:1) by +32% (plasma level difference: +0.017 μM, $p=2.67*10^{-4}$), octadecenoyl-L-carnitine (C18:1) by +22% (plasma level difference: +0.015 μM, $p=1.92*10^{-4}$) and octadecadienyl-L-carnitine (C18:2) by +27% (plasma level difference: +0.005 μM, $p=1.32*10^{-4}$). Short sleep duration increased acylcarnitines in both subgroups, indicating that the effect of short sleep on acylcarnitines was not dependent on having DM1 or being healthy. There was no interaction effect of the subgroup (healthy *vs.* DM1) with the sleep duration (short *vs.* normal) for the 13 increased acylcarnitines. Baseline acylcarnitine levels (i.e. after normal sleep) did not differ between healthy individuals and DM1, except for a higher level of C:12-DC in DM1 (0.087 ± 0.005 vs 0.101 ± 0.005 μM, $p<0.0001$) (Table S5). Acylcarnitines levels did not differ between healthy individuals and DM1 after short sleep (Table S6). We therefore conclude that a single night of short sleep specifically increased plasma acylcarnitines (Table 4).

DISCUSSION

The present study aimed to explore the metabolic pathways affected by sleep curtailment using targeted plasma metabolomics in individuals (healthy individuals and individuals with type 1 diabetes (DM1)) subjected to both short sleep (4 hours) and normal sleep (8 hours). As part of the same study, we previously reported that this short sleep intervention increased peripheral insulin resistance in both study groups as determined by hyperinsulinemic

Metabolite	Interaction P-value	Effect of sleep P-value	Effect of DM1 status P-value
C2	3.24 * 10-2	6.70 * 10-3$	8.33 * 10-1
C7-DC	1.10 * 10-3	<1.0 * 10-4#	4.53 * 10-1
C12	4.48 * 10-1	1.80 * 10-3#	2.35 * 10-1
C12:1	4.43 * 10-1	1.90 * 10-3#	2.25 * 10-1
C14	2.24 * 10-1	8.70 * 10-3#	1.01 * 10-1
C14:1	4.05 * 10-1	3.00 * 10-4#	1.68 * 10-1
C14:2	2.30 * 10-1	4.00 * 10-4#	4.22 * 10-1
C16	3.48 * 10-1	1.68 * 10-2$	2.09 * 10-1
C16:1	8.94 * 10-1	1.25 * 10-2$	3.82 * 10-1
C16:1-OH	1.42 * 10-1	3.30 * 10-3#	8.79 * 10-1
C16:2	8.34 * 10-2	4.30 * 10-3$	6.62 * 10-1
C18:1	5.97 * 10-1	3.00 * 10-4#	7.64 * 10-1
C18:2	1.35 * 10-1	<1.00 * 10-4#	1.81 * 10-1

Table 4. Interaction effects of diabetes status and short sleep on increased acylcarnitine levels. *DM1 = individuals with type 1 diabetes. Abbreviations of acylcarnitines are shown in Supplemental Table S3. $p<0.05, #p<0.004 (0.05/13) (two way repeated measure ANOVA).*

euglycemic clamp analysis [14, 15]. We now show that one night of short sleep specifically increases plasma levels of acylcarnitines, in both healthy individuals and DM1 patients.

Our study is the first to show that short sleep duration increased plasma acylcarnitines in concert with increased insulin resistance in both healthy individuals and individuals with DM1. This indicates that short sleep duration affects metabolism irrespective of pre-existing insulin producing capacity. The relationship between increased plasma acylcarnitine levels and increased insulin resistance is supported by association studies. Human studies showed increased plasma levels of acylcarnitines in individuals with impaired fasting glucose and with type 2 diabetes (DM2), compared to healthy controls [24, 25]. The significance of this association is still a matter of debate, since human intervention studies are lacking [26].

It is interesting to speculate about the biological relevance of increased plasma levels of acylcarnitines. Acylcarnitines are vital to energy homeostasis. They are esters of fatty acids and carnitine, which are transported over the outer and inner mitochondrial membranes by carnitine palmitoyl transferases (CPTs). Thus, acylcarnitines are essential to shuttle fatty acids from the cytoplasm into mitochondria were they can be oxidized and enter the tricarboxylic acid (TCA) cycle to generate ATP. An excess of acylcarnitines is generally viewed as a result from a mismatch between TCA flux and fatty acid oxidation (FAO) [27]. Previously reported causes of this mismatch include prolonged fasting and excessive muscle activity [28-30]. The present study, in which subjects participated in a protocol that controlled for food intake and physical activity, adds sleep deprivation as a provoking event. A mismatch between FAO and TCA flux has been related to mitochondrial dysfunction. Patients with inborn errors of FAO have increased plasma levels of especially

long chain acylcarnitines [31]. Interestingly, altered mitochondrial parameters have been frequently linked to insulin resistance in the context of both DM1 and DM2 [32-38]. Moreover, mitochondrial dysfunction in mice induces skeletal muscle insulin resistance [27] while TCA-FAO mismatch predisposes mice to diet-induced obesity and insulin resistance [39]. It is therefore tempting to speculate that in our model of insulin resistance due to short sleep deprivation, the increased plasma acylcarnitine levels are a sign of inefficient mitochondrial function.

The tissue distribution of acylcarnitines coincides with important targets of insulin, i.e. muscle and liver. The majority of the body's L-carnitine is stored in muscle (~ 97% of the body's L-carnitine), followed by liver which contains 1% of the total L-carnitine pool [40]. Acylcarnitine results from the acylation of L-carnitine, and is therefore dependent on the fatty acid pool of the tissue. Interestingly, animal studies demonstrate the distribution of acylcarnitines is different between metabolic organs. In mice, the muscle tissue contains relatively more long-chain acylcarnitines, including C14:1 and C18:1, while liver is richer in free carnitines and short-chain carnitines [41]. Collectively, these data suggest that plasma short-chain acyl- and free carnitines are mainly derived from the liver, as indeed demonstrated in pigs [42], while plasma long-chain acylcarnitines in plasma presumably originate from muscle tissue. These data thus suggest that the increase in long-chain acylcarnitine that we observe after a single night of short sleep is likely derived from muscle.

Mechanistically, increased acylcarnitine levels after short sleep duration could be a marker of altered metabolic processes: increased fatty acid oxidation (FAO), inefficient mitochondrial function or a disturbed metabolism of the branched-chain amino acids (BCAA) valine, isoleucine or leucine. Although disturbed BCAA metabolism has been associated with insulin resistance in humans [43], our data do not support a role of BCAA metabolism as short sleep duration did not increase BCAA plasma levels or short-chain acylcarnitines. Increased acylcarnitine levels due to increased FAO can be caused by either increased energy demand and/or prolonged fasting. In the present study, the length of fasting was equal; however energy expenditure was not measured. Therefore, we cannot exclude that the increased acylcarnitines after short sleep are due to increased FAO. Sleep is accompanied by lower resting energy expenditure than wakefulness [44] and therefore short sleep duration may increase energy demand. In fact, complete (24 h) sleep deprivation increases energy demand by 7% [45]. However, the effects of short sleep duration on energy expenditure are inconclusive [46]. A recent study shows that short sleep intervention for five consecutive days increased long-chain plasma acylcarnitines [19]. Interestingly, after one night of recovery sleep, plasma acylcarnitines did not normalize. Likely, the increased acylcarnitines were not due to differences in overnight energy expenditure. Besides being a marker of insulin resistance and/or mitochondrial processes, acylcarnitines could also play a causal role in development of insulin resistance. *In vitro* studies have shown that acylcarnitines have bioactive properties and indeed have pro-inflammatory effects [47, 48]. Of note, treatment of both rodent and human myotubes with acylcarnitines in a physiological concentration caused decreased insulin signaling and glucose uptake in response to insulin

[49]. Although this finding needs to be confirmed *in vivo*, it provides a putative causal link between acylcarnitines and insulin resistance.

Taken all these data together, it is interesting to speculate on a mechanistic model for the relationship between sleep curtailment and insulin resistance. Upon sleep curtailment, the energy demands of peripheral tissues increases at a time conflicting with the physiological circadian rhythm. The energy homeostasis is adapted to anticipate the changing energy need and availability throughout the day. Indeed, muscle tissue is also under circadian control [50]. These clock genes are also important in driving rhythmicity in energy producing capacity of the mitochondria, as evidenced by mice studies [51]. We hypothesize that the mismatch in energy producing capacity and demand could be the cause of incomplete FAO, leading to accumulation of intermediates of FAO. Acylcarnitine levels increase, which may increase insulin resistance either through direct interaction with insulin signaling or through increased inflammatory pathways.

Our findings are supported by three studies which have investigated the effects of sleep on the human metabolome. Davies *et al.* [20] subjected 12 healthy individuals to an extreme sleep deprivation of 24 hours and reported nine increased short and medium-chain acylcarnitines, including tetradecenoyl-L-carnitine. Bell *et al.* [18] reported a trend towards increased acylcarnitines after prolonged mild sleep curtailment of 8 consecutive nights of 5.5 hours sleep in 11 young individuals with family history of DM2. Weljie et al [19] also reported increased C18:1, C10:0 and C12:0 acylcarnitines upon five consecutive nights of 4 hours sleep. Strikingly, despite the difference in study populations and sleep curtailment protocols of the present and previous studies used, the acylcarnitines invariably increase after sleep curtailment.

In conclusion, the present study shows that a single night of 4 hours short sleep, which induces insulin resistance [14, 15], also increases plasma levels of acylcarnitines, in particular tetradecenoyl-L-carnitine, octadecenoyl-L-carnitine and octadecadienyl-L-carnitine. We propose that sleep curtailment impairs mitochondrial function, which coincides with insulin resistance. Our findings provide a basis for mechanistic studies to further elucidate the role of acylcarnitines in the complex relationship between short sleep and increased insulin resistance.

ACKNOWLEDGEMENTS

We thank Julia Scarpa, Werner Römisch-Margl and Katharina Faschinger for support with the metabolomics measurements performed at the Helmholtz Centrum München, Genome Analysis Center. **Author contributions.** R.v.d.B. wrote manuscript and performed analysis, D.O.M.K. and K.W.v.D. analyzed data and supervised metabolome analysis, E.D., M.v.D., and J.G.v.D. performed the initial study, G-J.L. and K.W.v.K. performed polysomnography, C.P. and J.A. performed metabolome analysis and quality assurance, and E.P.M.C, J.A.R, P.C.N.R. and N.R.B designed and supervised the study. All authors have approved final version of the manuscript. **Disclosure statement.** Authors declare no conflict of interest. **Funding.** This

study was supported by a pilot grant from the Dutch Diabetes Research Foundation and by grants from the European Foundation for the Study of Diabetes (J.A.R), the Netherlands Organization for Scientific Research (NWO-VENI grant 016.136.125 to N.R.B.) and the German Federal Ministry of Education and Research (BMBF) to the German Center Diabetes Research (DZD e.V.) (J.A.). P.C.N.R. is Established Investigator of the Dutch Heart Foundation (NHS2009T038). D.O.M.K. was supported by Dutch Science Organization (ZonMW-VENI Grant 916.14.023).

REFERENCES

1. Chillaron,JJ, Flores Le-Roux,JA, Benaiges,D, Pedro-Botet,J: Type 1 diabetes, metabolic syndrome and cardiovascular risk. *Metabolism* **63**:181-187, 2014
2. Fox,KM, Wu,Y, Kim,J, Grandy,S: Cardiovascular event rates and healthcare resource utilisation among high-risk adults with type 2 diabetes mellitus in a large population-based study. *Int J Clin Pract* **69**:218-227, 2015
3. Donga,E, Dekkers,OM, Corssmit,EP, Romijn,JA: Insulin resistance in patients with type 1 diabetes assessed by glucose clamp studies: systematic review and meta-analysis. *Eur J Endocrinol* **173**:101-109, 2015
4. Leproult,R, Van,CE: Role of sleep and sleep loss in hormonal release and metabolism. *Endocr Dev* **17**:11-21, 2010
5. Cappuccio,FP, D'Elia,L, Strazzullo,P, Miller,MA: Quantity and quality of sleep and incidence of type 2 diabetes: a systematic review and meta-analysis. *Diabetes Care* **33**:414-420, 2010
6. Borel,AL, Pepin,JL, Nasse,L, Baguet,JP, Netter,S, Benhamou,PY: Short sleep duration measured by wrist actimetry is associated with deteriorated glycemic control in type 1 diabetes. *Diabetes Care* **36**:2902-2908, 2013
7. Buxton,OM, Marcelli,E: Short and long sleep are positively associated with obesity, diabetes, hypertension, and cardiovascular disease among adults in the United States. *Soc Sci Med* **71**:1027-1036, 2010
8. Liu,Y, Croft,JB, Wheaton,AG, Perry,GS, Chapman,DP, Strine,TW, McKnight-Eily,LR, Presley-Cantrell,L: Association between perceived insufficient sleep, frequent mental distress, obesity and chronic diseases among US adults, 2009 behavioral risk factor surveillance system. *BMC Public Health* **13**:84, 2013
9. Najafian,J, Mohamadifard,N, Siadat,ZD, Sadri,G, Rahmati,MR: Association between sleep duration and diabetes mellitus: Isfahan Healthy Heart Program. *Niger J Clin Pract* **16**:59-62, 2013
10. Ohkuma,T, Fujii,H, Iwase,M, Kikuchi,Y, Ogata,S, Idewaki,Y, Ide,H, Doi,Y, Hirakawa,Y, Nakamura,U, Kitazono,T: Impact of sleep duration on obesity and the glycemic level in patientswith type 2diabetes. *Diabetes Care* **36**:611-617, 2013
11. Nedeltcheva,AV, Kessler,L, Imperial,J, Penev,PD: Exposure to recurrent sleep restriction in the setting of high caloric intake and physical inactivity results in increased insulin resistance and reduced glucose tolerance. *J Clin Endocrinol Metab* **94**:3242-3250, 2009
12. Spiegel,K, Leproult,R, Van,CE: Impact of sleep debt on metabolic and endocrine function. *Lancet* **354**:1435-1439, 1999
13. Buxton,OM, Pavlova,M, Reid,EW, Wang,W, Simonson,DC, Adler,GK: Sleep restriction for 1

week reduces insulin sensitivity in healthy men. *Diabetes* **59**:2126-2133, 2010

14. Donga,E, van,DM, van Dijk,JG, Biermasz,NR, Lammers,GJ, van Kralingen,KW, Corssmit,EP, Romijn,JA: A Single Night of Partial Sleep Deprivation Induces Insulin Resistance in Multiple Metabolic Pathways in Healthy Subjects. *J Clin Endocrinol Metab* **95**:2963-8, 2010
15. Donga,E, van,DM, van Dijk,JG, Biermasz,NR, Lammers,GJ, van,KK, Hoogma,RP, Corssmit,EP, Romijn,JA: Partial sleep restriction decreases insulin sensitivity in type 1 diabetes. *Diabetes Care* **33**:1573-1577, 2010
16. Gieger,C, Geistlinger,L, Altmaier,E, Hrabe de,AM, Kronenberg,F, Meitinger,T, Mewes,HW, Wichmann,HE, Weinberger,KM, Adamski,J, Illig,T, Suhre,K: Genetics meets metabolomics: a genome-wide association study of metabolite profiles in human serum. *PLoS Genet* 4:e1000282, 2008
17. Suhre,K: Metabolic profiling in diabetes. *J Endocrinol* **221**:R75-R85, 2014
18. Bell,LN, Kilkus,JM, Booth,JN, III, Bromley,LE, Imperial,JG, Penev,PD: Effects of sleep restriction on the human plasma metabolome. *Physiol Behav* **122**:25-31, 2013
19. Weljie,AM, Meerlo,P, Goel,N, Sengupta,A, Kayser,MS, Abel,T, Birnbaum,MJ, Dinges,DF, Sehgal,A: Oxalic acid and diacylglycerol 36:3 are cross-species markers of sleep debt. *Proc Natl Acad Sci U S A* **112**:2569-2574, 2015
20. Davies,SK, Ang,JE, Revell,VL, Holmes,B, Mann,A, Robertson,FP, Cui,N, Middleton,B, Ackermann,K, Kayser,M, Thumser,AE, Raynaud,FI, Skene,DJ: Effect of sleep deprivation on the human metabolome. *Proc Natl Acad Sci U S A* **111**:10761-6, 2014
21. DeFronzo,RA, Tobin,JD, Andres,R: Glucose clamp technique: a method for quantifying insulin secretion and resistance. *Am J Physiol* **237**:E214-E223, 1979
22. Römisch-Margl,W, Prehn,C, Bogumil,R, Röhring,C, Suhre,K, Adamski,J: Procedure for tissue sample preparation and metabolite extraction for high-throughput targeted metabolomics. *Metabolomics* **8**:133-142, 2012
23. Illig,T, Gieger,C, Zhai,G, Romisch-Margl,W, Wang-Sattler,R, Prehn,C, Altmaier,E, Kastenmuller,G, Kato,BS, Mewes,HW, Meitinger,T, de Angelis,MH, Kronenberg,F, Soranzo,N, Wichmann,HE, Spector,TD, Adamski,J, Suhre,K: A genome-wide perspective of genetic variation in human metabolism. *Nat Genet* **42**:137-141, 2010
24. Mai,M, Tonjes,A, Kovacs,P, Stumvoll,M, Fiedler,GM, Leichtle,AB: Serum levels of acylcarnitines are altered in prediabetic conditions. *PLoS One* 8:e82459, 2013
25. Mihalik,SJ, Goodpaster,BH, Kelley,DE, Chace,DH, Vockley,J, Toledo,FG, DeLany,JP: Increased levels of plasma acylcarnitines in obesity and type 2 diabetes and identification of a marker of glucolipotoxicity. *Obesity (Silver Spring)* 18:1695-1700, 2010
26. Schooneman,MG, Vaz,FM, Houten,SM, Soeters,MR: Acylcarnitines: reflecting or inflicting insulin resistance? *Diabetes* 62:1-8, 2013
27. Koves,TR, Ussher,JR, Noland,RC, Slentz,D, Mosedale,M, Ilkayeva,O, Bain,J, Stevens,R, Dyck,JR, Newgard,CB, Lopaschuk,GD, Muoio,DM: Mitochondrial overload and incomplete fatty acid oxidation contribute to skeletal muscle insulin resistance. *Cell Metab* 7:45-56, 2008
28. Chen,C, Krausz,KW, Shah,YM, Idle,JR, Gonzalez,FJ: Serum metabolomics reveals irreversible inhibition of fatty acid beta-oxidation through the suppression of PPARalpha activation as a contributing mechanism of acetaminophen-induced hepatotoxicity. *Chem Res Toxicol* 22:699-707, 2009
29. Xu,Q, Vu,H, Liu,L, Wang,TC, Schaefer,WH: Metabolic profiles show specific mitochondrial toxicities in vitro in myotube cells. *J Biomol NMR* 49:207-219, 2011
30. Soeters,MR, Sauerwein,HP, Duran,M, Wanders,RJ, Ackermans,MT, Fliers,E, Houten,SM, Serlie,MJ:

Muscle acylcarnitines during short-term fasting in lean healthy men. *Clin Sci (Lond)* **116**:585-592, 2009

31. Rinaldo,P, Cowan,TM, Matern,D: Acylcarnitine profile analysis. *Genet Med* **10**:151-156, 2008
32. Razak,F, Anand,SS: Impaired mitochondrial activity in the insulin-resistant offspring of patients with type 2 diabetes. Petersen KF, Dufour S, Befroy D, Garcia R, Shulman GI. N Engl J Med 2004; 350: 664-71. *Vasc Med* **9**:223-224, 2004
33. Morino,K, Petersen,KF, Dufour,S, Befroy,D, Frattini,J, Shatzkes,N, Neschen,S, White,MF, Bilz,S, Sono,S, Pypaert,M, Shulman,GI: Reduced mitochondrial density and increased IRS-1 serine phosphorylation in muscle of insulin-resistant offspring of type 2 diabetic parents. *J Clin Invest* **115**:3587-3593, 2005
34. Befroy,DE, Petersen,KF, Dufour,S, Mason,GF, de Graaf,RA, Rothman,DL, Shulman,GI: Impaired mitochondrial substrate oxidation in muscle of insulin-resistant offspring of type 2 diabetic patients. *Diabetes* **56**:1376-1381, 2007
35. Kelley,DE, He,J, Menshikova,EV, Ritov,VB: Dysfunction of mitochondria in human skeletal muscle in type 2 diabetes. *Diabetes* **51**:2944-2950, 2002
36. Ritov,VB, Menshikova,EV, He,J, Ferrell,RE, Goodpaster,BH, Kelley,DE: Deficiency of subsarcolemmal mitochondria in obesity and type 2 diabetes. *Diabetes* **54**:8-14, 2005
37. Mogensen,M, Sahlin,K, Fernstrom,M, Glintborg,D, Vind,BF, Beck-Nielsen,H, Hojlund,K: Mitochondrial respiration is decreased in skeletal muscle of patients with type 2 diabetes. *Diabetes* **56**:1592-1599, 2007
38. Cree-Green,M, Newcomer,BR, Brown,MS, Baumgartner,AD, Bergman,B, Drew,B, Regensteiner,JG, Pyle,L, Reusch,JE, Nadeau,KJ: Delayed skeletal muscle mitochondrial ADP recovery in youth with type 1 diabetes relates to muscle insulin resistance. *Diabetes* **64**:383-392, 2015
39. Muoio,DM, Noland,RC, Kovalik,JP, Seiler,SE, Davies,MN, DeBalsi,KL, Ilkayeva,OR, Stevens,RD, Kheterpal,I, Zhang,J, Covington,JD, Bajpeyi,S, Ravussin,E, Kraus,W, Koves,TR, Mynatt,RL: Muscle-specific deletion of carnitine acetyltransferase compromises glucose tolerance and metabolic flexibility. *Cell Metab* **15**:764-777, 2012
40. Reuter,SE, Evans,AM: Carnitine and acylcarnitines: pharmacokinetic, pharmacological and clinical aspects. *Clin Pharmacokinet* **51**:553-572, 2012
41. Schooneman,MG, Achterkamp,N, Argmann,CA, Soeters,MR, Houten,SM: Plasma acylcarnitines inadequately reflect tissue acylcarnitine metabolism. *Biochim Biophys Acta* **1841**:987-994, 2014
42. Schooneman,MG, Ten Have,GA, Van,VN, Houten,SM, Deutz,NE, Soeters,MR: Transorgan fluxes in a porcine model reveal a central role for liver in acylcarnitine metabolism. *Am J Physiol Endocrinol Metab*ajpendo, **1**;309(3):E256-64, 2015
43. Newgard,CB, An,J, Bain,JR, Muehlbauer,MJ, Stevens,RD, Lien,LF, Haqq,AM, Shah,SH, Arlotto,M, Slentz,CA, Rochon,J, Gallup,D, Ilkayeva,O, Wenner,BR, Yancy,WS, Jr., Eisenson,H, Musante,G, Surwit,RS, Millington,DS, Butler,MD, Svetkey,LP: A branched-chain amino acid-related metabolic signature that differentiates obese and lean humans and contributes to insulin resistance. *Cell Metab* **9**:311-326, 2009
44. Thearle,MS, Pannacciulli,N, Bonfiglio,S, Pacak,K, Krakoff,J: Extent and determinants of thermogenic responses to 24 hours of fasting, energy balance, and five different overfeeding diets in humans. *J Clin Endocrinol Metab* **98**:2791-2799, 2013
45. Jung,CM, Melanson,EL, Frydendall,EJ, Perreault,L, Eckel,RH, Wright,KP: Energy expenditure during sleep, sleep deprivation and sleep following sleep deprivation in adult humans. *J Physiol* **589**:235-244, 2011
46. Klingenberg,L, Sjodin,A, Holmback,U, Astrup,A, Chaput,JP: Short sleep duration and its associa-

tion with energy metabolism. *Obes Rev* **13**:565-577, 2012

47. Adams,SH, Hoppel,CL, Lok,KH, Zhao,L, Wong,SW, Minkler,PE, Hwang,DH, Newman,JW, Garvey,WT: Plasma acylcarnitine profiles suggest incomplete long-chain fatty acid beta-oxidation and altered tricarboxylic acid cycle activity in type 2 diabetic African-American women. *J Nutr* **139**:1073-1081, 2009
48. Rutkowsky,JM, Knotts,TA, Ono-Moore,KD, McCoin,CS, Huang,S, Schneider,D, Singh,S, Adams,SH, Hwang,DH: Acylcarnitines activate proinflammatory signaling pathways. *Am J Physiol Endocrinol Metab* **306**:E1378-E1387, 2014
49. Aguer,C, McCoin,CS, Knotts,TA, Thrush,AB, Ono-Moore,K, McPherson,R, Dent,R, Hwang,DH, Adams,SH, Harper,ME: Acylcarnitines: potential implications for skeletal muscle insulin resistance. *FASEB J* **29**:336-345, 2015
50. Harfmann,BD, Schroder,EA, Esser,KA: Circadian Rhythms, the Molecular Clock, and Skeletal Muscle. *J Biol Rhythms* **30**:84-94, 2015
51. Peek,CB, Affinati,AH, Ramsey,KM, Kuo,HY, Yu,W, Sena,LA, Ilkayeva,O, Marcheva,B, Kobayashi,Y, Omura,C, Levine,DC, Bacsik,DJ, Gius,D, Newgard,CB, Goetzman,E, Chandel,NS, Denu,JM, Mrksich,M, Bass,J: Circadian clock NAD+ cycle drives mitochondrial oxidative metabolism in mice. *Science* **342**:1243417, 2013

SUPPLEMENTARY APPENDIX

	Healthy	DM1
Females (%)	4 (44%)	4 (57%)
Age (years)	45 ± 14	43 ± 16
BMI (kg/m^2)	23.8 ± 2.2	23.5 ± 2.2
WHR	0.88 ± 0.05	0.81 ± 0.09

Table S1. General population characteristics of healthy individuals and patients with type 1 diabetes[1]. *DM1 = individuals with type 1 diabetes. BMI = body mass index. WHR = waist hip ratio. Healthy individuals n= 9, DM n= 7. Data are represented as mean ± SD (percentage). [1]Data previously published separately [14;15].*

	Healthy			DM1			Healthy vs. DM1	
	Normal sleep	Short sleep	Effect of sleep	Normal sleep	Short sleep	Effect of sleep	Normal sleep	Short sleep
Sleep characteristics			P-value			P-value	P-value	P-value
TST (min)	454 ± 26	228 ± 32	**<0.0001**	469 ± 22	222 ± 19	**<0.0001**	0.237	0.761
Stage 1 (% of TST)	10 ± 3	11 ± 6	0.490	11 ± 3	10 ± 6	0.868	0.577	0.664
Stage 2 (% of TST)	41 ± 7	35 ± 10	**0.006**	44 ± 7	41 ± 6	0.160	0.533	0.327
Stage 3 (% of TST) (SWS)	25 ± 5	33 ± 9	**0.007**	23 ± 9	35 ± 12	**0.006**	0.570	0.447
REM sleep (% of TST)	24 ± 5	21 ± 8	0.364	22 ± 4	14 ± 6	**0.038**	0.684	0.069
Sleep efficiency (%)	91 ± 5	90 ± 7	0.699	94 ± 2	93 ± 8	0.484	0.199	0.464
Plasma parameter								
Free fatty acids (mmol/l)	0.63 ± 0.15	0.62 ± 0.14	0.76	0.67 ± 0.31	0.59 ± 0.24	0.23	0.74	0.81
Insulin sensitivity parameters								
EGP (µmol*kg LBM^{-1}*min^{-1})	3.57 ± 0.6	4.43 ± 0.8	**0.017**	6.21 ± 1.9	6.88 ± 1.4	0.505	**0.003**	**0.001**
GDR (µmol*kg LBM^{-1}*min^{-1})	40.7 ± 14.3	32.5 ± 10.2	**0.009**	25.5 ± 6.4	22.1 ± 5.1	**0.039**	**0.028**	**0.035**
GIR (µmol*kg LBM^{-1}*min^{-1})	36.9 ± 14.4	27.8 ± 10.5	**0.006**	19.0 ± 7.0	14.9 ± 5.0	**0.041**	**0.014**	**0.014**

Table S2. Sleep and insulin sensitivity parameters of healthy individuals and patients with type 1 diabetes[1]. *DM1= individuals with type 1 diabetes. Insulin sensitivity parameters were determined by hyperinsulinemic euglycemic clamp. EGP = Endogenous glucose production, GDR = glucose disposal rate (glucose Rd), GIR = Glucose infusion rate. Sleep characteristics were determined by polysomnography. TST = total sleep time. SWS = slow wave sleep. Free fatty acids were measured in basal fasting plasma samples. Effect of sleep intervention was tested with paired Students T-test, significant differences shown in bold. Healthy individuals n= 9, DM1 n = 7. Data is presented as means ± SD. [1]Data previously published in separately [14;15].*

Table S3. (below and next pages) Metabolites determined by BiocratesIDQ™ p150 kit.

Metabolite Class	Short name	Biochemical Name
Acylcarnitines	C0	DL-Carnitine
	C2	Acetyl-L-carnitine
	C3	Propionyl-L-carnitine
	C3:1	Propenyl-L-carnitine
	C3-DC / C4-OH	Malonyl-L-carnitine / hydroxybutyryl-L-carnitine
	C3-DC-M / C5-OH	Methylmalonyl-L-carnitine / hydroxyvaleryl-L-carnitine
	C3-OH	Hydroxypropionyl-L-carnitine
	C4	Butyryl-L-carnitine
	C4:1	Butenyl-L-carnitine
	C4:1-DC / C6	Fumaryl-L-carnitine/Hexanoyl-L-carnitine
	C5	Valeryl-L-carnitine
	C5:1	Tiglyl-L-carnitine
	C5:1-DC	Glutaconyl-L-carnitine
	C5-DC / C6-OH	Glutaryl-L-carnitine/Hydroxyhexanoyl-L-carnitine
	C5-M-DC	Methylglutaryl-L-carnitine
	C6:1	Hexenoyl-L-carnitine
	C7-DC	Pimelyl-L-carnitine
	C8	Octanoyl-L-carnitine
	C8:1	Octenoyl-L-carnitine
	C9	Nonayl-L-carnitine
	C10	Decanoyl-L-carnitine
	C10:1	Decenoyl-L-carnitine
	C10:2	Decadienyl-L-carnitine
	C12	Dodecanoyl-L-carnitine
	C12:1	Dodecenoyl-L-carnitine
	C12-DC	Dodecanedioyl-L-carnitine
	C14	Tetradecanoyl-L-carnitine
	C14:1	Tetradecenoyl-L-carnitine
	C14:1-OH	Hydroxytetradecenoyl-L-carnitine
	C14:2	Tetradecadienyl-L-carnitine
	C14:2-OH	Hydroxytetradecadienyl-L-carnitine
	C16	Hexadecanoyl-L-carnitine
	C16:1	Hexadecenoyl-L-carnitine
	C16:1-OH	Hydroxyhexadecenoyl-L-carnitine
	C16:2	Hexadecadienyl-L-carnitine
	C16:2-OH	Hydroxyhexadecadienyl-L-carnitine
	C16-OH	Hydroxyhexadecanoyl-L-carnitine
	C18	Octadecanoyl-L-carnitine
	C18:1	Octadecenoyl-L-carnitine
	C18:1-OH	Hydroxyoctadecenoyl-L-carnitine
	C18:2	Octadecadienyl-L-carnitine

Metabolite Class	Short name	Biochemical Name
Sugars	H1	Hexose
Amino acids	Arg	Arginine
	Gln	Glutamine
	Gly	Glycine
	His	Histidine
	Met	Methionine
	Orn	Ornithine
	Phe	Phenylalanine
	Pro	Proline
	Ser	Serine
	Thr	Threonine
	Trp	Tryptophan
	Tyr	Tyrosine
	Val	Valine
	xLeu	xLeucine
Glycerophospholipids	lysoPC a C14:0	lysoPhosphatidylcholine acyl C14:0
	lysoPC a C16:0	lysoPhosphatidylcholine acyl C16:0
	lysoPC a C16:1	lysoPhosphatidylcholine acyl C16:1
	lysoPC a C17:0	lysoPhosphatidylcholine acyl C17:0
	lysoPC a C18:0	lysoPhosphatidylcholine acyl C18:0
	lysoPC a C18:1	lysoPhosphatidylcholine acyl C18:1
	lysoPC a C18:2	lysoPhosphatidylcholine acyl C18:2
	lysoPC a C20:3	lysoPhosphatidylcholine acyl C20:3
	lysoPC a C20:4	lysoPhosphatidylcholine acyl C20:4
	lysoPC a C24:0	lysoPhosphatidylcholine acyl C24:0
	lysoPC a C26:0	lysoPhosphatidylcholine acyl C26:0
	lysoPC a C26:1	lysoPhosphatidylcholine acyl C26:1
	lysoPC a C28:0	lysoPhosphatidylcholine acyl C28:0
	lysoPC a C28:1	lysoPhosphatidylcholine acyl C28:1
	lysoPC a C6:0	lysoPhosphatidylcholine acyl C6:0
	PC aa C24:0	Phosphatidylcholine diacyl C 24:0
	PC aa C26:0	Phosphatidylcholine diacyl C 26:0
	PC aa C28:1	Phosphatidylcholine diacyl C 28:1
	PC aa C30:0	Phosphatidylcholine diacyl C 30:0
	PC aa C30:2	Phosphatidylcholine diacyl C 30:2
	PC aa C32:0	Phosphatidylcholine diacyl C 32:0
	PC aa C32:1	Phosphatidylcholine diacyl C 32:1
	PC aa C32:2	Phosphatidylcholine diacyl C 32:2
	PC aa C32:3	Phosphatidylcholine diacyl C 32:3
	PC aa C34:1	Phosphatidylcholine diacyl C 34:1
	PC aa C34:2	Phosphatidylcholine diacyl C 34:2

Metabolite Class	Short name	Biochemical Name
Glycerophospholipids	PC aa C34:3	Phosphatidylcholine diacyl C 34:3
	PC aa C34:4	Phosphatidylcholine diacyl C 34:4
	PC aa C36:0	Phosphatidylcholine diacyl C 36:0
	PC aa C36:1	Phosphatidylcholine diacyl C 36:1
	PC aa C36:2	Phosphatidylcholine diacyl C 36:2
	PC aa C36:3	Phosphatidylcholine diacyl C 36:3
	PC aa C36:4	Phosphatidylcholine diacyl C 36:4
	PC aa C36:5	Phosphatidylcholine diacyl C 36:5
	PC aa C36:6	Phosphatidylcholine diacyl C 36:6
	PC aa C38:0	Phosphatidylcholine diacyl C 38:0
	PC aa C38:1	Phosphatidylcholine diacyl C 38:1
	PC aa C38:3	Phosphatidylcholine diacyl C 38:3
	PC aa C38:4	Phosphatidylcholine diacyl C 38:4
	PC aa C38:5	Phosphatidylcholine diacyl C 38:5
	PC aa C38:6	Phosphatidylcholine diacyl C 38:6
	PC aa C40:1	Phosphatidylcholine diacyl C 40:1
	PC aa C40:2	Phosphatidylcholine diacyl C 40:2
	PC aa C40:3	Phosphatidylcholine diacyl C 40:3
	PC aa C40:4	Phosphatidylcholine diacyl C 40:4
	PC aa C40:5	Phosphatidylcholine diacyl C 40:5
	PC aa C40:6	Phosphatidylcholine diacyl C 40:6
	PC aa C42:0	Phosphatidylcholine diacyl C 42:0
	PC aa C42:1	Phosphatidylcholine diacyl C 42:1
	PC aa C42:2	Phosphatidylcholine diacyl C 42:2
	PC aa C42:4	Phosphatidylcholine diacyl C 42:4
	PC aa C42:5	Phosphatidylcholine diacyl C 42:5
	PC aa C42:6	Phosphatidylcholine diacyl C 42:6
	PC ae C30:0	Phosphatidylcholine acyl-alkyl C 30:0
	PC ae C30:1	Phosphatidylcholine acyl-alkyl C 30:1
	PC ae C30:2	Phosphatidylcholine acyl-alkyl C 30:2
	PC ae C32:1	Phosphatidylcholine acyl-alkyl C 32:1
	PC ae C32:2	Phosphatidylcholine acyl-alkyl C 32:2
	PC ae C34:0	Phosphatidylcholine acyl-alkyl C 34:0
	PC ae C34:1	Phosphatidylcholine acyl-alkyl C 34:1
	PC ae C34:2	Phosphatidylcholine acyl-alkyl C 34:2
	PC ae C34:3	Phosphatidylcholine acyl-alkyl C 34:3
	PC ae C36:0	Phosphatidylcholine acyl-alkyl C 36:0
	PC ae C36:1	Phosphatidylcholine acyl-alkyl C 36:1
	PC ae C36:2	Phosphatidylcholine acyl-alkyl C 36:2
	PC ae C36:3	Phosphatidylcholine acyl-alkyl C 36:3

Metabolite Class	Short name	Biochemical Name
Glycerophospholipids	PC ae C36:4	Phosphatidylcholine acyl-alkyl C 36:4
	PC ae C36:5	Phosphatidylcholine acyl-alkyl C 36:5
	PC ae C38:0	Phosphatidylcholine acyl-alkyl C 38:0
	PC ae C38:1	Phosphatidylcholine acyl-alkyl C 38:1
	PC ae C38:2	Phosphatidylcholine acyl-alkyl C 38:2
	PC ae C38:3	Phosphatidylcholine acyl-alkyl C 38:3
	PC ae C38:4	Phosphatidylcholine acyl-alkyl C 38:4
	PC ae C38:5	Phosphatidylcholine acyl-alkyl C 38:5
	PC ae C38:6	Phosphatidylcholine acyl-alkyl C 38:6
	PC ae C40:0	Phosphatidylcholine acyl-alkyl C 40:0
	PC ae C40:1	Phosphatidylcholine acyl-alkyl C 40:1
	PC ae C40:2	Phosphatidylcholine acyl-alkyl C 40:2
	PC ae C40:3	Phosphatidylcholine acyl-alkyl C 40:3
	PC ae C40:4	Phosphatidylcholine acyl-alkyl C 40:4
	PC ae C40:5	Phosphatidylcholine acyl-alkyl C 40:5
	PC ae C40:6	Phosphatidylcholine acyl-alkyl C 40:6
	PC ae C42:0	Phosphatidylcholine acyl-alkyl C 42:0
	PC ae C42:1	Phosphatidylcholine acyl-alkyl C 42:1
	PC ae C42:2	Phosphatidylcholine acyl-alkyl C 42:2
	PC ae C42:3	Phosphatidylcholine acyl-alkyl C 42:3
	PC ae C42:4	Phosphatidylcholine acyl-alkyl C 42:4
	PC ae C42:5	Phosphatidylcholine acyl-alkyl C 42:5
	PC ae C44:3	Phosphatidylcholine acyl-alkyl C 44:3
	PC ae C44:4	Phosphatidylcholine acyl-alkyl C 44:4
	PC ae C44:5	Phosphatidylcholine acyl-alkyl C 44:5
	PC ae C44:6	Phosphatidylcholine acyl-alkyl C 44:6
Sphingolipids	SM (OH) C14:1	Hydroxysphingomyeline C 14:1
	SM (OH) C16:0	Hydroxysphingomyeline C 16:0
	SM (OH) C22:1	Hydroxysphingomyeline C 22:1
	SM (OH) C22:2	Hydroxysphingomyeline C 22:2
	SM (OH) C24:1	Hydroxysphingomyeline C 24:1
	SM C16:0	Sphingomyeline C 16:0
	SM C16:1	Sphingomyeline C 16:1
	SM C18:0	Sphingomyeline C 18:0
	SM C18:1	Sphingomyeline C 18:1
	SM C20:2	Sphingomyeline C 20:2
	SM C22:3	Sphingomyeline C 22:3
	SM C24:0	Sphingomyeline C 24:0
	SM C24:1	Sphingomyeline C 24:1
	SM C26:0	Sphingomyeline C 26:0
	SM C26:1	Sphingomyeline C 26:1

Table S4. (below and next pages) Metabolite changes after one night of short sleep duration.[1] *Difference in metabolite levels (μM) as measured by BiocratesIDQ™ p150 kit between short and normal sleep duration. Positive mean difference indicates an increase after short sleep duration. Negative mean difference indicates a decrease after short sleep duration.* [2]*Change (%) represents percentage of change in metabolite level in short compared to normal sleep (metabolite level (short sleep) – metabolite level (normal sleep)) / metabolite level (normal sleep). DM1 = individuals with type 1 diabetes. P-values are based on paired Students t-tests. Abbreviations of all metabolites are shown in Supplemental Table S3. N= 16 (healthy: n=9, DM1: n=7).*

	All subjects			Healthy			DM1		
Metabolite	**Mean difference**[1]	**Change (%)2**	**P-value**	**Mean difference**[1]	**Change (%)2**	**P-value**	**Mean difference**[1]	**Change (%)2**	**P-value**
C0	0.191	0.6%	$8.81*10^{-1}$	0.398	1.2%	$8.47*10^{-1}$	-0.075	-0.3%	$9.61*10^{-1}$
C2	0.662	16.8%	$2.28*10^{-2}$	0.184	4.3%	$5.40*10^{-1}$	1.276	35.6%	$1.33*10^{-2}$
C3	-0.006	-2.6%	$6.76*10^{-1}$	-0.002	-0.7%	$9.33*10^{-1}$	-0.012	-6.2%	$6.03*10^{-1}$
C3-DC (C4-OH)	0.007	11.3%	$4.55*10^{-1}$	0.006	8.0%	$7.20*10^{-1}$	0.009	17.7%	$2.87*10^{-1}$
C3-OH	0.001	3.3%	$5.03*10^{-1}$	0.002	8.5%	$5.91*10^{-2}$	-0.001	-2.1%	$8.24*10^{-1}$
C3:1	-0.001	-5.9%	$4.16*10^{-1}$	0.000	-0.1%	$9.93*10^{-1}$	-0.001	-12.3%	$1.58*10^{-1}$
C4	0.011	10.3%	$1.22*10^{-1}$	0.008	7.2%	$4.95*10^{-1}$	0.015	14.4%	$8.68*10^{-2}$
C4:1	0.002	6.7%	$2.90*10^{-1}$	0.002	8.7%	$2.55*10^{-1}$	0.001	4.8%	$6.58*10^{-1}$
C5	0.011	10.2%	$2.80*10^{-1}$	0.012	10.4%	$4.59*10^{-1}$	0.010	9.8%	$4.30*10^{-1}$
C5-DC (C6-OH)	-0.001	-4.1%	$4.87*10^{-1}$	-0.001	-8.3%	$2.56*10^{-1}$	0.000	0.7%	$9.45*10^{-1}$
C5-M-DC	0.000	0.3%	$9.32*10^{-1}$	0.000	-1.0%	$8.45*10^{-1}$	0.001	1.8%	$7.11*10^{-1}$
C5-OH (C3-DC-M)	0.000	0.3%	$9.40*10^{-1}$	0.000	-1.5%	$6.89*10^{-1}$	0.001	2.4%	$7.40*10^{-1}$
C5:1	0.000	1.0%	$8.74*10^{-1}$	-0.001	-2.5%	$7.86*10^{-1}$	0.001	5.0%	$6.20*10^{-1}$
C5:1-DC	0.000	2.6%	$6.75*10^{-1}$	-0.001	-4.8%	$5.96*10^{-1}$	0.002	12.5%	$1.27*10^{-1}$
C6 (C4:1-DC)	0.005	8.7%	$1.22*10^{-1}$	0.001	1.9%	$7.82*10^{-1}$	0.011	18.8%	$6.20*10^{-2}$
C6:1	0.001	2.6%	$3.99*10^{-1}$	0.001	3.5%	$3.35*10^{-1}$	0.000	1.5%	$8.05*10^{-1}$
C7-DC	0.005	19.9%	$5.41*10^{-4}$	0.002	8.4%	$8.50*10^{-2}$	0.008	34.8%	$3.21*10^{-4}$
C8	0.003	1.9%	$6.06*10^{-1}$	-0.005	-3.1%	$5.56*10^{-1}$	0.013	11.0%	$4.38*10^{-3}$

	All subjects			Healthy			DM1		
Metabolite	**Mean difference[1]**	**Change (%)2**	**P-value**	**Mean difference[1]**	**Change (%)2**	**P-value**	**Mean difference[1]**	**Change (%)2**	**P-value**
C8:1	0.012	15.4%	$1.62*10^{-1}$	0.008	11.8%	$3.93*10^{-1}$	0.017	18.9%	$3.09*10^{-1}$
C9	0.000	-0.4%	$9.47*10^{-1}$	-0.001	-4.7%	$5.73*10^{-1}$	0.001	5.3%	$5.51*10^{-1}$
C10	0.014	5.8%	$1.84*10^{-1}$	0.003	1.1%	$8.62*10^{-1}$	0.027	15.1%	$4.54*10^{-3}$
C10:1	0.008	6.9%	$2.68*10^{-1}$	-0.004	-3.1%	$6.68*10^{-1}$	0.022	23.9%	$2.72*10^{-2}$
C10:2	0.000	-0.7%	$8.65*10^{-1}$	0.000	-0.1%	$9.79*10^{-1}$	0.000	-1.3%	$8.51*10^{-1}$
C12	0.012	17.2%	$1.70*10^{-3}$	0.010	12.0%	$9.00*10^{-2}$	0.015	27.5%	$3.30*10^{-3}$
C12-DC	0.002	2.4%	$1.53*10^{-1}$	0.002	2.1%	$3.78*10^{-1}$	0.003	2.8%	$3.01*10^{-1}$
C12:1	0.017	23.6%	$1.74*10^{-3}$	0.014	17.0%	$8.32*10^{-2}$	0.021	35.2%	$5.85*10^{-3}$
C14	0.004	15.6%	$1.21*10^{-2}$	0.002	8.5%	$2.42*10^{-1}$	0.006	28.0%	$1.97*10^{-2}$
C14:1	0.020	32.4%	$2.67*10^{-4}$	0.017	23.5%	$2.34*10^{-2}$	0.024	49.1%	$6.55*10^{-3}$
C14:1-OH	0.001	6.2%	$3.79*10^{-1}$	0.000	-1.7%	$8.10*10^{-1}$	0.001	16.9%	$2.36*10^{-1}$
C14:2	0.006	26.1%	$5.48*10^{-4}$	0.005	17.3%	$5.01*10^{-2}$	0.008	41.5%	$4.17*10^{-3}$
C14:2-OH	0.000	5.0%	$3.64*10^{-1}$	0.000	6.4%	$2.91*10^{-1}$	0.000	3.3%	$7.48*10^{-1}$
C16	0.007	10.8%	$1.94*10^{-2}$	0.005	6.7%	$2.05*10^{-1}$	0.010	17.1%	$5.91*10^{-2}$
C16-OH	0.000	0.9%	$8.89*10^{-1}$	0.000	-3.4%	$5.84*10^{-1}$	0.000	6.0%	$6.49*10^{-1}$
C16:1	0.005	8.8%	$9.60*10^{-3}$	0.005	8.3%	$3.06*10^{-2}$	0.005	9.6%	$1.55*10^{-1}$
C16:1-OH	0.001	20.8%	$5.71*10^{-3}$	0.001	11.7%	$1.90*10^{-1}$	0.002	33.8%	$1.10*10^{-2}$
C16:2	0.001	21.3%	$9.72*10^{-3}$	0.001	9.6%	$2.39*10^{-1}$	0.002	39.5%	$1.91*10^{-2}$
C16:2-OH	0.000	2.1%	$6.29*10^{-1}$	0.000	3.8%	$5.45*10^{-1}$	0.000	-0.1%	$9.83*10^{-1}$
C18	0.003	10.8%	$7.34*10^{-2}$	0.002	9.6%	$3.04*10^{-1}$	0.003	12.5%	$1.18*10^{-1}$
C18:1	0.016	22.3%	$1.92*10^{-4}$	0.015	20.1%	$2.96*10^{-3}$	0.019	25.1%	$2.84*10^{-2}$
C18:1-OH	0.001	12.8%	$6.02*10^{-2}$	0.001	5.7%	$3.93*10^{-1}$	0.002	22.3%	$1.07*10^{-1}$
C18:2	0.007	27.0%	$1.32*10^{-4}$	0.005	20.7%	$9.01*10^{-4}$	0.010	34.4%	$1.38*10^{-2}$
Arg	4.297	6.0%	$2.74*10^{-1}$	6.988	10.0%	$2.66*10^{-1}$	0.838	1.1%	$8.57*10^{-1}$
Gln	13.186	4.5%	$2.52*10^{-1}$	10.500	3.6%	$4.88*10^{-1}$	16.641	5.7%	$4.00*10^{-1}$

	All subjects			Healthy			DM1		
Metabolite	**Mean difference[1]**	**Change (%)2**	**P-value**	**Mean difference[1]**	**Change (%)2**	**P-value**	**Mean difference[1]**	**Change (%)2**	**P-value**
Gly	-9.002	-4.7%	$2.84*10^{-1}$	-3.264	-1.9%	$7.57*10^{-1}$	-16.380	-7.4%	$2.69*10^{-1}$
His	0.533	1.0%	$8.27*10^{-1}$	-0.174	-0.3%	$9.57*10^{-1}$	1.441	3.0%	$7.32*10^{-1}$
Met	0.264	1.3%	$7.98*10^{-1}$	0.557	2.6%	$6.91*10^{-1}$	-0.113	-0.6%	$9.48*10^{-1}$
Orn	3.038	8.3%	$1.48*10^{-1}$	5.466	15.2%	$1.05*10^{-1}$	-0.083	-0.2%	$9.70*10^{-1}$
Phe	2.588	6.2%	$1.06*10^{-1}$	3.131	7.6%	$1.16*10^{-1}$	1.890	4.5%	$5.13*10^{-1}$
Pro	-3.161	-1.9%	$6.20*10^{-1}$	-0.909	-0.5%	$9.10*10^{-1}$	-6.057	-4.0%	$5.93*10^{-1}$
Ser	3.273	3.6%	$4.27*10^{-1}$	2.253	2.7%	$7.18*10^{-1}$	4.585	4.6%	$4.29*10^{-1}$
Thr	4.527	4.7%	$5.04*10^{-1}$	4.930	5.1%	$5.55*10^{-1}$	4.010	4.1%	$7.47*10^{-1}$
Trp	1.178	1.9%	$5.56*10^{-1}$	2.563	4.2%	$3.30*10^{-1}$	-0.602	-1.0%	$8.58*10^{-1}$
Tyr	4.638	9.8%	$1.05*10^{-1}$	6.966	14.7%	$1.30*10^{-1}$	1.644	3.5%	$6.12*10^{-1}$
Val	3.933	2.6%	$4.86*10^{-1}$	6.183	3.9%	$5.06*10^{-1}$	1.039	0.7%	$8.67*10^{-1}$
xLeu	9.916	6.4%	$1.56*10^{-1}$	9.156	5.7%	$3.55*10^{-1}$	10.892	7.3%	$3.24*10^{-1}$
lysoPC a C14:0	-0.047	-1.4%	$5.83*10^{-1}$	-0.022	-0.6%	$8.67*10^{-1}$	-0.079	-2.4%	$5.04*10^{-1}$
lysoPC a C16:0	-1.774	-2.4%	$5.84*10^{-1}$	0.872	1.3%	$8.39*10^{-1}$	-5.176	-6.6%	$3.34*10^{-1}$
lysoPC a C16:1	-0.144	-7.2%	$1.58*10^{-1}$	-0.061	-3.1%	$6.72*10^{-1}$	-0.249	-12.3%	$1.02*10^{-1}$
lysoPC a C17:0	-0.015	-1.3%	$7.88*10^{-1}$	0.005	0.5%	$9.46*10^{-1}$	-0.042	-3.4%	$6.57*10^{-1}$
lysoPC a C18:0	-0.003	0.0%	$9.97*10^{-1}$	1.077	6.4%	$3.22*10^{-1}$	-1.392	-6.9%	$4.33*10^{-1}$
lysoPC a C18:1	-0. 7	-2.9%	$5.91*10^{-1}$	-0.210	-1.6%	$7.91*10^{-1}$	-0.728	-4.2%	$6.67*10^{-1}$
lysoPC a C18:2	0.575	1.9%	$8.14*10^{-1}$	-1.447	-5.5%	$4.00*10^{-1}$	3.176	8.9%	$5.59*10^{-1}$
lysoPC a C20:3	0.008	0.4%	$9.43*10^{-1}$	0.080	4.0%	$5.80*10^{-1}$	-0.085	-4.5%	$6.19*10^{-1}$
lysoPC a C20:4	-0.248	-4.7%	$3.27*10^{-1}$	-0.302	-6.3%	$2.31*10^{-1}$	-0.179	-3.1%	$7.32*10^{-1}$
lysoPC a C24:0	-0.003	-0.5%	$9.28*10^{-1}$	0.014	3.1%	$6.56*10^{-1}$	-0.024	-4.7%	$6.56*10^{-1}$
lysoPC a C26:0	-0.009	-0.9%	$9.02*10^{-1}$	0.014	1.4%	$8.63*10^{-1}$	-0.039	-4.1%	$7.87*10^{-1}$
lysoPC a C26:1	-0.004	-1.1%	$8.81*10^{-1}$	-0.002	-0.6%	$9.42*10^{-1}$	-0.007	-1.7%	$9.03*10^{-1}$
lysoPC a C28:0	0.001	0.1%	$9.84*10^{-1}$	0.012	1.5%	$8.49*10^{-1}$	-0.013	-1.7%	$8.84*10^{-1}$

	All subjects			Healthy			DM1		
Metabolite	**Mean difference[1]**	**Change (%)2**	**P-value**	**Mean difference[1]**	**Change (%)2**	**P-value**	**Mean difference[1]**	**Change (%)2**	**P-value**
lysoPC a C28:1	-0.006	-0.6%	$9.28*10^{-1}$	0.010	1.1%	$8.84*10^{-1}$	-0.025	-2.6%	$8.31*10^{-1}$
lysoPC a C6:0	-0.002	-8.4%	$4.94*10^{-1}$	0.002	10.9%	$6.26*10^{-1}$	-0.007	-26.5%	$1.14*10^{-2}$
PC aa C24:0	-0.005	-1.8%	$7.93*10^{-1}$	-0.005	-1.9%	$8.42*10^{-1}$	-0.005	-1.8%	$8.78*10^{-1}$
PC aa C26:0	-0.028	-2.4%	$6.22*10^{-1}$	-0.040	-3.4%	$5.37*10^{-1}$	-0.013	-1.1%	$9.09*10^{-1}$
PC aa C28:1	0.061	2.7%	$3.74*10^{-1}$	0.089	3.9%	$2.47*10^{-1}$	0.026	1.1%	$8.47*10^{-1}$
PC aa C30:0	0.081	2.7%	$6.62*10^{-1}$	0.099	3.1%	$6.76*10^{-1}$	0.058	2.1%	$8.60*10^{-1}$
PC aa C30:2	0.002	1.2%	$9.33*10^{-1}$	0.010	7.0%	$7.71*10^{-1}$	-0.009	-4.3%	$8.40*10^{-1}$
PC aa C32:0	0.352	4.0%	$2.19*10^{-1}$	0.490	5.8%	$5.12*10^{-2}$	0.174	1.9%	$7.76*10^{-1}$
PC aa C32:1	0.370	3.7%	$6.36*10^{-1}$	1.063	9.4%	$3.68*10^{-1}$	-0.521	-6.5%	$6.17*10^{-1}$
PC aa C32:2	0.020	0.8%	$9.12*10^{-1}$	-0.038	-1.3%	$8.84*10^{-1}$	0.095	4.1%	$7.38*10^{-1}$
PC aa C32:3	0.001	0.2%	$9.68*10^{-1}$	-0.005	-1.3%	$7.93*10^{-1}$	0.007	1.9%	$7.90*10^{-1}$
PC aa C34:1	2.395	1.9%	$5.09*10^{-1}$	5.489	4.3%	$1.84*10^{-1}$	-1.583	-1.3%	$8.16*10^{-1}$
PC aa C34:2	7.304	3.7%	$1.04*10^{-1}$	6.544	3.3%	$1.31*10^{-1}$	8.282	4.1%	$3.78*10^{-1}$
PC aa C34:3	0.353	3.0%	$5.32*10^{-1}$	0.435	3.5%	$5.90*10^{-1}$	0.247	2.2%	$7.78*10^{-1}$
PC aa C34:4	-0.013	-1.2%	$8.47*10^{-1}$	-0.032	-2.7%	$7.55*10^{-1}$	0.012	1.3%	$8.98*10^{-1}$
PC aa C36:0	0.017	0.7%	$9.23*10^{-1}$	-0.046	-2.1%	$8.05*10^{-1}$	0.099	3.3%	$7.81*10^{-1}$
PC aa C36:1	1.673	5.8%	$1.72*10^{-1}$	2.555	8.7%	$1.40*10^{-1}$	0.538	1.9%	$7.75*10^{-1}$
PC aa C36:2	6.029	4.8%	$1.46*10^{-1}$	6.133	4.9%	$1.96*10^{-1}$	5.894	4.7%	$4.61*10^{-1}$
PC aa C36:3	3.808	4.5%	$1.64*10^{-1}$	6.521	7.5%	$5.27*10^{-2}$	0.320	0.4%	$9.47*10^{-1}$
PC aa C36:4	1.441	1.3%	$6.29*10^{-1}$	1.110	1.0%	$7.39*10^{-1}$	1.866	1.9%	$7.49*10^{-1}$
PC aa C36:5	-0.045	-0.3%	$9.65*10^{-1}$	0.559	4.1%	$7.51*10^{-1}$	-0.821	-6.8%	$3.50*10^{-1}$
PC aa C36:6	-0.010	-1.5%	$8.53*10^{-1}$	0.004	0.5%	$9.69*10^{-1}$	-0.028	-4.4%	$6.29*10^{-1}$
PC aa C38:0	0.050	2.0%	$6.68*10^{-1}$	0.039	1.7%	$8.06*10^{-1}$	0.065	2.3%	$7.41*10^{-1}$
PC aa C38:1	0.041	2.3%	$6.99*10^{-1}$	0.151	9.3%	$2.19*10^{-1}$	-0.101	-5.0%	$5.98*10^{-1}$
PC aa C38:3	2.020	7.5%	$6.46*10^{-2}$	3.788	12.9%	$1.68*10^{-2}$	-0.254	-1.1%	$8.48*10^{-1}$
PC aa C38:4	1.113	2.0%	$5.25*10^{-1}$	1.760	3.0%	$4.88*10^{-1}$	0.280	0.6%	$9.16*10^{-1}$
PC aa C38:5	0.060	0.2%	$9.55*10^{-1}$	0.609	2.3%	$7.31*10^{-1}$	-0.645	-2.6%	$5.62*10^{-1}$

	All subjects			Healthy			DM1		
Metabolite	**Mean difference[1]**	**Change (%)2**	**P-value**	**Mean difference[1]**	**Change (%)2**	**P-value**	**Mean difference[1]**	**Change (%)2**	**P-value**
PC aa C38:6	-0.622	-1.6%	$7.12*10^{-1}$	-0.987	-2.3%	$7.03*10^{-1}$	-0.154	-0.4%	$9.47*10^{-1}$
PC aa C40:1	0.020	2.5%	$6.90*10^{-1}$	0.060	8.0%	$3.34*10^{-1}$	-0.031	-3.5%	$7.38*10^{-1}$
PC aa C40:2	0.078	5.4%	$4.46*10^{-1}$	0.149	11.7%	$2.16*10^{-1}$	-0.012	-0.7%	$9.52*10^{-1}$
PC aa C40:3	0.068	4.6%	$4.70*10^{-1}$	0.136	10.5%	$2.55*10^{-1}$	-0.020	-1.2%	$9.04*10^{-1}$
PC aa C40:4	0.154	4.6%	$2.35*10^{-1}$	0.290	8.9%	$1.09*10^{-1}$	-0.021	-0.6%	$9.16*10^{-1}$
PC aa C40:5	0.232	4.1%	$3.01*10^{-1}$	0.540	9.3%	$9.49*10^{-2}$	-0.164	-3.0%	$5.89*10^{-1}$
PC aa C40:6	0.033	0.3%	$9.48*10^{-1}$	0.413	3.3%	$5.51*10^{-1}$	-0.454	-4.4%	$5.85*10^{-1}$
PC aa C42:0	0.028	4.0%	$2.80*10^{-1}$	0.040	6.2%	$2.00*10^{-1}$	0.012	1.6%	$8.01*10^{-1}$
PC aa C42:1	0.009	1.9%	$7.04*10^{-1}$	0.041	10.0%	$1.49*10^{-1}$	-0.033	-6.2%	$3.74*10^{-1}$
PC aa C42:2	0.020	3.1%	$6.55*10^{-1}$	0.054	9.5%	$3.06*10^{-1}$	-0.024	-3.1%	$7.75*10^{-1}$
PC aa C42:4	0.031	5.6%	$2.44*10^{-1}$	0.053	10.6%	$1.88*10^{-1}$	0.002	0.4%	$9.49*10^{-1}$
PC aa C42:5	0.029	5.5%	$1.84*10^{-1}$	0.047	9.7%	$1.34*10^{-1}$	0.005	0.8%	$8.81*10^{-1}$
PC aa C42:6	0.019	3.4%	$5.38*10^{-1}$	0.049	9.3%	$1.60*10^{-1}$	-0.020	-3.5%	$7.21*10^{-1}$
PC ae C30:0	0.002	0.5%	$9.20*10^{-1}$	0.012	3.5%	$6.07*10^{-1}$	-0.012	-3.6%	$5.95*10^{-1}$
PC ae C30:1	-0.003	-1.2%	$8.94*10^{-1}$	-0.003	-1.2%	$9.07*10^{-1}$	-0.004	-1.3%	$9.43*10^{-1}$
PC ae C30:2	0.006	2.5%	$6.96*10^{-1}$	0.011	5.1%	$5.28*10^{-1}$	-0.001	-0.3%	$9.81*10^{-1}$
PC ae C32:1	0.046	2.4%	$4.28*10^{-1}$	0.035	1.9%	$6.30*10^{-1}$	0.060	2.9%	$5.66*10^{-1}$
PC ae C32:2	0.011	2.2%	$4.36*10^{-1}$	0.017	3.7%	$3.50*10^{-1}$	0.003	0.6%	$8.99*10^{-1}$
PC ae C34:0	0.006	0.7%	$8.25*10^{-1}$	0.015	1.6%	$6.90*10^{-1}$	-0.005	-0.5%	$9.25*10^{-1}$
PC ae C34:1	0.159	2.7%	$3.75*10^{-1}$	0.202	3.3%	$4.23*10^{-1}$	0.105	1.8%	$7.15*10^{-1}$
PC ae C34:2	0.274	4.1%	$4.06*10^{-1}$	0.029	0.4%	$9.36*10^{-1}$	0.589	8.7%	$3.55*10^{-1}$
PC ae C34:3	0.213	3.9%	$3.04*10^{-1}$	0.093	1.8%	$7.10*10^{-1}$	0.368	6.3%	$3.34*10^{-1}$
PC ae C36:0	0.048	6.1%	$1.66*10^{-1}$	0.037	4.6%	$3.13*10^{-1}$	0.063	8.0%	$3.68*10^{-1}$
PC ae C36:1	0.832	6.7%	$3.11*10^{-1}$	0.792	6.9%	$3.45*10^{-1}$	0.883	6.4%	$5.98*10^{-1}$
PC ae C36:2	0.308	2.9%	$3.51*10^{-1}$	0.152	1.4%	$7.39*10^{-1}$	0.508	4.7%	$3.39*10^{-1}$
PC ae C36:3	0.143	2.8%	$5.30*10^{-1}$	0.044	0.9%	$8.77*10^{-1}$	0.272	5.4%	$5.13*10^{-1}$

	All subjects			Healthy			DM1		
Metabolite	**Mean difference[1]**	**Change (%)2**	**P-value**	**Mean difference[1]**	**Change (%)2**	**P-value**	**Mean difference[1]**	**Change (%)2**	**P-value**
PC ae C36:4	0.257	2.7%	$5.65*10^{-1}$	-0.112	-1.2%	$7.36*10^{-1}$	0.732	7.4%	$4.57*10^{-1}$
PC ae C36:5	0.079	1.2%	$7.36*10^{-1}$	-0.063	-0.9%	$8.10*10^{-1}$	0.260	3.7%	$5.64*10^{-1}$
PC ae C38:0	0.054	2.8%	$6.14*10^{-1}$	0.049	2.4%	$7.92*10^{-1}$	0.061	3.4%	$5.34*10^{-1}$
PC ae C38:1	0.263	6.4%	$4.50*10^{-1}$	0.411	11.8%	$3.06*10^{-1}$	0.073	1.5%	$9.13*10^{-1}$
PC ae C38:2	0.414	6.9%	$3.07*10^{-1}$	0.631	11.3%	$1.77*10^{-1}$	0.134	2.1%	$8.61*10^{-1}$
PC ae C38:3	0.776	7.3%	$1.96*10^{-1}$	0.799	7.6%	$2.04*10^{-1}$	0.745	6.9%	$5.38*10^{-1}$
PC ae C38:4	0.189	2.2%	$5.31*10^{-1}$	0.199	2.3%	$6.11*10^{-1}$	0.176	2.0%	$7.39*10^{-1}$
PC ae C38:5	0.132	1.3%	$7.42*10^{-1}$	-0.130	-1.3%	$7.68*10^{-1}$	0.470	4.4%	$5.50*10^{-1}$
PC ae C38:6	0.096	2.5%	$5.50*10^{-1}$	-0.033	-0.9%	$8.70*10^{-1}$	0.261	6.8%	$3.48*10^{-1}$
PC ae C40:0	0.010	0.3%	$9.35*10^{-1}$	0.044	1.1%	$8.20*10^{-1}$	-0.032	-0.9%	$8.54*10^{-1}$
PC ae C40:1	0.040	1.8%	$7.94*10^{-1}$	0.031	1.5%	$8.49*10^{-1}$	0.051	2.2%	$8.67*10^{-1}$
PC ae C40:2	0.144	5.2%	$3.60*10^{-1}$	0.233	8.5%	$2.19*10^{-1}$	0.031	1.1%	$9.15*10^{-1}$
PC ae C40:3	0.349	7.0%	$1.55*10^{-1}$	0.441	9.1%	$1.16*10^{-1}$	0.231	4.5%	$6.22*10^{-1}$
PC ae C40:4	0.223	4.5%	$3.41*10^{-1}$	0.332	7.1%	$2.64*10^{-1}$	0.082	1.6%	$8.42*10^{-1}$
PC ae C40:5	0.278	4.4%	$3.21*10^{-1}$	0.241	3.8%	$5.41*10^{-1}$	0.325	5.2%	$4.65*10^{-1}$
PC ae C40:6	0.051	1.8%	$6.17*10^{-1}$	0.057	2.0%	$7.26*10^{-1}$	0.044	1.5%	$7.36*10^{-1}$
PC ae C42:0	0.028	4.0%	$2.93*10^{-1}$	0.049	7.1%	$1.08*10^{-1}$	0.000	0.1%	$9.94*10^{-1}$
PC ae C42:1	0.044	4.5%	$4.52*10^{-1}$	0.075	8.4%	$2.37*10^{-1}$	0.004	0.3%	$9.75*10^{-1}$
PC ae C42:2	0.023	2.3%	$6.72*10^{-1}$	0.057	6.1%	$4.38*10^{-1}$	-0.020	-1.8%	$8.26*10^{-1}$
PC ae C42:3	0.047	3.4%	$5.37*10^{-1}$	0.090	7.0%	$3.21*10^{-1}$	-0.007	-0.5%	$9.59*10^{-1}$
PC ae C42:4	0.060	4.2%	$2.59*10^{-1}$	0.120	8.7%	$1.16*10^{-1}$	-0.017	-1.1%	$8.27*10^{-1}$
PC ae C42:5	0.119	4.3%	$1.96*10^{-1}$	0.149	5.4%	$2.06*10^{-1}$	0.081	2.9%	$6.20*10^{-1}$
PC ae C44:3	0.011	3.0%	$6.00*10^{-1}$	0.022	6.8%	$4.11*10^{-1}$	-0.003	-0.8%	$9.26*10^{-1}$
PC ae C44:4	0.016	3.3%	$2.93*10^{-1}$	0.040	8.1%	$5.12*10^{-2}$	-0.014	-2.7%	$5.62*10^{-1}$
PC ae C44:5	0.041	2.8%	$3.86*10^{-1}$	0.058	3.9%	$3.78*10^{-1}$	0.018	1.2%	$8.06*10^{-1}$

	All subjects			Healthy			DM1		
Metabolite	**Mean difference[1]**	**Change (%)2**	**P-value**	**Mean difference[1]**	**Change (%)2**	**P-value**	**Mean difference[1]**	**Change (%)2**	**P-value**
PC ae C44:6	0.021	1.9%	$6.18*10^{-1}$	0.060	5.7%	$2.69*10^{-1}$	-0.031	-2.7%	$6.51*10^{-1}$
SM (OH) C14:1	0.146	2.6%	$2.81*10^{-1}$	0.213	4.0%	$1.67*10^{-1}$	0.059	1.0%	$8.19*10^{-1}$
SM (OH) C16:1	0.096	3.7%	$1.60*10^{-1}$	0.084	3.3%	$3.39*10^{-1}$	0.111	4.2%	$3.54*10^{-1}$
SM (OH) C22:1	0.271	2.4%	$5.34*10^{-1}$	0.730	6.9%	$1.15*10^{-1}$	-0.320	-2.7%	$7.02*10^{-1}$
SM (OH) C22:2	-0.036	-0.4%	$8.93*10^{-1}$	0.084	1.0%	$7.57*10^{-1}$	-0.191	-2.0%	$7.29*10^{-1}$
SM (OH) C24:1	0.021	1.8%	$7.53*10^{-1}$	0.075	6.5%	$9.51*10^{-2}$	-0.049	-4.0%	$7.43*10^{-1}$
SM C16:0	3.468	3.9%	$1.56*10^{-1}$	4.587	5.4%	$8.66*10^{-2}$	2.030	2.1%	$6.71*10^{-1}$
SM C16:1	0.585	4.0%	$1.77*10^{-1}$	0.568	4.3%	$1.42*10^{-1}$	0.606	3.8%	$5.14*10^{-1}$
SM C18:0	0.859	5.0%	$9.13*10^{-2}$	0.375	2.1%	$5.47*10^{-1}$	1.482	8.9%	$9.81*10^{-2}$
SM C18:1	0.265	3.2%	$3.15*10^{-1}$	0.014	0.2%	$9.65*10^{-1}$	0.588	6.8%	$2.07*10^{-1}$
SM C20:2	0.024	5.5%	$3.80*10^{-1}$	0.010	2.3%	$7.28*10^{-1}$	0.042	9.9%	$4.41*10^{-1}$
SM C22:3	-0.017	-5.8%	$7.54*10^{-1}$	-0.021	-7.4%	$8.15*10^{-1}$	-0.061	-19.9%	$2.00*10^{-1}$
SM C24:0	1.132	5.0%	$1.61*10^{-1}$	2.201	9.9%	$3.84*10^{-2}$	-0.242	-1.0%	$8.48*10^{-1}$
SM C24:1	2.222	4.7%	$6.72*10^{-2}$	2.991	6.6%	$3.74*10^{-2}$	1.234	2.5%	$5.82*10^{-1}$
SM C26:0	0.032	51.0%	$1.31*10^{-1}$	0.023	24.4%	$3.09*10^{-1}$	0.050	139.3%	$9.71*10^{-2}$
SM C26:1	0.017	5.1%	$4.07*10^{-1}$	-0.008	-2.5%	$7.53*10^{-1}$	0.048	14.8%	$1.48*10^{-1}$
H1	419.618	7.8%	$3.58*10^{-1}$	126.200	2.8%	$3.61*10^{-1}$	796.870	12.3%	$4.65*10^{-1}$

	Healthy		DM1		Healthy *vs.* DM1
Metabolite	**Mean**	**SD**	**Mean**	**SD**	**P-value**
C0	31.9	5.8	26.6	4.8	0.073
C2	4.24	0.57	3.58	1.06	0.133
C3	0.273	0.043	0.192	0.042	0.002
C3:1	0.010	0.002	0.012	0.003	0.139
C3-DC (C4-OH)	0.074	0.062	0.049	0.011	0.304
C3-OH	0.020	0.003	0.024	0.005	0.020
C4	0.105	0.019	0.105	0.057	0.979
C4:1	0.022	0.003	0.031	0.007	0.005
C5	0.120	0.032	0.097	0.027	0.153
C5:1	0.022	0.003	0.024	0.004	0.148
C5:1-DC	0.020	0.004	0.019	0.002	0.628
C5-DC (C6-OH)	0.017	0.003	0.019	0.005	0.273
C5-M-DC	0.035	0.003	0.039	0.004	0.047
C5-OH (C3-DC-M)	0.023	0.003	0.025	0.004	0.405
C6 (C4:1-DC)	0.066	0.022	0.058	0.014	0.385
C6:1	0.027	0.003	0.026	0.002	0.828
C7-DC	0.025	0.008	0.024	0.008	0.975
C8	0.172	0.126	0.121	0.066	0.356
C8:1	0.065	0.009	0.088	0.043	0.151
C9	0.025	0.010	0.024	0.005	0.817
C10	0.274	0.228	0.181	0.073	0.321
C10:1	0.124	0.073	0.093	0.039	0.324
C10:2	0.027	0.006	0.028	0.004	0.593
C12	0.084	0.051	0.055	0.015	0.179
C12:1	0.080	0.035	0.059	0.018	0.163
C12-DC	0.087	0.005	0.101	0.005	**0.000#**
C14	0.029	0.008	0.022	0.004	0.044
C14:1	0.071	0.028	0.049	0.015	0.080
C14:1-OH	0.009	0.002	0.009	0.001	0.684
C14:2	0.027	0.016	0.020	0.008	0.300
C14:2-OH	0.007	0.001	0.007	0.001	0.277
C16	0.072	0.018	0.060	0.010	0.136
C16:1	0.059	0.004	0.056	0.006	0.231
C16:1-OH	0.006	0.001	0.005	0.001	0.174
C16:2	0.007	0.002	0.006	0.001	0.164
C16:2-OH	0.010	0.001	0.010	0.002	0.684
C16-OH	0.006	0.001	0.007	0.003	0.714
C18	0.025	0.007	0.024	0.007	0.798
C18:1	0.073	0.009	0.074	0.019	0.949
C18:1-OH	0.009	0.001	0.009	0.001	0.668
C18:2	0.025	0.006	0.028	0.006	0.467

Table S5: Acylcarnitine levels after normal sleep duration. *Mean = mean plasma metabolite level (μM). DM1 = individuals with type 1 diabetes. #P<0.001 (0.05/41). P-values are based on independent Students t-tests. Abbreviations of all metabolites are shown in Supplemental Table S3. Healthy individuals n=9, DM1 n=7.*

	Healthy		DM1		Healthy *vs.* DM1
Metabolite	**Mean**	**SD**	**Mean**	**SD**	**P-value**
C0	32.3	7.0	26.6	6.4	0.113
C2	0.287	0.212	0.208	0.078	0.434
C3	0.120	0.057	0.115	0.037	0.839
C3:1	0.027	0.005	0.028	0.005	0.680
C3-DC (C4-OH)	0.094	0.056	0.070	0.018	0.309
C3-OH	0.094	0.034	0.080	0.023	0.356
C4	0.089	0.006	0.104	0.011	0.004
C4:1	0.032	0.008	0.028	0.006	0.300
C5	0.087	0.032	0.073	0.026	0.336
C5:1	0.009	0.001	0.010	0.003	0.261
C5:1-DC	0.032	0.016	0.028	0.008	0.595
C5-DC (C6-OH)	0.007	0.001	0.008	0.002	0.447
C5-M-DC	0.077	0.016	0.070	0.014	0.398
C5-OH (C3-DC-M)	0.063	0.006	0.061	0.011	0.577
C6 (C4:1-DC)	0.007	0.002	0.007	0.002	0.610
C6:1	0.008	0.002	0.008	0.003	0.715
C7-DC	0.010	0.001	0.010	0.001	0.937
C8	0.006	0.001	0.007	0.002	0.213
C8:1	0.027	0.009	0.027	0.006	0.932
C9	0.088	0.014	0.092	0.024	0.664
C10	0.010	0.002	0.011	0.002	0.225
C10:1	0.031	0.006	0.037	0.009	0.103
C10:2	4.421	1.169	4.859	1.478	0.517
C12	0.271	0.065	0.180	0.039	0.006
C12:1	0.010	0.002	0.010	0.003	0.810
C12-DC	0.080	0.047	0.057	0.015	0.241
C14	0.021	0.003	0.024	0.005	0.255
C14:1	0.113	0.028	0.120	0.072	0.793
C14:1-OH	0.024	0.004	0.032	0.007	0.012
C14:2	0.132	0.038	0.106	0.036	0.188
C14:2-OH	0.021	0.005	0.026	0.006	0.121
C16	0.019	0.004	0.021	0.004	0.209
C16:1	0.015	0.003	0.019	0.003	0.028
C16:1-OH	0.034	0.005	0.040	0.007	0.086
C16:2	0.023	0.003	0.025	0.005	0.222
C16:2-OH	0.068	0.016	0.069	0.025	0.919
C16-OH	0.027	0.003	0.027	0.004	0.637
C18	0.027	0.008	0.033	0.008	0.159
C18:1	0.166	0.109	0.135	0.063	0.507
C18:1-OH	0.073	0.028	0.104	0.048	0.128
C18:2	0.024	0.007	0.025	0.005	0.645

Table S6: Acylcarnitine levels after short sleep duration. *Mean = mean plasma metabolite level (μM). DM1 = individuals with type 1 diabetes. P-values are based on independent Students t-tests. Abbreviations of all metabolites are shown in Supplemental Table S3. Healthy individuals n=9, DM1 n=7.*

Chapter 7

Familial longevity is characterized by high circadian rhythmicity of serum cholesterol in healthy elderly individuals

Rosa van den Berg, Raymond Noordam, Sander Kooijman, Steffy W.M. Jansen, Abimbola A. Akintola, P. Eline Slagboom, Hanno Pijl, Patrick C.N. Rensen, Nienke R. Biermasz, Diana van Heemst

Aging Cell 2017; 16: 237-243

ABSTRACT

The biological clock, whose function deteriorates with increasing age, determines bodily circadian (i.e. 24h) rhythms, including that of cholesterol metabolism. Dampening of circadian rhythms has been associated with ageing and disease. Therefore, we hypothesized that individuals with a familial predisposition for longevity have a higher amplitude circadian serum cholesterol concentration rhythm. We investigated circadian rhythmicity of serum cholesterol concentrations in offspring of nonagenarian siblings and their partners. Offspring from nonagenarian siblings (n=19), and their partners as controls (n=18), were recruited from the Leiden Longevity Study. Participants (mean age 65 years) were studied in a controlled in-hospital setting over a 24h period, receiving three isocaloric meals at 9:00h, 12:00h and 18:00h. Lights were off between 23:00h and 8:00h. Serum total cholesterol (TC), HDL-cholesterol (HDL-C), non-HDL-C and triglycerides (TG) were determined every 30 min over a 24h period. The serum TC concentrations were higher during day than during night in offspring (5.2 *vs.* 4.7 mM, p<0.001) and in controls (5.3 *vs.* 5.0 mM, p<0.001). The difference in TC concentrations between day and night tended to be greater in offspring than in controls (0.5 *vs.*0.3 mM, p=0.109), reaching statistical significance in females (p=0.045). Notably, the day-night serum differences in non-HDL-C were 2-fold greater in offspring than in controls (0.43 *vs.* 0.21 mM, p=0.044) and most explicit in females (0.53 *vs.* 0.22, p=0.078). We conclude that familial longevity is characterized by a high circadian rhythmicity of non-HDL-C in healthy elderly offspring from nonagenarian siblings.

INTRODUCTION

During the past decades, life expectancy has increased substantially, resulting in a growing number of individuals with a high age [1]. Ageing has been associated with an increased risk of dyslipidaemia [2]. Familial human longevity has been associated with a less atherogenic lipid profile, which includes a larger LDL particle size [3], and lower circulating concentrations of triglycerides [4]. Furthermore, multiple polymorphisms associated with human longevity were identified in genes involved in lipid metabolism, including several apolipoproteins (e.g., *APOA1* [5], *APOB* [6], *APOC1* [5] and *APOE* [7] which are involved in lipid transport), uncoupling protein-1 (which mediates triglyceride lowering effects through mediating thermogenesis in brown adipose tissue [8]), adiponectin (an anti-inflammatory adipokine that increases ß-oxidation and triglyceride clearance [9]), and cholesteryl ester transfer protein (involved in determining the lipoprotein balance by mediating transfer of cholesteryl esters from HDL to LDL [3, 7]).

Ageing and lipid metabolism have both been related to functioning of the biological clock [10]. The mammalian biological clock is a hierarchical system with a central clock, located in the suprachiasmatic nuclei (SCN) of the hypothalamus, and peripheral clocks at the tissue level [11]. The SCN conveys circadian timing signals, such as light information, to peripheral clocks in the body through neuronal and hormonal cues [11]. The biological clock ultimately serves to maintain circadian (i.e. 24h) rhythms in bodily functions, such as sleep-wake cycles, hormone levels and plasma metabolites. In fact, human plasma lipid concentrations, including those of triglycerides and cholesterol, are rhythmic over a 24h period [12], independent of feeding and waking conditions [13].

The capacity of the biological clock to sustain circadian rhythms deteriorates with increasing age, which is reflected by reduced size of the SCN in the elderly, lower melatonin secretion, and lower amplitudes of temperature rhythms [14]. Animal studies indicate a crucial role for high circadian rhythmicity, i.e. high amplitude rhythms, in maintenance of health. For example, transplantation of SCN grafts from young to old animals restores the amplitude of electrical activity in the SCN and prolongs the life span of aged hamsters [15]. Conversely, a lower amplitude of circadian rhythmicity in blood pressure has been associated with higher cardiovascular risk [16], independent of hypertension [17]. For this reason, we hypothesized that human familial longevity, which is associated with a lower risk of metabolic syndrome [18] and cardiovascular and cardiometabolic diseases at advanced middle-age [19], is associated with a higher rhythmicity in serum cholesterol concentrations. We investigated this hypothesis by comparing circadian rhythmicity of serum cholesterol concentrations between individuals with a familial predisposition for longevity and age-matched controls.

MATERIAL AND METHODS

Ethics statement

The Medical Ethical Committee of Leiden University Medical Center approved this study. The study was performed according to the Helsinki declaration. Written informed consent was obtained from all study participants.

Study participants

Participants were recruited from the Leiden Longevity Study, which aims to investigate genetic factors and biomarkers associated with familial longevity. A more detailed description of the study design and recruitment strategy of the Leiden Longevity Study has been described elsewhere [37]. In short, a total of 421 long-lived families were recruited, without selection based on health condition or demographics. Families were included when at least two long-lived siblings were still alive and fulfilled the age criteria of 89 years for men and 91 years for women. In total, 1671 offspring of these long-lived individuals were recruited and 744 partners thereof as controls.

Of these, a subsample of 38 healthy participants were recruited in the Switchbox study for in- depth endocrine and metabolic phenotyping [26], which included 24h venous blood sampling. To be included in the Switchbox study, participants had to have a fasting glucose level <7 mM, haemoglobin level <7.1 mM, a body mass index (BMI) between 19 kg/m^2 and 33 kg/m^2 and had to be free of any significant chronic disease. These conditions included, among others, renal, hepatic or endocrine diseases as well as the use of medication known to influence lipid concentrations or interfere with hormonal axes. A complete list of criteria that were considered prior to study inclusion has been published elsewhere [38]. Of the 38 participants, one participant was excluded because of a newly diagnosed hypertriglyceridemia, leaving 37 participants for the present study (19 offspring and 18 controls). Habitual sleep quality was assessed using the Pittsburgh sleep quality index (PSQI) questionnaire [39, 40]. With this questionnaire different aspects of sleep are subjectively assessed (e.g., sleep onset latency, sleep quality, and daytime dysfunction). A summary score was calculated to obtain an overall impression of a person's quality of sleep, ranging from a score of 0 (good sleep) to 21 (worse sleep). Chronotype was assessed using the Munich Chronotype Questionnaire, which has been described and validated before [41, 42]. For the present study, we assessed whether a person has any shortage of sleep during a normal week day.

Study and sampling procedure

After an overnight fast of 10-14 hours, a catheter was inserted before start of the study, and blood sampling started at 09:00h. During 24 hours, every 10 minutes 1.2 ml and 2 ml blood was collected in a K_3-EDTA tube and a serum separator (SST)-tube respectively. Participants received three standardized meals at three fixed time points (namely, between 09:00h-10:00h, 12:00h-13:00h and 18:00h-19:00h). All meals consisted of 600 kcal Nutridrink, containing a standard percentage of energy derived from fat (35 %),

carbohydrates (49 %) and protein (16 %) (Nutricia Advanced Medical Nutrition, Zoetermeer, the Netherlands). All participants were sampled year-round in the same room with standardized ambient conditions. Offspring and control couples were studied on the same day. Participants were not allowed to sleep during the day and except for lavatory use no physical activity was allowed during the study period; lights were turned off between 23:00h to 08:00h to allow the participants to sleep.

Biochemical analyses

After blood withdrawal, the serum tubes were kept at room temperature and immediately centrifuged when the samples were clotted. Serum was aliquoted into 500 µl tubes and stored at -80°C. For the present study, we determined serum concentrations of total cholesterol (TC), high-density lipoprotein cholesterol (HDL-C), non-HDL-C and triglycerides (TG) every 30 minutes. TC and TG were analysed by a commercially available enzymatic kit according to the manufacturer's protocols (Roche, Mannheim, Germany), with an inter-assay coefficient of variation (CV) of 7% and intra-assay CV of 3%. HDL was isolated by precipitation of ApoB-containing lipoproteins, with an inter-assay CV of 13% and intra-assay CV of 4%. Hereto, 20% polyethylene glycol (Sigma Aldrich) in 200 mM glycine buffered saline (pH 10) was added to serum, centrifuged for 30 minutes at 6,000 rpm, and HDL-C was determined in the supernatant. Non-HDL-C was calculated by subtracting HDL-C from TC.

Anthropometrics

At the study centre, we measured the height, weight and body fat percentage of the participants. Weight (in kg) was divided by the squared height (in m) to calculate the body mass index (BMI). The percentage of body fat was measured using a bioelectrical impedance analysis (BIA) meter at a fixed frequency of 50 kHz (Bodystat® 1500 Ltd, Isle of Man, British Isles).

Statistical analyses

We calculated the overall mean TC, HDL-C and non-HDL-C per participant for the whole 24h study period, for the day period (9.00h – 23.00h and 8.00h – 9.00h), and the night period (23.00h – 8.00h). Comparisons between offspring and controls were performed using independent sample Student's T-tests (continuous outcomes) and with chi square statistics (dichotomous outcomes). We used paired sample Student's T-tests to analyse differences between day and night serum cholesterol values. To assess whether the differences in mean TC, HDL-C, non-HDL-C and TG between day and night were different between offspring and controls, we calculated the individual mean difference between mean day and night values and tested the differences using independent sample T-tests. All analyses for the comparisons between offspring and controls were additionally stratified by sex. All statistical analyses were conducted using SPSS v.20 for Windows (SPPS Inc., Chicago, IL, USA). Data are presented as means ± SEM. Two-sided p-values below 0.05 were considered statistically significant.

RESULTS

Characteristics of the study population

We performed 24h venous blood sampling in 37 participants under highly controlled conditions at our research facility. During the 24h study period, participants minimized physical activity, received three isocaloric meals (at 9.00h, 12.00h and 18.00h) and were allowed to sleep from 23.00h to 8.00h. The total study population consisting of 19 offspring from nonagenarian siblings (9 men, 10 women) and 18 of their partners as controls (10 men, 8 women), with a mean age of 65.0 ± 1.2 *vs.* 64.7 ± 1.2 years, respectively. The characteristics of the study population were similar between offspring and controls (Table 1), except that the mother's age at death or at inclusion of the study participants was higher in the offspring than in controls (92.1 ± 1.8 *vs.* 78.6 ± 3.3 years, p<0.01). Habitual sleep quality and chronotype were similar between offspring and controls (Table 1). We first characterized circadian rhythms in cholesterol concentrations for the entire study population. Serum total cholesterol (TC) and high-density lipoprotein cholesterol (HDL-C) concentrations were measured in samples collected every 30 min over the 24h period and from these measurements corresponding concentrations of non-HDL-C were derived. Twenty-four hour mean concentration profiles for TC, HDL-C and non-HDL are shown in Figure 1 together with the overall mean TC, HDL-C and non-HDL-C concentration during the day period and night period. In the entire study population, serum concentrations of TC, HDL-C and non-HDL-C exhibited an intra-individual coefficient of variation (CV) of 13%, 19% and 14%, respectively. The mean concentrations of TC, HDL-C and non-HDL-C were higher during the day than during the night (p<0.001).

Comparison of circadian rhythmicity in serum cholesterol between offspring and controls

Mean serum concentrations of TC, HDL-C and non-HDL-C are presented for every 30 min for 24h stratified for offspring and controls in Figure 2 together with the overall mean TC, HDL-C and non-HDL-C concentration during the day period and night period. We observed no difference between offspring and controls in the 24h mean TC (p=0.36), HDL-C (p=0.63) and non-HDL-C (p= 0.59) (Table 2). The serum cholesterol concentrations as measured during the first and last time point of the 24 h period were not statistically significantly different (data not shown). Both offspring and controls had higher serum concentrations of TC during the day than during the night (offspring: 5.2 ± 0.2 *vs.* 4.7 ± 0.2 mM; p<0.001; controls: 5.3 ± 0.1 *vs*. 5.0 ± 0.1 mM; p<0.001) (Figure 2a, b) (Table 3). However, the day-night difference in TC concentrations tended to be larger in offspring than in controls (0.51 ± 0.10 *vs.* 0.31 ± 0.07 mM, p=0.109). Mean HDL-C concentrations were also higher during the day than during the night in both offspring (1.3 ± 0.1 *vs.* 1.2 ± 0.1 mM, p=0.002) and controls (1.3 ± 0.1 *vs*. 1.2 ± 0.1 mM, p=0.001) (Figure 2c, d) (Table 3). However, the day-night difference in mean HDL-C was similar between offspring and controls (p=0.928). In line with the TC concentrations, the mean non-HDL-C concentrations were also higher during the day than during the night, both in offspring (4.0 ± 0.2 *vs.* 3.5 ± 0.2 mM, p<0.001) and controls

	Offspring (n = 19)	Controls (n = 18)	P-value
Men, n (%)	9 (47%)	10 (56%)	0.75
Age, years	65.3 ± 1.2	64.7 ± 1.2	0.71
Men	67.0 ± 2.2	64.9 ± 1.3	0.42
Women	63.9 ± 1.1	64.5 ± 2.1	0.78
BMI, kg/m2	24.5 ± 0.9	25.7 ± 1.0	0.32
Men	25.0 ± 1.1	25.9 ± 1.0	0.57
Women	24.0 ± 1.3	25.5 ± 1.9	0.50
Fat mass, %	31.8 ± 1.9	31.2 ± 2.0	0.83
Men	24.7 ± 1.1	25.0 ± 1.0	0.89
Women	38.3 ± 1.6	38.2 ± 2.0	0.99
Age father, years	82.3 ± 4.5	76.8 ± 2.2	0.28
Men	80 ± 8.2	76 ± 2.9	0.66
Women	85 ± 4.6	78 ± 3.4	0.27
Age mother, years	92.1 ± 1.8	78.6 ± 3.3	<0.01
Men	93 ± 2.6	82 ± 2.2	0.01
Women	92 ± 2.7	75 ± 6.9	0.03
Chronotype >0 min disturbance, N (%)[1]	5 (26.3)	4 (22.2)	0.77
Men	4 (44.4)	2 (20.0)	0.25
Women	1 (10.0)	2 (25.0)	0.40
Chronotype >30 min disturbance, N (%)	3 (15.8)	2 (11.1)	0.68
Men	3 (33.3)	1 (10.0)	0.21
Women	0 (0.0)	1 (12.5)	0.25
Sleep Quality PSQI, median (IQR)[2]	4.0 (2.0 – 7.0)	3.0 (1.0 – 5.0)	0.91
Men	3.0 (1.0 – 4.0)	2.0 (1.0 – 5.0)	0.78
Women	6.0 (4.0 – 9.0)	4.0 (1.0 – 6.0)	0.15

Table 1: Characteristics of the study population. *Abbreviations: BMI, body mass index. Data are presented as the mean ± SEM, unless indicated otherwise. BMI and fat mass were missing for 1 participant. P-value calculated for offspring vs. controls, Student's T-test.*

[1] Scores obtained from Munich Chronotype Questionnaire (P-values calculated with Mann-Whitney test).

[2] Scores obtained from Pittsburg sleep quality index, ranging from 0 (good sleep) to 21 (worse sleep) (P-values calculated with Mann-Whitney test).

(4.0 ± 0.2 *vs.* 3.8 ± 0.2 mM, p=0.002). Notably, the day-night difference in mean non-HDL-C concentrations was significantly larger in offspring than in controls (0.43 ± 0.09 *vs.* 0.21 ± 0.06 mM, p=0.044) (Figure 2e, f) (Table 3). Since the non-HDL lipoproteins transport triglycerides (TG) in addition to cholesterol, we determined TG concentrations. Similar to the HDL-C concentrations, TG concentrations showed a difference between day and night, but this day-night difference was not different between offspring and controls (p=0.852) (Figure S1a-b).

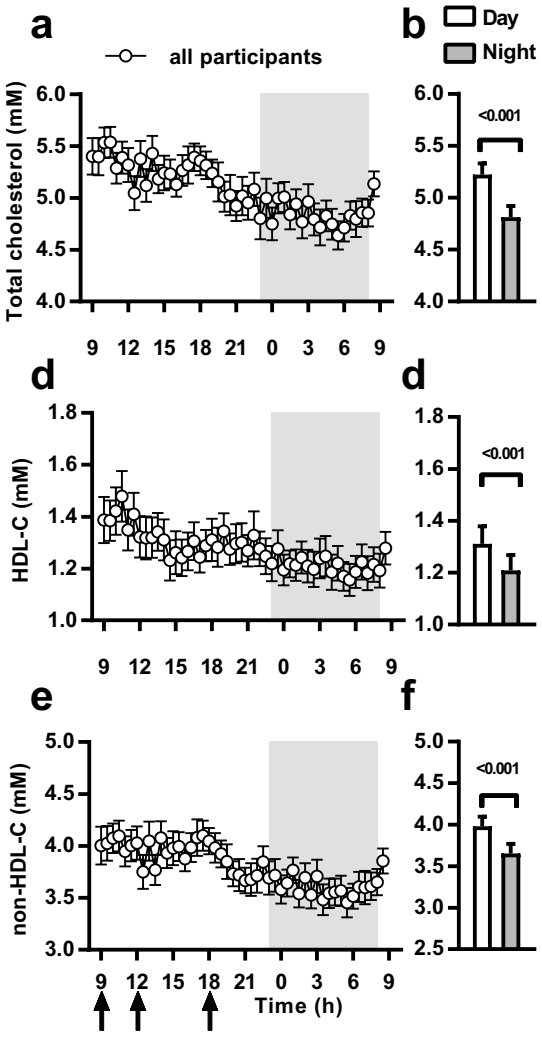

Figure 1: Circadian pattern of serum cholesterol concentrations in all participants combined. *Mean serum cholesterol concentrations are displayed every 30 min over a 24h period for all participants combined (n=37); total cholesterol (TC) (a), HDL-cholesterol (HDL-C) (c), and non-HDL-cholesterol (non-HDL-C) (e) Shaded area indicates dark/sleeping period. Black arrows indicate the time of three isocaloric meals (9:00h, 12:00h, and 18:00h). Figures b, d, and f present the mean ± SEM serum cholesterol concentrations during the day and night period for TC, HDL-C, and non-HDL-C, respectively.*

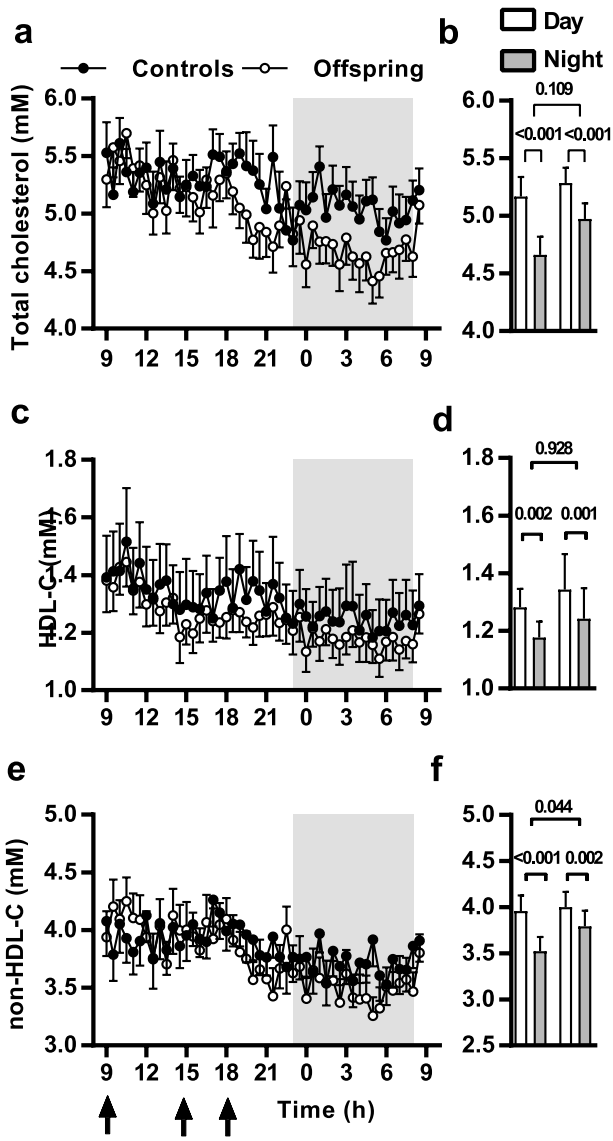

Figure 2: Serum cholesterol concentrations in offspring and controls. *Mean serum cholesterol concentrations are displayed every 30 min over a 24h period stratified for offspring (n=19) (open circles) and controls (n=18) (solid circles); total cholesterol (TC) (a), HDL-cholesterol (HDL-C) (c), and non-HDL-cholesterol (non-HDL-C) (e). Shaded area indicates dark/sleeping period. Black arrows indicate the time of three isocaloric meals (9:00h, 12:00h, and 18:00h). Figures b, d, and f present the mean ± SEM serum cholesterol concentrations during the day and night period for TC, HDL-C, and non-HDL-C, respectively.*

	Offspring (n=19)	Controls (n=18)	P-value
Total cholesterol (mM)	5.0 ± 0.2	5.2 ± 0.1	0.36
Men	4.9 ± 0.3	5.1 ± 0.2	0.58
Women	5.1 ± 0.2	5.3 ± 0.2	0.38
HDL-C (mM)	1.2 ± 0.1	1.3 ± 0.1	0.63
Men	1.2 ± 0.1	1.1 ± 0.1	0.23
Women	1.3 ± 0.1	1.6 ± 0.2	0.14
Non-HDL-C (mM)	3.7 ± 0.2	3.9 ± 0.2	0.59
Men	3.7 ± 0.3	4.0 ± 0.2	0.41
Women	3.8 ± 0.2	3.7 ± 0.2	0.81

Table 2: Mean 24h serum cholesterol concentrations. *Abbreviations: HDL-C = HDL-cholesterol, non-HDL-C = non-HDL cholesterol. Mean 24h parameters were calculated using the individual 24h serum cholesterol concentrations. Data are presented as means ± SEM. P-value calculated for offspring vs. controls, Student's T-test.*

Comparison in cholesterol rhythmicity between offspring and controls, stratified by sex

The analyses stratified by men and women are displayed in Table 3 and Supplemental Figure 2 (Figure S2). Both in men and women, the mean serum TC concentrations during the day were higher than during the night (p<0.05) (Table 3) (Figure S2a-d). In both men and women, the day-night difference seemed higher in offspring than in controls, however this was only statistically significant in women (0.68 ± 0.11 *vs.* 0.36 ± 0.09 mM, p=0.045) and not in men (0.31 ± 0.14 *vs.* 0.27 ± 0.10 mM, p=0.822). The HDL-C concentrations in women were higher during the day than during the night in both offspring and controls (p<0.05) (Table 3) (Figure S2e,f), while this was not observed in men (p>0.05) (Table 3) (Figure S21g, h). In line with the observations in all subjects combined, both in men and women there was no difference between offspring and controls in the day-night difference in HDL-C concentrations. The mean non-HDL-C concentrations were higher during the day than during the night in both men and women (p<0.05) (Table 3) (Figure S2i-l). In women, the day-night differences in non-HDL-C tended to be larger in offspring than in controls (0.53 ± 0.13 *vs.* 0.22 ± 0.08 mM; p=0.078) (Table 3). Similarly, day-night differences in non-HDL-C concentrations in men were also slightly larger in offspring than in controls, but this was not statistically significant (0.33 ± 0.12 *vs.* 0.20 ± 0.08 mM; p=0.388) (Table 3).

DISCUSSION

The present study aimed to investigate differences in circadian rhythmicity of serum cholesterol concentrations between individuals with and without a familial predisposition for longevity. Irrespective of the study groups, we observed that serum cholesterol

concentrations displayed a 24h rhythm with mean concentrations being higher during the day compared to the night. Previous studies on the daily variation in serum cholesterol concentrations have been conflicting. Some studies reported no variation during the day [20, 21], while others reported circadian variation in serum cholesterol with a CV up to 4% [12] and circadian variation in cholesterol precursors [22] or cholesterol production rate [23]. However, in all these studies, sampling frequency was at most every 1.5 hours and the study populations included up to 25 young adults, and the studies showing no circadian rhythm in cholesterol included only 5 individuals. Within the current study sampling rate was every 30 minutes in 37 individuals, which therefore gives more detailed data about possible rhythmicity. Within our study population of 37 healthy older participants, we found a 24h variation in serum TC concentrations with a CV of 13%. Moreover, we observed a clear difference between day and night serum total cholesterol concentrations, showing that in this population of healthy elderly, cholesterol concentrations are rhythmic.

We observed that participants with a predisposition for familial longevity had a higher circadian rhythmicity (observed by a greater day-night difference) in cholesterol concentrations compared with their partners as controls. Ageing has been associated with a decreased functioning of the biological clock, with respect to hormonal rhythms, core body temperature and sleep-wake cycles [14]. Likely, the age-related changes originate within the central biological clock, the SCN. Post-mortem analysis showed that in individuals over 50 years of age, the SCN has decreased neuronal activity and rhythmicity compared to the SCN of younger individuals, as determined by arginine vasopressin expression [24]. Notably, the number of active SCN neurons correlated with the amplitude in activity patterns in elderly [25]. Previously, we observed within the Leiden Longevity Study cohort that familial longevity is associated with higher mean thyroid stimulating hormone (TSH) concentrations, in the absence of differences in free T3 or T4 serum concentrations [26]. We also observed a stronger temporal association between TSH and free T3 in offspring compared to in controls, which is indicative of a stronger correlation between circadian TSH and free T3 rhythms [27]. Based on the current study, we speculate that a familial predisposition of longevity is characterized by subtle changes in some rhythmic parameters rather than their 24h mean serum concentrations resulting from a preserved biological clock function.

In the complete Leiden Longevity Study cohort, no difference in unfasted HDL-C concentrations between offspring and controls was observed [4], in contrast to observations of Barzilai *et al.* in offspring of Ashkenazi Jewish centenarians and controls [28]. In line with the larger Leiden Longevity Study cohort, in the present subset no difference in HDL-C rhythms between offspring and controls were found. The differences observed in the current study between offspring and controls were specifically in non-HDL-C concentrations during day and night, independent of triglyceride concentrations, habitual lifestyle and food intake. Therefore, there is likely an intrinsic difference in non-HDL-C metabolism in individuals with familial longevity.

The higher rhythmicity in non-HDL-C concentrations in offspring compared to controls could be a marker of a maintained clock function at a higher age. Alternatively, the increased

rhythmicity in serum non-HDL-C concentrations could directly contribute to the increased life expectancy that is associated with familial longevity. The differences between the offspring and control group were mainly observed in non-HDL-C concentrations. This is particularly interesting with respect to life expectancy since non-HDL-C concentrations are implicated as causal in the pathogenesis of cardiovascular disease, which represents the number one cause of death world-wide. In humans, non-HDL-C concentrations mainly represent LDL-C [29]. LDL can be modified and taken up by macrophages, triggering atherosclerotic lesion development [29]. Indeed, Mendelian randomization studies have demonstrated that life-long low-range LDL-C concentrations (compared to higher LDL-C concentrations) decreases cardiovascular risk [30]. Accordingly, long-term high-range cholesterol concentrations are associated with a significantly increased cardiovascular risk [31]. It is therefore tempting to speculate that a stronger day-night rhythm of non-HDL-C (likely LDL-C) contributes to a lower cardiovascular disease risk.

We investigated the sex-specific effects on cholesterol rhythms in this study. Both men and women tended to display a higher rhythmicity in offspring than in controls in TC and non-HDL-C concentrations, but not in HDL-C concentrations. However, this day-night difference was more prominent in women than in men, where the differences between offspring and controls did not reach significance, while in women day-night difference in TC concentrations was significantly different and the day-night difference in non-HDL-C concentrations showed a trend. Of note, there is evidence pointing towards sex specific differences with respect to activity of the SCN. The SCN is sensitive to regulation by gonadal hormones [32]. Furthermore, in mice, ageing-induced decrease of the locomotor activity is higher in male mice than in female mice [33]. These data imply that also ageing may affect biological clock function in a sex-specific manner. This observation may also account for any possible sex differences in cholesterol rhythmicity in our study.

In this study, we observed that familial longevity is characterized by larger difference between night and day serum non-HDL-C concentrations. For human metabolism, the transition from night to day indicates the switch from fasting to feeding and thus from a catabolic to an anabolic state. This is for example apparent by the morning increase in insulin sensitivity [34]. Since cholesterol is a major substrate for synthesis of membranes and hormones, the observed increase of non-HDL-C upon waking may be a function of this anabolic state. The lower night concentrations of non-HDL-C are analogous to the diurnal rhythm of blood pressure. The absence of a decrease in blood pressure during the night, a phenomenon which is called 'non-dipping', has been associated with increased cardiovascular risk [16], independent of hypertension [17]. However, as these studies were done in observational settings, the question remains whether the lower amplitude in blood pressure is a marker of underlying disease or a causal factor affecting cardiovascular disease risk. Animal studies support a causal role for dampened rhythms in metabolic disease. We previously showed that constant light exposure induces a dampened rhythm in SCN electrical activity as well as feeding and locomotor rhythms [35]. Interestingly, constant light increased weight gain independent of total food intake and activity, but by decreasing energy expenditure by decreasing brown adipose tissue activity [36].

	Offspring (n=19)			Controls (n=18)			Offspring (n=19)	Controls (n=18)	
	Day	Night	P-value[1]	Day	Night	P-value[1]	Day – Night difference	Day – Night difference	P-value[2]
Total cholesterol (mM)	5.2 ± 0.2	4.7 ± 0.2	<0.001	5.3 ± 0.1	5.0 ± 0.1	<0.001	0.51 ± 0.10	0.31 ± 0.07	0.109
Men	5.0 ± 0.3	4.7 ± 0.3	0.062	5.1 ± 0.2	4.9 ± 0.2	0.023	0.31 ± 0.14	0.27 ± 0.10	0.822
Women	5.3 ± 0.2	4.6 ± 0.2	<0.001	5.5 ± 0.2	5.1 ± 0.2	0.004	0.68 ± 0.11	0.36 ± 0.09	0.045
HDL-C (mM)	1.3 ± 0.1	1.2 ± 0.1	0.002	1.3 ± 0.1	1.2 ± 0.1	0.001	0.10 ± 0.03	0.10 ± 0.03	0.928
Men	1.2 ± 0.1	1.2 ± 0.1	0.332	1.1 ± 0.1	1.0 ± 0.1	0.135	0.05 ± 0.04	0.05 ± 0.03	0.918
Women	1.4 ± 0.1	1.2 ± 0.1	<0.001	1.7 ± 0.2	1.5 ± 0.2	0.003	0.16 ± 0.03	0.16 ± 0.04	0.905
Non-HDL-C (mM)	4.0 ± 0.2	3.5 ± 0.2	<0.001	4.0 ± 0.2	3.8 ± 0.2	0.002	0.43 ± 0.09	0.21 ± 0.06	0.044
Men	3.9 ± 0.3	3.6 ± 0.3	0.025	4.1 ± 0.2	3.9 ± 0.2	0.038	0.33 ±. 0.12	0.20 ± 0.08	0.388
Women	4.0 ± 0.2	3.5 ± 0.2	0.003	3.8 ± 0.2	3.6 ± 0.2	0.026	0.53 ± 0.13	0.22 ± 0.08	0.078

Table 3: Mean serum cholesterol concentrations during day and night. *Abbreviations: HDL-C = HDL-cholesterol, non-HDL-C = non-HDL cholesterol. Day (9:00h – 23:00h and 8.00h – 9.00h) and night (23:00h – 8:00h) mean values were calculated using the individual 24h serum cholesterol concentrations. Day – Night difference was calculated by subtracting the individual mean night value from mean day value. Data are presented as means ± SEM. [1]P-value calculated between day and night based on paired Student's T-test; [2] P-value calculated of day-night difference between offspring and controls, Student's T-test.*

A limitation of the current study is the relatively small sample size. Although our study cohort was larger than previous cohorts that studied 24h cholesterol rhythms, our sample size of 37 individuals is likely too limited to find subtle differences. This was also apparent from the stratification by sex. Visually, the HDL-C concentrations in female control individuals seemed higher than those of female offspring, however only two out of the eight female control individuals displayed elevated 24h HDL-C concentrations. Likewise, the differences in day-night non-HDL-C serum concentrations were larger in offspring than in controls, but only significant in women. Possibly, effects are more subtle in men, which were therefore not detected in a small study such as the present one.

In conclusion, we show that in advanced middle-age, familial longevity is characterized by a high rhythmicity of serum non-HDL-C concentrations in a subset of healthy individuals. Our study supports the hypothesis that high amplitude rhythms may contribute to healthy ageing and therefore, decreased rhythmicity may be an additional risk factor for development of disease. Increasing circadian rhythmicity may be an attractive target to promote longevity.

ACKNOWLEDGEMENTS

We thank all participants, the secretarial staff (M. van der Star and E. Bemer-Oorschot), the research nurse (R. de Wilde), the research assistant (B. Ladan), and database manager (S. Henquet). Furthermore, we thank J.P. van der Elst for excellent technical assistance to measure the serum cholesterol concentrations. **Disclosure Statement:** The authors have nothing to disclose. **Funding**: PCN Rensen is an Established Investigator of the Dutch Heart Foundation (grant 2009T038). This study was supported by the Netherlands Organisation for Scientific Research (NWO-VENI grant 016.136.125 to NR Biermasz) and funded by the European funded projects Switchbox (FP7, Health- 2010-259772) and HUMAN (FP7, Health-2013-INNOVATION-1-602757). **Author contributions:** RvdB designed the study, supervised the cholesterol measurements, conducted the analyses and wrote the initial version of the manuscript. RN designed the study, conducted the analyses and wrote the initial version of the manuscript. SK designed the study and wrote the initial version of the manuscript. SWJ and AAA included the study participants and collected the biomaterials and data of the Switchbox Study. HP, PES, NRB, PCNR and DvH supervised the project. All authors critically commented on the initial versions of the manuscript and approved the final version of the manuscript for submission.

REFERENCES

1. Oeppen, J. and J.W. Vaupel, *Demography. Broken limits to life expectancy.* Science, 2002. **296**(5570): p. 1029-31.
2. Steinhagen-Thiessen, E., *et al.*, *Dyslipidemia in primary care--prevalence, recognition, treatment and control: data from the German Metabolic and Cardiovascular Risk Project (GEMCAS).* Cardiovasc Diabetol, 2008. **7**: p. 31.
3. Barzilai, N., *et al.*, *Unique lipoprotein phenotype and genotype associated with exceptional longevity.* JAMA, 2003. **290**(15): p. 2030-2040.
4. Vaarhorst, A.A., *et al.*, *Lipid metabolism in long-lived families: the Leiden Longevity Study.* Age (Dordr.), 2011. **33**(2): p. 219-227.
5. Garasto, S., *et al.*, *The study of APOA1, APOC3 and APOA4 variability in healthy ageing people reveals another paradox in the oldest old subjects.* Ann. Hum. Genet, 2003. **67**(Pt 1): p. 54-62.
6. G., D.B., *et al.*, *DNA multiallelic systems reveal gene/longevity associations not detected by diallelic systems. The APOB locus.* Hum. Genet, 1997. **99**(3): p. 312-318.
7. Soerensen, M., *et al.*, *Evidence from case-control and longitudinal studies supports associations of genetic variation in APOE, CETP, and IL6 with human longevity.* Age (Dordr.), 2013. **35**(2): p. 487-500.
8. Rose, G., *et al.*, *Two variants located in the upstream enhancer region of human UCP1 gene affect gene expression and are correlated with human longevity.* Exp. Gerontol, 2011. **46**(11): p. 897-904.
9. Roszkowska-Gancarz, M., *et al.*, *Total and high molecular weight adiponectin and level-modifying polymorphisms of ADIPOQ in centenarians.* Endokrynol. Pol, 2012. **63**(6): p. 439-446.
10. Froy, O., *Circadian rhythms, aging, and life span in mammals.* Physiology (Bethesda), 2011. **26**(4): p. 225-35.
11. Reppert, S.M. and D.R. Weaver, *Coordination of circadian timing in mammals.* Nature, 2002. **418**(6901): p. 935-941.
12. Rivera-Coll, A., X. Fuentes-Arderiu, and A. Diez-Noguera, *Circadian rhythmic variations in serum concentrations of clinically important lipids.* Clin. Chem, 1994. **40**(8): p. 1549-1553.
13. Chua, E.C., *et al.*, *Extensive diversity in circadian regulation of plasma lipids and evidence for different circadian metabolic phenotypes in humans.* Proc. Natl Acad. Sci. U. S. A, 2013. **110**(35): p. 14468-14473.
14. Hofman, M.A. and D.F. Swaab, *Living by the clock: the circadian pacemaker in older people.* Ageing Res. Rev, 2006. **5**(1): p. 33-51.
15. Hurd, M.W. and M.R. Ralph, *The significance of circadian organization for longevity in the golden hamster.* J Biol Rhythms, 1998. **13**(5): p. 430-6.
16. White, W.B., *Ambulatory blood pressure monitoring: dippers compared with non-dippers.* Blood Press Monit, 2000. **5 Suppl 1**: p. S17-23.
17. Hermida, R.C., *et al.*, *Blunted sleep-time relative blood pressure decline increases cardiovascular risk independent of blood pressure level--the "normotensive non-dipper" paradox.* Chronobiol Int, 2013. **30**(1-2): p. 87-98.
18. Rozing, M.P., *et al.*, *Favorable glucose tolerance and lower prevalence of metabolic syndrome in offspring without diabetes mellitus of nonagenarian siblings: the Leiden longevity study.* J Am Geriatr Soc, 2010. **58**(3): p. 564-9.
19. Westendorp, R.G., *et al.*, *Nonagenarian siblings and their offspring display lower risk of mortality and morbidity than sporadic nonagenarians: The Leiden Longevity Study.* J Am. Geriatr. Soc, 2009. **57**(9): p. 1634-1637.
20. Mirani-Oostdijk, C.P., *et al.*, *Diurnal changes in serum triglycerides as related to changes in lipolytic enzymes, (apo) lipoproteins and hormones in normal subjects on a carbohydrate-rich diet.* Eur J Clin Invest, 1983. **13**(4): p. 301-9.

21. Persson, L., *et al., Circulating proprotein convertase subtilisin kexin type 9 has a diurnal rhythm synchronous with cholesterol synthesis and is reduced by fasting in humans.* Arterioscler. Thromb. Vasc. Biol, 2010. **30**(12): p. 2666-2672.
22. Miettinen, T.A., *Diurnal variation of cholesterol precursors squalene and methyl sterols in human plasma lipoproteins.* J Lipid Res, 1982. **23**(3): p. 466-73.
23. Jones, P.J. and D.A. Schoeller, *Evidence for diurnal periodicity in human cholesterol synthesis.* J Lipid Res, 1990. **31**(4): p. 667-73.
24. Hofman, M.A., J.N. Zhou, and D.F. Swaab, *Suprachiasmatic nucleus of the human brain: an immunocytochemical and morphometric analysis.* Anat. Rec, 1996. **244**(4): p. 552-562.
25. Wang, J.L., *et al., Suprachiasmatic neuron numbers and rest-activity circadian rhythms in older humans.* Ann Neurol, 2015. **78**(2): p. 317-22.
26. Jansen, S.W., *et al., Human longevity is characterised by high thyroid stimulating hormone secretion without altered energy metabolism.* Sci. Rep, 2015. **5**: p. 11525.
27. Jansen, S.W., *et al., Familial Longevity Is Associated With Higher TSH Secretion and Strong TSH-fT3 Relationship.* J Clin Endocrinol Metab, 2015. **100**(10): p. 3806-13.
28. Barzilai, N., *et al., Offspring of centenarians have a favorable lipid profile.* J Am Geriatr Soc, 2001. **49**(1): p. 76-9.
29. Graham, I., *et al., Dyslipidemias in the prevention of cardiovascular disease: risks and causality.* Curr. Cardiol. Rep, 2012. **14**(6): p. 709-720.
30. Postmus, I., *et al., LDL cholesterol still a problem in old age? A Mendelian randomization study.* Int J Epidemiol, 2015. **44**(2): p. 604-12.
31. Pletcher, M.J., *et al., Nonoptimal lipids commonly present in young adults and coronary calcium later in life: the CARDIA (Coronary Artery Risk Development in Young Adults) study.* Ann Intern Med, 2010. **153**(3): p. 137-46.
32. Bailey, M. and R. Silver, *Sex differences in circadian timing systems: implications for disease.* Front Neuroendocrinol, 2014. **35**(1): p. 111-39.
33. Stowie, A.C. and J.D. Glass, *Longitudinal Study of Changes in Daily Activity Rhythms over the Lifespan in Individual Male and Female C57BL/6J Mice.* J Biol Rhythms, 2015. **30**(6): p. 563-8.
34. Yoshino, J., *et al., Diurnal Variation in Insulin Sensitivity of Glucose Metabolism Is Associated With Diurnal Variations in Whole-Body and Cellular Fatty Acid Metabolism in Metabolically Normal Women.* J Clin Endocrinol. Metab, 2014: p. jc20141579.
35. Coomans, C.P., *et al., Detrimental effects of constant light exposure and high-fat diet on circadian energy metabolism and insulin sensitivity.* FASEB J, 2013. **27**(4): p. 1721-1732.
36. Kooijman, S., *et al., Prolonged daily light exposure increases body fat mass through attenuation of brown adipose tissue activity.* Proc. Natl Acad. Sci. U. S. A, 2015. **112**(21): p. 6748-6753.
37. Schoenmaker, M., *et al., Evidence of genetic enrichment for exceptional survival using a family approach: the Leiden Longevity Study.* Eur. J Hum. Genet, 2006. **14**(1): p. 79-84.
38. Akintola, A.A., *et al., A simple and versatile method for frequent 24 h blood sample collection in healthy older adults.* MethodsX, 2015. **2**: p. 33-38.
39. Carpenter, J.S. and M.A. Andrykowski, *Psychometric evaluation of the Pittsburgh Sleep Quality Index.* J Psychosom Res, 1998. **45**(1): p. 5-13.
40. Buysse, D.J., *et al., The Pittsburgh Sleep Quality Index: a new instrument for psychiatric practice and research.* Psychiatry Res, 1989. **28**(2): p. 193-213.
41. Roenneberg, T., A. Wirz-Justice, and M. Merrow, *Life between clocks: daily temporal patterns of human chronotypes.* J Biol Rhythms, 2003. **18**(1): p. 80-90.
42. Zavada, A., *et al., Comparison of the Munich Chronotype Questionnaire with the Horne-Ostberg's Morningness-Eveningness Score.* Chronobiol Int, 2005. **22**(2): p. 267-78.

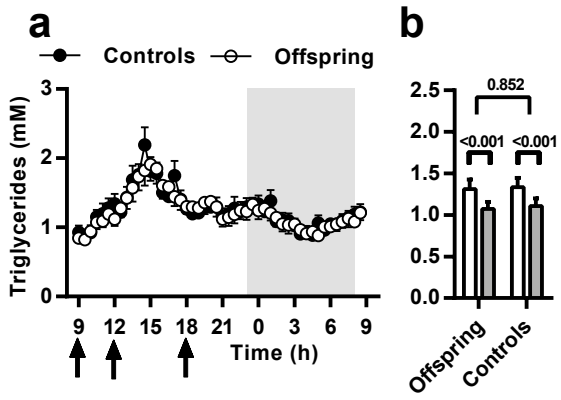

Supplemental Figure 1: Serum triglyceride concentrations in offspring and controls. *Mean serum triglycerides (TG) concentrations are displayed every 30 min over a 24h period stratified for offspring (n=19) (open circles) and controls (n=18) (solid circles) (**a**), the mean ± SEM serum TG concentrations during the day and night period (**b**). Shaded area indicates dark/sleeping period. Black arrows indicate the time of three isocaloric meals (9:00h, 12:00h, and 18:00h).*

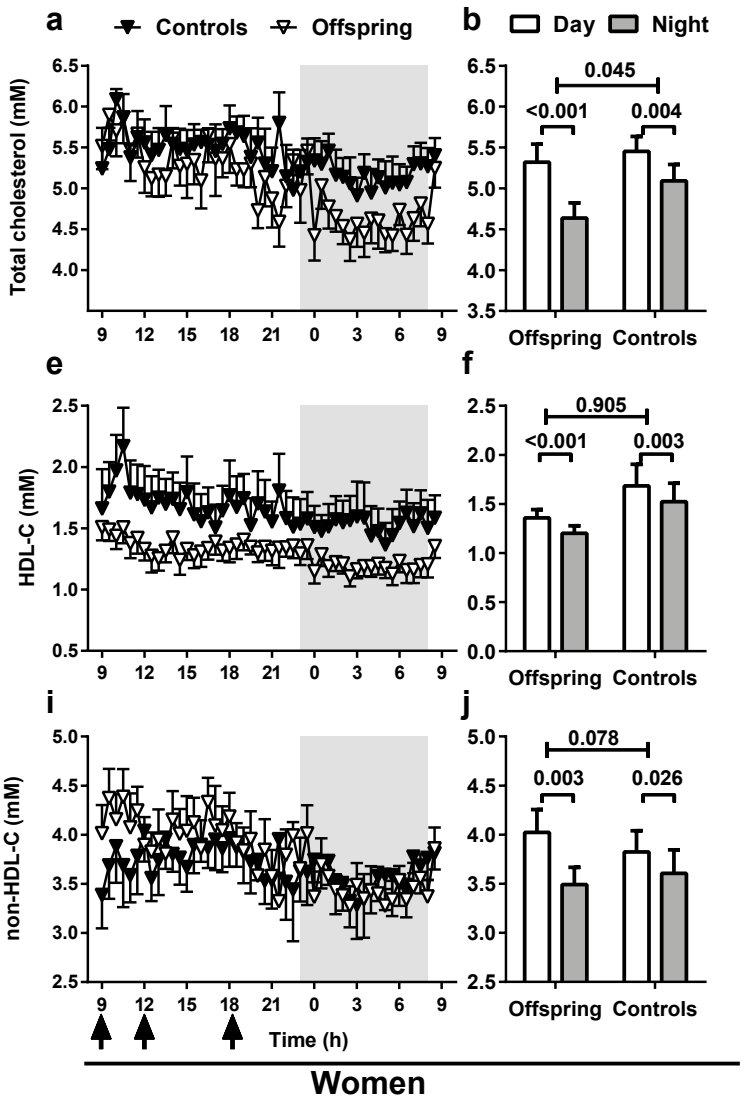

Supplemental Figure 2: (continues on right page) Serum cholesterol concentrations in offspring and controls in women and men. *Mean serum cholesterol concentrations are displayed every 30 min over a 24h period separately for women (triangles) and men (squares), and stratified for offspring (open symbols) and controls (solid symbols); total cholesterol (TC)* ***(a;c)****, HDL-cholesterol (HDL-C)* ***(e;g)****, and non-HDL-cholesterol (non-HDL-C)* ***(i;k)****. Shaded area indicates dark/sleeping period. Black arrows indicate the time of three isocaloric meals (9:00h, 12:00h, and 18:00h). Figures* ***b****,* ***d****,* ***f****,* ***h****,* ***j****, and* ***l*** *present the mean ± SEM serum cholesterol concentrations during the day and night period for TC* ***(b, d)****, HDL-C* ***(f, h)****, and non-HDL-C* ***(j, l)****, respectively.*

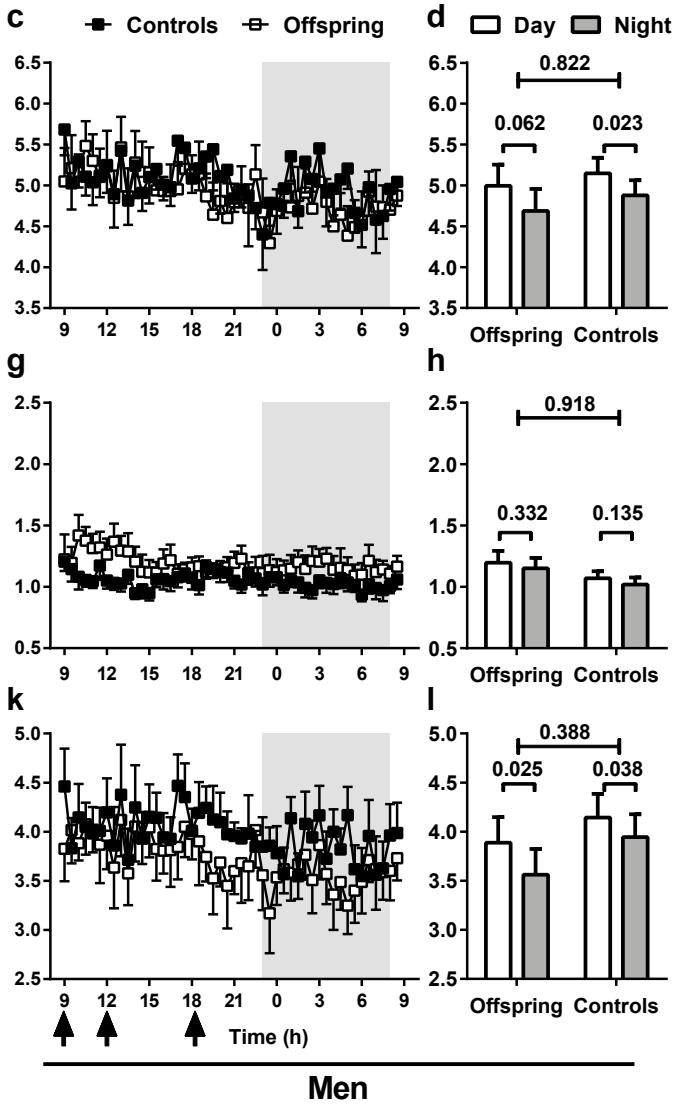
c
Controls
Offspring
d
Day
Night
0.822
0.062
0.023
Offspring
Controls
g
0.918
0.332
0.135
Offspring
Controls
k
l
0.388
0.025
0.038
Offspring
Controls
Time (h)
Men

Chapter 8

General Discussion and Future Perspectives

GENERAL DISCUSSION AND FUTURE PERSPECTIVES

For centuries, the use of artificial light permitted man to stay awake after dark. From campfires in prehistoric times, to the use of an oil lamp ancient Greece, humans have invented ways to bring light. The invention of the light bulb in 1879 by Thomas Edison is heralded as the birth of 'artificial light'. This coincided with the advent of the industrial revolution, and the increased need to working at night commenced to have a large impact on society. In the 19th century, factory labor was among the hardest shift work circumstances with shift work rotations of 12 hours for two weeks straight, without a day rest [1]. Today, it is estimated that in Europe, approximately 20% of the working population is involved in some form of shift work [2]. The 24 hour economy is not just exemplified by the common use of shift work but also by shifting of social activities to nightly hours. This habit has only further encouraged shift work, as nowadays leisure businesses are also open 24/7, including supermarkets, bars, gas stations and restaurants. In terms of our biological clock, these habits are severely disturbing via at least three different pathways. Firstly, humans are widely exposed to bright light during the natural occurring night. Since light exposure directly acts on the central biological clock, the mistimed light exposure may disrupt synchronization of the clock. Secondly, in our modern society physical activity, wakefulness and food intake take place throughout the light-dark cycle. This induces a misalignment between the metabolic demand, *i.e.* energy intake, storage and expenditure, and the endogenous circadian rhythms of metabolic organs, which are entrained to the light-dark cycle. Thirdly, staying up late in the evening and night for work or leisure has led to shortened sleep duration [3]. All of these human circadian disruptions have been associated with metabolic disease.

In this thesis we have investigated which metabolic pathways may mediate the interaction between the biological clock and energy metabolism. To gain more insight in how circadian disruption causes metabolic disease, we studied the effect of light exposure on metabolic phenotypes in mice (**Part I**). We demonstrated that prolonged light exposure attenuates brown adipose tissue (BAT) activity, thereby increasing adiposity (**Chapter 2**). Subsequently, we demonstrated that BAT activity displays a marked 24h rhythm, which determines the 24h rhythm in plasma lipid levels (**Chapter 3**), and which is attenuated upon dampening of the endogenous glucocorticoid rhythm (**Chapter 4**). Finally, we show that mistimed light exposure can aggravate atherosclerosis development in dyslipidemic mice (**Chapter 5**). In **Part** II, we evaluated the relationship between circadian rhythms and metabolism in humans. We showed that shortened sleep duration increases acylcarnitines in plasma, suggesting a defect in mitochondrial fatty acid oxidation (**Chapter 6**). Finally, we demonstrate 24h rhythms in plasma cholesterol and observed a higher rhythmicity in plasma cholesterol in the context of longevity (**Chapter 7**). In this chapter, I will discuss these novel findings in the context of the three pathways – mistimed light exposure, behavioral misalignment and short sleep – that mediate the relationship between light exposure and metabolic disease (see graphical summary). I will conclude by discussing the implications for future research and possible therapeutic strategies.

The rhythm in brown adipose tissue in relation to cardiometabolic disease

A very recent study on light pollution reports that an astonishing 83% of the world population lives under light-polluted skies [4]. In the US and Europe, this proportion even reaches 99%. The human retina has three photoreceptors sensitive to light: rods and cones, which are crucial for visual perception, and the melanopsin-containing intrinsically photoreceptive retinal ganglion cells (ipRGCs) [5]. The ipRGCs transmit light-dark information directly to the SCN, although mice lacking melanopsin can still entrain to light-dark cycle [6, 7]. Conversely, ipRGCs are also sufficient to entrain to light-dark cycle [8]. The illumination levels that constitute light pollution [4] not only reach the human retina, but are also sufficient to trigger the photoreceptors [9]. Evidence is accumulating that in humans, light exposure at night associates with increased body weight [10-13]. Although constant light exposure has previously been shown to induce a fast increase in weight gain due to a decrease in 24h energy expenditure in mice [14], it remained unknown which tissues contributed to this difference. In chapter 2, we provide evidence that BAT plays a crucial role. BAT is a highly metabolically active tissue that burns glucose and fatty acids (FA) to produce heat. Activation of BAT increases energy expenditure, decreases and prevents diet-induced obesity and decreases dyslipidemia [15-18]. We showed that prolonged light exposure duration decreases SNS output towards BAT and reduces the capacity of BAT to take up TG-derived FA from the circulation [19]. Without compensation in food intake, this led to increased storage of energy in WAT. Specific sympathetic denervation of BAT abolished the rhythm-attenuating effect of prolonged light exposure.

Our findings support recent human studies demonstrating that exposure to light can alter metabolism. Healthy individuals that were exposed to low levels of blue light in the evening showed a lower energy expenditure in the morning, without alterations in sleep duration or quality [20]. Other evidence for the effect of light exposure on metabolism in humans is mainly derived from epidemiological studies. Light duration inversely correlates to detectability of BAT throughout the year, as shown by uptake of [^{18}F]fluorodeoxyglucose. This association is stronger and more significant than the association between ambient temperature and BAT activity [21]. Take together with our findings in mice, it can be hypothesized that short light duration, presumably via the SCN, increases basal BAT activity in humans. Since light duration is a more stable predictor for seasonal changes than ambient temperature, this mechanism seems to have biological relevance: shortening of days predicts the approach of winter, a season in which higher BAT activity is needed for heat generation to maintain body temperature. Therefore, turning up the heat by activation of BAT as the days grow shorter may more likely be an adaptive mechanism than merely a reaction to the outside temperature. Whether light exposure duration regulates BAT activity in humans as well remains to be investigated.

Besides showing that disruption of circadian rhythm lowers BAT activity, we demonstrated a marked diurnal rhythm in TG-rich lipoprotein-derived FA uptake by BAT in mice (chapter 3). This diurnal rhythm aligns with the known rhythms of energy expenditure and core body temperature, which peak before the start of the wakeful period in both day-

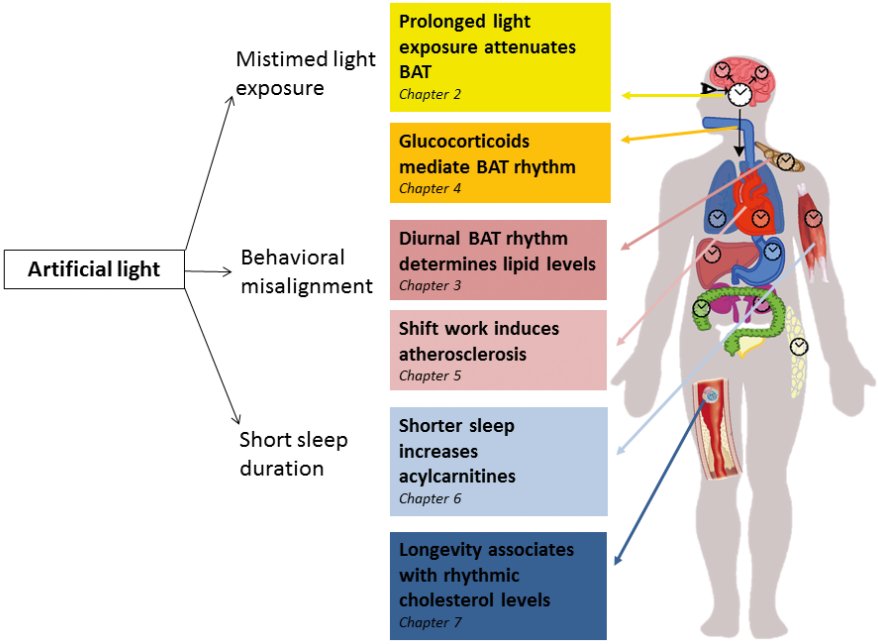

Figure 1. Graphical Summary representing the main conclusions based on the studies described in this thesis. *See text for explanation.*

active and night-active mammals [22]. In our study, prolonged and shortened light exposure shifted the peak time in BAT activity to the respective onsets of the dark (active) period. This was accompanied by a fast postprandial lipid clearance at the onset of the dark period irrespective of the light exposure period. These data suggest that BAT should be influenced by circadian misalignment. Indeed, an experimental jet-lag protocol of 6 days in healthy individuals led to decreased energy expenditure and a decreased thermic effect of food [23]. These results may be explained by misalignment between food intake and the endogenous BAT rhythm. In another misalignment study, 10 healthy individuals were subjected to 7 repeated cycles of a 28h 'day'. Metabolic hormones changed, including decreased total leptin levels, increased insulin levels, but interestingly also decreased plasma epinephrine [24]. This suggests that reduced sympathetic output towards BAT may play a role in lowering BAT activity upon circadian disruption.

Although humans are day-active and mice are night-active, it is likely that the circadian BAT activity found in mice is analogous to humans, *i.e.* highest activity at wakening. A recent human study found a circadian rhythm in supraclavicular temperature, a proxy for human BAT activity, which was low during the night and higher during daytime. Furthermore, human brown adipose tissue explants sustain a circadian rhythm in gene expression [25]. Circumstantial evidence also points towards a circadian human BAT activity with a trough at night and peak at wakening. In humans, BAT activation also contributes to energy

expenditure [15] and decreases free FA [18]. Energy expenditure displays a robust circadian rhythm in humans [26]. Our data demonstrate that plasma free FA display a circadian rhythm, with low FA in the morning, which is not explained by food intake (chapter 3). From an evolutionary point of view, a circadian rhythm in BAT constitutes an energy saving ability. BAT developed to maintain body temperature in homeotherms, however keeping BAT constitutively active would be a 'waste' of energy. Moreover, circadian body temperature may serve as a synchronization signal for peripheral clocks. *In vitro*, temperature cycles specifically regulate the cyclic expression of cold-inducible RNA-binding protein (CIRP) and mice lacking CIRP have a decreased circadian amplitude in rhythmic gene expression [27]. Since BAT contributes to body temperature, the diurnal BAT rhythm may be important in the synchronization circadian rhythms throughout the body and contribute to wakening. Together, human data support the hypothesis that circadian BAT activity is high at wakening and low during sleep.

A key question remains to be elucidated: how does the SCN regulate the rhythm in BAT activity? Possible pathways can be divided in indirect *vs*. direct regulation of BAT by the SCN. Meal timing has been shown to entrain peripheral circadian clocks in metabolic tissues, and is therefore a likely indirect regulator of rhythmic BAT activity. Restricting food intake to the usual sleep period of rodents induces a shift in the rhythm of metabolic tissues, both in clock gene expression and metabolic function [28]. The SCN itself however is not affected by the restricted feeding regimens [29]. Therefore, food intake rhythm has an independent effect on synchronizing metabolic tissues. The SCN does align food intake behavior to the light-dark cycle. SCN lesioned rats display arrhythmic locomotor activity and food intake behavior [30, 31]. Light exposure duration induces adaptations in food intake rhythms in wild type animals [32]. These adaptations are dependent on intact SCN functioning, as VIP-knockout mice (a genetic model for SCN dysfunction) cannot entrain to light exposure duration [33]. The effect of food intake rhythm on BAT activity has not extensively been characterized. Under normal chow feeding, there is no effect of night-restricted feeding on gene expression rhythms of BAT. However, after 20 weeks of high fat diet feeding, night time restriction of food intake increases overall BAT activity and improves the rhythm in gene expression of several thermogenic genes [34]. The authors attribute this effect to increased bile acid synthesis during feeding within the liver. Due to increased production by liver after a meal, the spill-over into the circulation would ultimately result in higher bile acid plasma levels that can directly increase BAT activity [34]. Hormones released upon feeding such as insulin and GLP-1 are also known to increase BAT activity [35, 36]. Changes in hormone release due to changes in food intake behavior may provide additional indirect pathways by which the SCN regulates rhythmic BAT.

The SCN may also directly signal towards BAT. I will start by evaluating how the SCN in general synchronizes peripheral tissues. Presumably, the SCN synchronizes peripheral organs through the sympathetic nervous system (SNS) and through endocrine output [37]. In case of metabolic tissues, it is demonstrated in rats that specific ablation of the SCN abolishes circadian both at both gene expression level and the functional level, *e.g.* production of insulin and leptin. Furthermore, liver denervation abolishes the circadian

rhythm in glucose plasma levels [38], demonstrating that the SNS is necessary to sustain a circadian rhythm in liver function. BAT is densely innervated by the SNS. The best known trigger for SNS activation towards BAT is cold sensing [39]. Tracing studies in Siberian hamsters demonstrated a direct neural connection between the SCN and BAT [40]. In rats, administration of the excitatory neurotransmitter glutamate to the retinohypothalamic tract or directly to the SCN induced a thermogenic response of BAT [41, 42]. Furthermore, we found that light exposure duration dose dependently decreased noradrenergic outflow as demonstrated by reduced tyrosine hydroxylase staining within BAT. In our study, prolonged light exposure duration was associated with decreased intracellular β-adrenergic signaling, such as CREB phosphorylation. Specific denervation of the BAT depots abolished the attenuating effects of prolonged light exposure on BAT activity, suggesting mediation via SNS [19] (chapter 2). The SCN likely accomplishes the SNS output towards BAT by signaling through the ventromedial hypothalamus (VMH). Specific knock out of clock gene *Bmal1* in the VMH dampened energy expenditure and body temperature rhythms, and dampened the naturally occurring increase in nocturnal expression of *Ucp1* and mitochondrial genes *Nrf1* and *Cpt1b* within BAT. From these data, it seems that the VMH produces an intrinsic rhythm in SNS output towards BAT. Light exposure modulates SCN output towards brain areas including the VMH, thereby changing the amplitude and timing of SNS output [43]. For the SCN to be able to signal towards BAT, an intact signaling via VMH and SNS is thus at least necessary.

Besides SNS input, endocrine systems have been implicated in synchronizing peripheral tissue activity. Glucocorticoid rhythms are a likely candidate to transmit the timing signal. *In vitro*, non-SCN cells do not retain rhythmicity in gene expression [44, 45]. Synchronization of these *in vitro* rhythms can be accomplished by at least three methods: heat shock, serum shock or administration of the glucocorticoid receptor (GR) agonist dexamethasone [46-48]. Interestingly, the intracellular mechanisms by which heat shock and serum shock achieve synchronization are not fully understood. Moreover, attempts to identify which factors within serum synchronize the cells have failed. In this respect, it is intriguing that the dexamethasone is the only single molecule known to synchronize cells *in vitro*. There is some evidence that glucocorticoids can synchronize the rhythm in BAT activity. In chapter 4, we provide evidence that dampening of glucocorticoid rhythms flatten the TG-derived FA uptake by BAT. The finding that the peak corticosterone aligns with peak FA uptake by BAT may seem surprising. Previous studies showed that high concentrations of dexamethasone strongly inhibit BAT activity *in vivo* and *in vitro* [49, 50]. The peak concentration of corticosterone during circadian peak is two-fold lower than the corticosterone peak in response to stress [51]. Therefore, we hypothesize that the concentration of corticosterone is crucial in determining whether BAT is activated or inhibited. In our laboratory, we have investigated the effect of a high versus a low dose of dexamethasone on brown adipocytes. Indeed, our preliminary data show that only high concentrations of dexamethasone downregulate thermogenic gene expression, but that both a high and a low dose of dexamethasone are able to synchronize clock gene expression of brown adipocytes.

Taken together, the link between artificial light and cardiometabolic disease in humans may be mediated via decreased BAT activity. What are the implications to prevent or treat cardiometabolic diseases? Firstly, exposure to artificial light at otherwise dark periods could be reduced or altered. Blue light is the most potent signal for the SCN [52]. Indeed, exposure to light-emitting screens in the evening disturbs sleep in healthy individuals [53]. One study investigated whether selectively removing blue light wavelength prevents adverse health effects. Although sleepiness was indeed improved without blue light exposure, effects on physical parameters, such as cortisol and melatonin levels, were not significant [54]. More studies are needed to further investigate whether blue light specifically mediates the effects of artificial light on metabolism, which would support the use of blue light filters of screens to maintain cardiometabolic health. Although there are no systematic data available, the amount of smartphone software-applications to filter out blue light from smartphone and tablet screens is increasing; the newest Windows operating system has a blue light filter incorporated aimed at "reducing blue light at night to help you sleep" [55]. Secondly, pharmacological activation of BAT may be tailored to the circadian rhythm of its activity. This concept of 'chronotherapy' is gaining ground in various research areas [56]. For example, cancer cells are not synchronized in their circadian rhythm of cell proliferation, making them relatively more susceptible to chemotherapy during the night compared to healthy cells, as these are in their resting phase during night time [57]. In cardiovascular disease, it has been known that myocardial infarctions occur mostly in the morning [58], coinciding with the circadian rise in blood pressure [59] and increased platelet aggregation [60]. In fact, aspirin therapy in the evening more effectively lowers the morning peak in platelet aggregation function than aspirin in the morning [61]. Interestingly, preliminary data have shown that cooling of individuals in the morning increases their energy expenditure more than cooling in the evening (Kooijman, unpublished data), suggesting that activation of BAT may be optimal in the morning, when it is presumably peaking in humans.

Of note, impaired BAT activity may also explain the relationship between disturbed glucocorticoid rhythms and obesity in humans. Individuals who depend on oral supplementation of glucocorticoids, *e.g.* with adrenal insufficiency, have increased risk of metabolic syndrome even though they are adequately treated [62]. Current standard replacement therapy of glucocorticoids attempts to mimic the circadian rhythm with 2-3 doses divided over the day; one high dose in the morning and two lower doses in the afternoon and evening. Even so, the resulting glucocorticoid levels poorly resemble the endogenous circadian – not the mention ultradian – rhythm [63]. If glucocorticoid rhythms are indeed an important synchronizer for BAT activity in humans, individuals on exogenous glucocorticoids may have a disturbed rhythm of BAT, which may lead to decreased thermogenesis and subsequent increased lipid levels and adiposity.

The role of light exposure in the relationship between shift work and atherosclerosis

While studies have established a clear association between shift work and cardiovascular events in humans [64], proving a direct causal relationship is challenging. Shift work is accompanied by many confounding factors. Shift workers may adopt a different life style due to their irregular working hours, as their sleep pattern, physical activity and food intake habits may be different compared to non-shift workers [65, 66]. Furthermore, there is a difference among individuals in shift work tolerance, which is commonly defined as the ability to carry out shift work without adverse consequences [67]. On the other hand, the causes of cardiovascular diseases (CVD) are multifactorial. Contributing factors include dyslipidemia, a pro-inflammatory state, hypertension, pro-thrombotic state and obesity. Shift work and/or circadian rhythm disturbances have been linked independently to all of these individual contributing factors. The work described in this thesis aimed to dissect the contributing pathways, in particular whether mistimed light exposure can induce CVD.

The data described in chapter 5 are the first to demonstrate that mistimed light exposure is a causal factor in atherosclerosis formation. We previously showed that continuous light (LL) exposure in mice decreases SCN amplitude, decreases energy expenditure [14] and decreases BAT activity [19]. Since pharmacological activation of BAT lowers the levels pro-atherogenic VLDL and chylomicron remnants in dyslipidemic mice by accelerating their clearance from plasma [16], it stands to reason that LL would be pro-atherogenic by reducing BAT activity. Although we did observe increased total cholesterol levels, gene expression of BAT activation markers and lipid content within BAT was not affected by chronic LL exposure. Possibly, LL transiently disturbs the rhythm in mice and consequently, transiently lowers BAT activity. A five week LL exposure in wild type male mice induced an arrhythmic phenotype, evidenced by arrhythmic locomotor behavior and flattened plasma corticosterone levels [14]. Exposing dyslipidemic mice to 15 weeks of LL induced arrhythmic locomotor behavior in a small subset of mice (chapter 5). In contrast to LL exposure, 15 weeks of mistimed light exposure did aggravate atherosclerosis development. The lesion size and severity depended on the severity of SCN disturbance. The SCN is disturbed more by a 12 h shift than by a 6 h shift. Moreover, the SCN adapts faster to phase delays than to phase advances [68]. In mice, phase advance but not delay was shown to increase mortality [69]. Atherosclerosis development was not affected by 6 h delay, modestly affected by 6 h advance and severely affected by 12 h reversal of the light-dark cycle. Therefore, the extent (i.e. 6 h vs 12 h) and direction (advance vs delay) of circadian disruption possibly correlates to the extent of atherosclerosis formation.

A crucial question is how mistimed light exposure induces a pro-atherogenic phenotype. Although plasma cholesterol concentrations play a dominant role in atherosclerosis development we did not find an increase in total cholesterol exposure after exposure to 12h reversal and 6h phase advance for 15 weeks compared to a regular LD light regime. However, absence of increased plasma cholesterol levels do not exclude the possibility that mistimed light exposure may affect cholesterol metabolism in various other ways and thereby contributes to atherosclerosis development. LDL particles may be more prone to

oxidation, which makes them prone to be taken up by macrophages, resulting in foam cell formation. Furthermore, the cholesterol efflux capacity of macrophages may play a role. Efflux capacity depends on expression of cholesterol transporters on the macrophages, which is at least partly regulated by circadian genes. For instance, C*lock* regulates the expression of *Abca1*. Macrophages from *Clock*$^{\Delta 19/\Delta 19}$*Apoe-/-* mice have an impaired cholesterol efflux capacity [70].

Another explanation that we did not observe increased total cholesterol levels after mistimed light may be the timing of sampling. Plasma cholesterol levels display a modest diurnal rhythm in humans [71]; we confirmed an oscillation of approximately 2 mM during the day in APOE*3-Leiden.CETP dyslipidemic mice (van den Berg, unpublished data). Since the biological clock adapts to light shifts during the first days after the light regime changes, the 24h rhythms in plasma cholesterol are possibly in phase between the groups. The cholesterol levels of different groups could be similar at a specific time point, even though the groups exhibit different 24h rhythms in plasma cholesterol levels. To determine whether total cholesterol exposure is affected by mistimed light exposure, repeated 24h plasma curves of cholesterol levels should therefore be determined in future studies.

Alternatively, mistimed light exposure may induce atherosclerosis without modulating cholesterol metabolism but via inducing a proinflammatory phenotype, since the biological clock also influences the immune system. Circulating leukocytes and monocytes display a circadian rhythm [72]. Macrophages from mice with *Clock*$^{\Delta 19/\Delta 19}$,an arrhythmic mouse model, were previously shown to be more proinflammatory and to exacerbate metabolic syndrome upon high fat feeding [73]. Macrophages from *Rev-erbα-/-* mice were also shown to be more proinflammatory [74]. We infer that inflammatory cells are regulated by the biological clock and that its disturbance induces a proinflammatory phenotype. Therefore, disturbance of the biological clock via other pathways, such as mistimed light exposure, likely also induce a proinflammatory state.

From clock disturbance to metabolic disease: scientific challenges and future perspectives

The relationship between the circadian clock and metabolism is steadily being unraveled. Animal studies, including those described in this thesis, have convincingly shown that a malfunctioning clock causes metabolic disease. Nevertheless, there are some challenges ahead. Future research has yet to answer the following questions: 1) What are the timing signals for peripheral tissues? 2) What are the intracellular pathways that cause metabolic derangements upon circadian rhythm disturbances? 3) Which data from animal experiments are translatable to humans and which are not? 4) How can we 'cure' our diseased clock, if at all? 5) Since timing determines virtually every tissue function, how should we integrate this fourth dimension into other research fields? These questions are challenging due to the several aspects in the current research on this topic, of which I will discuss the following three.

I. The use of knock out models. Many studies on circadian disturbances have been performed by studying the effect of knock out or mutant clock genes on metabolism using

genetically modified mice. Although very useful to uncover vital functions of genes, the use of genetic animal models has drawbacks. Any genetic model has the downside that animals develop without the gene of interest. Any phenotype may therefore be a developmental problem and compensatory mechanisms may have occurred. This issue may be solved by using conditional knock-out mice. To date, these have not been used in the context of circadian research. In addition, genetic manipulation of a clock gene always affects both the central and peripheral clocks, since they share the same molecular mechanism. This issue is slowly being solved by the use of tissue-specific knock-out mice, although the tissue specificity is often an issue. For example, in adipose tissue-specific *Bmal1* knock-out mice, both WAT and BAT are affected, while only WAT was studied [75]. The SCN-specific *Bmal1* knock-out mouse has been developed using a synaptotagmin10-Cre driven mouse strain, which is specifically expressed in the SCN [76, 77]. SCN-specific *Bmal1* knock-out leads to disturbed gene expression rhythm in WAT, showing that SCN specific rhythm is necessary for rhythmic gene expression in metabolic tissues [78]. Whether the gene expression disturbance translates to disturbed tissue function and whether that results in metabolic disease remains to be investigated. Another drawback of genetic manipulation is that the translatability of findings in mice to human settings of circadian disruptions is very limited. We have shown that, by using artificial light exposure in our studies to manipulate the clock, the human exposure to artificial light can be mimicked, making it possible to study metabolic consequences in an intact animal model. Therefore, findings obtained by varying light exposure regimes are likely more translatable to the human situation compared with genetic intervention. Future research in humans should prove whether indeed BAT activity is influenced by light exposure regimes.

II. Discovery of intracellular mechanisms. It is becoming increasingly clear which metabolic organs mediate the relationship between disturbed clock function and metabolic disease. Nevertheless, the intracellular mechanisms involved are still obscure. Gene expression analysis is the most widely used method to investigate rhythms. However, gene expression analysis alone may be insufficient to predict functional rhythms in organs. We demonstrated a clear adaptive rhythm in BAT with respect to its capacity to take up FA from TG-rich lipoproteins. Upon examination of gene expression, many canonical BAT 'activity' genes, such as *Ucp1,* did not display a clear rhythmicity (chapter 3). In general, regulation of gene expression is only one layer of rhythmic regulation within the cell. In an extensive paper by Koike *et al.* [79], immunochromatin precipitation-sequencing of seven core clock genes showed thousands of genes with bound clock proteins. They compared intronic and exonic RNA expression and concluded that only 22% of cycling transcripts are driven by transcriptional regulation, demonstrating that oscillating mRNA levels depend more on non-transcriptional regulation, *e.g.* post-transcriptional regulation. The highly rhythmic gene *Nocturnin* regulates poly-adenylation of mRNA transcripts [80]. This is likely the tip of the iceberg of non-transcriptional circadian regulation.

Another challenge in elucidating intracellular mechanisms is to obtain human tissue. Gene expression rhythms in humans are often assessed in easily accessible peripheral blood mononuclear cells [81-83]. Subcutaneous white adipose tissue was also shown to

display rhythmic gene expression [84]. In a recent study, repeated muscle biopsies were taken from healthy men under regular feeding and sleep-wake conditions. Oxidative capacity of muscle displayed a rhythm with a peak in the afternoon. While mitochondrial genes did not show oscillations, protein involved in mitochondrial dynamics did oscillate [85]. We also obtained evidence for the involvement of mitochondria in circadian rhythm of metabolism in humans. After one night of short sleep, we found an increase in plasma of specifically the metabolite class of acylcarnitines, which may indicate a mitochondrial dysfunctional (chapter 6). To examine the hypothesis that acylcarnitines derive from muscle tissue and are a result of mitochondrial dysfunction, we are currently investigating the effect of short sleep energy metabolism, including measuring mitochondrial function directly in muscle and white adipose tissue. Although taking human biopsies is invasive, these studies will be necessary to advance the knowledge on intracellular mechanisms in the context of circadian disturbances of energy metabolism.

III. Microbiome involvement. We are not alone. Humans are a symbiosis of human cells and bacteria. The importance of the microbiome for metabolism in general is increasingly recognized. Interestingly, circadian rhythms are also present in the function and composition of gut microbiota [86]. Disturbance of the circadian clock either by genetic modification or by jet-lag resulted in a loss of circadian rhythms of microbiota in mice. Restricting the feeding time to the dark period – the natural feeding time – rescued this effect. Thus, timed feeding controls the circadian rhythm in microbiome [87]. Interestingly, the same group recently reported that the inverse relationship holds true as well. Rhythmicity in the microbiota influences the metabolic pathways in the intestine and in the liver, as loss of rhythmicity in the microbiota changed rhythmic expression in metabolic pathways in these organs [88]. In these studies, rhythms in adipose depots were not established. Since the gut microbiome has been shown to influence the function of both brown and white adipose tissue, it seems highly likely that these organs are also under control of the microbiome [89, 90]. Sleep fragmentation in mice was shown to both change the gut microbiome and lead to inflammation of visceral WAT [91]. Thus, disturbed circadian rhythms may indeed lead to metabolic diseases via changes in gut microbiota, although this relationship needs to be investigated in more detail.

Concluding remarks

The data presented in this thesis have added to the growing body of literature demonstrating that disturbances of the biological clock can lead to cardiometabolic disease. We show that BAT plays a crucial role in mediation of these effects and that this is regulated by both the sympathetic nervous system and glucocorticoid rhythms. The clinical implications of these observations are that prevention of disturbances to our day-night rhythms provides additional handles to improve cardiometabolic health of both the general population and CVD patients. These can be summarized as follows: 1) diminishing (blue) light exposure at dark (inactive) periods, 2) aligning behavior (*e.g.* food intake, physical activity and sleep) to the natural light-dark cycle, 3) aiming to sleep at least 7 hours per night, 4) use of chronotherapy in CVD, 5) BAT activating strategies, probably restricted to

the early wakeful phase, 6) administration of glucocorticoids aimed to mimic the circadian rhythm. Our data showing marked day-night rhythms in metabolism also have diagnostic implications. Measuring lipids at multiple daily time points may give better predictive value for development of CVD. For other CVD risk factors such as blood pressure, it is already common practice to measure multiple times. Blood pressure 'dips' during the night, and 'non-dippers' are known to have an increased risk of CVD in absence of hypertension [92]. Analogous to the 24h blood pressure monitoring, repeated determination of plasma lipid levels may refine risk assessments.

Future research should investigate whether humans display a diurnal rhythm in TG-derived FA uptake by BAT and whether specific flattening of BAT rhythm contributes to cardiometabolic disease. The timing signals and intracellular pathways that synchronize peripheral tissues need further elucidation, *e.g.* with respect to whether the SNS outflow towards BAT is rhythmic. If so, this would provide an additional target for pharmacological activation. In conclusion, the circadian clock crucially regulates energy metabolism. Increasing our understanding of the interplay between clock and energy metabolism will provide new avenues to improve cardiometabolic health.

REFERENCES

1. Circadian. *Managing 24/7: History of Shiftwork*. 24-04-2017]; Available from: http://www.circadian.com/solutions-services/publications-a-reports/newsletters/managing-247-enewsletter/managing-247-history-of-shiftwork.html.
2. Parent-Thirion, A.M., EnriqueHurley, JohnVermeylen, Greet, *Fourth European Working Conditions Survey*. 2007, EurWORK: Dublin: European Foundation for the Improvement of Living and Working Conditions.
3. Leproult, R. and C.E. Van, *Role of sleep and sleep loss in hormonal release and metabolism.* Endocr. Dev, 2010. **17**: p. 11-21.
4. Falchi, F., *et al.*, *The new world atlas of artificial night sky brightness.* Science Advances, 2016. **2**(6): p. e1600377.
5. Sexton, T., E. Buhr, and R.N. Van Gelder, *Melanopsin and Mechanisms of Non-visual Ocular Photoreception.* The Journal of Biological Chemistry, 2012. **287**(3): p. 1649-1656.
6. Panda, S., *et al.*, *Melanopsin (Opn4) requirement for normal light-induced circadian phase shifting.* Science, 2002. **298**(5601): p. 2213-6.
7. Ruby, N.F., *et al.*, *Role of melanopsin in circadian responses to light.* Science, 2002. **298**(5601): p. 2211-3.
8. Freedman, M.S., *et al.*, *Regulation of mammalian circadian behavior by non-rod, non-cone, ocular photoreceptors.* Science, 1999. **284**(5413): p. 502-4.
9. Do, M.T.H., *et al.*, *Photon capture and signalling by melanopsin retinal ganglion cells.* Nature, 2009. **457**(7227): p. 281-287.
10. McFadden, E., *et al.*, *The Relationship Between Obesity and Exposure to Light at Night: Cross-Sectional Analyses of Over 100,000 Women in the Breakthrough Generations Study.* Am. J Epidemiol, 2014.
11. Pattinson, C.L., *et al.*, *Environmental Light Exposure Is Associated with Increased Body Mass*

in Children. PLoS One, 2016. **11**(1): p. e0143578.

12. Rybnikova, N.A., A. Haim, and B.A. Portnov, *Does artificial light-at-night exposure contribute to the worldwide obesity pandemic?* Int J Obes. (Lond), 2016.
13. Obayashi, K., *et al.*, *Exposure to light at night, nocturnal urinary melatonin excretion, and obesity/dyslipidemia in the elderly: a cross-sectional analysis of the HEIJO-KYO study.* J Clin Endocrinol. Metab, 2013. **98**(1): p. 337-344.
14. Coomans, C.P., *et al.*, *Detrimental effects of constant light exposure and high-fat diet on circadian energy metabolism and insulin sensitivity.* FASEB J, 2013. **27**(4): p. 1721-1732.
15. Bakker, L.E., *et al.*, *Brown adipose tissue volume in healthy lean south Asian adults compared with white Caucasians: a prospective, case-controlled observational study.* Lancet Diabetes Endocrinol, 2014. **2**(3): p. 210-217.
16. Berbee, J.F., *et al.*, *Brown fat activation reduces hypercholesterolaemia and protects from atherosclerosis development.* Nat. Commun, 2015. **6**: p. 6356.
17. Boon, M.R., *et al.*, *Peripheral cannabinoid 1 receptor blockade activates brown adipose tissue and diminishes dyslipidemia and obesity.* FASEB J, 2014. **28**(12): p. 5361-5375.
18. Bartelt, A., *et al.*, *Brown adipose tissue activity controls triglyceride clearance.* Nat. Med, 2011. **17**(2): p. 200-205.
19. Kooijman, S., *et al.*, *Prolonged daily light exposure increases body fat mass through attenuation of brown adipose tissue activity.* Proc. Natl Acad. Sci. U. S. A, 2015. **112**(21): p. 6748-6753.
20. Kayaba, M., *et al.*, *The effect of nocturnal blue light exposure from light-emitting diodes on wakefulness and energy metabolism the following morning.* Environ Health Prev Med, 2014. **19**(5): p. 354-61.
21. Au-Yong, I.T., *et al.*, *Brown adipose tissue and seasonal variation in humans.* Diabetes, 2009. **58**(11): p. 2583-2587.
22. Coomans, C.P., A. Ramkisoensing, and J.H. Meijer, *The suprachiasmatic nuclei as a seasonal clock.* Front Neuroendocrinol, 2015. **37**: p. 29-42.
23. McHill, A.W., *et al.*, *Impact of circadian misalignment on energy metabolism during simulated nightshift work.* Proc Natl Acad Sci U S A, 2014. **111**(48): p. 17302-7.
24. Scheer, F.A., *et al.*, *Adverse metabolic and cardiovascular consequences of circadian misalignment.* Proc. Natl. Acad. Sci. U. S. A, 2009. **106**(11): p. 4453-4458.
25. Lee, P., *et al.*, *Brown Adipose Tissue Exhibits a Glucose-Responsive Thermogenic Biorhythm in Humans.* Cell Metab, 2016.
26. Thearle, M.S., *et al.*, *Extent and determinants of thermogenic responses to 24 hours of fasting, energy balance, and five different overfeeding diets in humans.* J Clin Endocrinol. Metab, 2013. **98**(7): p. 2791-2799.
27. Morf, J., *et al.*, *Cold-Inducible RNA-Binding Protein Modulates Circadian Gene Expression Posttranscriptionally.* Science, 2012. **338**(6105): p. 379-383.
28. Boulos, Z. and M. Terman, *Food availability and daily biological rhythms.* Neurosci Biobehav Rev, 1980. **4**(2): p. 119-31.
29. Damiola, F., *Restricted feeding uncouples circadian oscillators in peripheral tissues from the central pacemaker in the suprachiasmatic nucleus.* Genes Dev, 2000. **14**: p. 2950-2961.
30. Patton, D.F. and R.E. Mistlberger, *Circadian adaptations to meal timing: neuroendocrine mechanisms.* Frontiers in Neuroscience, 2013. **7**: p. 185.
31. Stephan, F.K. and I. Zucker, *Circadian Rhythms in Drinking Behavior and Locomotor Activity of Rats Are Eliminated by Hypothalamic Lesions.* Proceedings of the National Academy of Sciences, 1972. **69**(6): p. 1583-1586.
32. Ebling, F.J. and P. Barrett, *The regulation of seasonal changes in food intake and body weight.* J Neuroendocrinol, 2008. **20**(6): p. 827-33.
33. Lucassen, E.A., *et al.*, *Role of vasoactive intestinal*

peptide in seasonal encoding by the suprachiasmatic nucleus clock. European Journal of Neuroscience, 2012. **35**(9): p. 1466-1474.

34. Teodoro, J.S., *et al., Enhancement of brown fat thermogenesis using chenodeoxycholic acid in mice.* Int J Obes (Lond), 2014. **38**(8): p. 1027-34.
35. Cypess, A.M., *et al., Insulin/IGF-I regulation of neccdin and brown adipocyte differentiation via CREB- and FoxO1-associated pathways.* Endocrinology, 2011. **152**(10): p. 3680-9.
36. Beiroa, D., *et al., GLP-1 agonism stimulates brown adipose tissue thermogenesis and browning through hypothalamic AMPK.* Diabetes, 2014. **63**(10): p. 3346-3358.
37. Reppert, S.M. and D.R. Weaver, *Coordination of circadian timing in mammals.* Nature, 2002. **418**(6901): p. 935-941.
38. Cailotto, C., *et al., The suprachiasmatic nucleus controls the daily variation of plasma glucose via the autonomic output to the liver: are the clock genes involved?* Eur. J. Neurosci, 2005. **22**(10): p. 2531-2540.
39. Cannon, B. and J. Nedergaard, *Brown adipose tissue: function and physiological significance.* Physiol Rev, 2004. **84**(1): p. 277-359.
40. Bamshad, M., C.K. Song, and T.J. Bartness, *CNS origins of the sympathetic nervous system outflow to brown adipose tissue.* Am. J. Physiol, 1999. **276**(6 Pt 2): p. R1569-R1578.
41. Amir, S., *Retinohypothalamic tract stimulation activates thermogenesis in brown adipose tissue in the rat.* Brain Res, 1989. **503**(1): p. 163-166.
42. Amir, S., P. Shizgal, and P.P. Rompre, *Glutamate injection into the suprachiasmatic nucleus stimulates brown fat thermogenesis in the rat.* Brain Res, 1989. **498**(1): p. 140-144.
43. Orozco-Solis, R., *et al., The Circadian Clock in the Ventromedial Hypothalamus Controls Cyclic Energy Expenditure.* Cell Metab, 2016. **23**(3): p. 467-478.
44. Brown, S.A., *et al., The period length of fibroblast circadian gene expression varies widely among human individuals.* PLoS Biol, 2005. **3**(10): p. e338.
45. Yoo, S.-H., *et al., PERIOD2::LUCIFERASE real-time reporting of circadian dynamics reveals persistent circadian oscillations in mouse peripheral tissues.* Proceedings of the National Academy of Sciences of the United States of America, 2004. **101**(15): p. 5339-5346.
46. Balsalobre, A., *Resetting of circadian time in peripheral tissues by glucocorticoid signaling.* Science, 2000. **289**: p. 2344-2347.
47. Balsalobre, A., F. Damiola, and U. Schibler, *A serum shock induces circadian gene expression in mammalian tissue culture cells.* Cell, 1998. **93**: p. 929-937.
48. Buhr, E.D., S.H. Yoo, and J.S. Takahashi, *Temperature as a universal resetting cue for mammalian circadian oscillators.* Science, 2010. **330**(6002): p. 379-385.
49. Soumano, K., *et al., Glucocorticoids inhibit the transcriptional response of the uncoupling protein-1 gene to adrenergic stimulation in a brown adipose cell line.* Mol Cell Endocrinol, 2000. **165**(1-2): p. 7-15.
50. Strack, A.M., M.J. Bradbury, and M.F. Dallman, *Corticosterone decreases nonshivering thermogenesis and increases lipid storage in brown adipose tissue.* Am J Physiol, 1995. **268**(1 Pt 2): p. R183-91.
51. Meijer, O.C., R.V. Van Oosten, and E.R. De Kloet, *Elevated basal trough levels of corticosterone suppress hippocampal 5-hydroxytryptamine(1A) receptor expression in adrenally intact rats: implication for the pathogenesis of depression.* Neuroscience, 1997. **80**(2): p. 419-26.
52. Lockley, S.W., G.C. Brainard, and C.A. Czeisler, *High sensitivity of the human circadian melatonin rhythm to resetting by short wavelength light.* J Clin Endocrinol Metab, 2003. **88**(9): p. 4502-5.
53. Chang, A.M., *et al., Evening use of light-emitting eReaders negatively affects sleep, circadian timing, and next-morning alertness.* Proc Natl Acad Sci U S A, 2015. **112**(4): p. 1232-7.

54. Heo, J.-Y., *et al.*, *Effects of smartphone use with and without blue light at night in healthy adults: A randomized, double-blind, cross-over, placebo-controlled comparison.* Journal of Psychiatric Research, 2017. **87**: p. 61-70.
55. 26-4-2017]; Available from: http://www.pcmag.com/news/347526/report-windows-10-adding-blue-light-reduction-option.
56. Griffett, K. and T.P. Burris, *The mammalian clock and chronopharmacology.* Bioorg. Med Chem. Lett, 2013. **23**(7): p. 1929-1934.
57. Sancar, A., *et al.*, *Circadian Clock, Cancer, and Chemotherapy.* Biochemistry, 2015. **54**(2): p. 110-123.
58. Kono, T., *et al.*, *Circadian variations of onset of acute myocardial infarction and efficacy of thrombolytic therapy.* J Am Coll Cardiol, 1996. **27**(4): p. 774-8.
59. Giles, T., *Relevance of blood pressure variation in the circadian onset of cardiovascular events.* J Hypertens Suppl, 2005. **23**(1): p. S35-9.
60. Ridker, P.M., *et al.*, *Aspirin, platelet aggregation, and the circadian variation of acute thrombotic events.* Chronobiol Int, 1991. **8**(5): p. 327-35.
61. Bonten, T.N., *et al.*, *Effect of aspirin intake at bedtime versus on awakening on circadian rhythm of platelet reactivity. A randomised cross-over trial.* Thromb Haemost, 2014. **112**(6): p. 1209-18.
62. Johannsson, G., *et al.*, *Adrenal insufficiency: review of clinical outcomes with current glucocorticoid replacement therapy.* Clin Endocrinol. (Oxf), 2015. **82**(1): p. 2-11.
63. Debono, M., R.J. Ross, and J. Newell-Price, *Inadequacies of glucocorticoid replacement and improvements by physiological circadian therapy.* Eur. J Endocrinol, 2009. **160**(5): p. 719-729.
64. Esquirol, Y., *et al.*, *Shift work and cardiovascular risk factors: new knowledge from the past decade.* Arch Cardiovasc Dis, 2011. **104**(12): p. 636-68.
65. Peplonska, B., *et al.*, *Night shift work and modifiable lifestyle factors.* Int J Occup Med Environ Health, 2014. **27**(5): p. 693-706.
66. Hemio, K., *et al.*, *Food and nutrient intake among workers with different shift systems.* Occup Environ Med, 2015. **72**(7): p. 513-20.
67. Saksvik-Lehouillier, I., *et al.*, *Towards a more comprehensive definition of shift work tolerance.* Ind Health, 2015. **53**(1): p. 69-77.
68. Rohling, J.H., *et al.*, *Phase resetting of the mammalian circadian clock relies on a rapid shift of a small population of pacemaker neurons.* PLoS One, 2011. **6**(9): p. e25437.
69. Davidson, A.J., *et al.*, *Chronic jet-lag increases mortality in aged mice.* Curr Biol, 2006. **16**(21): p. R914-6.
70. Pan, X., X.C. Jiang, and M.M. Hussain, *Impaired Cholesterol Metabolism and Enhanced Atherosclerosis in Clock Mutant Mice.* Circulation, 2013.
71. Rivera-Coll, A., X. Fuentes-Arderiu, and A. Diez-Noguera, *Circadian rhythmic variations in serum concentrations of clinically important lipids.* Clin. Chem, 1994. **40**(8): p. 1549-1553.
72. Labrecque, N. and N. Cermakian, *Circadian Clocks in the Immune System.* J Biol Rhythms, 2015. **30**(4): p. 277-90.
73. Nguyen, K.D., *et al.*, *Circadian Gene Bmal1 Regulates Diurnal Oscillations of Ly6Chi Inflammatory Monocytes.* Science, 2013. **341**(6153): p. 1483-1488.
74. Ma, H., *et al.*, *Increased Atherosclerotic Lesions in LDL Receptor Deficient Mice With Hematopoietic Nuclear Receptor Rev-erbalpha Knock- Down.* J. Am. Heart Assoc, 2013. **2**(4): p. e000235.
75. Paschos, G.K., *et al.*, *Obesity in mice with adipocyte-specific deletion of clock component Arntl.* Nat. Med, 2012. **18**(12): p. 1768-1777.
76. Husse, J., *et al.*, *The light-dark cycle controls peripheral rhythmicity in mice with a genetically ablated suprachiasmatic nucleus clock.* Faseb j, 2014. **28**(11): p. 4950-60.
77. Husse, J., *et al.*, *Synaptotagmin10-Cre, a driver to*

disrupt clock genes in the SCN. J Biol Rhythms, 2011. **26**(5): p. 379-89.

78. Kolbe, I., *et al.*, *The SCN Clock Governs Circadian Transcription Rhythms in Murine Epididymal White Adipose Tissue.* J Biol Rhythms, 2016. **31**(6): p. 577-587.
79. Koike, N., *et al.*, *Transcriptional architecture and chromatin landscape of the core circadian clock in mammals.* Science, 2012. **338**(6105): p. 349-354.
80. Douris, N., *et al.*, *Nocturnin regulates circadian trafficking of dietary lipid in intestinal enterocytes.* Curr. Biol, 2011. **21**(16): p. 1347-1355.
81. Cuesta, M., N. Cermakian, and D.B. Boivin, *Glucocorticoids entrain molecular clock components in human peripheral cells.* Faseb j, 2015. **29**(4): p. 1360-70.
82. Chen, A., *The circadian rhythm of expression of Bmal1 and Cry1 in peripheral blood mononuclear cells of preterm neonates.* J Matern Fetal Neonatal Med, 2010. **23**(10): p. 1172-5.
83. Kavcic, P., *et al.*, *The impact of sleep deprivation and nighttime light exposure on clock gene expression in humans.* Croat Med J, 2011. **52**(5): p. 594-603.
84. Otway, D.T., *et al.*, *Rhythmic diurnal gene expression in human adipose tissue from individuals who are lean, overweight, and type 2 diabetic.* Diabetes, 2011. **60**(5): p. 1577-81.
85. van Moorsel, D., *et al.*, *Demonstration of a day-night rhythm in human skeletal muscle oxidative capacity.* Mol Metab, 2016. **5**(8): p. 635-45.
86. Leone, V., *et al.*, *Effects of diurnal variation of gut microbes and high-fat feeding on host circadian clock function and metabolism.* Cell Host Microbe, 2015. **17**(5): p. 681-9.
87. Thaiss, C.A., *et al.*, *Transkingdom control of microbiota diurnal oscillations promotes metabolic homeostasis.* Cell, 2014. **159**(3): p. 514-29.
88. Thaiss, C.A., *et al.*, *Microbiota Diurnal Rhythmicity Programs Host Transcriptome Oscillations.* Cell, 2016. **167**(6): p. 1495-1510.e12.
89. Geurts, L., *et al.*, *Gut microbiota controls adipose tissue expansion, gut barrier and glucose metabolism: novel insights into molecular targets and interventions using prebiotics.* Benef Microbes, 2014. **5**(1): p. 3-17.
90. Suarez-Zamorano, N., *et al.*, *Microbiota depletion promotes browning of white adipose tissue and reduces obesity.* Nat Med, 2015. **21**(12): p. 1497-501.
91. Poroyko, V.A., *et al.*, *Chronic Sleep Disruption Alters Gut Microbiota, Induces Systemic and Adipose Tissue Inflammation and Insulin Resistance in Mice.* Sci Rep, 2016. **6**: p. 35405.
92. Fabbian, F., *et al.*, *Dipper and non-dipper blood pressure 24-hour patterns: circadian rhythm-dependent physiologic and pathophysiologic mechanisms.* Chronobiol Int, 2013. **30**(1-2): p. 17-30.

ADDENDUM

SUMMARY

Cardiovascular diseases (CVD) are the leading cause of death worldwide, and disturbances in day-night rhythms have recently been implicated as a novel risk factor for CVD. **Chapter 1** provides an overview of both lipid metabolism and the biological clock system and their role in the pathogenesis of CVD is outlined. We introduce the various research question that were addressed by a combination of studies in animal models and humans.

Part I of this thesis focuses on the effects of modulating circadian rhythms on energy metabolism using animal models. Disruption of circadian rhythmicity in humans, *e.g.* through exposure to light at night, is associated with obesity and related disorders, including type 2 diabetes and CVD. The underlying mechanism is unclear. Therefore, we investigated the effect on the duration of light exposure on the metabolic phenotype in **Chapter 2**. Mice that were exposed to day lengths of 16 h and 24 h light, compared to regular 12 h light, showed increased adiposity without food intake or locomotor activity being affected. Mechanistically, we demonstrated that prolonged day length decreases sympathetic input into brown adipose tissue (BAT) and reduces β3-adrenergic intracellular signaling in BAT. As a consequence, prolonging day length decreased the uptake of FAs from TG-rich lipoproteins as well as glucose from plasma selectively by BAT. We concluded that impaired BAT activity is an important mediator in the association between disturbed circadian rhythm and adiposity. Therefore, we anticipate that activation of BAT may overcome the adverse metabolic consequences of disturbed circadian rhythmicity.

Since BAT activity is subject to seasonal regulation, we hypothesized that BAT is also subjected to a circadian, i.e. 24 h, regulation by the central biological clock. In **Chapter 3** we characterized the 24 h rhythm of BAT activity and its implications for lipid metabolism. We observed a high amplitude 24 h rhythm in the TG-derived FA uptake by BAT. The highest uptake was observed at the onset of the active period which was explained by high *Lipoprotein lipase* (*Lpl)* expression and low *Angioprotein-like 4 (Angptl4)* expression, resulting in high LPL protein levels in BAT. Since BAT takes up TG-derived FA to produce heat, we examined fasting and postprandial lipid levels at various time points, and observed that circadian rhythmicity in BAT activity determined daily fluctuations in plasma lipid concentrations as well as lipid clearance. Strikingly, in mice as well as humans we found postprandial lipid excursions to be nearly absent at the onset of the active period and high before sleep, consistent with the diurnal BAT activity pattern. We hypothesize that diurnal rhythm in BAT activity explains previous findings that restriction of food intake to the early wakeful period improves metabolic health.

From the previous chapters, we concluded that the biological clock regulates BAT activity rhythm. However, the mechanisms underlying the regulation of BAT rhythmicity were still unclear. We hypothesized that the circadian rhythm of plasma glucocorticoids, referring to cortisol in humans and corticosterone in rodents, plays a crucial role. In **Chapter 4** we thus addressed this hypothesis by implanting mice with subcutaneous pellets containing a low concentration of corticosterone, which markedly dampened the endogenous corticosterone rhythm. After one week of corticosterone pellet treatment,

the ability of BAT to take up TG-derived FAs from the circulation was determined at AM (onset of the light period) and PM (onset of the dark period). In control mice receiving vehicle, FA uptake by BAT displayed a large AM-PM fluctuation that was in accordance with data shown in Chapter 3. Interestingly, this AM-PM fluctuation was abolished in mice with dampened corticosterone rhythms by preventing the rise in FA uptake PM. Examination of cellular pathways in BAT revealed that dampened rhythm in FA uptake was accompanied by dampened rhythms of the expression of *Lpl* and phosphorylation of CREB, a downstream β3-receptor signaling target. In contrast, known glucocorticoid-responsive element-controlled genes retained rhythmic expression patterns, suggesting that glucocorticoids did not act on brown adipocytes directly. We concluded that short-term dampening of corticosterone rhythm flattens the rhythmicity of BAT activity with respect to the uptake of TG-derived FAs in mice. Our data imply that the biological clock regulates rhythmicity of BAT activity via circadian glucocorticoid levels.

Shift work is a risk factor for atherosclerotic disease, however which aspect(s) of shift work causally induce(s) atherosclerosis remains to be elucidated. In **Chapter 5** we investigated the contribution of mistimed light exposure to atherosclerosis development by performing studies in female APOE*3-Leiden.CETP mice fed a Western-type diet, which is a well-established model for human-like lipoprotein metabolism and atherosclerosis. In two separate experiments, mice were either subjected to constant light (LL) or to three different rotating light-dark schedules, compared to control 12h light-dark (LD) schedule, during 15 weeks of Western-type diet feeding. While LL disturbed the circadian physical activity rhythm to some extent, atherosclerotic lesion development was not affected. In contrast, a weekly 6 h advance light schedule increased plaque severity. Moreover, weekly reversal of LD schedule, which is possibly most effective to disturb circadian rhythmicity, increased plaque severity as well as plaque size. Interestingly, increased atherosclerotic development could not be attributed to higher plasma cholesterol levels, which may suggest that other factors including regulation of immune function by the biological clock may play a role. In conclusion, mistimed light exposure aggravates atherosclerotic development in mice, which may at least partly explain the association between shift work and CVD in humans. Future studies should focus on whether this is mediated via cholesterol metabolism or inflammatory pathways.

Part II of this thesis focuses on the effects of altered day night rhythm and longevity on human lipid metabolism. In **Chapter 6** we investigated the effects of shortened sleep on metabolism. We previously showed that acute sleep curtailment induces insulin resistance, in healthy individuals as well as in patients with type 1 diabetes. Therefore, disturbances in sleep might play a causal role in the pathogenesis of insulin resistance, independent of endogenous insulin production. However, the underlying mechanisms remained unclear. This study aimed to explore the metabolic pathways affected by sleep loss using targeted metabolomics in human fasting plasma samples. Healthy individuals and patients with type 1 diabetes were studied after a single night of short sleep (4 h) versus normal sleep (8 h) in a cross-over design. Remarkably, one night of short sleep specifically increased the plasma levels of acylcarnitines, essential intermediates in mitochondrial FA oxidation. Specifically,

short sleep increased plasma levels of tetradecenoyl-L-carnitine (C14:1), octadecanoyl-L-carnitine (C18:1), and octadecadienyl-L-carnitine (C18:2). Since increased plasma acylcarnitine levels could be a sign of disturbed FA oxidation, it is possible that sleep curtailment acutely induces inefficient mitochondrial function. Inefficient mitochondrial function has been associated to insulin resistance. Also, acylcarnitines have been shown to have pro-inflammatory properties *in vitro* that could disturb insulin signaling. Our observations provide a basis for further research into the role of acylcarnitines as a potential mechanistic pathway by which sleep deprivation – even short term – causes adverse metabolic effects, such as insulin resistance.

In **Chapter 7** we investigated whether longevity may determine circadian rhythms in cholesterol concentrations. The function of the biological clock function deteriorates with increasing age, and aging is associated with dampening of circadian rhythms. Therefore, we hypothesized that individuals with a familial predisposition for longevity have a higher amplitude circadian rhythm in serum cholesterol concentrations. We investigated circadian rhythmicity of serum cholesterol concentrations in offspring of nonagenarian siblings and their partners. Offspring from nonagenarian siblings and their partners as controls were studied in a controlled in-hospital setting over a 24 h period, receiving three isocaloric meals. Serum total cholesterol, HDL-cholesterol and non-HDL-cholesterol were determined every 30 min over a 24 h period. The serum total cholesterol concentrations were higher during day than during night in offspring and in controls. The difference in total cholesterol concentrations between day and night tended to be greater in offspring than in controls, reaching statistical significance in females. Notably, the day-night serum differences in non-HDL-cholesterol were 2-fold greater in offspring than in controls and most explicit in females. We conclude that familial longevity is characterized by a high circadian rhythmicity of non-HDL- cholesterol in healthy elderly offspring from nonagenarian siblings.

Finally, in **Chapter 8**, we discuss the clinical implications and future perspectives of the research described in this thesis. Using animal studies we observed that BAT is strongly regulated by the biological clock, possibly via circadian glucocorticoid rhythms, and attenuated BAT activity through prolonged light exposure increases adiposity. Research focusing on the rhythm in human BAT, and regulation thereof, is necessary to confirm the translational value of our findings. We also observed that mistimed light exposure enhances atherosclerosis development, which may provide a mechanistic link between the known association between shift work and CVD. We anticipate that living according to the natural circadian rhythms presumably contributes to cardiometabolic health. Since disturbances in day-night rhythms are inevitable in modern society, in the future we may advise individuals at risk for development of CVD refrain from shift work and short sleep duration. In addition, data in this thesis may be useful to design strategies to avoid the disadvantageous metabolic effects of shift work.

NEDERLANDSE SAMENVATTING

Hart- en vaatziekten vormen gezamenlijk wereldwijd de belangrijkste doodsoorzaak. Deze ziekten worden meestal veroorzaakt door slagaderverkalking, ook wel 'atherosclerose' genoemd. Verhoogde concentraties van vetten in het bloed, voornamelijk cholesterol en triglyceriden, vormen de belangrijkste risicofactor voor de ontwikkeling van atherosclerose. Hoewel er effectieve cholesterolverlagende medicijnen zijn, kunnen we daarmee atherosclerose niet geheel voorkómen. Het is daarom van belang om meer factoren te ontdekken die bijdragen aan een verstoorde vetstofwisseling, zodat we die ook kunnen moduleren. Het is in de afgelopen jaren aan het licht gekomen dat verstoring van de biologische klok van ons lichaam een risico vormt voor hart- en vaatziekten, mogelijk via verstoring van de vetstofwisseling. Het exacte werkingsmechanisme is echter onbekend. In dit proefschrift is gekeken naar het verband tussen de biologische klok en vetstofwisseling en de gevolgen die verstoringen van de biologische klok kunnen hebben op de ontwikkeling van hart- en vaatziekten.

In **deel 1** van dit proefschrift onderzochten we de relatie tussen de biologische klok en vetstofwisseling door gebruik te maken van muismodellen. In **Hoofdstuk 1** wordt uitgelegd hoe de vetstofwisseling en de biologische klok in elkaar zitten. Daarna wordt de onderlinge verhouding tussen de vetstofwisseling en de biologische klok uiteengezet. Elke lichaamscel heeft energie nodig om te kunnen functioneren. Deze energie wordt geleverd door suikers en vetzuren. Suikers en vetzuren, in de vorm van 'vrije' vetzuren dan wel triglyceriden, worden via de bloedbaan naar cellen getransporteerd die deze energiebronnen nodig hebben. Omdat vet niet oplost in water, worden triglyceriden verpakt in bolletjes omgeven door zeepachtige moleculen en eiwitten. Deze zogenaamde 'lipoproteïnen' transporteren niet alleen triglyceriden, maar ook het vettige molecuul cholesterol, een voor cellen essentiële bouwsteen. Energie in de vorm van suiker en vetzuren is afkomstig uit voeding. Een overschot aan energie kan worden opgeslagen in met name wit vetweefsel en in mindere mate in de lever en in spierweefsel. De lichaamseigen aanmaak van suiker en vet vindt met name in de lever plaats. Sinds enkele jaren is het bekend dat er nog een type vetweefsel bestaat wat bijdraagt aan de stofwisseling in mensen, namelijk bruin vetweefsel. Bruin vet is als het ware de kachel van het lichaam; door de verbranding van suikers en vetzuren produceren bruine vetcellen warmte, met als doel de lichaamstemperatuur op peil te houden. Dit 'gratis' energieverbruik heeft bruin vet tot een aantrekkelijk doelwit gemaakt voor het verlagen van een overschot aan opgeslagen en circulerende vetten, waarmee stofwisselingsziekten zoals suikerziekte (ofwel type 2 diabetes) en hart- en vaatziekten bestreden zouden kunnen worden. Hierom wordt er veel onderzoek gedaan naar medicijnen die bruin vet aanzetten tot verbranding van suikers en vetten.

De biologische klok beïnvloedt vrijwel alle aspecten van de stofwisseling en zorgt ervoor dat de energiebalans afgestemd is op onze omgeving. Menselijk gedrag, zoals eten, bewegen en slapen, volgt een regelmatig dag-nacht patroon. Door ervoor te zorgen dat de werking van organen ook een dag-nacht patroon volgt kan het lichaam efficiënt omgaan met energie. Licht is het belangrijkste signaal voor de centrale klok in het brein, de zogenaamde suprachiasmatische nucleus (SCN), om aan te geven 'welk tijdstip van de

dag' het is. In de afgelopen eeuw heeft het gebruik van kunstmatige verlichting een enorme vlucht genomen. Hierdoor zijn de dag-nacht ritmes in menselijke bezigheden losgekoppeld van de natuurlijke 24-uurs licht-donker cyclus en de jaarlijkse seizoensritmes. Dit heeft geleid tot de mogelijkheid van werken in ploegendiensten, maar tot het besteden van vrije tijd in nachtelijke uren. Deze ontkoppeling van dag-nacht ritmes van de natuurlijke licht-donker cyclus heeft grote effecten op onze gezondheid. Kortere slaapduur, lichtvervuiling en werken in ploegendiensten zijn allemaal in verband gebracht met verstoringen in de stofwisseling, en leiden met name tot een verhoogd risico op overgewicht, type 2 diabetes en hart- en vaatziekten.

In deel 1 hebben de relatie tussen In **hoofdstuk 2** hebben we onderzocht via welke organen lichtblootstelling de stofwisseling beïnvloedt. Hiertoe werden muizen blootgesteld aan een normale licht-donker cyclus (12 uur licht, 12 uur donker), of aan dagen met 16 uur of 24 uur licht. Hoe langer de lichtblootstelling, hoe meer vetstapeling in het witte vetweefsel, 'de voorraadkamer' van het lichaam, plaatsvond. Daarentegen nam het bruine vetweefsel, de 'kachel' van het lichaam, juist minder vetten op uit bloed. Bruin vet wordt in belangrijke mate aangestuurd door het zenuwstelsel. Als het we de zenuwbanen naar het bruine vet doorknipten, was er geen effect meer van lichtblootstelling op bruin vetweefsel. Lichtblootstelling is dus een belangrijk signaal voor de seizoensgebonden activiteit van bruin vetweefsel en voor het doorgeven van dit signaal is het zenuwstelsel blijkbaar onmisbaar. In **hoofdstuk 3** hebben we het 24-uurs ritme van bruin vet in muizen onderzocht. In tegenstelling tot andere organen, vertoonde bruin vetweefsel een opmerkelijk ritme in de opname van vetzuren gedurende de dag. De piek in vetzuuropname vond plaats bij de start van de wakkere periode, wat in muizen overeenkomt met het begin van de nacht. Bovendien paste dit patroon zich aan wanneer muizen aan korte of lange dagen werden blootgesteld: de vetzuuropname door bruin vet was steeds het hoogst aan het begin van de donkere periode. Vervolgens hebben we gekeken of dit uitgesproken 24-uurs ritme gevolgen had voor de vetstofwisseling over de dag. Aangezien activatie van bruin vet vetniveaus in het bloed kan verlagen, hebben we in muizen met verhoogde vetten in het bloed het effect van de bruin vet ritmiek op bloedvetten onderzocht. We vonden dat de piek in bruin vet activiteit altijd samen viel met het laagste niveau van bloedvetten. Ook als we de muizen een standaard hoeveelheid vet toedienden in de vorm van olijfolie, waren de vetniveaus in het bloed heel laag bij het ontwaken en hoog voor het slapen gaan. Vervolgens hebben we onderzocht of bloedvetten eenzelfde dag-nacht ritme vertonen in mensen. In een groep van gezonde mensen van middelbare leeftijd zagen we dat de vrije vetzuren in het bloed ook een 24-uurs patroon volgden. Ondanks het feit dat de proefpersonen drie identieke maaltijden toegediend kregen als ontbijt, lunch en diner, waren na de maaltijd de vetzuren in het bloed veel lager na het ontbijt van na de lunch of het diner. We concluderen daarom dat consumptie van vetten op het moment dat bruin vet heel actief is leidt tot het snel verbranden van deze vetten door bruin vet waardoor de vetten niet in de bloedbaan blijven circuleren en de bloedniveaus dus laag blijven. Zowel in muizen als mensen is dit waarschijnlijk rond het moment van ontwaken. Ons onderzoek kan verklaren waarom vroege eters gemiddeld minder aankomen dan late eters en heeft een wetenschappelijke basis gegeven aan de oude volkswijsheid 'Ontbijt als een keizer, lunch als een koning en dineer als een bedelaar'.

De centrale biologische klok kan zowel zenuwbanen als hormonen gebruiken om het ritme in organen te bepalen. De hormonen die hierbij waarschijnlijk een rol spelen zijn de glucocorticoïden. Glucocorticoïden vertonen een opvallend 24-uurs ritme in het bloed dat gelijk valt met het hierboven beschreven ritme in de opname van vetzuren door bruin vet. Daarom hebben we in **hoofdstuk 4** onderzocht in hoeverre het 24-uurs ritme in bruin vet door glucocorticoïden worden gereguleerd. Het natuurlijke 24-uurs ritme van het glucocorticoïde corticosteron werd afgevlakt door muizen een continue lage dosis corticosteron toe te dienen onder de huid. Afvlakking van het corticosteronritme leidde ertoe dat bruin vet geen piek meer in vetzuuropname vertoonde. Hierdoor konden we concluderen de SCN bruin vet niet alleen door zenuwbanen maar waarschijnlijk ook door glucocorticoïden aanstuurt.

Ploegendienst werkers hebben zoals gezegd een verhoogd risico op hart- en vaatziekten. Een mogelijke oorzaak zou de verandering in lichtblootstelling kunnen zijn. In mensen is dit niet goed te onderzoeken omdat er veel levensstijlveranderingen zijn die dit verband beïnvloeden: ploegendienst werkers eten, bewegen en slapen op andere tijden dan niet-ploegendienst werkers. Daarom hebben wij in muizen onderzocht of een veranderde lichtblootstelling atherosclerose kan veroorzaken. In **hoofdstuk 5** laten we zien dat verandering in lichtblootstelling inderdaad tot een versnelde ontwikkeling van atherosclerose kan leiden. Muizen die gedurende 15 weken aan continu licht werden blootgesteld hadden verhoogde cholesterolconcentraties in het bloed in vergelijking met dieren die in een regelmatige licht-donker (12 uur licht, 12 uur donker) cyclus leefden, maar geen toename in atherosclerosevorming. Een mogelijke verklaring hiervoor is dat de dieren gewend raakten aan het regelmatige continue licht, gezien de meeste dieren nog steeds een zeer regelmatig bewegingsritme lieten zien. Daarom voerden we een tweede experiment uit waarin gedurende 15 weken de licht-donkercyclus wekelijks werd opgeschoven, waarmee een 'jetlag' werd nagebootst. De vorming van atherosclerose werd niet verergerd als de donkerfase wekelijks 6 uur werd verlaat. Echter, wanneer we de donkere periode van muizen wekelijks 6 uur vervroegden, wat voor de mens vergelijkbaar is met vliegen naar het oosten, zagen we wél een toename in atherosclerosevorming. Wanneer muizen elke week werden blootgesteld aan een omgekeerde licht-donkercyclus, wat overeenkomt met een wekelijkse jetlag van 12 uur, ontwikkelden zij bijna twee keer zoveel atherosclerose dan onder normale licht-donker omstandigheden.

In **deel 2** hebben we diverse aspecten van de biologische klok in relatie tot de vetstofwisseling onderzocht in mensen. We hebben gekeken naar twee veel voorkomende omstandigheden waardoor dag-nachtritmes in mensen veranderd zijn, namelijk korte slaapduur en veroudering. Type 2 diabetes kenmerkt zich door ongevoeligheid voor het hormoon insuline, waardoor de lever meer suiker en vet produceert en andere organen minder suiker en vet opnemen. Hierdoor stijgt de suiker- en vetspiegel in het bloed, wat veel schadelijke gevolgen heeft voor de functie van organen en een verhoogd risico voor hart- en vaatziekten geeft. Het is onbekend of korte slaapduur een oorzaak is voor het ontstaan van suikerziekte. Mocht dit zo zijn, dan zou langdurige slaapbeperking de suikerstofwisseling nadelig kunnen beïnvloeden. In een vorige studie hebben we bevestigd dat één nacht van 4 uur slaap al leidt tot insulineongevoeligheid van organen. In **hoofdstuk 6** hebben we de

mogelijke mechanismen van deze ongevoeligheid onderzocht door een groep mensen te onderzoeken die één nacht 'normaal' (8 uur) en één nacht kort (4 uur) hadden geslapen. We hebben in het bloed een groot aantal 'metabolieten' gemeten. Dat zijn moleculen die worden gevormd als resultaat van stofwisselingsprocessen en daarmee informatie geven over deze processen. We ontdekten dat na korte slaap één bepaalde klasse metabolieten verhoogd was, en wel de acylcarnitines. Dit wijst op een mogelijk probleem in het energieverbruik in specifieke organellen binnen cellen, zogenaamde mitochondriën, die vetten en suikers omzetten in energie.

Veroudering is geassocieerd met een verminderde werking van de biologische klok, wat zich uit in slechtere slaapritmes, maar ook afgevlakte ritmes in hormoonafgifte. Aan de andere kant is langlevendheid juist geassocieerd met behoud van ritmiek in bijvoorbeeld hormonen in het bloed. Langlevenden hebben daarnaast in het algemeen een gunstigere verdeling van vetten in het bloed. In **hoofdstuk 7** hebben we onderzocht of langlevendheid ook geassocieerd is met een verhoogde dag-nachtritmiek in bloedvetten. Hiervoor onderzochten we de cholesterolspiegels in een groep mensen met een genetische aanleg voor langlevendheid en hun partners die deze aanleg niet zonder meer hebben als controles. Zowel de langlevenden als de controles vertoonden een dag-nachtverschil in cholesterolspiegels maar dat verschil was groter in langlevenden. We concluderen hieruit dat de cholesterolspiegels meer ritmiek vertonen in mensen van middelbare leeftijd die aanleg hebben voor langlevendheid.

In **hoofdstuk 8** werden de resultaten van dit proefschrift besproken als ook de gevolgen van de nieuwe bevinden voor toekomstig onderzoek en de gezondheid. We toonden aan dat langere blootstelling van muizen aan licht tot overgewicht leidde en dat deze relatie verklaard kon worden door vermindering van de bruin vetactiviteit. Op basis van deze gegevens kan gesteld worden dat het reduceren van licht in nachtelijke uren kan bijdragen aan vermindering van overgewicht in mensen. Verder hebben we laten zien dat 24-uurs ritmes in bruin vet bepalend zijn voor de bloedvetconcentratie. Hoewel nog dient te worden aangetoond dat bruin vet een vergelijkbare ritmiek in mensen vertoont en dan het meest bijdraagt aan de verbranding van vet aan het begin van de dag, sluiten onze bevindingen aan bij studies die laten zien dat afvallen effectiever is wanneer maaltijden met name 's ochtends worden gegeten. Tevens zou dit impliceren dat bruin vet op het goede moment geactiveerd kunnen worden met bijvoorbeeld medicijnen. Het maakt dus niet alleen uit wát we eten, maar ook wannéér we eten. We lieten ook zien dat verschuivingen in licht-donkercycli atherosclerosevorming kunnen verergeren. Deze bevinding vormt een wetenschappelijke onderbouwing van de vele observationele studies die laten zien dat werken in ploegendiensten een risicofactor voor hart- en vaatziekten is. Op basis hiervan zouden wij aanbevelen om mensen met een verhoogd cardiovasculair risicoprofiel uit te sluiten van ploegendienst werk. Er blijven nog steeds belangrijke vragen over, bijvoorbeeld hoe het brein precies de 24-uurs ritmes in bruin vet reguleert. We hebben laten zien dat glucocorticoïden hierbij een rol spelen, maar de exacte rol en relatie tot aansturing door zenuwen moet nog verder uitgezocht worden.

LIST OF PUBLICATIONS

Rosa van den Berg,*, Sander Kooijman*, Raymond Noordam, Gustavo Abreu-Vieira, Ashna Ramkisoensing, Wieneke Dijk, Lauren L. Tambyrajah, Isabel M. Mol, Barbara Kramar, Rosanna Caputo, Laura Sardón Puig, Evelien M. de Ruiter, Linda W.M. van Kerkhof, Constantinos Christodoulides, Fredrik Karpe, Sander Kersten, Zachary Gerhart-Hines, Johanna H. Meijer, Claudia P. Coomans, Diana van Heemst, Nienke R. Biermasz, Patrick C.N. Rensen. Circadian rhythmicity of fatty acid uptake by brown fat determines plasma lipid metabolism. Submitted. **authors contributed equally*

Rosa van den Berg, Raymond Noordam, Sander Kooijman, Steffy W.M. Jansen, Abimbola A. Akintola, P. Eline Slagboom, Hanno Pijl, Patrick C.N. Rensen, Nienke R. Biermasz, Diana van Heemst. Familial longevity is characterized by high circadian rhythmicity of serum cholesterol in healthy elderly individuals. Aging Cell 2017; 16: 237-43.

Rosa van den Berg, Dennis O. Mook-Kanamori, Esther Donga, Marieke van Dijk, J. Gert van Dijk, Gert-Jan Lammers, Klaas W. van Kralingen, Cornelia Prehn, Jerzy Adamski, Johannes A. Romijn, Ko Willems van Dijk, Eleonora P.M. Corssmit, Patrick C.N. Rensen, Nienke R. Biermasz. A single night of sleep curtailment increases plasma acylcarnitines: Novel insights in the relationship between sleep and insulin resistance. Arch Biochem Biophys 2016; 589: 145-51.

Rosa van den Berg*, Sander Kooijman*, Ashna Ramkisoensing, Mariette R. Boon, Eline N. Kuipers, Marieke Loef, Tom C. Zonneveld, Eliane A. Lucassen, Hetty C. Sips, Iliana A. Chatzispyrou, Riekelt H. Houtkooper, Johanna H. Meijer, Claudia P. Coomans, Nienke R. Biermasz, Patrick C.N. Rensen. Prolonged daily light exposure increases body fat mass through attenuation of brown adipose tissue activity. Proc Natl Acad Sci USA 2015; 112: 6748-53. **authors contributed equally*

Sjoerd D. Joustra, Roland D. Thijs, Rosa van den Berg, Marieke van Dijk, Alberto M. Pereira, Gert-Jan Lammers, Eus van Someren, Johannes A. Romijn, Nienke R. Biermasz. Alterations in diurnal rhythmicity in patients treated for nonfunctioning pituitary macroadenoma; a controlled study and literature review. Eur J Endocrinol 2014; 171: 217-28.

Claudia P. Coomans, Sjoerd A. van den Berg, Thijs Houben, Jan B. van Klinken, Rosa van den Berg, Amanda C. Pronk, Louis M. Havekes, Johannes A. Romijn, Ko Willems van Dijk, Nienke R. Biermasz, Johanna H. Meijer Detrimental effects of constant light exposure and high-fat diet on circadian energy metabolism and insulin sensitivity. FASEB J 2013; 27: 1721-32.

CURRICULUM VITAE

Rosa van den Berg werd op 2 april 1985 geboren te Voorburg. In 2003 behaalde zij het gymnasium diploma aan het Zandvliet college in Den Haag, waarna zij begon aan de studie Biomedische Wetenschappen aan de Universiteit Leiden. In 2006 behaalde zij haar bachelor diploma. Hierna maakte zij gedurende één collegejaar deel uit van het bestuur van Vereniging te Studerenden te Leiden Catena in de functie van penningmeester sociëteit, ondersteund door een beurs van de Universiteit Leiden. Zij solliciteerde voor het dubbeltraject programma van de Universiteit, die het mogelijk maakt om zowel de Master Biomedische Wetenschappen als de studie Geneeskunde af te ronden. Zij werd hiervoor toegelaten en startte in 2007 met de Master Biomedische Wetenschappen. In 2008 startte zij in het derde jaar van het doctoraal programma van Geneeskunde. In het kader van de Master Biomedische Wetenschappen rondde zij twee stages af binnen het domein van de Interne Geneeskunde, te weten bij de afdeling Reumatologie (onder supervisie van prof. dr. R.E.M. Toes) en de afdeling Endocrinologie (onder supervisie van prof. dr. J.A. Romijn). In 2010 werd zij toegelaten tot de Honours Class 'Medicine and Literature', begeleid door medisch psycholoog prof. dr. A.A. Kaptein. Op 30 augustus 2012 behaalde Rosa haar Master diploma Biomedische Wetenschappen en op 31 augustus 2012 verkreeg zij het doctoraal diploma Geneeskunde en het artsexamen, met lof. Zij startte als arts assistent interne geneeskunde in het Alrijne Ziekenhuis te Leiderdorp. In mei 2013 begon zij als arts-onderzoeker aan haar promotieonderzoek naar de rol van de biologische klok in het energiemetabolisme. Per 1 september 2017 zal zij als arts in opleiding tot specialist beginnen in het Haaglanden Medisch Centrum in het kader van de opleiding tot medisch specialist Interne Geneeskunde.

DANKWOORD

Promoveren is een vierjarig project waar je zelf de regie over hebt. Het is echter alles behalve eenzaam en ik zou dan ook dit proefschrift willen afsluiten met een dankwoord aan de mensen zonder wiens hulp, steun en advies ik dit resultaat nooit had kunnen bereiken.

Allereerst wil ik mijn promotor, Prof. dr. Rensen noemen. Beste Patrick, bedankt voor je benaderbare en enthousiasmerende manier van supervisie. Ik heb geleerd dat de combinatie van inhoud en vorm van vitaal belang zijn in het bedrijven van wetenschap.

Van evenveel belang is mijn copromotor dr. Biermasz. Beste Nienke, bedankt voor je vertrouwen om mij aan te stellen op je prachtige onderzoekslijn naar de invloed van circadiaan ritme op gezondheid. Dankzij jouw genuanceerde advies hielden we de relevantie voor de mens in het vizier en leerde ik tegelijkertijd dat er niet zoiets bestaat als 'dé patiënt'.

Voordat ik mijn collega's ga noemen, wil ik benadrukken dat helpen bij experimenten van mij een bijzondere opgave was, aangezien dit meestal betekende dat mensen op de meest barre tijdstippen aan mochten treden. Dank aan allen voor de vroege en late uurtjes. Sander, nog voordat mijn aanstelling inging had je me al op sleeptouw genomen, hetgeen uitmondde in een prachtige onderzoekslijn naar bruin vet ritmiek. Bedankt voor het mij leren delegeren. Edwin, bedankt voor je onverstoorbaarheid. Jan; je laat zien dat er zoiets bestaat als ontspannen promoveren. Yanan, a conversation with you resulted invariably in good advice, be it scientific, private or fashion. Gustavo, thanks for being my guinea pig. Padmini en Jimmy voor de praktische en theoretische inleiding in het atherosclerose onderzoek.

Endomeiden van het eerste uur: Andrea, Geerte, José, Lisa vW, Mariëtte, en endomeiden van het 'tweede uur' Eline, Kimberly, Laura, Lisanne, Lisa K, Maaike en natuurlijk de endo'heren' Huub, Enchen, Zhuang. Bedankt voor de hoognodige pauzepraat, comic relief en congresbezoekplezier. De goede sfeer zorgde ervoor dat ik met plezier naar werk ging.

Graag wil ik van het endolab Chris, Trea, Hetty en Janny bedanken voor praktische ondersteuning en koffiepauze ontspanning. Isabel, bedankt voor je eindeloze inzet, dag en nacht, bij kamertemperatuur en bij 'thermoneutraal', in licht en donker.

Alle studenten die stage hebben gelopen bij mij: Rosanna, Julia, Laura, Tom, Karina, Evelien, Eveline, Nikki, Sebas. Ik leerde altijd ook iets van jullie. Thank you for all your enthusiasm and efforts.

Er waren verder veel andere afdelingen waarmee ik zeer prettig heb samenwerkt. Van de afdeling Humane genetica: Ko, Vanessa, Jan, Lisa H, Amanda, Sam, Saeed, Mattijs, Lianne. Dennis, voor een inleiding in grote data-analyse. Van de afdeling ouderengeneeskunde: Diana, Steffy, Abi en Raymond, ik heb erg veel plezier gehad in ons gezamenlijk project. Het RIVM; Harry, Linda, Martijn en Conny, dank voor de samenwerking met het jet-lag project. Ten slotte was de samenwerking met de afdeling neurofysiologie (MCB) onontbeerlijk voor alle ritme studies. Joke, Claudia, Ashna, Erno en Eliane, ik heb ontzettend veel van jullie geleerd.

Dan wil ik nog een aantal mensen noemen die op één of andere manier belangrijk zijn geweest. Jolanda, bedankt dat je me ooit het dubbeltraject in loodste. Alberto, bedankt dat je je over mij ontfermde ten aanzien van mijn verdere loopbaan. Onno, gesprekken met jou

kunnen gaan over muziek, studenten, zombies of cortisol, altijd met hetzelfde enthousiasme en inzet. Je aandacht voor studenten en onderwijs is een voorbeeld voor me.

Het avontuur van het opzetten en (deels) uitvoeren van een klinische slaapstudie had heel wat voeten in de aarde. Van het klinisch onderzoekscentrum wil ik Bep en Sabrina bedanken voor de praktische hulp. Van de afdeling dermatologie wil ik Sjan en Abdoel bedanken voor het meedenken en van Unilever wil ik Harry, Timo en Louise bedanken voor de input. Iris, zonder jou had mijn laatste promotiejaar er heel anders uitgezien, bedankt voor alle slapeloze nachten.

Promoveren was alleen mogelijk geweest met morele steun van vrienden en familieleden. Hierbij wil ik in het bijzonder de volgende mensen noemen. Soraia, voor je eerlijke mening. Fransje, voor onze stimulerende discussies over het wetenschappelijk bedrijf (en life, the universe and everything). Joke, voor hulp in barre tijden. Karin, voor het voorbeeld dat geneeskunde en een bruisend sociaal leven prima te combineren zijn. Petra, voor je energie. Annemarie en Martijn, voor een luisterend oor. Marina, voor je volste vertrouwen in mijn wetenschappelijke kwaliteiten, ook als ik het zelf niet zo zeker wist. Chiara, voor het inzicht van het belang van een goede werk-privé balans, voor durven te dromen. Floris, bedankt dat ik altijd op je kan rekenen. Alberto, le distanze non si misurano in kilometri; grazie per tenermi presente nei tuoi pensieri. Quirien, Didi, Job; jullie hebben mij mijn hele promotietraject bijgestaan. Bedankt voor jullie geduld als ik weekenden, avonden en vakanties doorwerkte, voor het ophalen en brengen naar het lab met mijn gebroken enkel en nog veel meer. Aurora, cara mamma, grazie per il sostegno morale tramite telefonate, pranzi e cene. Martin, paps, discussies over slaap brachten onze werk/hobby's onverwachts en tot mijn grote vreugd bij elkaar. Bedankt voor jullie onvoorwaardelijke steun.